CR-72543
DAC-63240

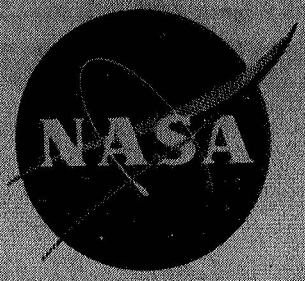

DEVELOPMENT AND DEMONSTRATION OF CRITERIA FOR LIQUID FLUORINE FEED SYSTEM COMPONENTS

JUNE 1969

Prepared Under Contract No. NAS 3-11195

by
D.L. Endicott and L.H. Donahue

McDonnell Douglas Astronautics Company
McDonnell Douglas Corporation
5301 Bolsa Avenue
Huntington Beach, California 92647

for
NASA Lewis Research Center
Cleveland, Ohio
L.H. Gordon, Project Manager
Liquid Rocket Technology Branch
NATIONAL AERONAUTICS AND SPACE ADMINISTRATION

MCDONNELL DOUGLAS ASTRONAUTICS COMPANY
WESTERN DIVISION

CR-72543
DAC-63240

DEVELOPMENT AND DEMONSTRATION OF CRITERIA FOR LIQUID FLUORINE FEED SYSTEM COMPONENTS

JUNE 1969

Prepared Under Contract No. NAS 3-11195

by
D.L. Endicott and L.H. Donahue

McDonnell Douglas Astronautics Company
McDonnell Douglas Corporation
5301 Bolsa Avenue
Huntington Beach, California 92647

for
NASA Lewis Research Center
Cleveland, Ohio
L.H. Gordon, Project Manager
Liquid Rocket Technology Branch
NATIONAL AERONAUTICS AND SPACE ADMINISTRATION

MCDONNELL DOUGLAS ASTRONAUTICS COMPANY
WESTERN DIVISION

ABSTRACT

A five-part program was completed to supplement the design criteria of flight-weight fluorine feed systems development under Contract NASw-1351. The five parts of the program included the following:

1. Conceptual design studies of 2-in. shutoff valves and vent-relief valves with special emphasis on a poppet type shutoff valve.
2. Studies of contaminants in LF_2 systems with emphasis on potential hazards of water-ice in liquid fluorine. The ice was found to be less hazardous than anticipated.
3. Material compatibility tests on Titanium Ti-5Al-2.5SN (ELI) alloy and thin TFE coatings. The corrosion rate of the titanium was found to be acceptable while both the titanium and the commercial TFE coating were found to be impact sensitive in LF_2 at 72 ft-lb.
4. Filter compatibility tests to evaluate filter elements of high purity nickel and Al_2O_3 materials in full-size fluorine filters. Both materials were found to be acceptable.
5. Compatibility tests on various types of explosively actuated valves in both liquid and gaseous fluorine. Potential failure mechanisms were noted.

FOREWORD

The work described herein, which was conducted by the McDonnell Douglas Astronautics Company - Western Division, was performed under NASA contract NAS 3-11195. The work was done under the management of the NASA Project Manager, Mr. L. H. Gordon, Liquid Rocket Technology Branch, NASA Lewis Research Center.

CONTENTS

FIGURES

TABLES

SECTION I

SUMMARY

Under the guidance of the NASA Lewis Research Center, a five-part program was completed to supplement the design criteria of flight-weight fluorine systems developed under Contract NASw-1351. The previous work was applicable to flight-weight fluorine feed systems in general and is described in a Final Report CR 72063, and in the Fluorine System Handbook, CR 72064. The objectives and results of the Tasks conducted in this supplemental program are presented in this section.

A fluorine valve design study was conducted to provide valve designs which were optimized for fluorine service and which would not exceed the NASA leakage requirements of 10^{-6} lb/sec (4.5×10^{-7} kg/sec) of fluorine. Poppet vent-and-relief valves and both poppet and butterfly shutoff valves were studied. Parker Aircraft Company assisted with the vent-and-relief valve studies, and AiResearch Manufacturing Company assisted with the butterfly shutoff-valve studies. The poppet shutoff-valve study was done by McDonnell Douglas Astronautics Company-Western Division (MDAC-WD), Advanced Propulsion Department liquid fluorine program group. The poppet shutoff valve was of special interest because it featured a bellows shaft seal, a bellows-mounted compliant seat, and a pressure-energized poppet closure. Configuration drawings, material lists, manufacturing methods, cleaning procedures and inspection procedures were prepared for all three valve types.

The extent of the contamination which could occur from moisture entrapment in a fluorine system was investigated. This study included predictions of the amount of moisture which would normally be expected in a closed system, and determination of the problems which would result from the presence of water. The explosive potential of the frozen water ice and the corrosive nature of the hydrogen fluoride contamination were evaluated. It was found that the amount of moisture existing in a tank dried to a level of 200 ppm (present LOX requirement) and pressurized with helium gas with a dew point (D.P.) of -75°F (214°K) would not present an explosion hazard or corrosive condition (high hydrogen fluoride content) under typical flight-vehicle conditions. However, wet helium gases in the -75°F (214°K) dewpoint range would not be recommended because of potential freezing of flow passages or component mechanisms.

A separate study was conducted to determine the solubility limits for hydrogen fluoride in liquid fluorine (LF_2) and it was found that only a negligible quantity of hydrogen fluoride will dissolve in liquid fluorine.

Analytical studies of hydrogen fluoride contamination showed hydrogen fluoride levels which were lower than those on the previous hydrogen fluoride corrosive tests conducted on contract NASw-1351.

A series of material compatibility tests were conducted on titanium alloy Ti-5Al-2.5Sn (ELI), commercial Teflon TFE coating, and the proprietary MDAC-WD Astrocoat-T polymer coating. It was found that the titanium alloy

was impact sensitive in LF_2 at the 72 lb-ft (10 kg-m) energy level and would not be recommended for the LF_2 feed system. The corrosive rate of this alloy was found to be similar to the rates measured for the various aluminum alloys and would be acceptable for fluorine feed systems.

The commercial Teflon TFE coatings were found to be impact sensitive in LF_2 at the 72 lb-ft (10 kg-m) energy level and thus are not considered acceptable for fluorine service. The Astrocoat-T was found to be acceptable at the 72 lb/ft (10 kg-m) impact level and no erosion was detectable at flow velocities up to 200 fps (6.79 x 10 m/sec). This material is considered acceptable for LF_2 service.

A study was made to evaluate available filters in the 2-in.-line size range which would be suitable for fluorine service. No off-the-shelf filter was found that would meet the requirements; however, several LOX filters were found that could be modified for LF_2 service. A filter housing and four interchangeable filter elements were purchased and tested on this program. The element rating sizes and materials were as follows:

1. 25-micron (2.5×10^{-5} m) sintered high-purity porous nickel;
2. 10-micron (10^{-5} m) sintered high-purity porous nickel;
3. 40-micron (4×10^{-5} m) sintered aluminum oxide (Al_2O_3); and
4. 60-micron (6×10^{-5} m) sintered high-purity nickel wire.

These elements were tested using both uncontaminated fluorine, and fluorine contaminated with premixed stainless steel, aluminum metal particles, and hydrogen fluoride ice. All of the elements were found to be compatible with LF_2. A sintered, 25-micron (2.5×10^{-5} m) nickel element was tested under conditions which produced a total flow of over 11,000 lb (4.99×10^3 kg) of LF_2 and a flow time of over 900 sec. A 10 micron (1.0×10^{-5} m) nickel element was tested with a total flow of over 11,000 lb (4.99×10^3 kg) for 800 sec.

A study was made to evaluate available explosively actuated valves which would be suitable for fluorine service. No off-the-shelf valves were found which were completely acceptable for fluorine service; however, a number of valves were found which could be modified for fluorine service without difficulty. Flow tests of 20 different valves (1/4-in. (6.35×10^{-3} m) size were conducted in gaseous and liquid fluorine on both normally open (N/O) and normally closed (N/C) types. Four different failure mechanisms were evaluated. Pretest and posttest leakage rates of the valves were found to vary from 9×10^{-2} ccs (gaseous helium) (9×10^{-8} m^3/sec) to less than 10^{-10} ccs (10^{-6} m^3/sec).

In addition, a series of three tests was conducted to evaluate the compatibility of three different types of unfired squib assemblies. These squibs failed on test; however, it was concluded that the squib failures were caused by a small amount of nylon remaining in the threads of the squib housing even after the removal of the thread lock and recleaning the thread area. New squibs of the type that failed were tested successfully after elimination of the contamination problem.

SECTION II

INTRODUCTION

The potential gains in vehicle payload which are made possible by the use of liquid fluorine, or other interhalogen oxidizers, have been determined through analytical studies. To utilize this potential performance increase it will be necessary to develop engines that are optimized for liquid fluorine (LF_2) service, and to develop propellant feed systems which can handle this highly reactive oxidizer.

To provide the latter technology, NASA Headquarters has sponsored a program for the development and demonstration of criteria for liquid fluorine feed-system components. This effort, under the technical guidance of NASA Lewis Research Center, covered system and subsystem analytical studies, component and subcomponent testing, and an extensive literature survey. Under contract (NASw-1351) a Fluorine Systems Handbook NASA CR 72064 (Reference 1) and Final Report NASA CR 72063 (Reference 2) were published. The present contract (NAS 3-11195) was funded by NASA-LeRC to continue the criteria studies in specific areas.

The object of this program was to verify the criteria generated under the previous NASw-1351 contract by applying those criteria to the conceptual design of two major feed-system components and to provide additional criteria in areas where insufficient data were available. The approach that was used to achieve these objectives during the 16-month period was to:

1. Demonstrate the applicability of the design criteria by performing conceptual design studies of two major components: a vent-and-relief valve and a propellant shutoff valve.

2. Develop adequate data and formulate design criteria in selected areas of system contamination for application to airborne LF_2 feed systems, including the contamination effects of moisture introduced during assembly and launch operation.

3. Conduct material compatibility testing of a titanium alloy and special polymeric materials.

4. Conduct studies to determine the availability of, and complete evaluation testing necessary for, three types of full-size feed-system filters that are suitable for use in LF_2 systems.

5. Conduct studies to determine the availability of, and complete evaluation testing necessary for, explosive valves that are suitable for use in LF_2 and gaseous fluorine service.

6. Prepare addenda, where applicable, for the above items for the Fluorine Systems Handbook, NASA CR 72064.

This approach was implemented by a five-task program as summarized below.

1.0 TASK I: FLUORINE VALVE DESIGN STUDY

The objective of this task was to conduct a design study to provide conceptual designs of a vent-and-relief valve and a propellant-shutoff valve.

Preliminary conceptual design studies and detail component and subcomponent analyses were conducted for both valves to establish the parameters for the detail design effort. These analyses included selection of materials, design, loads, fabrication techniques, inspection procedures, cleaning, and handling requirements. Two component subcontractors assisted in providing detailed component and subcomponent designs.

The design activities of the two component subcontractors were supplemented with independent design studies conducted by MDAC-WD. The results of the detail designs were shown on reproducible drawings and are suitable for inclusion in the Fluorine Systems Handbook.

2.0 TASK II: CONTAMINANT EFFECTS ON FLUORINE FEED SYSTEMS

An engineering study and a program of material compatibility testing was conducted to evaluate the effects of various contaminants on fluorine-feed systems. Emphasis was given to the problem of contamination of the system with various amounts of moisture, particularly the moisture content of the helium gas used for pressurization and purge operations. The frequency of occurrence and the quantity of contaminants was studied and a probable level of hydrogen fluoride contamination was determined. Laboratory testing was conducted to determine the solubility limit of hydrogen fluoride in liquid fluorine.

Additional testing was conducted to evaluate the rate and type of ice buildup in a typical fluorine-feed system and to determine the explosive potential of this condition.

3.0 TASK III: MATERIAL COMPATIBILITY STUDY

Compatibility tests were conducted to provide design criteria covering the use of the titanium alloy Ti-5Al-2.5Sn (ELI) and two forms of polymeric coatings.

The titanium evaluation tests consisted of open-cup LF_2 impact tests and static immersion corrosion tests in LF_2/liquid oxygen environments. The two thin Teflon coatings that were evaluated were standard commercial coatings which did not contain binders or undercoatings and the proprietary Douglas-Astropower in situ polymerized coatings. Open-cup LF_2 impact tests were conducted with both materials, and erosive testing was conducted on the in situ polymerized coating.

4.0 TASK IV: FILTER COMPATIBILITY TESTS

A study was made to evaluate the suitability of existing propellant filters for fluorine service, and evaluation tests of three types of filter elements were conducted. The evaluation tests were conducted by using both uncontaminated fluorine and fluorine which contained controlled amounts of contaminants. Solid particulates and solid hydrogen fluoride were used as contaminants. Full-size test items that were suitable for flowrates of 20 lb/sec (9.08 kg/sec) at 50 psi (3.45×10^5 pascals) supply pressure were tested.

The filter-mesh size requirements were studied and a final size was selected based on the results of the Task II study.

The effectiveness of the filters was evaluated on the basis of differential pressure across the filter, durability, and particle removal.

5.0 TASK V: EXPLOSIVE VALVE COMPATIBILITY TESTS

This effort consisted of a study to evaluate the suitability of existing explosively actuated shutoff valves for fluorine service and evaluation testing of 12 types of valves. The valve designs were selected for testing on the basis of which could provide the most information on these critical design variables. The evaluation testing included component leakage tests, squib compatibility tests, and full-flow tests of complete valve assemblies in LF_2 and gaseous fluorine. The valves were tested at 100 psig (6.90×10^5 pascals) for the gaseous fluorine tests and at 400 psig (2.76×10^6 pascals) for the LF_2 tests.

6.0 SIGNIFICANCE OF PROGRAM RESULTS

The work done on these five tasks has provided important new design criteria for use in designing flight-weight LF_2 feed systems and in providing verification of important criteria generated on the previous NASw-1351 contract. The conceptual design of the poppet shutoff valve has provided a basic design configuration that is suitable for use on high-energy upper stages. The principal features of this valve are suitable for long-term missions. The work on LF_2 filters has provided a significant step forward in fluorine technology. The feasibility of filtering large quantities of LF_2 was demonstrated and filter element designs suitable for this service are available to the industry for the first time. The feasibility of using low-leakage explosive valves in LF2 was demonstrated for the first time. This information will be of significant value for vehicles designed for long-term storage missions.

7.0 RECOMMENDATIONS

The following recommendations are based on the results of the work completed on this contract:

1. The oxidizer shutoff valve (1T32095) evolved under the Task I conceptual design studies should be built and tested at rated operating conditions with LF_2.

2. A detailed evaluation should be made to determine the desirability of using inert liners in the test apparatus used for static corrosion testing of materials in LF_2.

3. A service filter should be developed for vehicle loading of LF_2.

4. The fluorine compatibility of large-size explosive valves, 1-1/2 to 2-in. (3.81×10^{-2} m to 5.08×10^{-2} m) line size, should be investigated.

SECTION III

DESIGN DATA

1.0 TASK I: FLUORINE VALVE DESIGN STUDY

1.1 Introduction

The Task I valve design study of this program was a continuation of the design effort on feed system components, initiated under NASA Contract NASw-1351 (Development and Demonstration of Criteria for Liquid Fluorine Feed System Components) and reported in Reference 2. The purpose of Task I was to produce component designs for flight-weight shutoff valves and vent-and-relief valves for use with liquid fluorine, liquid oxygen, and mixtures of these propellants. This goal was achieved in three steps: (1) conceptual valve design study; (2) preliminary component design; and (3) final component design study.

1.2 Summary

The initial phase of Task I consisted of a survey to determine valve designs that could reasonably be expected to operate in liquid fluorine. From this survey, 10 shutoff-valve and 8 vent-and-relief-valve conceptual sketches were prepared for further evaluation. These conceptual designs were based on analyses of design loads, fabrication techniques, selection of materials, quality control requirements, and cleaning and handling requirements. The 18 conceptual valve designs were reviewed and modified by MDAC-WD and a master comparison chart was prepared. The 18 designs were then presented to the NASA LeRC Project Manager, together with the comparison chart, for a preliminary component design review.

From this design review, two configurations each of poppet shutoff valves, butterfly shutoff valves, and poppet vent-and-relief valves were selected for further study for the preliminary design effort. The preliminary design and analysis of these components included a resolution of the tradeoffs between valve spring and actuator force requirements, closure contact areas and surface-finish specifications, and poppet, bellows, and shaft areas; detailed materials selection; and investigation of the performance of cryogenic seals for actuator pistons, and the effect of seal performance on valve force balances.

The configurations included subcomponent designs of housings, static and dynamic seals, shafts, drives, and bearings, actuation devices, and valve closures. In addition, consideration was given to special valve drive mechanisms which would not require shaft seals. All the devices considered in this category were based upon the principle of transmitting motion through an elastic, hermetically sealed membrane. In this category, the single-ply metal bellows appeared to provide the optimal solution to the drive seal problem.

Preliminary design layouts and subcomponent sketches were prepared for the two poppet shutoff valves, the two butterfly shutoff valves, and the two poppet vent-and-relief valves. Instructions for fabrication, assembly, inspection, cleaning, and handling were prepared for each of these valves. At the conclusion of the preliminary valve-design effort, a final design review was conducted to select the most promising valve design for the final component design effort. As a result of this review, a poppet shutoff valve design was selected for further study. The chosen design was a variation of one of the two poppet shutoff valves reviewed. The final component design effort consisted of a complete preliminary analysis, including pressure and flow losses through the valve, static forces acting on valve poppet during actuation, valve leakage calculations, critical stress calculations, material selection, and critical thermal contraction calculations.

1.3 Conceptual Valve Design Study

A conceptual valve design study was conducted during the Task I effort to evaluate configurations of vent-and-relief and main propellant shutoff valves to meet the design objectives and specifications listed in Table 1. The study effort required to meet these design objectives and specifications consisted of both analytical and design efforts.

1.3.1 Analysis

The conceptual valve-design effort included work in the following areas.

1. The seal leakage investigation initiated under Contract NASw-1351 was continued during the present contract. A modified method of calculating seal leakage was developed to permit analytical predictions of poppets with circular lay finish.

2. The possible types of valve closures for fluorine service were reviewed. This review was directed toward the use of metal-to-metal sealing elements to eliminate the use of rubber or plastic seals in this service.

3. Preliminary design analysis methods for single-ply, flexible metal bellows were reviewed. Of principal interest was the determination of cycle life limits for a given bellows design.

1.3.1.1 Leakage Analysis

The leakage study conducted in Task I made use of the leakage evaluation methods developed under Contract NASw-1351 and in the Fluorine Systems Handbook. The leakage curves shown in the handbook were applied to a valve closure configuration selected to meet the leakage requirements of Table 1. The valve closure consisting of a flat-on-flat poppet closure with a 0.010-in. (2.540×10^{-4} m) land-width sealing surface was selected based upon leakage testing experience gained during the previous program. The initial values of valve-closure leakage taken from the curves in the handbook indicated that a seat stress of 20,000 psi (6.895×10^{7} pascals) is required to meet the leakage requirements of Table 1. This high seat stress appeared to be unrealistic, and so a study was made which showed that a much lower stress would be required if a different surface finish was used.

Table 1 (page 1 of 2)

VALVE DESIGN OBJECTIVES AND SPECIFICATION

1. Fluid:
   a. Liquid oxygen (in accordance with MIL-O-25508)
   b. Liquid fluorine (98.7% LF_2, Min)
      (0.3% (by Wt) Max HF, CH_4)
      (1.0% (by Wt) Max O_2, N_2, Other Inerts)
   c. Mixtures of (a) and (b)
   d. Helium (Grade A Bureau of Mines)
   e. Liquid nitrogen (MIL-P-27401)
2. Temperature:
   Fluid: -320°F (77.6°K)
3. Fluid Pressure:
   Oxidizer: 100 psig max. operating (6.90×10^5 pascals)
   250 psig proof (1.72×10^6 pascals)
   250 x 1.5 = 375 psig burst (2.58×10^6 pascals)
4. Actuation:
   Helium: 500 psig (3.45×10^6 pascals)
   x 1.2 = 600 psig proof (4.14×10^6 pascals)
   x 1.5 = 750 psig burst (5.17×10^6 pascals)

   To open at propellant differential pressures at 100 psig (6.90×10^5 pascals)
5. Flow Rate: 90 GPM (5.68×10^{-3} m^3/sec)
6. Pressure differential at rated flow rate:
   10 psig max (6.90×10^4 pascals)
   5 psig target (3.44×10^4 pascals)
7. Line Size: 2 in. ID (5.08×10^{-2} m)
8. Leakage Rate: (both valves)
   a. Between propellant and actuator: Zero scim H_e (0 m^3/sec)
   b. Main seat leakage: 10^{-6}/sec F_2 (4.5×10^{-7} kg/sec)
9. Material:

   Main flow passage must be compatible with fluorine. Only metallic fluoride lubricants shall be permitted in the propellant cavities, should such lubricants be desirable for sliding contacts, etc.

Table 1 (page 2 of 2)

10. Environmental Conditions:
    a. This valve shall be designed to function properly with an ambient pressure from 0 psia (0 pascals) to 14.7 psia (1.0×10^5 pascals), an ambient temperature of -250°F to +140°F (116.5°K to 333.2°K), humidity from 0% to 100%, salt spray of 50 hr (1.8×10^5 sec), vibrations ±0.25 in. ($\pm 6.35 \times 10^{-3}$ m), amplitude from 5 cps (Hz) to 31 cps (Hz), and 25 g's from 31 cps (Hz) to 2,000 cps (Hz).
    b. Accelerations: 12.0 g's parallel and perpendicular.
11. Special Considerations:
    a. The valves shall be designed for maximum internal passivation with fluorine gas.
    b. Positive isolation between propellant and actuator. Redundancy shall be considered.
    c. Valve envelope limitations established under Contract NASw-1351 shall not be exceeded.
    d. The vent and relief valve shall fail-safe open under normal operating conditions. The main propellant shutoff valve shall fail-safe closed under normal operating conditions.

The analytical method to calculate the leakage that was published in the handbook is primarily based on theoretical considerations, and has not been correlated with extensive empirical data. A search was made for metal-to-metal seal test data with which to verify further the analytical results in the handbook. This search included a review of leakage study reports that have been published since the completion of the literature survey that was conducted during the NASw-1351 contract effort.

Recently published information (References 3 and 4) show that two distinct surface-finish conditions must be considered when determining the leakage rates of metal-to-metal sealing surfaces. The microscopic ridges and furrows, or asperities, that make up the surface of a finished metal part have a more-or-less uniform size and direction that depends on how the surface finish was applied. This direction, or lay, of the surface finish can be classified into two categories: circular and multidirectional. Circular finishes are generated by rotation of the seal with respect to the grinder or lap surface; the multidirectional finish is generated by random motion of the seal with respect to the lap.

Because leakage flow crosses the finished surface of a metal-to-metal seal in a radial direction, it always crosses the lay at right angles to a circular finish; however, with a multidirectional finish, the leakage can flow parallel to the lay in some areas. The difference in leakage rate across a seal with circular lay compared to a seal with multidirectional lay is significant. It is possible to correlate measured seal-leakage flowrates to apparent seat stress for flat seals if the data are first separated according to surface finish direction.

Based on the empirical leakage-test data presented in Reference 3, a simplified method for hand calculation of predicted leakage flow rates was developed. This simplified method is given in Appendix A. Sample calculations of predicted gaseous and liquid fluorine leakage by this simplified method are shown in Figure 1. In this figure, the hand calculations, based upon empirical data, are shown plotted against the computer-generated predictions based upon theoretical considerations, given in the Fluorine Systems Handbook. The curves from the handbook shown were computed for a condition corresponding to multidirectional asperities. All of the curves plotted are based upon surfaces finishes of 4 μin. Peak-to-Valley (1.017×10^{-7} m PTV).

Within the elastic range of the seal, good agreement is obtained between the hand-calculated and the computer-generated values. However, the simplified method curves become invalid when stress levels are reached which cause gross plastic deformation of the seal surfaces. It can be concluded from these curves that the simplified method of hand calculation provides good preliminary answers so long as the elastic range of the seals is not exceeded. However, when it is necessary to determine where the effect of plastic deformation occurs, the leakage curves in the handbook are recommended.

1.3.1.2 Valve Closure Selection Study

A study was conducted to provide criteria for the selection of the optimal valve closure for the metal-to-metal sealing requirements of a liquid fluorine shutoff or vent-and-relief valve. A valve closure may be defined as a subassembly of a valve consisting of two components: a stationary seat and a movable element (such as poppet, gate, blade, disk, ball or butterfly), which are forced together in such a way as to produce a sealing interface. A tabulation of the types of closures that were considered for fluorine service is given in Table 2.

The criteria that were determined to be potentially most useful in making a selection were flow resistance, sealing ability, and complexity. A detailed discussion of these criteria are given in Appendix B, together with the results of an examination of their effects on several candidate closure concepts. In addition to the material presented in Appendix B, the results of the subcontracted study efforts of Parker Aircraft Company in this area are reported in Reference 5.

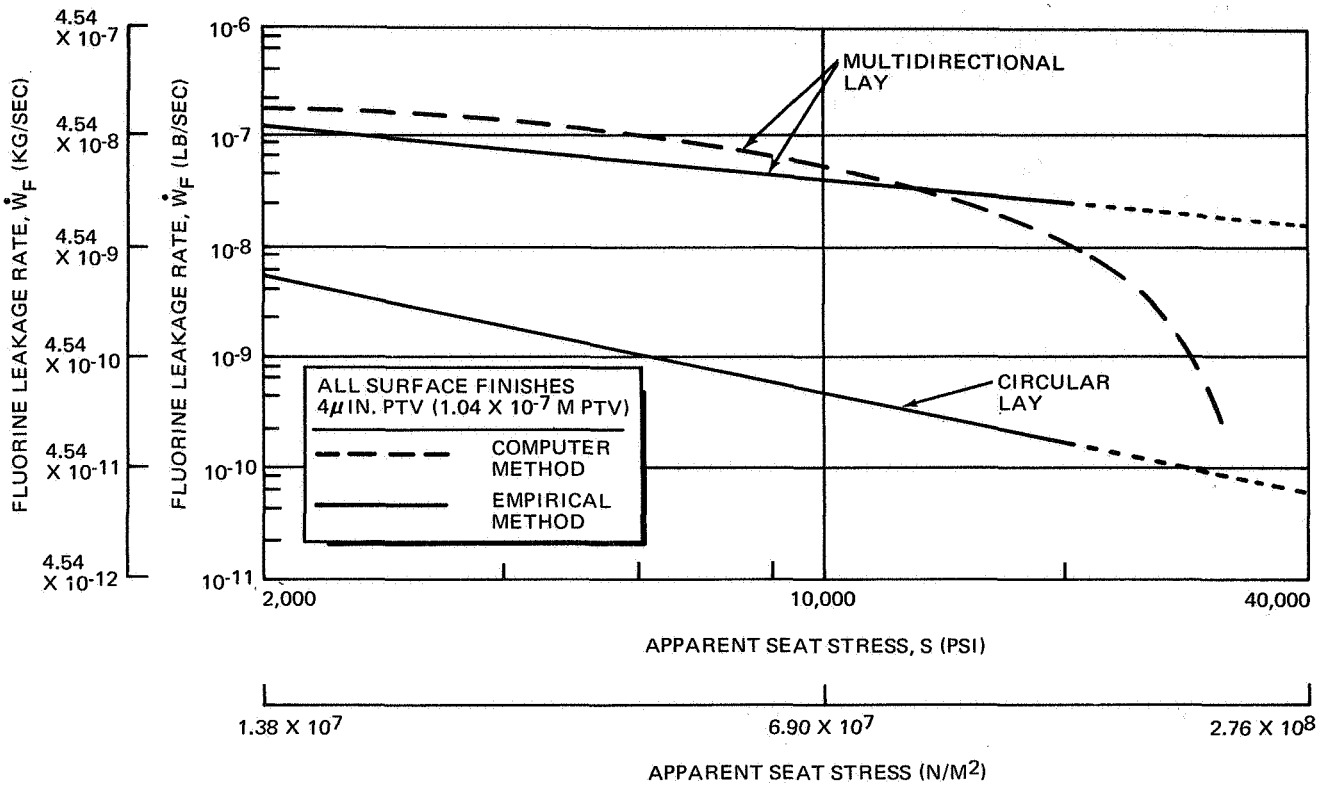

a.—GASEOUS FLUORINE LEAKAGE

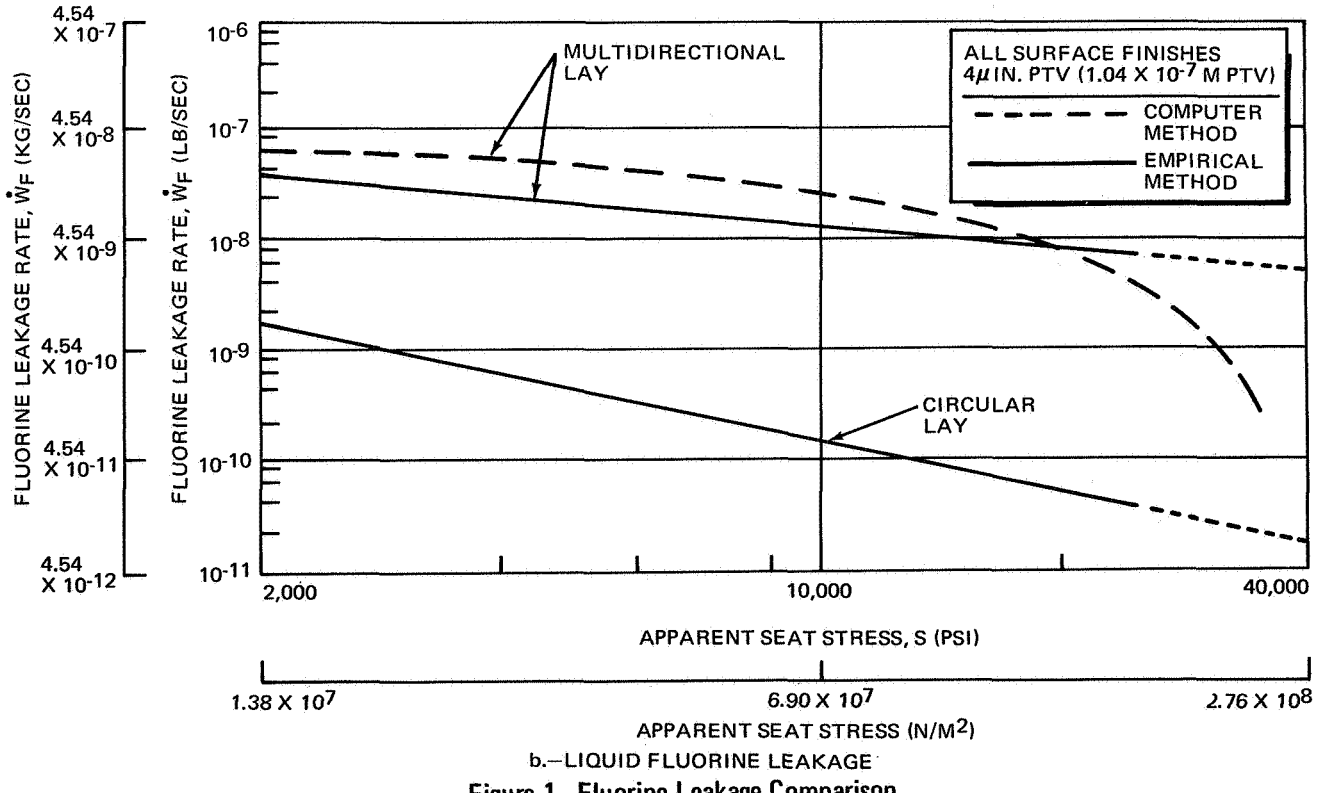

b.—LIQUID FLUORINE LEAKAGE

Figure 1. Fluorine Leakage Comparison

Table 2

VALVE CLOSURE CATEGORIES

Ball Valve Family
Ball
Segmented Ball
Rotary Plug
GateValve Family
Gate
Blade
Rotary Slide
Butterfly Valve
Poppet Valve Family
Inline Valve
Angle Valve
Y-Valve

The valve closures included in the conceptual valve design study, and the valves for the preliminary and final design efforts, were selected on the basis of the results of this valve closure study.

1.3.1.3 Bellows Investigation

The valve design specification given in Table 1 stipulates positive isolation between propellant and actuator. Based upon MDAC-WD sealing experience during the previous contract (NASw-1351), and the results of drive seal investigations conducted during Task I, a bellows seal appears to be the most acceptable shaft seal for LF_2 service. Therefore, as a part of the conceptual valve design study, a review of the parameters affecting performance of metal bellows was undertaken. This review included further evaluation of the bellows test data developed during the NASw-1351 program, assessment of the bellows analysis, and test data published by the Battelle Institute in Reference 6, and a survey of the quasi-empirical design and analysis techniques published by various bellows manufacturers.

The intent of this review was to determine the optimal means of sizing and prestressing a bellows for a given duty cycle. To optimize a bellows design, it is necessary to establish the critical parameters influencing selection of bellows material, and the relationship between bellows deflection and fatigue life.

Additional goals in bellows design are to reduce component envelope and weight. The cycle-life requirements for most missile and space system applications are low, and one method of achieving the design goals is to operate the bellows material partially in the plastic range. For the bellows materials that have been used extensively, there are sufficient test data to predict service life under these conditions reasonably accurately. However, for new bellows materials, and those for which there are limited data, cycle-life prediction is difficult; therefore, it is to be expected that the recommendations made by the different bellows manufacturers will vary.

Two bellows manufacturers were contacted, Gardner Bellows Corp., and Stainless Steel Products, Inc., to obtain information for a valve sealing bellows with a design life of 10,000 cycles. Gardner recommended that the bellows be designed to operate entirely in the compression mode. They stated it would be permissible to operate into the extension mode for a maximum of 50% of the stroke; however, the total stroke in both directions should not exceed the maximum stroke allowable for compression only.

The Stainless Steel Products recommendation was less conservative, using both tension and compression modes to almost the design limit stress. They cited the results of the bellows segment tests on the NASw-1351 program (Reference 2) as support for this recommendation.

The factors which influence fatigue life were also discussed with Battelle Memorial Institute. Battelle has completed a 2-1/2 year program to develop analytical techniques for bellows and diaphragm design. Battelle's recommendation for the limits on the operating stroke was essentially the same as that of Gardner Bellows Corp.: either 100% compression or, if extension operation is desired, a maximum of 50% extension with 50% compression. A further recommendation was to fatigue test at least three bellows specimens to 20,000 cycles to provide a reasonable confidence level or a design life of 10,000 cycles.

In summary, based on the results of Task I investigation, together with previous MDAC-WD fluorine design and test experience, the following design and fabrication constraints for fluorine valve bellows were compiled:

- A LF_2 compatible-material must be used.
- The bellows should be designed for a fatigue life of 10,000 cycles (minimum) to assure an adequate service life, even though the expected number of operating cycles will be only a small percentage of this value.
- Total bellows deflection should be based on the allowable deflection in the compression mode. It is permissible to operate into the extension mode for a maximum of 50% of the stroke; however, the total stroke should not exceed the maximum stroke allowable for compression only.
- Convoluted hydroformed, spun, or rolled bellows are preferred for fluorine service because the cold working enhances the endurance properties of the bellows.

- A single-ply bellows should be used because there is danger of contamination between laminated sheets and adequate cleaning would be impossible.

- Edge-welded bellows are not recommended for fluorine service because of the possibility of contamination and the difficulty of cleaning the welded areas.

- The safety factor used must allow for a potential loss of cycle life in LF_2 service as discussed in Reference 2.

1.3.2 Design

Following the analytical studies, 18 conceptual designs of shutoff and vent-and-relief valves were initially completed which would meet the requirements summarized in Table 1. These 18 conceptual designs were systematically reviewed for critical design characteristics including material selection, design loads, leakage potential, fabrication and assembly techniques, quality control, cleaning, and handling requirements. These 18 designs are summarized in the comparison chart in Table 3.

Following the conceptual design review, several variations of the initial 18 designs were developed. The more promising concepts developed during this design study are pictured in Figures 2 through 9. These concepts are described in the following paragraphs.

The first concept, shown in Figure 2, is an inline poppet shutoff valve with a self-contained actuator piston. The actuator piston and the valve poppet are mounted on opposite ends of a rigid shaft, with a bellows between to provide positive separation. The actuator and poppet housings form an island in the center of the concentric flow path of the valve.

The second configuration, Figure 3, consists of a right-angle version of the inline valve in Figure 2. By moving the actuator out of the flow path and eliminating the concentric flow channel, it is possible to reduce the complexity of the actuator design and assembly and at the same time simplify the sealing, material compatibility, and cryogenic problems. The tradeoff is one of flowrate performance for reliability and cost.

Both of the poppet shutoff valves shown in Figures 2 and 3 utilize bellows mountings for the valve seats. This design provides a compliant mounting of the seat to absorb misalignment between the valve poppet and the seat and enhances the sealing ability of the valve. In the two design configurations, the valve-sealing force is developed by a combination of the actuator spring and the inlet pressure acting over the upstream side of the poppet. The actuator piston is not bottomed under normal operational conditions due to the spring force of the compliant seat.

Figure 4 presents another configuration which is an alternative to that shown in Figure 3. This alternative consists basically of reversing the flow through the valve so that a minimum of seals are exposed to the LF_2 during long-term storage; however, to use the upstream pressure for sealing the valve, it was necessary to reverse the bellows-mounted seat as well as the flow. This

Table 3. (page 1 of 4)

CONCEPTUAL DESIGN COMPARISON CHART

(a) SHUTOFF VALVES

Configuration	Main Closure				Amount of Sliding Friction	Static Seals		Bellows						Assembly Provisions	Failure and Malfunction Modes
	Design and Material		Potential Leakage Perimeter in. (m)	Alignment Provisions		Potential Leakage Perimeter		Quantity	Dimensions L/OD in. (m)	Pressure Application	Deflection Mode	Vulnerability to Physical Damage	Cleaning and Inspection Provisions		
	Stationary Member	Moveable Member				Inlet in. (m)	Outlet in. (m)								
1. Conventional, Center Drive, Butterfly Shutoff Valve (Figure 6)	Conical Seat, A286	Butterfly Disk, Center Actuated, Copper	6.28 (1.59×10^{-1})	Compliant Seat	Moderate	13 (3.30×10^{-1})	33.5 (8.50×10)	1	2.06/0.88 (5.23×10^{-2}/ 2.24×10^{-2})	External	Compression	Relatively long bellows. Column buckling could cause rubbing on housing during compressive loading.	Outside (F_2 side) may be easily cleaned and inspected. Inside cannot be visually inspected after welding, but surfaces are accessible for solution cleaning technique.	Straightforward assembly except two spacers must be machined to provide seat-to-butterfly preload adjustment.	Valve fails: a. Closed (by spring) if actuation signal or pressure fails. b. Open (by butterfly area force unbalance) if actuator linkage fails. c. Closed if butterfly seizes in seat. The final positioning of butterfly into seat is a sliding action where galling could occur if the seat preload is not correctly adjusted and the seating force is too great. The two pin joints in the actuation link also are sliding surfaces but should not gall if the bearing stress is kept low.
2. Center Drive Butterfly Shutoff Valve with Aluminum Body)	Conical Seat, A286	Butterfly Disk, Center Actuated, Copper	6.28 (1.59×10^{-1})	Compliant Seat	Moderate	13 (3.30×10^{-1})	33.5 (8.50×10)	1	2.06/0.88 (5.23×10^{-2}/ 2.24×10^{-2})	External	Compression	Relatively long bellows. Column buckling could cause rubbing on housing during compressive loading.	Outside (F_2 side) may be easily cleaned and inspected. Inside cannot be visually inspected after welding, but surfaces are accessible for solution cleaning technique.	Straightforward assembly expect one spacer must be machined to provide seat-to-butterfly preload adjustment.	Valve fails: a. Closed (by spring) if actuation signal or pressure fails. b. Open (by butterfly area force unbalance) if actuator linkage fails. c. Closed if butterfly seizes in seat. The final positioning of butterfly into seat is a sliding action where galling could occur if the seat preload is not correctly adjusted and the seating force is too great. The two pin joints in the actuation link also are sliding surfaces but should not gall if the bearing stress is kept low.
3. Bell Crank Drive Butterfly Shutoff Valve	Conical Seat, A286	Butterfly Disk, Bell Crank Actuated, Copper	6.28 (1.59×10^{-1})	Compliant Seat	Moderate	13 (3.30×10^{-1})	33 (8.38×10^{-1})	1	1.56/0.88 (5.23×10^{-2}/ 2.24×10^{-2})	External	Compression	Relatively long bellows. Column buckling could cause rubbing on housing during compressive loading.	Outside (F_2 side) may be easily cleaned and inspected. Inside cannot be visually inspected after welding, but surfaces are accessible for solution cleaning technique.	Straightforward assembly except two spacers must be machined to provide seat-to-butterfly preload adjustment.	Valve fails: a. Closed (by spring) if actuation signal or pressure fails. b. Open (by butterfly area force unbalance) if actuator linkage fails. c. Closed if butterfly seizes in seat. The final positioning of butterfly into seat is a sliding action where galling could occur if the seat preload is not correctly adjusted and the seating force is too great. The two pin joints in the actuation link also are sliding surfaces but should not gall if the bearing stress is kept low.
4. In-Line Poppet Shutoff Valve (Figure 2)	Conical Seat, A286	Spherical Poppet, Copper	6.28 (1.59×10^{-1})	Compliant Seat	Low to Moderate	87 (2.21×10^{0})	13 (3.30×10^{-1})	1	2.88/1.25 (7.32×10^{-2}/ 3.18×10^{-2})	External/ Internal	Compression	Relatively long bellows. Column buckling could cause rubbing on housing during compressive loading.	Outside (F_2 side) may be easily cleaned and inspected. Inside cannot be visually inspected after welding, but surfaces are accessible for solution cleaning technique.	Conventional assembly, except care must be exercised to prevent bellows damage during assembly of poppet and piston.	Valve fails: a. Closed (by spring and F_2 pressure) if actuation signal or pressure fails. b. Closed if actuator shaft fails. c. Closed if poppet seizes in seat. The actuator piston as well as the poppet shaft are sliding surfaces which although isolated by seals are buried in the F_2 flow stream and use of lubricants or non-compatible materials is prohibited. May not gall because side forces are inherently small. A flat seat and poppet would eliminate possibility of seat galling.
5. Angle Poppet Shutoff Valve (Figure 3)	Conical Seat, A286	Spherical Poppet, Copper	6.28 (1.59×10^{-1})	Compliant Seat	Low to Moderate	41 (1.04×10^{0})	13 (3.30×10^{-1})	1	2.88/1.25 (7.32×10^{-2}/ 3.18×10^{-2})	External	Compression	Relatively long bellows. Column buckling could cause rubbing on housing during compressive loading.	Outside (F_2 side) may be easily cleaned and inspected. Inside cannot be visually inspected after welding, but surfaces are accessible for solution cleaning technique.	Conventional assembly, except care must be exercised to prevent bellows damage during assembly of poppet and piston.	Valve failure position is indeterminate if piston or poppet shaft seizes. The poppet shaft is a sliding surface which although isolated by seals is buried in the F_2 flow stream and use of lubricants or non-compatible materials is prohibited. Vulnerability to piston galling is eliminated because Teflon piston ring and seal are permissible.

Table 3. (page 2 of 4)

Configuration	Main Closure					Static Seals		Bellows						Assembly Provisions	Failure and Malfunction Modes
	Design and Material		Potential Leakage Perimeter in. (m)	Alignment Provisions	Amount of Sliding Friction	Potential Leakage Perimeter		Quantity	Dimensions L/OD in. (m)	Pressure Application	Deflection Mode	Vulnerability to Physical Damage	Cleaning and Inspection Provisions		
	Stationary Member	Moveable Member				Inlet in. (m)	Outlet in. (m)								
6. Double Bellows Bell Crank Drive Butterfly Shutoff Valve	Conical Seat, S-Monel	Butterfly Disk, Bell Crank Actuated, Copper	5.50 (1.40×10^{-1})	Compliant Seat	Moderate	26.5 (6.73×10^{-1})	69 (1.75×10^{0})	2	1.75/1.13 (4.45×10^{-2}/ 2.87×10^{-2})	External	Compression	Long stroke relative to bellows free length indicates a low spring rate. Bellows probably has a low natural frequency and may be vulnerable to vibration failure.	Edge welded bellows are not acceptable for use in F_2 because of impossibility to clean and inspect. Hydroformed bellows would have to be used and the length would be excessive for the stroke shown.	Possibility of alignment problems with 3-bearing shafts for both the butterfly and actuator. Also seat flange must be machined to fit to obtain seat-to-butterfly preload adjustment.	Valve fails: a. Closed (by spring) if actuation signal or pressure fails. b. Open (by butterfly area force unbalance) if actuator linkage fails. c. Closed if butterfly seizes in seat. d. Indeterminate if butterfly shaft seizes in bushings or actuator shaft seizes in its guide bushings. Highly vulnerable to galling at plain bushings on butterfly shaft, as well as at sliding contact spots on actuator shaft. Also final positioning of butterfly into seat is a sliding action.
7. Single Bellows Bell Crank Drive Butterfly Shutoff Valve	Conical Seat, S-Monel	Butterfly Disk, Bell Crank Actuated, Copper	5.50 (1.40×10^{-1})	Compliant Seat	Moderate	26.5 (6.73×10^{-1})	53.5 (1.36×10^{0})	1	4.13/1.13 (1.05×10^{-1}/ 2.87×10^{-2})	External	Compression	Very long stroke relative to bellows free length indicates a low spring rate. Bellows probably has a low natural frequency and may be vulnerable to vibration failure.	Outside (F_2 side) may be easily cleaned and inspected. Inside cannot be visually inspected after welding, but surfaces are accessible for solution cleaning technique.	Reasonably straightforward to assemble and safety.	Valve fails: a. Closed (by spring) if actuation signal or pressure fails. b. Open (by butterfly area force unbalance) if actuator linkage fails. c. Closed if butterfly seizes in seat. d. Indeterminate if butterfly shaft seizes in bushings or actuator shaft seizes in its guide bushings. Highly vulnerable to galling at plain bushings on butterfly shaft, as well as at sliding contact spots on actuator shaft. Also final positioning of butterfly into seat is a sliding action.
8. Rocking Bellows Drive Butterfly Shutoff Valve A (Figure 7)	Conical Seat, S-Monel	Butterfly Disk, Center Actuated, Copper	5.50 (1.40×10^{-1})	Compliant Seat	Moderate	26.5 (6.73×10^{-1})	37 (9.40×10^{-1})	1	1.13/1.00 (2.87×10^{-2}/ 2.54×10^{-2})	External	Bending	Relatively safe from moving contact with other components due to short L/D ratio and low deflection.	Outside (F_2 side) may be easily cleaned and inspected. Inside cannot be visually inspected after welding, but surfaces are accessible for solution cleaning technique.	Straightforward assembly except seat flange must be machined to fit to obtain seat-to-butterfly preload adjustment.	Valve fails: a. Closed (by spring) if actuation signal or pressure fails. b. Open (by butterfly area force unbalance) if actuator linkage fails. c. Closed if butterfly seizes in seat. d. Indeterminate if butterfly trunnions seize in bushings. Highly vulnerable to galling at plain bushings on butterfly shaft, as well as at sliding contact spots on actuator shaft. Also final positioning of butterfly into seat is a sliding action. Actuator linkage is less vulnerable to galling and butterfly shaft has one less bushing.
9. Rocking Bellows Drive Butterfly Shutoff Valve B	Conical Seat S-Monel	Butterfly Disk, Bell Crank Actuated, Copper	5.50 (1.40×10^{-1})	Compliant Seat	Moderate	26.5 (6.73×10^{-1})	47.5 (1.21×10^{0})	1	1.13/1.00 (2.87×10^{-2}/ 2.54×10^{-2})	External	Bending	Relatively safe from moving contact with other components due to short L/D ratio and low deflection.	Outside (F_2 side) may be easily cleaned and inspected. Inside cannot be visually inspected after welding, but surfaces are accessible for solution cleaning technique.	Straightforward assembly except seat flange must be machined to fit to obtain seat-to-butterfly preload adjustment.	Valve fails: a. Closed (by spring) if actuation signal or pressure fails. b. Open (by butterfly area force unbalance) if actuator linkage fails. c. Closed if butterfly seizes in seat. d. Indeterminate if butterfly trunnions seize in bushings. Highly vulnerable to galling at plain bushings on butterfly shaft, as well as at sliding contact spots on actuator shaft. Also final positioning of butterfly into seat is a sliding action. Actuator linkage is less vulnerable to galling and butterfly shaft has one less bushing. One additional bushing on butterfly shaft increases galling vulnerability.
10. Precessing Bellows Drive Butterfly Shutoff Valve	Conical Seat, S-Monel	Butterfly Disk, Bell Crank Actuated, Copper	5.50 (1.40×10^{-1})	Compliant Seat	Moderate	26.5 (6.73×10^{-1})	41 (1.04×10^{0})	1	1.88/1.00 (4.78×10^{-2}/ 2.54×10^{-2})	External	Bending and Twisting	Other than possible vibration induced damage, should have low vulnerability because of low relative motion with respect to other components.	Outside (F_2 side) may be easily cleaned and inspected. Inside cannot be visually inspected after welding, but surfaces are accessible for solution cleaning technique.	Straightforward assembly except seat flange must be machined to fit to obtain seat-to-butterfly preload adjustment. Adjusting components to obtain an acceptable fit between the two bell-crank arms will be difficult.	Valve fails: a. Closed (by spring) if actuation signal or pressure fails. b. Open (by butterfly area force unbalance) if actuator linkage fails. c. Closed if butterfly seizes in seat. d. Indeterminate if butterfly trunnions seize in bushings. Highly vulnerable to galling at plain bushings on butterfly shaft, as well as at sliding contact spots on actuator shaft. Also final positioning of butterfly into seat is a sliding action. Actuator linkage is less vulnerable to galling and butterfly shaft has one less bushing. Use of ball bearings in actuation mechanism reduces galling vulnerability.

Table 3. (page 3 of 4)

(b) VENT AND RELIEF VALVES

Configuration	Main Closure					Static Seals		Bellows						Assembly Provisions	Failure and Malfunction Modes
	Design and Material		Potential Leakage Perimeter in. (m)	Alignment Provisions	Amount of Sliding Friction	Potential Leakage Perimeter		Quantity	Dimensions L/OD in. (m)	Pressure Application	Deflection Mode	Vulnerability to Physical Damage	Cleaning and Inspection Provisions		
	Stationary Member	Moveable Member				Inlet in. (m)	Outlet in. (m)								
1. Spherical Poppet Vent and Relief Valve	Conical Seat, A286	Spherical Poppet, Copper	6.28 (1.59×10^{-1})	Compliant Seat	Moderate	37 (9.40×10^{-1})	53.5 (1.36×10^{0})	2	3.65/1.38 (9.27×10^{-2}/ 3.50×10^{-2})	External	Compression	Relatively long bellows. Column buckling could cause rubbing on guide during compressive loading.	Outside can be easily cleaned and inspected. Inside cannot be visually inspected but can be solution cleaned.	Screw together attachment of poppet and vent piston shafts can damage static seal in relief piston cavity.	Valve fails: a. Open with large size hole in primary bellows or if pilot valve sticks open. b. Closed if pilot valve sticks closed. Hole in secondary bellows would permit external leakage when valve relieves, but will have negligible effect on valve opening or closing. The relief piston, poppet guide bushing, vent piston, and vent piston rod seal are sliding components. Their vulnerability varies directly with size and contact force.
2. Flexible Flat Poppet Vent and Relief Valve	Flat Seat, K-Monel	Flat Poppet, Inconel	6.76 (1.72×10^{-1})	Flexible Poppet	Negligible	39 (9.90×10^{-1})	48 (1.22×10^{0})	2	2.06/1.38 (5.23×10^{-2}/ 3.50×10^{-2})	External	Tension/ Compression	Relatively long bellows. Column buckling could cause rubbing on guide during compressive loading.	Outside can be easily cleaned and inspected. With both ends open, inside can be solution cleaned by flushing through.	Reasonably straightforward to assemble and safety.	Valve fails: a. Open with large size hole in primary bellows or if pilot valve sticks open. b. Closed if pilot valve sticks closed. Hole in secondary bellows would permit external leakage when valve relieves, but will have negligible effect on valve opening or closing. The relief piston and poppet guide are sliding surfaces during the relief function. The vent piston and its rod seal are additional sliding surfaces during vent function only. Vulnerability similar to I.
3. Poppet Vent and Relief Valve with Pinned Shaft	Flat Seat, K-Monel	Flat Poppet, Inconel	6.76 (1.72×10^{-1})	Flexible Poppet	Negligible	41 (1.04×10^{0})	54.5 (1.38×10^{0})	2	2.06/1.38 (5.23×10^{-2}/ 3.50×10^{-2})	External	Tension/ Compression	Relatively long bellows. Column buckling could cause rubbing on guide during compressive loading.	Outside can be easily cleaned and inspected. With both ends open, inside can be solution cleaned by flushing through.	Reasonable to assemble, except for joining of poppet and vent piston shafts which can damage relief piston cavity seal.	Valve fails: a. Open with large size hole in primary bellows or if pilot valve sticks open. b. Closed if pilot valve sticks closed. Hole in secondary bellows would permit external leakage when valve relieves, but will have negligible effect on valve opening or closing. The relief piston and poppet guide are sliding surfaces during the relief function. The vent piston and its rod seal are additional sliding surfaces during vent function only. Vulnerability similar to I.
4. Butterfly Vent and Relief Valve	Conical Seat, A286	Butterfly Disk, Copper	6.28 (1.59×10^{-1})	Compliant Seat	Moderate	40 (1.02×10^{0})	58 (1.47×10^{0})	1	2.06/1.38 (5.23×10^{-2}/ 3.50×10^{-2})	External	Tension/ Compression	Relatively long bellows. Column buckling could cause rubbing on guide during compressive loading.	Outside can be easily cleaned and inspected. Inside cannot be visually inspected but can be solution cleaned.	Reasonably straightforward assembly, except the machine-to-fit spacer for preload adjustment of butterfly.	Valve fails: a. Open with large size hole in primary bellows or if pilot valve sticks open. b. Closed if pilot valve sticks closed. Hole in secondary bellows would permit external leakage when valve relieves, but will have negligible effect on valve opening or closing. The relief piston and poppet guide are sliding surfaces during the relief function. The vent piston and its rod seal are additional sliding surfaces during vent function only. Vulnerability similar to I.

Table 3. (page 4 of 4)

Configuration	Main Closure					Static Seals		Bellows						Assembly Provisions	Failure and Malfunction Modes
	Design and Material		Potential Leakage Perimeter in. (m)	Alignment Provisions	Amount of Sliding Friction	Potential Leakage Perimeter		Quantity	Dimensions L/OD in. (m)	Pressure Application	Deflection Mode	Vulnerability to Physical Damage	Cleaning and Inspection Provisions		
	Stationary Member	Moveable Member				Inlet in. (m)	Outlet in. (m)								
5. Rigid Flat Poppet Vent and Relief Valve	Flat Seat, K-Monel	Flat Poppet, Inconel	6.76 (1.72×10^{-1})	Compliant Seat	Negligible	42.5 (1.08×10^{0})	48 (1.22×10^{0})	2	1.75/1.81 (4.54×10^{-2}/ 4.60×10^{-2})	External	Tension/ Compression	Relatively long bellows. Column buckling could cause rubbing on guide during compressive loading.	Outside can be easily cleaned and inspected. With both ends open, inside can be solution cleaned by flushing through.	Reasonably straightforward to assemble and safety.	Valve fails: a. Open with large size hole in primary bellows or if pilot valve sticks open. b. Closed if pilot valve sticks closed. Hole in secondary bellows would permit external leakage when valve relieves, but will have negligible effect on valve opening or closing. The relief piston and poppet guide are sliding surfaces during the relief function. The vent piston and its rod seal are additional sliding surfaces during vent function only. Vulnerability similar to I.
									2.06/1.38 (5.23×10^{-2}/ 3.50×10^{-2})	External	Tension/ Compression				
6. Flexible Flat Poppet Vent and Relief Valve	Flat Seat, Inconel-718	Flat Poppet, K-Monel	6.48 (1.65×10^{-1})	Compliant Poppet	Negligible	35 (8.88×10^{-1})	41.5 (1.05×10^{0})	2	2.00/1.28 (5.08×10^{-2}/ 3.25×10^{-2})	Internal/ External	Compression	May be vulnerable to rubbing due to internal pressurization and relatively large L/D ratio.	Cannot be visually inspected, but can be solution cleaned.	Reasonably straightforward to assemble and safety.	Failure of either bellows will cause external F_2 leakage. If pilot valve sticks open, valve will fail open. If pilot valve sticks closed, valve will fail closed. The relief piston is a sliding surface during the relief function. The vent piston is an additional sliding surface during the vent function. Sliding surface area is larger than II, but side forces should be about same.
									1.15/1.75 (2.92×10^{-2}/ 4.45×10^{-2})	External	Compression	Relatively safe from rubbing due to low L/D ratio and short stroke.	Can be easily inspected, and easily cleaned.		
7. Bellows Actuated All Welded Poppet Vent and Relief Valve (Figure 9)	Flat Seat, Inconel 718	Flat Poppet, K-Monel	6.48 (1.65×10^{-1})	Flexible Poppet	Negligible	0	0	3	4.30/4.75 (1.09×10^{-1}/ 1.21×10^{-1})	External	Compression	Relatively low L/D ratio should preclude rubbing.	Inaccessible for cleaning, and the effectiveness of any cleaning is doubtful.	Assembly problems are directly related to ability to achieve acceptable welds.	Large hole in bellows #1 will cause valve to fail closed; in bellows #2 would preclude vent mode operation; in #3 will cause external F_2 leakage. If pilot valve sticks closed, valve will fail closed, and will fail open if pilot valve sticks open. No sliding surfaces.
									2.30/2.87 (5.84×10^{-2}/ 7.29×10^{-2})	Internal	Compression	May be vulnerable to rubbing because moving end is unguided, however, low L/D ratio may counteract any rubbing tendency			
									1.15/1.75 (2.92×10^{-2}/ 4.45×10^{-2})	External	Compression	Relatively low L/D ratio should preclude rubbing.			
8. Bellows Actuated Poppet Vent and Relief Valve (Figure 8)	Flat Seat, Inconel 718	Flat Poppet, K-Monel	6.48 (1.65×10^{-1})	Flexible Poppet	Negligible	34.5 (8.75×10^{-1})	45.5 (1.15×10^{0})	3	4.30/4.75 (1.09×10^{-1}/ 1.21×10^{-1})	External	Compression	Relatively low L/D ratio should preclude rubbing.	#1 outside can be inspected and cleaned. Inside cannot be inspected, but can be solution cleaned. #2 inside can be inspected with optical equipment and solution cleaned. Impossible to inspect outer surface and any cleaning is doubtful. #3 inside difficult to inspect, but can be solution cleaned. Outside impossible to inspect, and any cleaning is doubtful.	Mechanical joints are reasonably straightforward to assemble and safety. Some welds may be difficult to achieve.	Large hole in bellows #1 will cause valve to fail closed; in bellows #2 would preclude vent mode operation; in #3 will cause external F_2 leakage. If pilot valve sticks closed, valve will fail closed, and will fail open if pilot valve sticks open. No sliding surfaces.
									2.30/2.87 (5.84×10^{-2}/ 7.29×10^{-2})	Internal	Compression	May be vulnerable to rubbing because moving end is unguided, however, low L/D ratio may counteract any rubbing tendency			
									1.15/1.75 (2.92×10^{-2}/ 4.45×10^{-2})	External	Compression	Relatively low L/D ratio should preclude rubbing.			

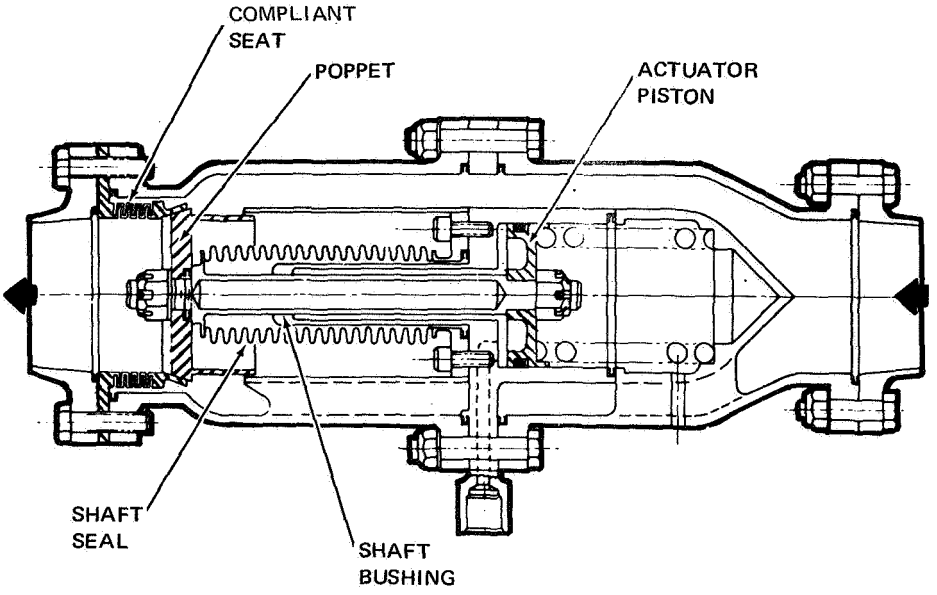

Figure 2. Inline Poppet Valve

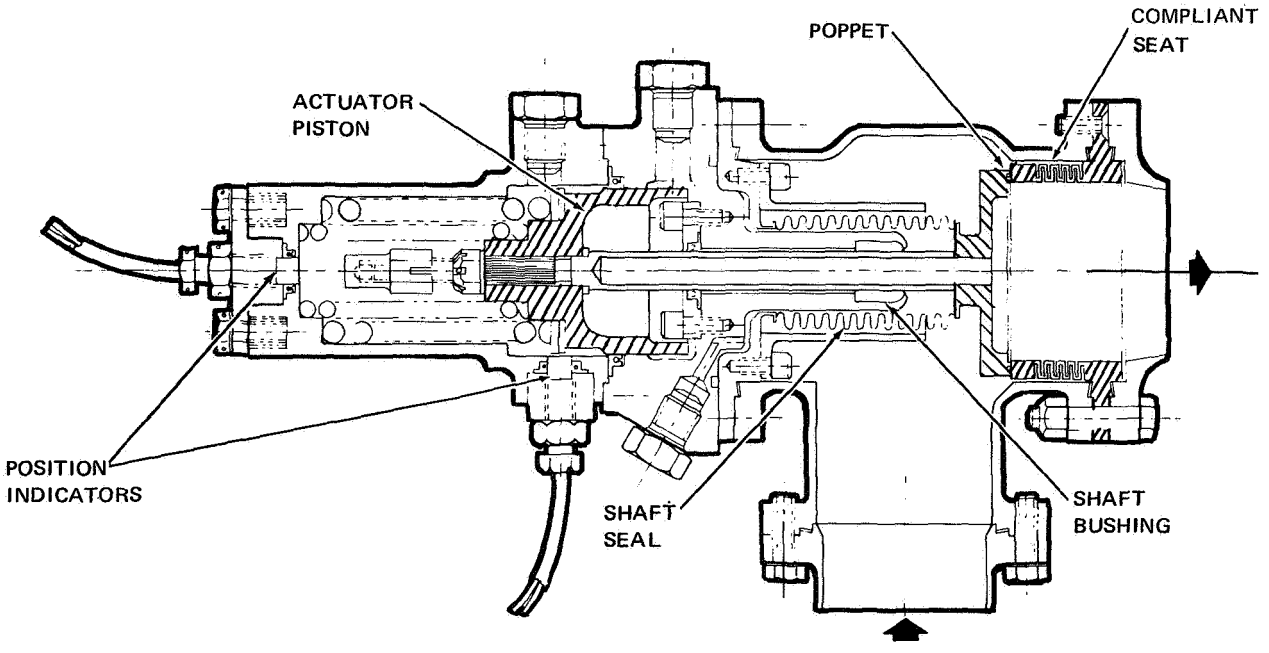

Figure 3. Angle Poppet Valve

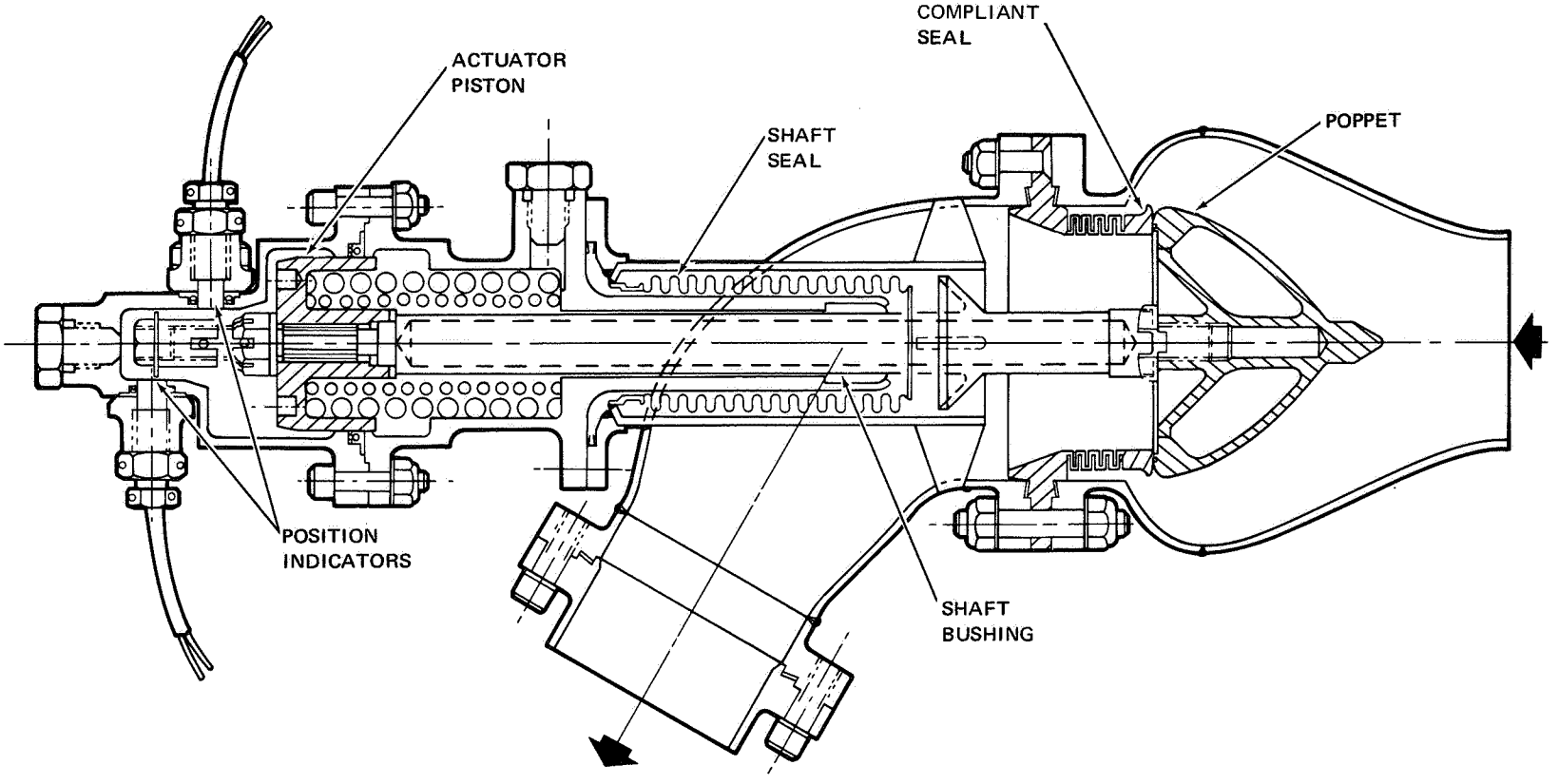

Figure 4. Angle Poppet Valve

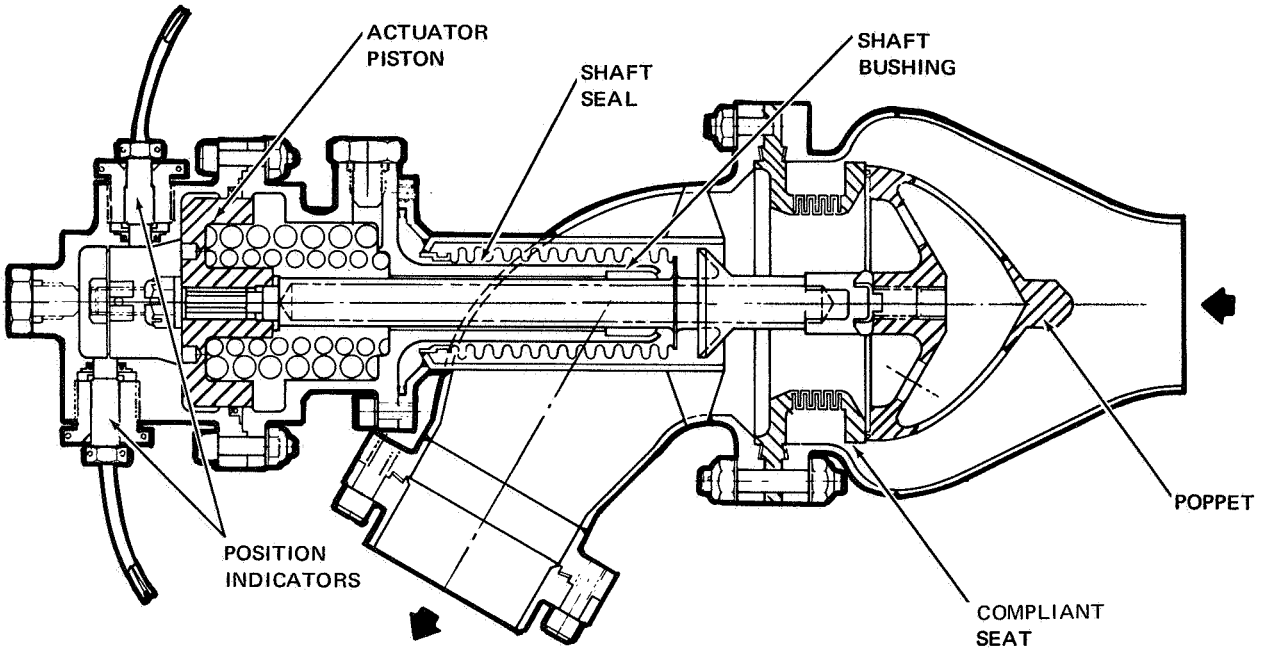

Figure 5. Angle Poppet Valve

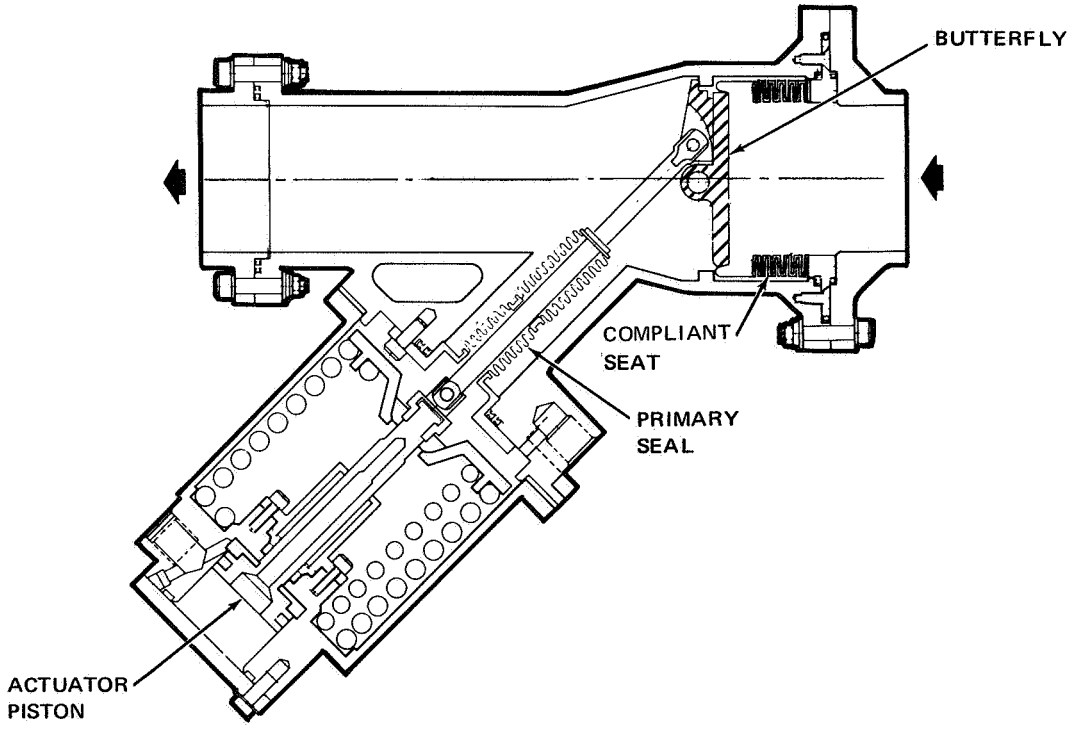

Figure 6. Conventional Butterfly Valve

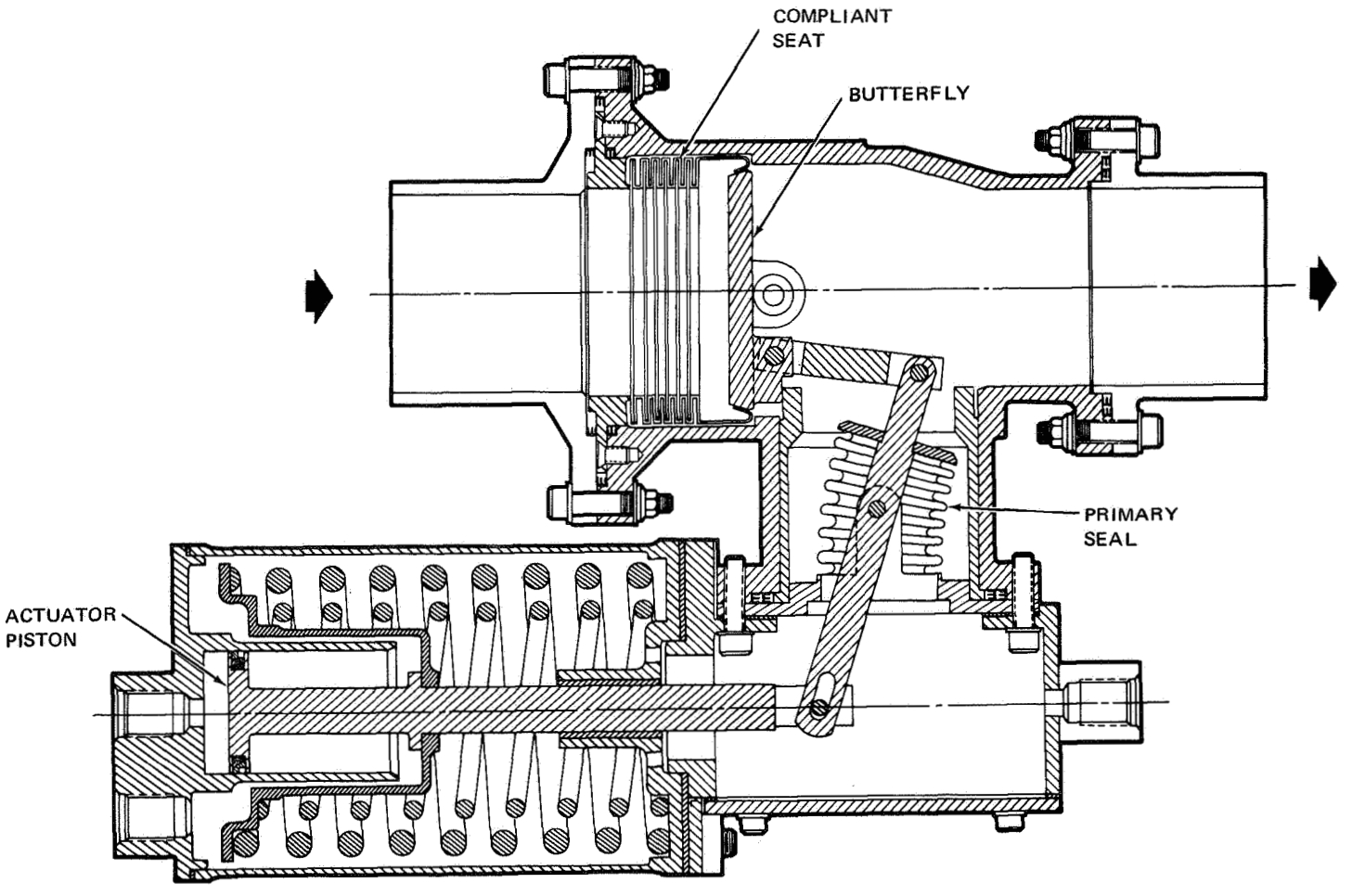

Figure 7. Offset Butterfly Valve

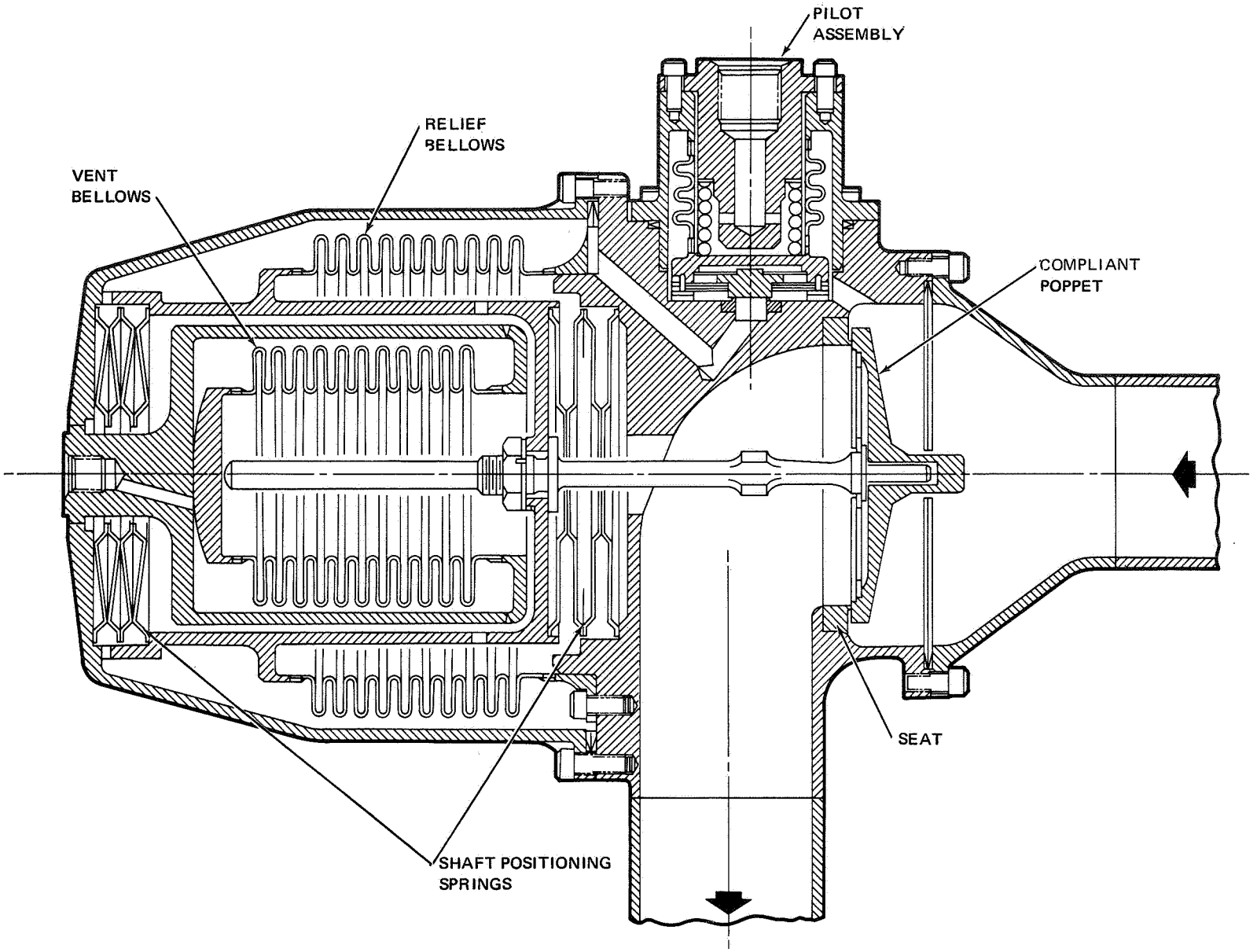

Figure 8. Bolted Vent and Relief Valve

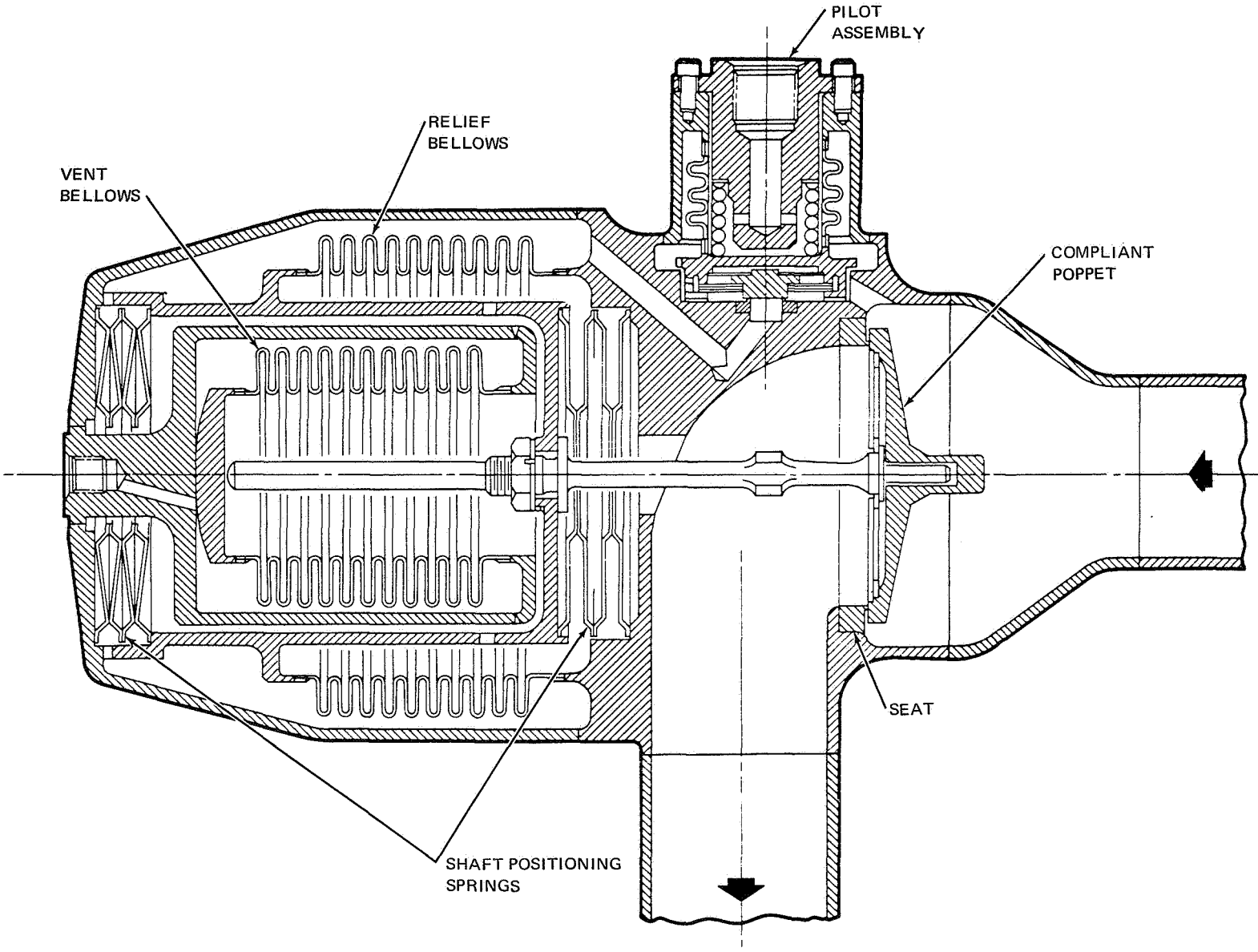

Figure 9. Welded Vent and Relief Valve

caused the poppet and poppet shaft of the valve to be considerably lengthened from the previous configurations. Several design variations were studied to optimize the tradeoff between the poppet overhang length and the valve flow losses induced by shortening the shaft length. A suitable compromise between these two conditions was attained in the configuration shown in Figure 4.

Another area in which further design effort was required as a result of this modification is the poppet attachment method. With the valve poppet on the upstream side of the closure and the actuator on the downstream side, the actuation shaft must pass through the closure. This made it desirable that the poppet be detachable from the shaft to permit valve assembly. A number of alternate poppet attachment schemes were considered, including threading the poppet onto the shaft, fastening the poppet onto the shaft with an external nut, and welding the poppet onto the shaft. The figure shows one method: i.e., threading the poppet onto the shaft and securing it with a tab washer that is locked by reaching through the valve closure.

A modification of this valve is shown in Figure 5, which uses a different sealing-force arrangement. In this valve configuration, the actuator piston is forced to the bottom of the actuator cylinder by large actuator springs. The entire poppet-shaft-and-piston assembly is therefore rigid and stationary when the valve is closed. Sealing forces for this configuration are provided from two sources. First, the compliant seat is compressed when the actuator piston bottoms, thus providing some sealing force. Secondly, the seat is flanged with the poppet sealing near the outer edge of the inlet face, providing an annular area under the back face of the flange on which the inlet pressure can act to load the seat against the poppet.

Figures 6 and 7 show the two of the configurations of butterfly shutoff valves that were considered during this study. Figure 6 portrays the more conventional piston-actuator drive arrangement, while Figure 7 shows the alternate rocking-linkage drive.

Figure 8 represents one of the poppet vent-and-relief valve concepts. The valve shown here is a version which can be disassembled in the field. An alternative design shown in Figure 9 is similar to this vent-and-relief valve, but features all-welded construction to minimize external leakage.

1.4 Preliminary Design Study

After the conceptual design studies were completed, a formal preliminary design review was held with NASA and, as a result of this review, six designs were selected from the 18 conceptual designs for further effort in the preliminary design phase of Task I. The six valve designs selected are the two poppet shutoff valves shown in Figures 4 and 5, the two butterfly shutoff valves shown in Figures 6 and 7, and the two vent and relief valves shown in Figures 8 and 9.

The preliminary design study included further effort in the areas of valve-leakage performance, loads and stresses, material selection, methods of fabrication and assembly, and quality control, cleaning, and handling of final valve assemblies. The preliminary designs included configurations of housings, static seals, closure elements, actuator mechanisms, drive shafts, bearings, and shaft seals.

The two butterfly shutoff valve concepts, while potentially identical in performance capabilities, differ in external configurations and in the methods used to apply actuation force to the butterfly disk. The results of the preliminary design study of these butterfly shutoff valves are given in Appendix C.

The preliminary design study results of the two selected poppet vent-and-relief valve configurations, Figures 8 and 9, are contained in Appendix D.

The results of the preliminary design effort for the two selected poppet shutoff valves shown in Figures 4 and 5 are essentially identical to the preliminary study efforts performed on the final design. These results are given in the following section.

1.5 Final Component Design

Based upon the results of the preliminary design effort, a final design review was held, and a single valve configuration was chosen by NASA for further preliminary design study. The valve configuration selected, shown in Figure 10, is a modification of the two poppet shutoff valves considered during the initial preliminary design study. The detailed results of the final design study on the poppet shutoff valve are presented in the following paragraphs. These results are representative of the preliminary design study effort for the two initial poppet shutoff valves analyzed during this phase of the study.

1.5.1 Description

The final fluorine shutoff valve design, 1T32095, shown in Figure 10, is a normally closed, pneumatically actuated poppet valve which weighs approximately 11.5 lb (5.2 kg). A weight breakdown on the valve is shown in Table 4. The valve-closing forces are provided by both the upstream fluorine pressure acting on the poppet and two helical springs. In the event of actuator failure, this valve will fail-safe in the closed position per the requirement of Table 1.

MDAC-WD research under Contracts NASw-1351 and NAS 3-11195 showed that none of the available plastic or rubber seal materials are satisfactory for use with fluorine. The closure of the valve, therefore, consists of a metal poppet that seals against a metal seat. The mounting of the valve seat on a complaint member isolates the closure from distortions of the valve body and allows it to absorb misalignment between the valve poppet and the seat. This arrangement also ensures the low leakage of the valve with fluorine-compatible materials.

The flat poppet and seat combination was selected because MDAC-WD experience with metal-to-metal seals has shown that low leakage can be maintained over a long operational life with this shape. To obtain leakage of 10^{-8} lb/sec (4.54×10^{-9} kg/sec) on a 2-in. (5.08×10^{-2} m) valve closure, a 2 μin. AA (5.08×10^{-8} m AA) surface finish is required. This fine surface finish can be obtained in commercial practice, but sliding or scuffing of the poppet on the seat during valve cycling must be minimized to maintain the finish.

Table 4

WEIGHT BREAKDOWN

Poppet assembly	0.95 lb	(0.43 kg)
Valve seat	1.22 lb	(0.56 kg)
Valve body	3.93 lb	(1.78 kg)
Inlet flange	1.86 lb	(0.84 kg)
Outlet flange	0.73 lb	(0.33 kg)
Actuator assembly	1.42 lb	(0.64 kg)
Fasteners and seals	1.43 lb	(0.65 kg)
Total	11.54 lb	(5.23 kg)

Leakage is also minimized by placing the poppet on the inlet side of the valve. This reduces the number of seals that are exposed to the working fluid during long-term space storage of propellant, assures fewer leak paths, and therefore reduces leakage.

Subcomponent and component testing was conducted by MDAC-WD as a part of the Contract NASw-1351 effort to determine the optimum approach to the selection of dynamic shaft seals for fluorine service. These tests included sliding-seal leakage and wear tests and cycle-stress tests of hydroformed metal bellows segments. Based on the results of these tests (Reference 2), a hydroformed metal bellows was selected as the dynamic seal for the poppet shaft of the proposed valve. When the valve poppet moves from closed to open, this metal bellows flexes, preventing LF_2 leakage from the valve body.

In keeping with the specified use of the valve as a flight-weight demonstration component, the valve has been designed so that both the poppet and the seat may be removed for inspection or refurbishment. With the poppet removed, it is possible to inspect the sealing surfaces of both the poppet and the seat. The seat may also be separated from the valve by removing the threaded fasteners around the outer flange.

The body of the valve, which incorporates the LF_2 flow passage, consists of two lathe-turned and welded components. Flange joints permit easy installation of the valve in the propellant system. Direct mounting of the valve inlet flange on a vehicle propellant tank is also made possible by this design arrangement.

The actuator assembly is made of aluminum to minimize the overhung weight and the total weight of the valve. Positive position indicators on the valve actuator, both valve open and valve closed, will provide reference data for demonstration testing.

1.5.2 Design Analysis

The final valve design (Figure 10) that was submitted to NASA for design approval at the completion of Task I was supported by analysis in areas that included sizing, flow performance, static actuation forces, main closure leakage, and valve response characteristics. Each of these analytical areas are discussed in the following paragraphs, and detailed calculations are given in Appendix E.

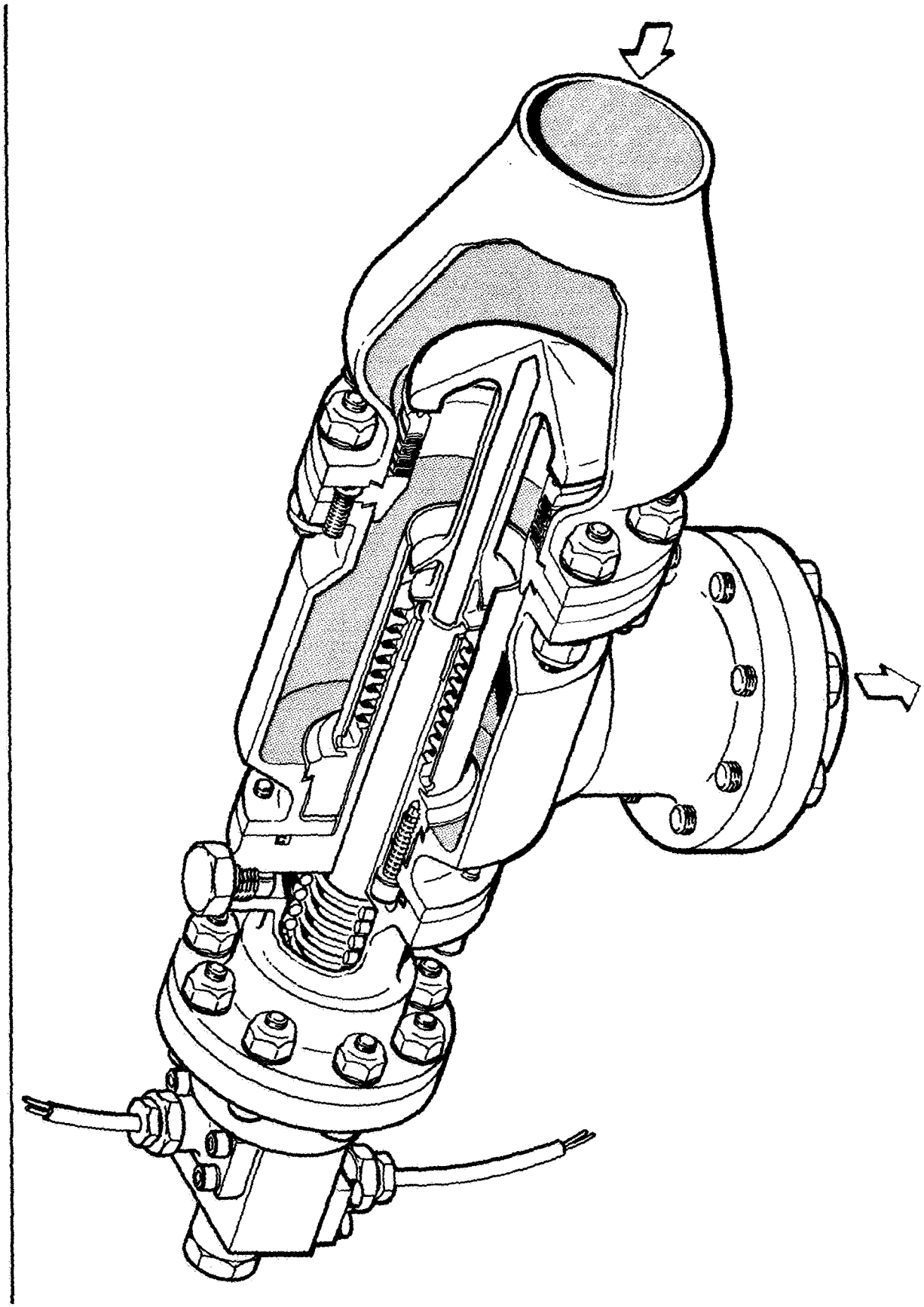

Figure 10. Final Poppet Shutoff Valve Design 1T32095

1.5.2.1 Valve Sizing

The analytical design of the valve consisted of the determination of the optimal sizes of the critical elements of the valve. In sizing these valve elements, a number of factors were considered. The overall valve size had been dictated by the line size and the flow rate specified in Table 1. The valve performance was also specified in terms of low leakage and pressure loss. Based on these primary inputs, an effective seat and poppet diameter of 2.10 in. (5.33×10^{-2} m) and a poppet stroke of 0.50 in. (1.27×10^{-2} m) were selected.

1.5.2.2 Flow Performance

The specified flow-rate and pressure-loss requirements were conservatively met by the final valve design. As shown in Figure 11, the pressure loss through the valve at the maximum rate flow of LF_2 at -320° F (22.2° K) has been calculated to be less than 5.4 psid (3.7×10^4 pascals). The flow-rate and pressure-loss calculations are based on the use of empirical constants derived from tests of similar valves. Table 5 summarizes the preliminary flow performance analysis.

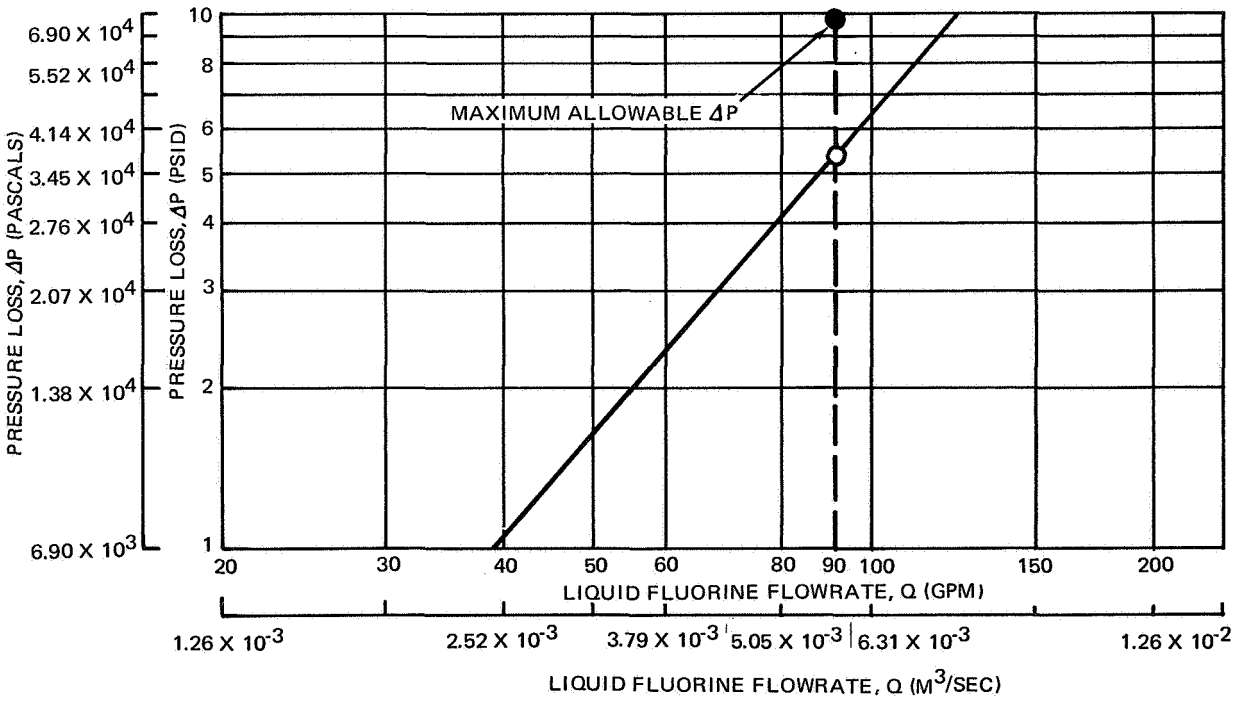

Figure 11. Pressure Losses vs LF_2 Flowrate

Table 5

PRELIMINARY FLOW PERFORMANCE SUMMARY

Pressure drop, psid (pascals)	< 5.3	(<3.7 x 10^4)
Rate flow, gpm (m^3/sec)	90	(5.68 x 10^{-3})
Temperature, °F (°K)	-320	(77.6)
Density, fluorine, lb/ft^3 (kg/m^3)	97	(1.55 x 10^3)
Flow velocity across seal, fps (m/sec) (valve fully open)	9.2	(2.8)
Equivalent flow area, $in.^2$ (m^2)	3.14	(2.03 x 10^{-4})
Resistance factor, K	6	

1.5.2.3 Static Actuation Forces

Figure 12 shows the static forces that act on the poppet of the proposed valve design. The net 500 lb (2.23 x 10^2 N) unbalanced force acts on the valve poppet in the closing direction, but this force varies with valve position. The valve actuator was designed to overcome this closing force with a safety factor greater than two. Therefore, if the specified nominal actuation pressure of 500 psi (3.45 x 10^6 pascals) is available, the actuator provides 1,040 lb (4.63 x 10^2 N) of force on the valve poppet shaft. If the actuation pressure falls to 250 psi (1.72 x 10^6 pascals), the actuator will still provide enough force to open the valve from any position. A summary of static actuation force parameters is given in Table 6.

1.5.2.4 Main Closure Leakage

Figure 13 shows the predicted LF_2 leakage through the shutoff valve as a function of the differential pressure across the closure. The leakage values shown are for a poppet and seat surface finish of 2 μin. (5.08 x 10^{-8} m) AA with a circular lay. With this selected configuration, a differential pressure across the closed valve of 100 psia (6.90 x 10^5 pascals) will result in a leakage of 10^{-8} lb/sec (4.54 x 10^{-9} kg/sec) of LF_2 through the closure. Increases in differential pressure will increase the apparent seat stress and cause a net decrease in valve leakage as shown in the figure; decreases in differential pressure will also reduce the leakage because of reduced potential across the seal. A further discussion of the mechanism of leakage through metal-to-metal seals is given in Appendix A.

Liquid fluorine leakage through the valve for a range of surface finishes is shown in Figure 14 at a differential pressure of 100 psid. Based on the leakage requirement of 10^{-6} lb/sec (4.54 x 10^{-7} kg/sec) LF_2 leakage, a circular lay, 2-μin. -AA (5.08 x 10^{-8} m AA) surface roughness has been chosen as the design finish for the poppet and seats. This finish is readily obtainable in the present state of the art, and it will provide an order-or-magnitude safety factor on the required leakage. A summary of the parameters affecting main closure leakage is given in Table 7.

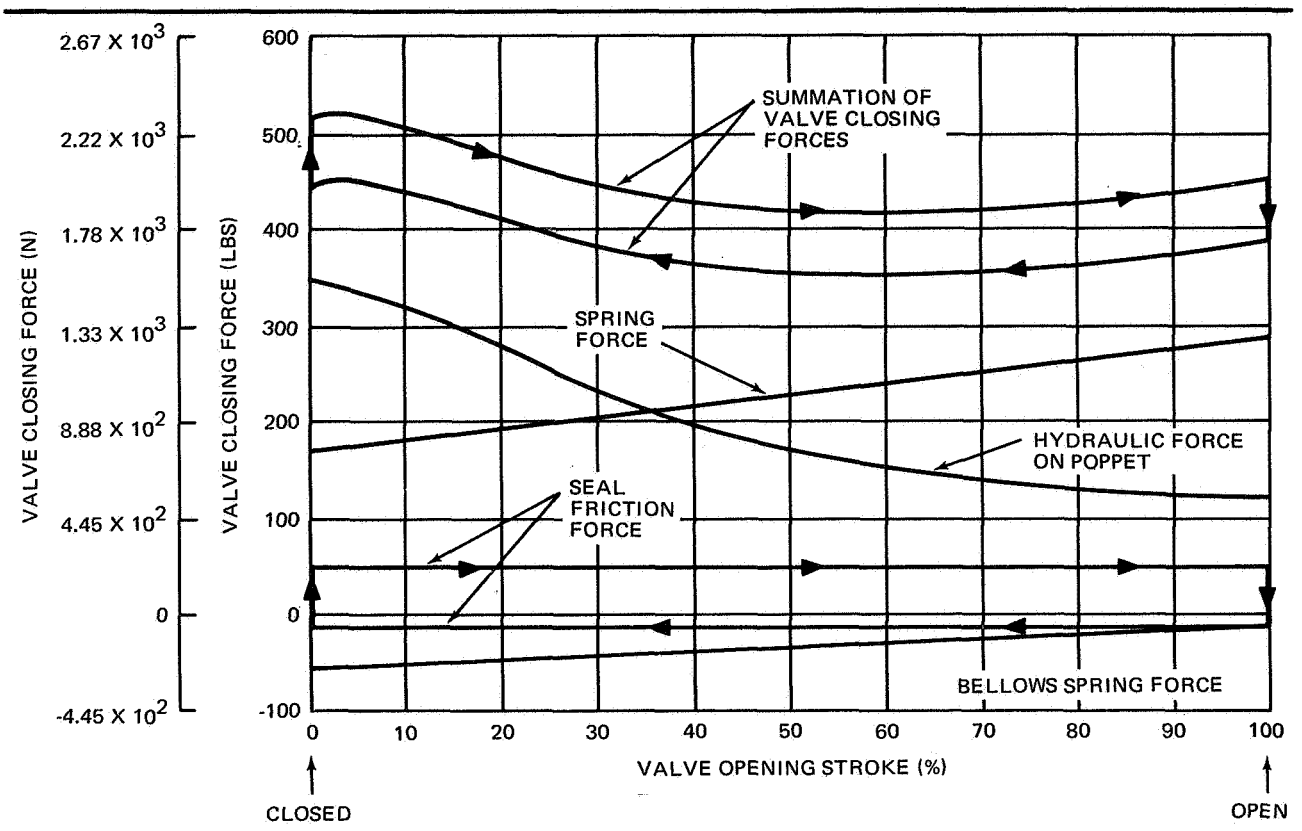

Figure 12. Typical Valve Closing Forces

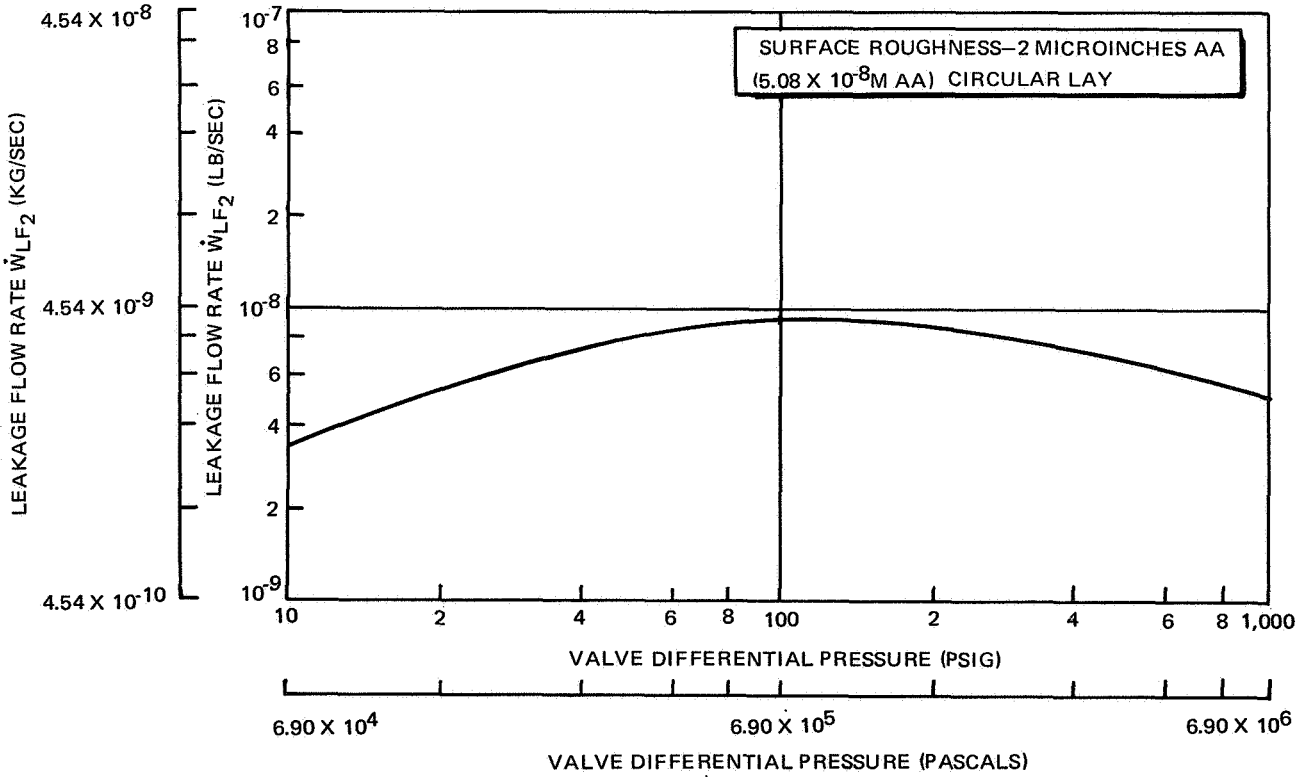

Figure 13. Estimated LF_2 Leakage vs Differential Pressure

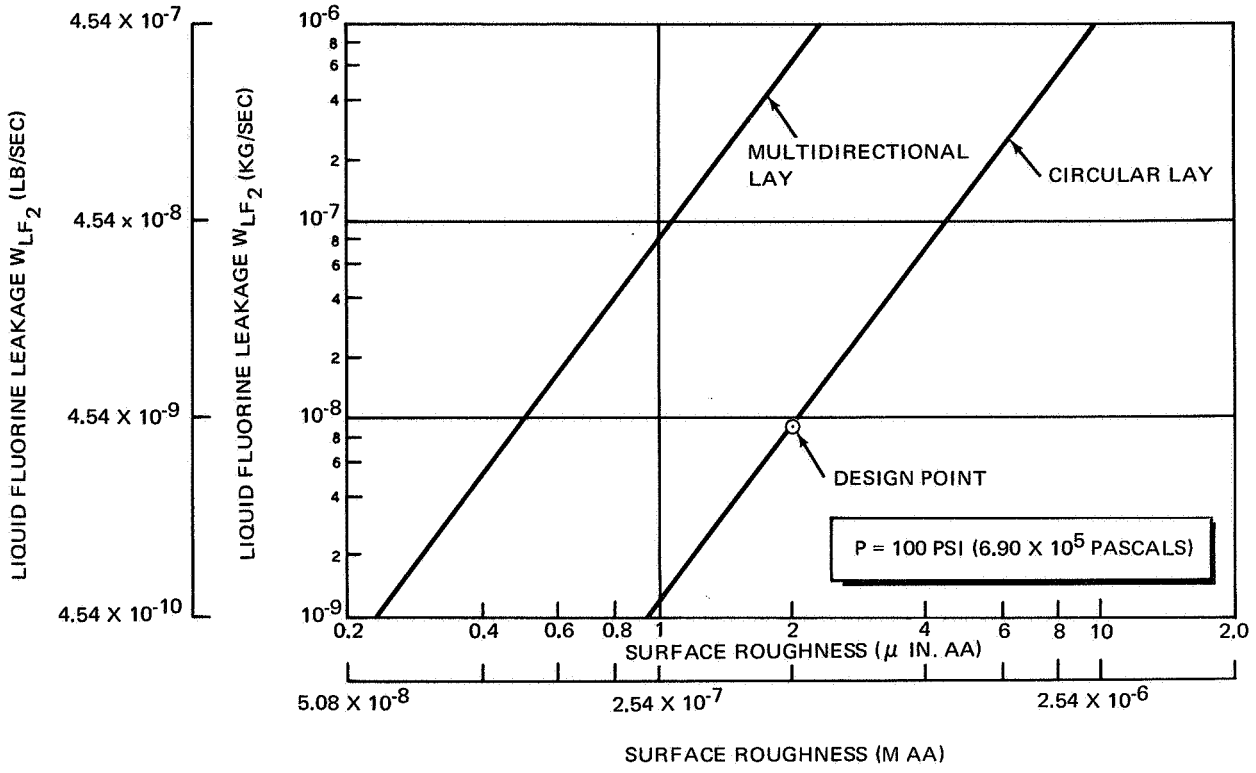

Figure 14. LF_2 Leakage vs Surface Roughness

Table 6

STATIC ACTUATION FORCE PARAMETERS SUMMARY

Pneumatic operating pressure, psig (pascals)		
Nominal	500	(3.45×10^6)
Minimum	250	(1.73×10^6)
Actuator pressure area, in.^{2} (m^2)	2.07	(1.33×10^{-3})
Shaft seal bellows		
Inside diameter, in. (m)	0.90	(2.29×10^{-2})
Outside diameter, in. (m)	1.26	(3.20×10^{-2})
Effective area, in.^{2} (m^2)	0.92	(5.94×10^{-4})
Spring rate, lb/in. (N/m)	147	(2.63×10^3)
Material	Inconel 718	
Springs		
Preload, lb (N)	170	(7.71×10^1)
Spring rate, lb/in. (N/m)	230	(4.11×10^3)
Material	CRES 316	
Poppet pressure area, in.^{2}	3.45	(2.22×10^{-3})

Table 7

MAIN CLOSURE LEAKAGE PARAMETERS SUMMARY

Rated differential pressure, psid (pascals) (valve closed)	100	(6.90×10^{5})
Mean seat diameter, in. (m)	2.1	(5.34×10^{-2})
Seat width, in. (m)	0.010	(2.54×10^{-4})
Seat area, $in.^2$ (m^2)	0.066	(4.25×10^{-5})
Apparent seat stress, psi (N/m^2)	8,000	
Materials poppet/seat	Inconel 718/ CRES A286	
Surface roughness, μin. (m) (circular lay)	2AA	(5.08×10^{-8}AA)
Flatness, in. (m) (PTV wave height)	10	(2.54×10^{-7})
Poppet/seat angular misalignment compensation, degrees (radians)	1	(1.75×10^{-2})
LF_2 Leakage, lb/sec (kg/sec)	10^{-8}	(4.54×10^{-9})

2.0 TASK II: CONTAMINANT EFFECTS ON FLUORINE FEED SYSTEMS

2.1 Introduction

An engineering study and a field survey were conducted to determine the amount and type of contaminants which would be expected to be present in a typical fluorine feed system. Particular attention was given to the potential concentration of moisture and its effects on corrosion rate and explosive hazard to the overall system. The analytical effort was followed by a series of tests that were selected to verify and supplement the analytical effort. The original program was to have included the following tests:

1. Corrosion rate measurements of 6061 and A356 aluminum at an aqueous hydrogen fluoride level equivalent to the maximum concentration predicted from the analytical study.

2. A test to establish structure, growth rate, and concentration of ice formed from helium gas containing moisture levels of -70, -80, and -90°F dew point (D. P.) (216.5, 210.9, and 205.4°K).

3. A series of tests to evaluate the explosive hazard of ice in various LF_2 environments.

From the analytical study it was determined that the maximum predicted concentrations of aqueous hydrogen fluoride in LF_2 would normally be less than the 0.3% (volume) level which had been tested previously on Contract NASw-1351. Because corrosion rate testing at such a low level of hydrogen fluoride would be of limited value to the overall program, a change was made in the testing program. This change resulted in the addition of a test designed to measure the solubility limit of hydrogen fluoride in LF_2 and the deletion of the aqueous hydrogen fluoride corrosion tests. The ice formation and hazards tests were conducted as schedule in the original plan.

2.2 Summary and Conclusions

2.2.1 Contaminant Study

The analytical study was made in conjunction with a field survey of contamination in conventional liquid oxygen feed systems and purity of field deliveries of bulk LF_2. A representative value of hydrogen fluoride in delivered LF_2 was established as the first step of this effort. This analysis indicated that 98% of all bulk LF_2 delivered for rocket propellant use would likely have an hydrogen fluoride level of less than 0.172% by volume (0.086% by weight). A series of typical purge and pressurization cycles was then studied to determine the amount of moisture that would be added to the system under various conditions and how this moisture would change the level of hydrogen fluoride contamination.

A representative number for these operations indicated that the percent of hydrogen fluoride would increase about 3×10^{-5}% by weight each time the fluorine was detanked to a system which had been exposed to the atmosphere. Therefore, the value of hydrogen fluoride contaminant increase after

10 cycles of neither purging or pressurization would be only $3 \times 10^{-4}\%$ by weight, and it was concluded that the moisture in the pressurant gases is not significant from the standpoint of gross moisture addition to the system.

The moisture added to the fluorine from residual moisture retained in the skin of the propellant tank was estimated to be much smaller than the moisture contained in the pressurant gases, and therefore was not considered to make a significant contribution to gross moisture addition. It can be concluded that limitations on pressurant moisture levels will be based on localized icing conditions and not on the generation of corrosive hydrogen fluoride in the flight-type vehicle.

A field survey was made of feed-line contamination at both the Kennedy Space Center and at the Vandenberg launch facility. The liquid oxygen fill-line filters were back flushed after the filter had been in service for more than one launch operation. Both sides of the filters were examined and found to have particles that were larger than 2,500 microns (2.5×10^{-3} m) in size. In all cases, the vehicle tank side of the filters was found to contain a larger quantity of particulate than did the ground support equipment (GSE) side of the filter. This study indicates that a service-type flourine filter will be satisfactory for filtering the propellant being loaded into the vehicle tank but that the present liquid oxygen clean standards and procedures will not be acceptable for LF_2 tankage because of the effects of the large particles on the all metal sealing surfaces used on components of the LF_2 system.

A third study effort was completed by Pratt and Whitney Aircraft Co., West Palm Beach, Florida to determine:

1. The particle size limitation of the LF_2 rocket engine (if different than the requirements for a conventional liquid oxygen engine).

2. The filter size required for use on the LF_2 engine.

The results of this study indicated the following:

1. The LF_2 engine will be similar to the liquid oxygen engine with respect to contaminant tolerance.

2. Very little data exist on the tolerance of liquid oxygen engines to contaminants.

3. Methods for evaluating the tolerance of engines to contaminants are standardized for the gas turbine engine industry, and these methods could serve as guidelines for similar work within the rocket engine industry.

2.2.2 Hydrogen Fluoride Solubility Tests

A series of hydrogen fluoride solubility tests were conducted using the etched glass (EG) method described in Reference 2. It was found that the measurement of the solubility limit of hydrogen fluoride in LF_2 varies with the filter size used to remove the solid hydrogen fluoride particles from the

test solution. These tests showed that the solubility limit is lower than the generally accepted value and approaches zero (less than 0.01% weight) and that hydrogen fluoride will only exist in LF_2 as frozen particles.

2.2.3 Ice Formation Tests

A series of ice formation tests were conducted using gaseous helium with various levels of moisture contamination in the gases. The rate of ice formation was found to increase with moisture content and decrease with flow velocity in both metal and glass tubing; this rate was found to be similar for both the glass and stainless steel tubing under similar test conditions.

2.2.4 Ice Reaction Tests

A series of ice reaction tests was conducted to evaluate the potential hazards that could occur from ice formation of block-type and frost-type ice under steady-state LF_2 flow conditions and under high-velocity LF_2 impact conditions. No potentially explosive conditions were found to occur in any of the tests conducted although there were indications that a rise in system pressure may occur from the chemical reaction which occurs when the LF_2 contacts the ice formations. These data indicate that water ice is not potentially hazardous in a LF_2 feed system, and only the usual design constraints for plugging or physical damage to the operating parts caused by ice buildup need to be applied to the LF_2 systems.

2.3 Technical Discussion

2.3.1 Contamination Study

The analytical portion of this task consisted of three separate study efforts.

2.3.1.1 Moisture Addition Study

An investigation was conducted to determine the contamination of the cryogenic propellant systems of the MDAC-WD Thor booster and the Saturn S-IVB stage. This investigation included visiting facilities at West Palm Beach and Cape Kennedy, Florida. A review was made of the methods and techniques used at the launch areas to measure and to limit the contaminants in the vehicle tanks, both before and after propellant loading. It was found that the moisture content in the propellant tanks for the Thor booster and the Saturn S-IVB stage is kept below a specified limit of 200 ppm by purging the tanks with nitrogen or helium gas having a moisture level lower than 200 ppm.

A study to determine the moisture content in bottled pressurization and purge gases was conducted. The available specifications on helium and nitrogen do not limit the moisture content of bottled helium. Investigation shows that drying of helium by molecular sieves and other devices will probably be needed to maintain the total moisture content of the pressurant gas at a level that will prevent freezing of mechanical parts of the system. This level is presently limited to 2 ppm of moisture. This type of drying is now state of the art and is presently used as a normal procedure at the engine test sites and Cape Kennedy.

A study was completed to determine the maximum possible hydrogen fluoride contamination that could be anticipated in LF_2 stored at a typical test site. A statistical evaluation of 14 batches of LF_2 showed delivered fluorine to have a mean hydrogen fluoride content of 0.048% (by weight) and a standard deviation of 0.019% (by weight). Therefore, if the hydrogen fluoride is normally distributed from batch to batch, 98% of all delivered liquid fluorine will contain less than 0.086% (by weight) of hydrogen fluoride. These figures are based on the analysis sheet supplied with LF_2 deliveries from the propellant supplier.

An additional study indicated that each time a quantity of LF_2 is taken from one sealed system and flowed to another, additional water content is added to the fluorine. This water reacts with the LF_2 to produce hydrogen fluoride, gradually raising the hydrogen fluoride level of the fluorine. There are two sources which increase the water content in the typical fluorine system. The first is the moisture content of the atmosphere in the tank into which the fluorine is being introduced. The second source of moisture is the molecular film of water vapor that adheres to the surface of the metal tank into which the fluorine is introduced. An analysis was made to evaluate the magnitude of these two effects. These results show that the moisture on the skin surface of a tank constitutes a very small amount (less than 2×10^{-4} lb (9.08×10^{-5} kg) of water for a tank with a surface area of 300 ft^2 (2.79×10^1 m^2) of actual water, and can be neglected for calculation of formation of hydrogen fluorine in liquid fluorine tanks. Also, it was found that the normal upper limit of moisture in vehicle propellant tanks, i.e., 200 ppm, would result in the formation of only a relatively small amount of hydrogen fluoride. This small amount of hydrogen fluoride would not normally be significant from a corrosion standpoint during the short time of exposure in a flight-type propellant tank. Appendix F provides further details of this analysis.

2.3.1.2 Field Survey of Service Filters

A survey was made to determine the type of contamination which is being filtered by typical oxidizer fill line filters in normal service. Results were obtained from a filter in service at the Kennedy Space Center and Vandenberg Air Force Base. The filter was used in liquid oxygen service and was located in the propellant fill line. Because the loaded propellant is off loaded through the same filter (in the reverse direction), the results obtained yield typical values of contaminant in the storage tank complex (forward direction) and in the vehicle propellant tank (reverse direction). The samples were taken during routine filter servicing by back flushing in both directions and collecting the freed particles with standard inspection filters. The measured particle count is shown in Table 8.

The spectrographic analysis of the sample taken at Vandenberg Air Force Base is shown in Table 9 and the Kennedy Space Center samples are shown in Table 10. The breakdown of these specimens indicate a makeup of contaminants consisting of:

1. White cotton thread
2. Krytox grease
3. Aluminum chips
4. Stainless steel chips
5. Silver brazing remnants
6. Copper chips

Table 8

LIQUID OXYGEN CONTAMINANT PARTICLE DISTRIBUTION FOR TYPICAL THOR LAUNCH

Location	Number of Particles	Particle Size (microns) (10^{-6} m)
Storage tank Side	1	>2500
	5	700 to 2500
	31	175 to 700
Vehicle tank Side	4*	>2500
	145	700 to 2500
	775	175 to 700

*Includes one particle with a 5/16 in. (8,000 microns) (8×10^{-3} m) maximum dimension.

2.3.1.3 Rocket Engine Contaminant Tolerance Study

The Pratt and Whitney Aircraft Company conducted a brief study to identify potential areas of sensitivity to propellant contamination in a typical LF_2 rocket engine. For this study, a fluorine/hydrogen version of the RL10A-3-3 engine (the RL10A-3-3F, a relatively minor modification) was selected as a typical upper-stage engine. No effort was made to define contaminant level; engine requirements were considered independently.

Experience with RL10 oxygen/hydrogen engines was used to establish the base for contaminant tolerance. Model specifications for RL10 engines require that the oxidizer supplied at the engine inlet contains no particles larger than 175 microns (1.75×10^{-4} m). There is evidence that RL10 engines have operated successfully on propellants containing contaminants of larger sizes. This has been documented for both the engine fuel system and oxidizer system, but for only a limited number of tests. Additional testing, on a statistical basis, would be required to provide definition of limits. Therefore, until such demonstrations are accomplished, it is assumed that specification requirements have been observed, and that the acceptable upper-limit particle size is 175 microns (1.75×10^{-4} m). Based

Table 9

RESULTS OF SPECTROGRAPHIC ANALYSIS
VANDENBERG AFB

Sample Description	Elements			
	Principal	Major	Minor	Trace
Upstream Side	Fe	Ca, Br Si, Mn	Mg, Zn, Sn	Ag
Black				
Dull copper	Cu	Sn	Ni, Zn, Pe	Mg, Fe, Ag, Si
Shiny	Fe	Cu, Ni, Br	Mn, Sn, Si Mo, Pb	Mg, Al, Ag
Mixed particles		Ti, Zn	Si, Mn, Mg B, Fe, Al	Ca, Cu, Cr
Brown	Fe		Si, Mg, Mn Cr	Cu, Al, Zm
Downstream Side				
Mixed particles	Fe	Al, Cu	Mn, Mg, Mo, Ag, Ti, Ni, Cr	Si, Zn, Cd, Ca
Aluminum shaving	Al	Cu	Si, Mg, Fe, Cr	
White (paper-like)			Si, Mg	Al
Green-black	Fe		Si, Ni, Cr, Cu, Ti, Al	B, Mg
Aluminum appearance	Al	Cu, Cd	Fe, Si, Mg, Mn, Cr	
Resin				Mg, Ca

Table 10

RESULTS OF SPECTROGRAPHIC ANALYSIS
KENNEDY SPACE CENTER

Sample Description	Elements			
	Principal	Major	Minor	Trace
Upstream Side				
Black	Organic Material			
Dull copper	Cu, Ag	Cd, Zn	Ni, Cr, Fe	
Shiny			Cd	
Mixed particles	Fe, Ag	Al, Cu, Zn, Cd	Si, Mn, Mg	B, Sn
Brown			Si, Mg	Cu
Downstream Side				
Mixed particles	Fe	Al, Cu	Mn, Mg, Mo, Ag, Ti, Ni, Cr	Si, Zn, Cd, Ca
Aluminum shaving		Al, Cu	Si, Mg, Mn, Fe, Mo, Cr	
White (paper-like)		Zn	Si, Fe, Mg, Sn	Al, Cu
Green-black		Fe, Cr	Si, Sn, Pb, Cu, Cu, Zn, Ti, Al	
Aluminum appearance	Al	Cu	Fe, Si, Mg, Ag, Ni, Co, Cr	Mo, Zn, Ti
Resin			Fe	Mg, Cu, Cr
Plastic appearance	Fe	Al, Cu	Mn, Mg, Mo, Ag, Ti, Ni, Cr	Si, Zn, Cd Ca

on this study, it was concluded that a fluorine/hydrogen RL10 derivative engine would have the same tolerance to particulate contaminants in the oxidizer as does the basic oxygen/hydrogen system. At this time the limit on particle size must be set at 175 microns (1.75×10^{-4} m). However, there are indications that this limit is extremely conservative.

If studies to define particle sizes and concentrations that may be present in LF_2 show that particles larger than those which the engine will accept may typically be encountered in vehicle oxidizer systems, it will be necessary to either subject the engine to further development to increase its tolerance to contaminants, or filter the oxidizer in the vehicle line upstream of the engine.

If a filter is used in the vehicle oxidizer line, compensation for pressure reductions at the engine inlet caused by partial plugging can be accomplished down to the predicted cavitation limit of the pump, 4.5 psi (3.10×10^4 pascals) above vapor pressure, or 19 psia (1.31×10^5 pascals) at a propellant temperature of 153°R (85.4°K). The adjustment provided in the oxidizer flow-control valve of the RL10A-3F engine for vehicle propellant utilization could be employed, but this would compromise ability to respond to vehicle demands. Therefore it would be recommended that a separate flow adjustment be added if large changes in filter pressure drop are anticipated.

Experience in development of aircraft jet engines, where demonstration of contamination tolerance is required, has shown that the susceptibility of components to deterioration because of fluid contamination cannot readily be established through analysis. It is therefore necessary to base judgment on experience for a particular type component. This implies that evaluation must be based on specific designs.

A review of available jet engine data did not reveal any information that was directly applicable to rocket engines. Therefore, it was necessary to rely solely on oxygen/hydrogen experience with respect to particulate contaminants. It was assumed that this should be applicable to the case of a fluorine engine if component differences were not significant. Expected differences between the oxygen/hydrogen and fluorine/hydrogen engines were analyzed, and their effects were considered. The effect on engine performance of inlet pressure reductions that might result from use of a full-flow filter upstream of the engine to provide protection was evaluated.

Techniques applied in the design of aircraft jet engine components to assure tolerance to contaminants can be applied to rocket engines if further rocket engine contaminant tolerance development is necessary.

2.3.2 Hydrogen Fluoride Solubility Test

There are no accurate measurements available of the solubility of hydrogen fluoride in liquid fluorine. Previous work reported in Reference 7 gives the solubility as less than 0.5 mole % at -320°F (77.6°K). Based on observations in the laboratory it was believed that the true solubility is in the neighborhood of 0.2 mole %. It had been observed that gaseous fluorine containing more than 0.2% by volume hydrogen fluoride shows a visible precipitate of hydrogen fluoride crystals when condensed to liquid. (Mole

percent equals percent by volume in gas phase.) This observation was confirmed by personnel of Allied Chemical Research for condensation at -320°F (77.6°K) (LN_2 temperature).

The etched glass method was used for investigating the equilibrium solubility of solid hydrogen fluoride in LF_2 at two temperatures: -320°F (77.6°K) (liquid nitrogen temperature) and -306°F (85.4°K) (LF_2 boiling point).

The apparatus is depicted in Figure 15. The tube at the left of the drawing is the stainless steel saturator which connects to a calibrated glass receiver through an eductor tube equipped with stainless steel filter and through a diaphragm valve. The valve is connected in reverse of the normal flow pattern to limit liquid downstream and the entire line leading from the saturator to the receiver slopes downward at approximately a 15° (2.62×10^{-1} radians) angle.

The procedure for determining solubility is as follows. The apparatus is first cleaned and dried. The calibrated glass receiver is then weighed with an analytical balance to the nearest 0.1 mg (1.0×10^{-7} kg). The system is assembled as shown in the figure and evacuated. The diaphragm valve is closed and liquid nitrogen poured into the Dewar vessel to the approximate coolant level shown. Fluorine gas containing a concentration of 0.5 to 0.6 mole % hydrogen fluoride in the fluorine is used.

After condensing the mixture, it is allowed to stand for a minimum of 10 min to allow completion of the precipitation of the hydrogen fluoride and to assure thermal equilibrium with the liquid nitrogen bath. Meanwhile a valve connecting the receiver to the manifold is closed and the receiver left under vacuum. The diaphragm valve is then opened carefully and the saturated fluorine aspirated from the saturator through the filter and into the calibrated glass receiver. A slight pressure of helium is applied to the saturator to force the last traces of liquid over. After allowing a few minutes for drainage, the volume of the fluorine saturated with hydrogen fluoride in the calibrated receiver is measured.

The concentration of hydrogen fluoride in the resulting liquid sample was determined by the etched glass method. This procedure was described in the Final Report for the NASw-1351 program (Reference 2) and involves evaporation of the fluorine at -320°F (77.6°K) leaving the nonvolatile hydrogen fluoride behind. The hydrogen fluoride is allowed to attack the glass forming volatile silicon fluoride which is pumped off. The hydrogen fluoride content is calculated from the loss of weight of the glass receiver. The determinate errors involving estimation of sample volume and weighing should not exceed 4% in total.

A total of four test runs were conducted at -320°F (77.6°K) and a fifth run made at -306°F (85.4°K) using the filter shown on Figure 15. The results of these runs are shown in Table 11.

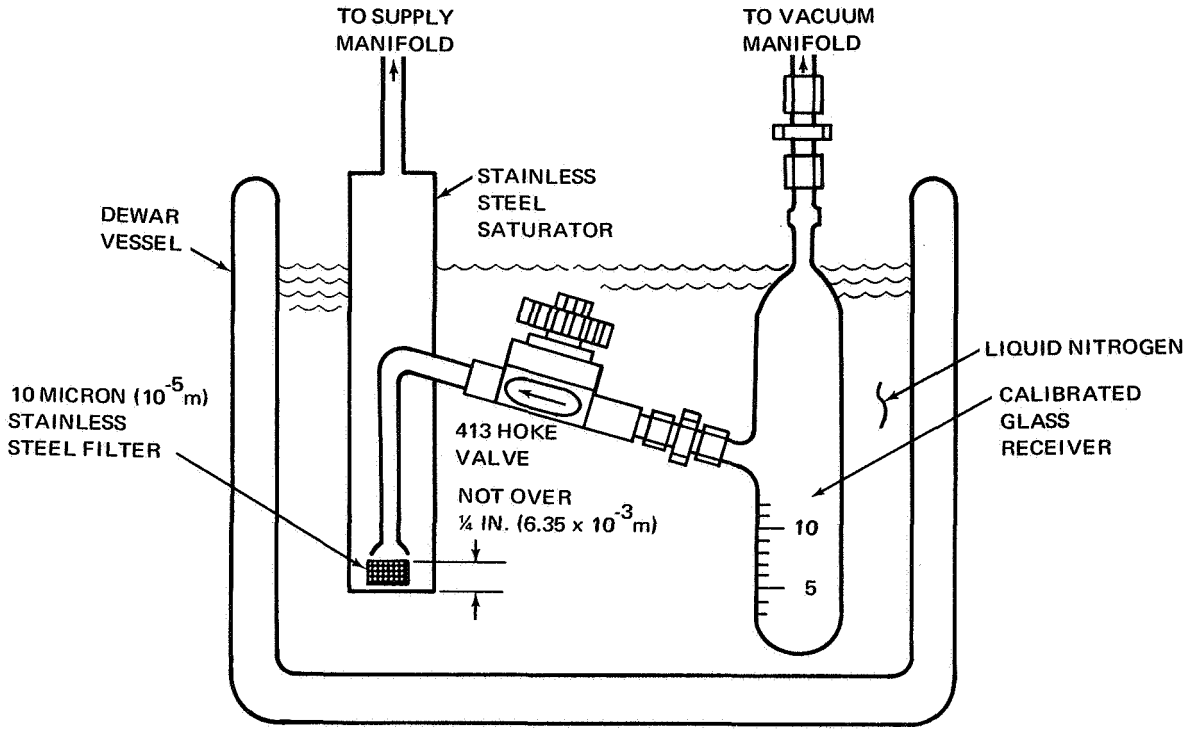

Figure 15. HF Solubility Test Apparatus

Table 11

HYDROGEN FLUORIDE SOLUBILITY LIMIT TESTS

Run No.	Temperature	Solubility Limit	
		Weight Percent	Volume Percent
1	-320°F (77.6°K)	0.007	0.014
2	-320°F (77.6°K)	0.013	0.026
3	-320°F (77.6°K)	0.028*	0.056*
4	-320°F (77.6°K)	0.009	0.018
5	-307°F (84.9°K)	0.007	0.014
Average		0.009	0.018

*This reading is questionable and is not included in the average. The reading was made by weighing the pieces of the glass container which was broken during the test.

tests were conducted. The object of the test series was to determine the ice buildup rate as a function of flow velocity, total moisture content of the helium, and the type of material used in the construction of the flow tubing. Tubing material determination was necessary to verify the validity of using glass tubing in the ice reaction tests to permit monitoring the tests with a high-speed movie camera. The apparatus for this test series is shown schematically in Figure 16.

The test plan specified a total of nine helium bottles which contained gases at three different controlled levels of moisture content. The three levels were gases with dew points (D. P.) of -70°, -80° and -90°F (216.5°, 210.9°, and 205.4°K). This range of dew points was selected as being representative of the variation which would be expected when using undried Bureau of Mines, Grade A, helium.

A search was conducted to obtain nine bottles of helium at the desired moisture level from all local sources including the MDAC-WD in-plant bottle farm. It was found that although the Grade A helium is not limited to moisture level, no helium with a higher dew point than -90°F (205.4°K) was available. To provide samples for testing, a supply of wet helium was synthesized by adding distilled water to helium, and then mixing this wet helium with dry helium to provide test gases with the desired moisture level. This method met with only limited success because the moisture added to the helium would not disperse evenly enough to provide a stable moisture level when mixed with the dry gas. It was found necessary to mix the gases at approximate mixture ratios, analyze each test bottle with a CEC moisture

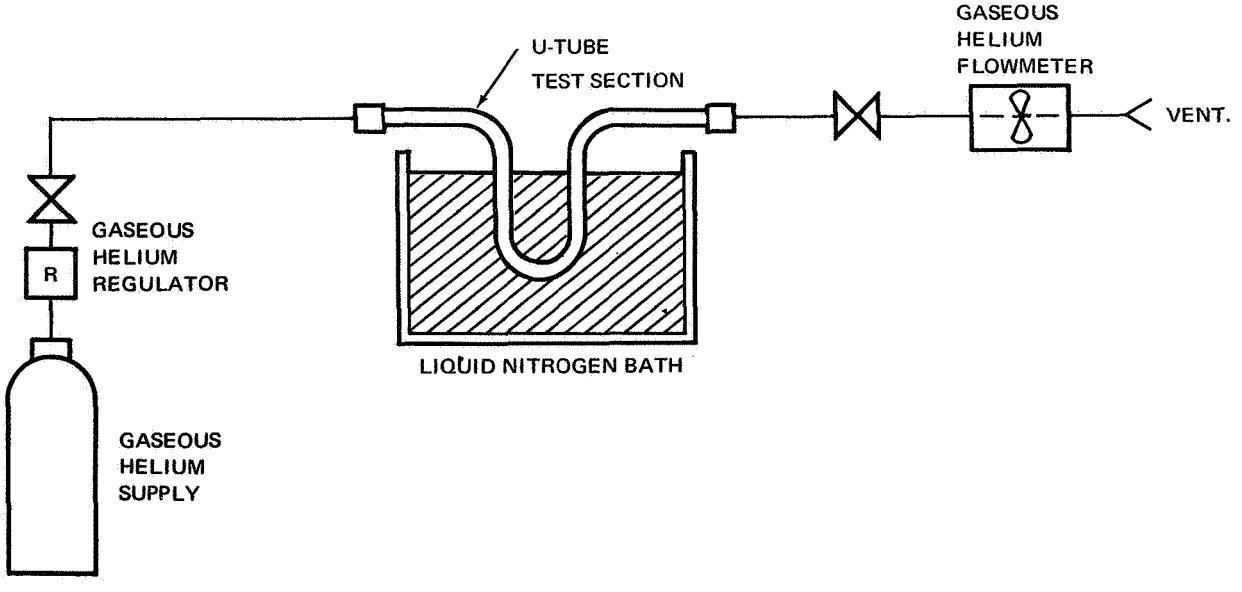

Figure 16. Helium Moisture Test Installation

A single test was then conducted to evaluate the effects of the filter size used in the basic hydrogen fluoride solubility tests. The basic tests were conducted using a filter rated at a nominal 4 microns (4×10^{-6} m), or 11 microns (1.1×10^{-5} m) absolute, between the hydrogen fluoride mixing chamber and the glass reaction tube. With that filter size a value of less than 0.01% by volume was obtained for the solubility of hydrogen fluoride in LF_2. The recheck was made using a filter rated at a nominal 25 microns (2.5×10^{-5} m), or 68 microns (6.8×10^{-5} m) absolute. Using this filter, a value of 0.015% by volume was obtained for the solubility. These results indicate that 30 to 35% more of the hydrogen fluoride which was formed was able to enter the gas reaction section. This would indicate the approximately one-third of the hydrogen fluoride particles which were formed in the mixing section were between 11 microns (1.1×10^{-5} m) and 68 microns (6.8×10^{-5} m) in size and that if a filter smaller than the 11-micron (1.1×10^{-5} m) element were to be used, the apparent solubility limit of hydrogen fluoride in LF_2 would continue to approach a value of zero.

It should be noted that the larger particles which entered the test chamber with the larger filter were sufficiently large to give the LF_2 a very dirty appearance which was readily detectable visually.

2.3.3 Ice Formation Tests

To evaluate the growth rate and resultant explosive hazard potential of the moisture contained in a wet pressurant gas, a series of helium moisture monitor, and then cross plot the final data to allow for this variation in dew points. The dew points measured by actual analysis are shown in the results of these tests in Table 12 and Figures 17 and 18. The percentage of moisture trapped was obtained by comparing the weight of moisture trapped with the theoretical moisture contained in each gas sample.

The measured weight of moisture trapped was determined by weighing the U-tube test section on a precision laboratory balance scale both before and after the test run. The weight gain of the test section was assumed to be due to the increase in moisture collected in the test section.

To minimize the inclusion of atmospheric moisture in the test apparatus, an all metal pressure regulator was used for all tests in this series and the complete test setup was evacuated with a vacuum pump at the start of each test run. Each individual bottle was analyzed with the CEC moisture monitor to evaluate the moisture level of the helium supply gases and the value obtained from these readings used to compute the percent of moisture trapped.

The first test result indicated that more moisture was collected in the trap than was supposed to be in the complete gas supply. Therefore the monitoring method was revised to make a separate moisture reading of each test bottle of gas at the start of each test run.

Table 12

HELIUM MOISTURE TESTS

Run Number	Dew Point (°F) (°K)	Flowrate (cfm) (m^3/sec)	Material	Moisture Trapped (%)
1	-81 (210.5)	1 (4.72×10^{-4})	Metal	70.0
2	-76 (213.2)	1 (4.72×10^{-4})	Metal	96.5
3	-76 (213.2)	1 (4.72×10^{-4})	Glass	92.0
4	-62 (220.9)	5 (2.36×10^{-3})	Metal	50.0
5	-76 (213.2)	5 (2.36×10^{-3})	Metal	12.0
6	-69 (217.1)	5 (2.36×10^{-3})	Metal	40.0
7	-81 (210.5)	10 to 15* (4.72×10^{-3} to 7.08×10^{-3})	Metal	0.0

*The helium regulator was not capable of maintaining the specified 10 cfm (4.72×10^{-3} m^3/sec) the timed heading indicated a flowrate varying between 10 and 15 cfm (4.72×10^{-3} to 7.08×10^{-3} m^3/sec).

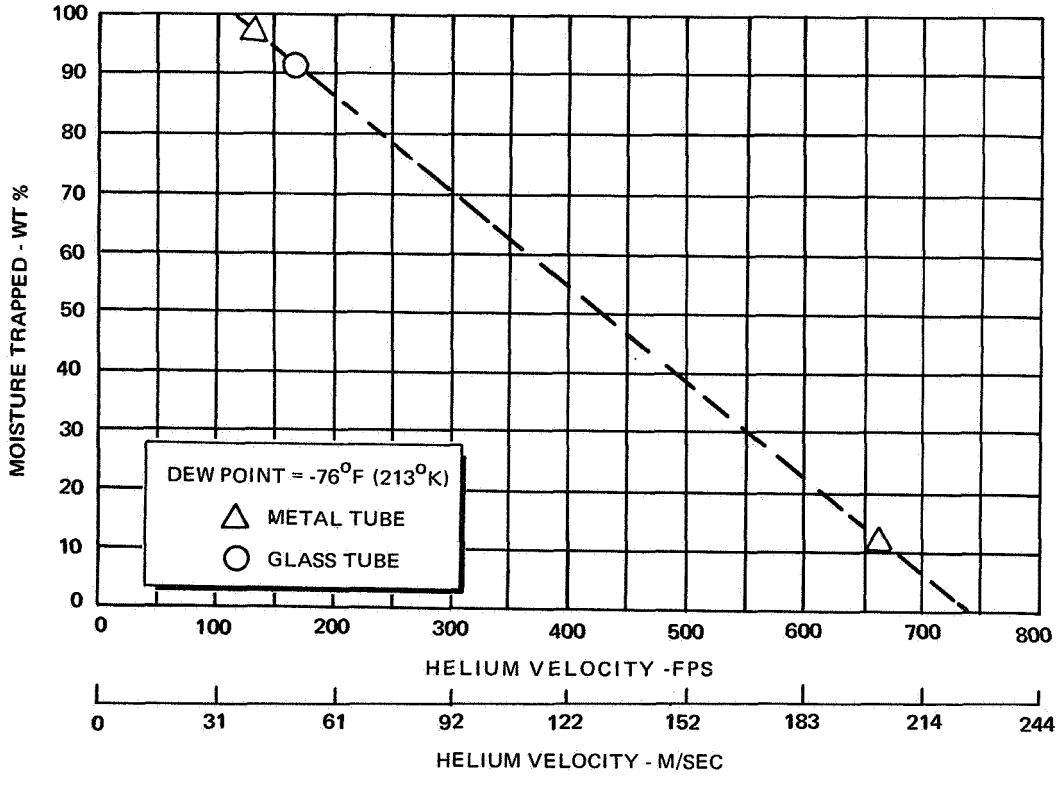

Figure 17. Effect of Helium Velocity on Trapped Moisture

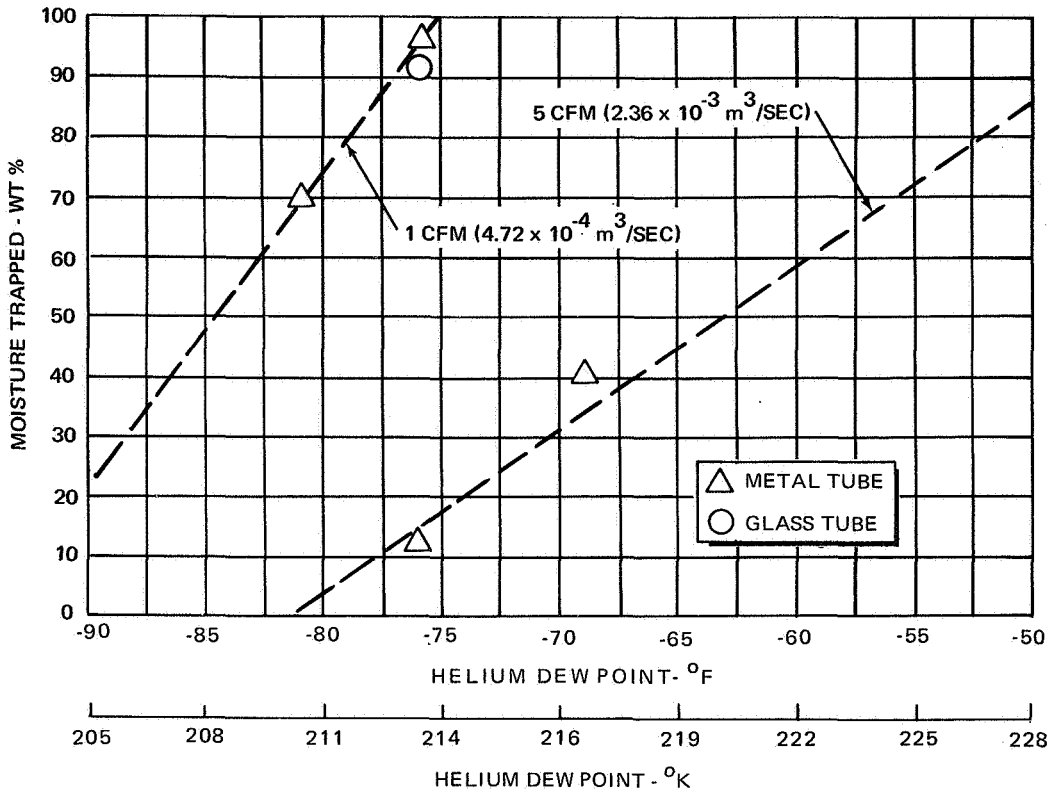

Figure 18. Effect of Helium Dew Point on Trapped Moisture

The correlation of test data was then considered to be acceptable and the results were as anticipated.

Because a low flow velocity may exist in a normal system in the fittings and component housings even when the mean flow velocity in the system piping is high, it becomes important to give consideration to the possibility of a high percentage of moisture freeze out in the components chilled to cryogen storage temperatures. The results of these test runs were used in establishing the test indicators of the ice reaction tests.

2.3.4 Ice Reaction Tests

The ice reaction tests were designed to determine the potential hazard which could exist in LF_2 feed lines when the feed lines are purged with wet helium gases prior to the transfer of LF_2 through the feed lines. These tests were made in a test apparatus which included a glass test section of the type used in the ice formation tests discussed above. The ice was allowed to form in the glass test section in several ways and then a high-speed movie camera (200 frames per sec) was used to record the events during a transfer of LF_2 through the test section. This test setup is shown in Figure 19.

The three LF_2-frost ice reaction tests were completed with no LF_2-ice reactions observed. One LF_2 reaction occurred when the vent line glass-to-metal joint failed. However, this reaction was remote from the location of the ice and cannot be attributed to a LF_2-ice reaction. A total of five test runs was required to obtain three satisfactory tests, and the results of the five tests are summarized below.

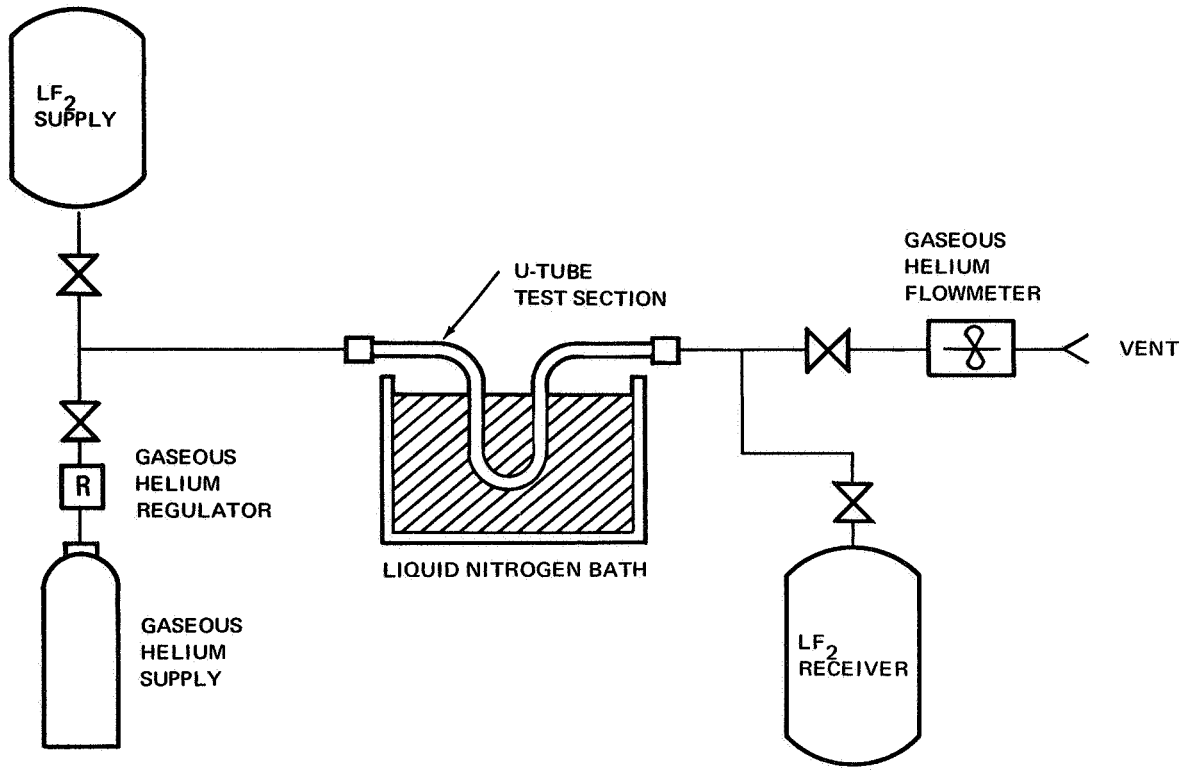

Figure 19. LF_2-Ice Reaction Test Installation

Test 1. A flow of 0.5 lb (2.27×10^{-1} kg) of LF_2 was scheduled to flow at 50 psig (3.45×10 pascals) through the glass U-tube which was submerged in a liquid nitrogen cold trap. Frost ice was formed by passing helium gas with a dew point of -76°F (213.2°K) through the cold trap at 1 cfm (4.72×10^{-4} m^3/sec) flow rate. One full bottle of helium was used for this test. This test was unsuccessful because the remote fluorine-shutoff solenoid valve did not open as required. This was caused by failure to obtain the required 28-Vdc power to the LF_2 control solenoid. The complete roll of movie film was expended before the failure was detected and the system secured.

Test 2. This test was a repeat of Test 1. The 0.5 lb (2.27×10^{-1} kg) of LF_2 was transferred through the glass test tube with no observable reaction. The movie film did indicate a greater amount of bubbling on the outside of the U-tube in the liquid nitrogen in the approximate vicinity of the ice, but no other visible reaction. No ice movement was detected in the LF_2 stream leaving the test section.

Test 3. This test was to be similar to the first test except that saturated nitrogen gas was to be used to deposit the ice in the test section. When this was attempted it was found that the condensing of the gaseous nitrogen into liquid prevented the formation of the ice on the glass wall. The ice that was formed floated on the liquid nitrogen and would not attach to the glass wall. The test plan was then changed and saturated helium gas was used to deposit the ice in the test chamber. It was then found that no LF_2 would flow through the system because of complete freeze up of the water in the test section.

Test 4. This was a repeat of Test 3 with the time of helium gas flow reduced to prevent complete freezing of the test section. This test was completed successfully, and again, no LF_2-ice reaction was observed. However, the bubbling of the liquid nitrogen coolant in the vicinity of the ice was more pronounced.

Test 5. This test was similar to the preceding tests except that the ice was formed by placing distilled water in the bottom of the U-tube. The level of the water was controlled so that the ice reduced the flow area of the tube to approximately 50% of the normal flow area. This test ended with a reaction, but not between the fluorine and the ice as anticipated. A posttest analysis of the movie film showed that the glass-to-metal joint at the outlet of the U-tube failed under pressure with enough force to break the U-tube in the middle of the test section. The remainder of the LF_2 spilled out over the top of the coolant beaker and reacted with the supporting structure below the test system. This reaction was violent and destroyed the remainder of the glass hardware used on the test. No other equipment was damaged during this test.

This test completed the scheduled LF_2-ice flow reaction tests. Based on the results of this work, it would appear that consideration should be given to additional testing with the system temperature brought up to a higher value before the LF_2 is passed through the test section to increase the possibility of a reaction.

It can be tentatively concluded from the results of these tests that water ice trapped in a normal LF_2 system line may not be a hazardous condition from a reactivity standpoint. Therefore, the normal liquid oxygen design criteria used to prevent physical damage or flow blockage resulting from the formation of ice in a flow system will apparently apply to the LF_2 system.

At the completion of the LF_2-ice flow tests, a completely separate series of LF_2 impact reaction tests were conducted. These tests were designed to evaluate the efforts of impacting a high-velocity stream of LF_2 on a stationary surface of block type ice. The higher energy involved in this type of test was suspected of being more susceptible to a hazardous reaction.

The flowing liquid explosive sensitivity tester consists of a modified Black, Sivalls, and Bryson 1-in. (2.54×10^{-2} m) diameter safety head assembly (see Figure 20). The upstream high-pressure helium safety head test section is 5.2 in. (1.32×10^{-1} m) long to accommodate 90 cc (9.0×10^{-5} m) of LF_2, and the downstream vacuum side is 3 in. (7.62×10^{-2} m) deep to provide sufficient distance for the moving LF_2 mass to accelerate to the proper theoretical fluid velocity and impact on the 2-cc (2×10^{-6} m) thin sheet of water frozen at the bottom of the well. These dimensions are based on LF_2 impact with a theoretical fluid velocity of 200 fps (6.10×10^{1} m/sec) at the instant it strikes the block of ice.

The LF_2-ice impact tester was cleaned in acetone, air dried, dipped in Oakite cleaner for 2 min, flushed in distilled water, and dried with gaseous nitrogen. After cleaning, the test components were assembled and leak checked at 1-1/2 times the operating pressure. Care was taken to maintain an equal pressure on both sides of the rupture disk.

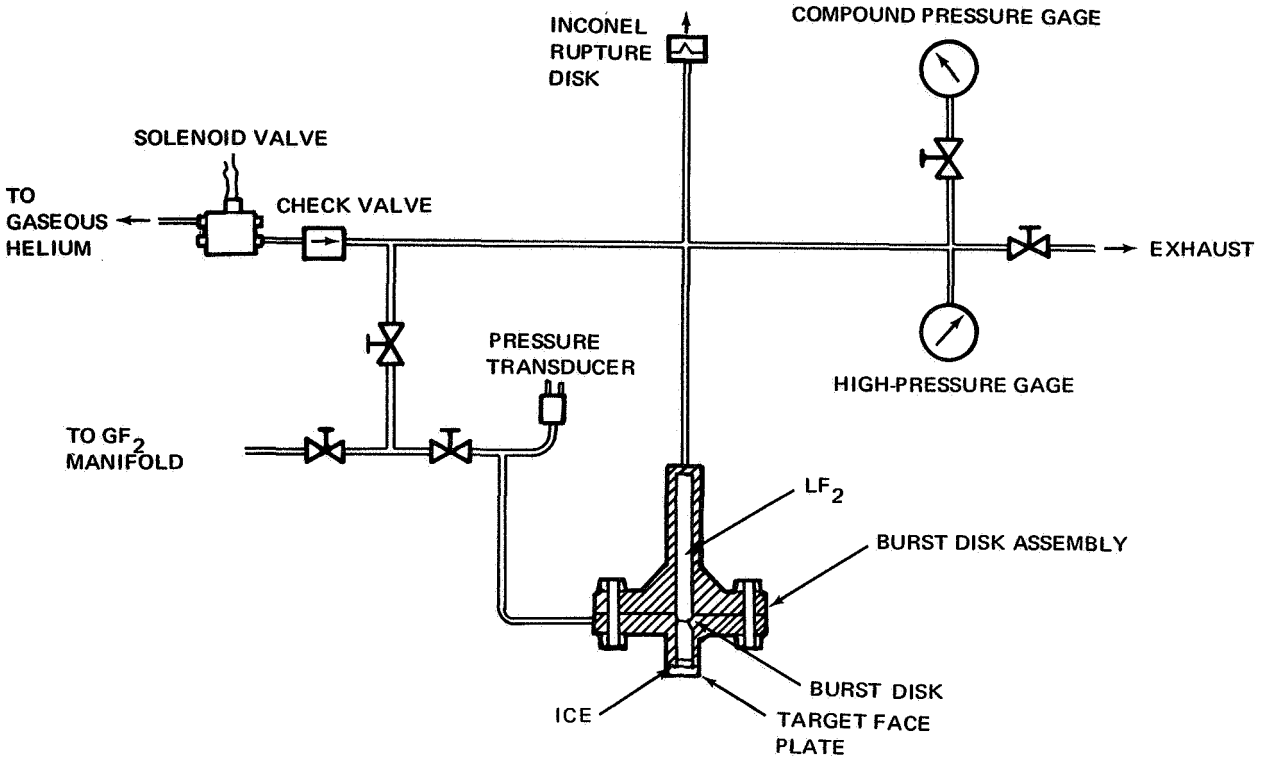

Figure 20. LF_2-Ice Impact Test System

Two cubic centimeters (2. x 10^{-6} m^3) of distilled water were placed in the lower test section by means of a syringe through an entrance port. The test unit was then cooled to -320°F (77.6°K) and helium leak checked once more. The lower chamber was evacuated and 90 cc (9.0 x 10^{-5} m^3) LF_2 condensed in the upper chamber.

The upstream side of the high-pressure solenoid valve was pressurized to slightly above the rupture disk burst pressure. The solenoid switch was actuated and the rupture disk burst, allowing the mass of fluorine to accelerate toward the ice sheet at the bottom of the lower section.

A rise in pressure above the rupture disk value indicated that a reaction had occurred. These pressure transients were recorded on a Brush Recorder Mark II from the input of a Statham pressure transducer and read directly from the high-pressure sight gage. A schematic of the LF_2-ice impact test system is given in Figure 20.

The LF_2 remaining in the fixture was removed by lowering the liquid nitrogen bath and allowing the fluorine to heat up and vent out of the system. A final nitrogen sweep was used to purge the residual fluorine gas out. The LF_2-ice impact tester was then removed and the lower test section examined for other signs of reaction at the bottom of the wall.

The first two LF_2-ice impact tests were conducted at -320°F (77.6°K) using a Continental Disc Corporation Inconel rupture disk. A reaction was recorded for both tests either by the pressure transducer or by visual

reading of the high-pressure sight gage. In both cases, the pressure rose to 1200 psig (8.28×10^6 pascals). The Inconel rupture disks did not fail at their rated values, but burst at 750 psig (5.17×10^5 pascals) for test 1 and 400 psig (2.76×10^5 pascals) for test 2. Theoretical LF_2 velocities for these burst pressures were calculated to be 216 fps (6.57×10^1 m/sec) and 158 fps (4.81×10^1 m/sec) respectively.

Figures 21, 22, and 23 illustrate the magnitude of the explosive reaction that occurred in these LF_2-ice tests at -320°F (77.6°K).

Because it could not be established whether the reaction observed occurred by LF_2-ice impact or by Inconel metal fragments impacting on the ice in fluorine at -320°F (77.6°K), further tests were run to verify which one of the possible phenomena was correct. A second pair of LF_2-ice impact tests were run using scored aluminum rupture disks manufactured by Black, Sivalls, and Bryson. These rupture disks did not fragment in the test runs. However, they did not burst at the rated 485 psi (3.34×10^6 pascals) value at -320°F (77.6°K). It was necessary to pressurize the upstream side to 900 psig (6.21×10^6 pascals). This provides a theoretical fluid velocity on impact of 240 fps (7.30×10^1 m/sec).

Two LF_2-ice impact tests were run at this burst pressure. In the first test, No. 3, there was a 950 psi (6.55×10^6 pascals) rise in pressure above the 900 psi (6.21×10^6 pascals) in the test unit (increased to 1850 psi (1.28×10^7 pascals)). The 1000 psi (6.90×10^6 pascals) safety disk burst on this test. In the second test, No. 4, there was only a 410 psi (2.82×10^6 pascals)

Figure 21. Fluorine – Ice Impact Test Reaction No. 1

(A) CORROSION DEPOSIT ON LOWER FLANGE PLATE

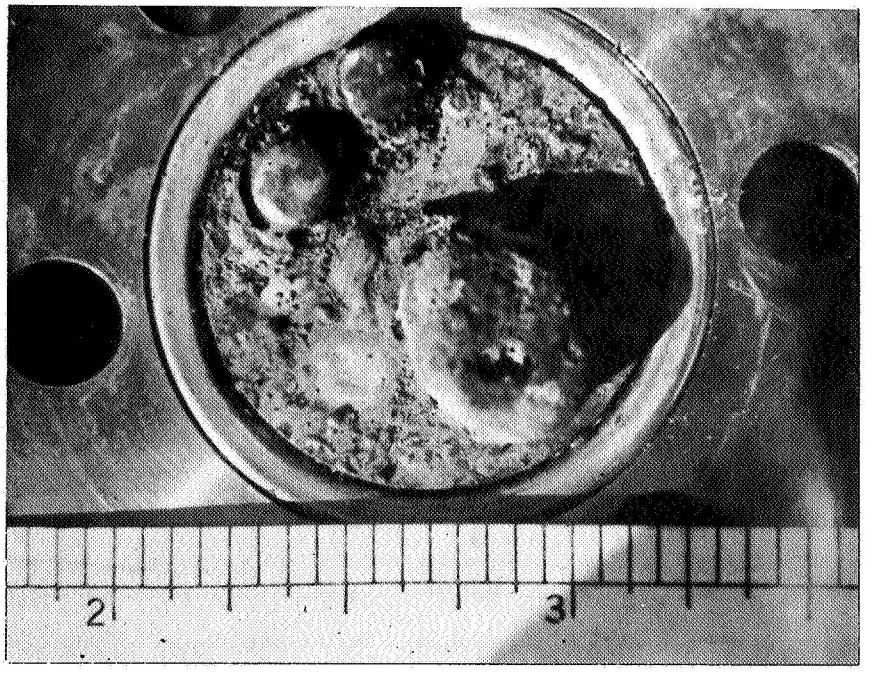

(B) LOWER FLANGE PLATE AFTER CORROSION REMOVAL

Figure 22. Liquid Fluorine-Ice Impact Test 2

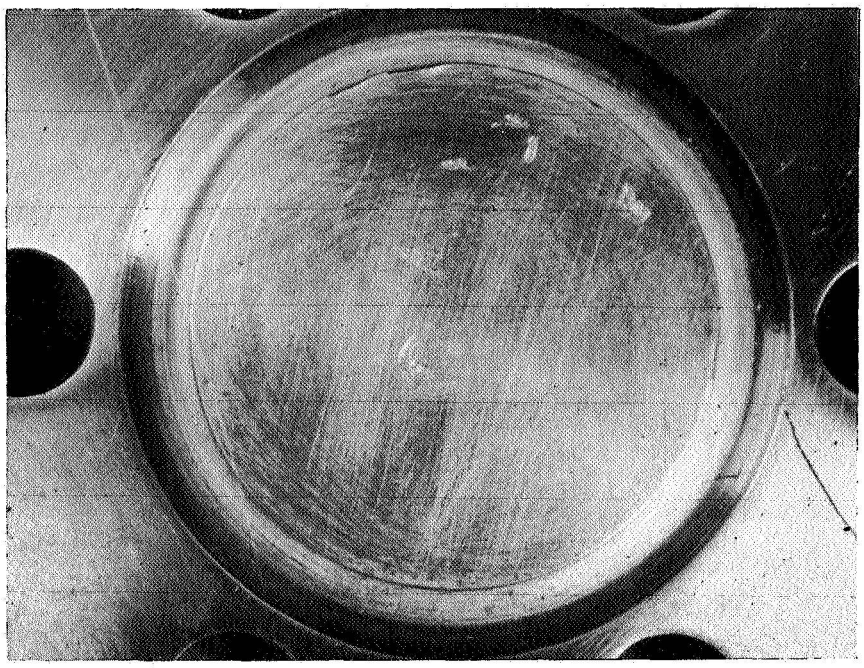

Figure 23. Liquid Fluorine – Ice Impact Test 4

pressure rise recorded above the 900 psig (6.21×10^6 pascals) burst pressure. No reaction sites were observed on the target-plate. See Figure 24. One cubic centimeter (10^{-6} m) of liquid reaction product (aqueous hydrogen fluoride) was collected for each test.

The high-pressure level and slow decay time observed on these tests is partly due to the response characteristics of the pressure recording equipment, and partly due to a mild chemical reaction between the high-velocity LF_2 and the ice. Other than the system pressure rise due to the chemical reaction of the LF_2 with the ice, no explosive conditions were indicated by these tests. No hot spots or burning of the basic metal parts were detected during these two tests which were conducted without fragmentation of the burst disk elements.

These tests concluded the investigation of the potential hazards of exposing LF_2 to water ice. Based on the results of these tests, the following conclusions are made:

1. A pressure rise may occur from the forced chemical reaction of LF_2 with water ice.

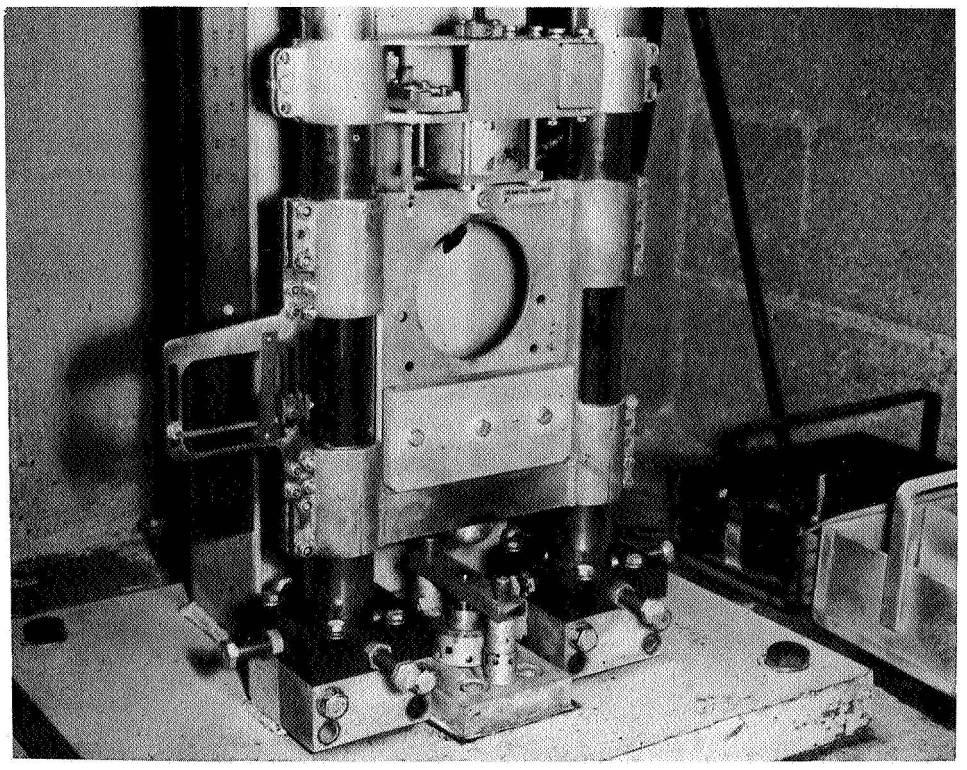

Figure 24. Open-Cup Impact Tester

2. No tendency to detonate or burn was observed under all the flow conditions tested on this program and therefore, the presence of water ice in a LF_2 system would not appear to be hazardous under normal flow conditions. Previous tests (Reference 8) have shown water ice to be explosive if impacted with a CRES plunger at a 72 lb-ft (10 kg-m) energy level.

These results would indicate that the limits of moisture which can be permitted in a typical flight-weight feed system will be based on considerations of corrosion and component malfunction and not on the potential hazard of detonation or burnout of the system.

3.0 TASK III MATERIAL COMPATIBILITY

3.1 Introduction

The material compatibility portion of this program supplements the experimental and analytical work which had been previously accomplished on Contract NASw-1351. These current tests were conducted at the Materials Laboratory at the McDonnell Douglas Gypsum Canyon Test Site (A12). The materials tested for compatibility with fluorine were:

1. Titanium alloy Ti-5Al-2.5Sn(ELI); a new material.
2. Teflon TFE commercial coating; a rerun of an earlier test.
3. Astrocoat-T coating; additional tests.
4. Silver friction tests; a new test.

3.2 Summary

The performance of these four materials under the various methods of testing are summarized in the following paragraphs.

1. Titanium alloy Ti-5Al-2.5Sn(ELI). This titanium alloy was found to be impact sensitive in LF_2, liquid oxygen, and gaseous oxygen environments when subjected to ABMA open-cup impact tests at 72 lb-ft (10 kg-m) energy levels. This material was found to be acceptable for gaseous fluorine service, and it has an acceptable static corrosion rate when exposed to LF_2 under nonimpact conditions.
2. Commercial Teflon TFE coatings. Commercial Teflon TFE coating material was found to be impact sensitive in a LF_2 medium when subjected to the 72 lb-ft (10 kg-m) ABMA open-cup impact test method. These results agreed with the data obtained earlier on the NASw-1351 program.
3. Astrocoat-T in-situ polymerized coating. This fluorocarbon material was found to be nonreactive at the 72 lb-ft (10 kg-m) energy level when tested in LF_2 using the ABMA open-cup impact test method, and no reaction or erosion was detected on a special LF_2 flow erosion test at velocities between 200 and 300 fps (6.08×10 and 9.11×10 m/sec).
4. Silver friction test. The combination of plated silver, sliding on 321 CRES, in a gaseous fluorine environment produces a low coefficient of friction, indicating that the silver fluorine film is an acceptable dry lubricant under the conditions tested. This testing was conducted on a special friction testing device. Additional tests on standardized equipment would be recommended to verify these preliminary results.

3.3 Technical Discussion

3.3.1 Titanium Alloy Ti-5Al-2.5Sn(ELI)

3.3.1.1 Impact Tests

Open-cup impact tests on this material in 100% fluorine and 100% oxygen were conducted first, in both the liquid and gaseous form. Individual tests were repeated until either reactions were observed in two tests, or until the statistically valid number of 20 tests were completed. The results of these tests, shown in Table 13, indicated that the Ti-5Al-2.5Sn(ELI) material was impact sensitive to both the LF_2 and liquid oxygen when

Table 13

OPEN-CUP IMPACT TESTS

Item	Test Material	Thickness in. (m)	No. of Tests	No. of Reactions	Remarks
1.	Ti-5Al-2.5Sn (ELI)	0.020 (5.08×10^{-4})	20	0	Gaseous fluorine at 62°F (289.8°K)
2.	Ti-5Al-2.5Sn (ELI)	0.020 (5.08×10^{-4})	2	2	LF_2 at -320°F (77.6°K)
3.	Ti-5Al-2.5Sn (ELI)	0.020 (5.08×10^{-4})	20	2	Gaseous oxygen at 62°F; (289.8°K) moderate reaction
4.	Ti-5Al-2.5Sn (ELI)	0.020 (5.08×10^{-4})	4	2	Liquid oxygen at -320°F; (77.6°K) moderate reaction
5.	Commercially coated TFE on 321 CRES				
	brown coating	0.025 (6.35×10^{-4}) base	8	4	LF_2 at -320°F; (77.6°K) one moderate, 3 faint reactions
	blue-grey coating	0.025 (6.35×10^{-4}) base	10	2	LF_2 at -320°F; (77.6°K) faint reaction
	Total		18	6	
6.	Astrocoat-T on 321 CRES	0.025 (6.35×10^{-4}) base	20	3	LF_2 at -320°F; (77.6°K) 3 faint sparks(?)

measured at the 72 lb-ft (10 kg-m) energy level. As no useful purpose would be achieved, tests with various FLOX mixtures were not conducted as had originally been planned.

The test specimens in this test series were made from a sheet of material which was 0.020 in. (5.08×10^{-9} m) thick and which was made available to this program by the NASA-LeRC program office. The material source was utilized to expedite the test program when no commercial source was found that had certified material of the required thickness in small quantities. The specimens were coined to provide 225 disks which were 5/8 in. (1.59×10^{-2} m) in diameter. The disks are checked for flatness and any that were dished were flattened. All disks were then deburred. The test specimens were then cleaned using the following steps:

1. Rinsed in acetone
2. Dried with gaseous nitrogen (filter)
3. Dipped for 2 minutes in Oakite 33 solution (50% Oakite 50% distilled water)
4. Rinsed in distilled water
5. Dried with gaseous nitrogen
6. Degreased with trichloroethylene at 192°F (362.0°K)
7. Rinsed in Freon TF
8. Dried with gaseous nitrogen

After this cleaning process, the specimens were bagged in individual plastic bags and transferred to the test area. The test control disks were made from 304 CRES, cleaned using the same procedure as used for the test specimens, bagged, and moved to the test area at the same time.

The propellants used for this test series consisted of Gaseous Fluorine, Douglas Specification, Grade 1; and Gaseous Oxygen, Aviator's Breathing Grade, Extra Dry. The liquid forms of these propellants were obtained by condensing the gases in a liquid nitrogen jacket container. The gaseous fluorine was passed through a sodium fluoride (NaF) scrubber before use as a gas or condensation as a liquid.

The open-cup drop weight impact tests were carried out on the MDAC-WD Astropower LF_2-ABMA impact tester used for the testing completed on the NASw-1351 contract. The details of this test equipment is shown in Figures 24 and 25.

The apparatus, including the drop weight tester, the test cubicle, sample trays, striker pins, and sample cups, was cleaned by appropriate techniques. Using care to avoid contamination, titanium specimen disks and blank CRES test disks were placed in aluminum cups and the loaded cups were placed in a covered CRES tray. Similarly, the striker pins and guide bars were placed in a second CRES tray and covered.

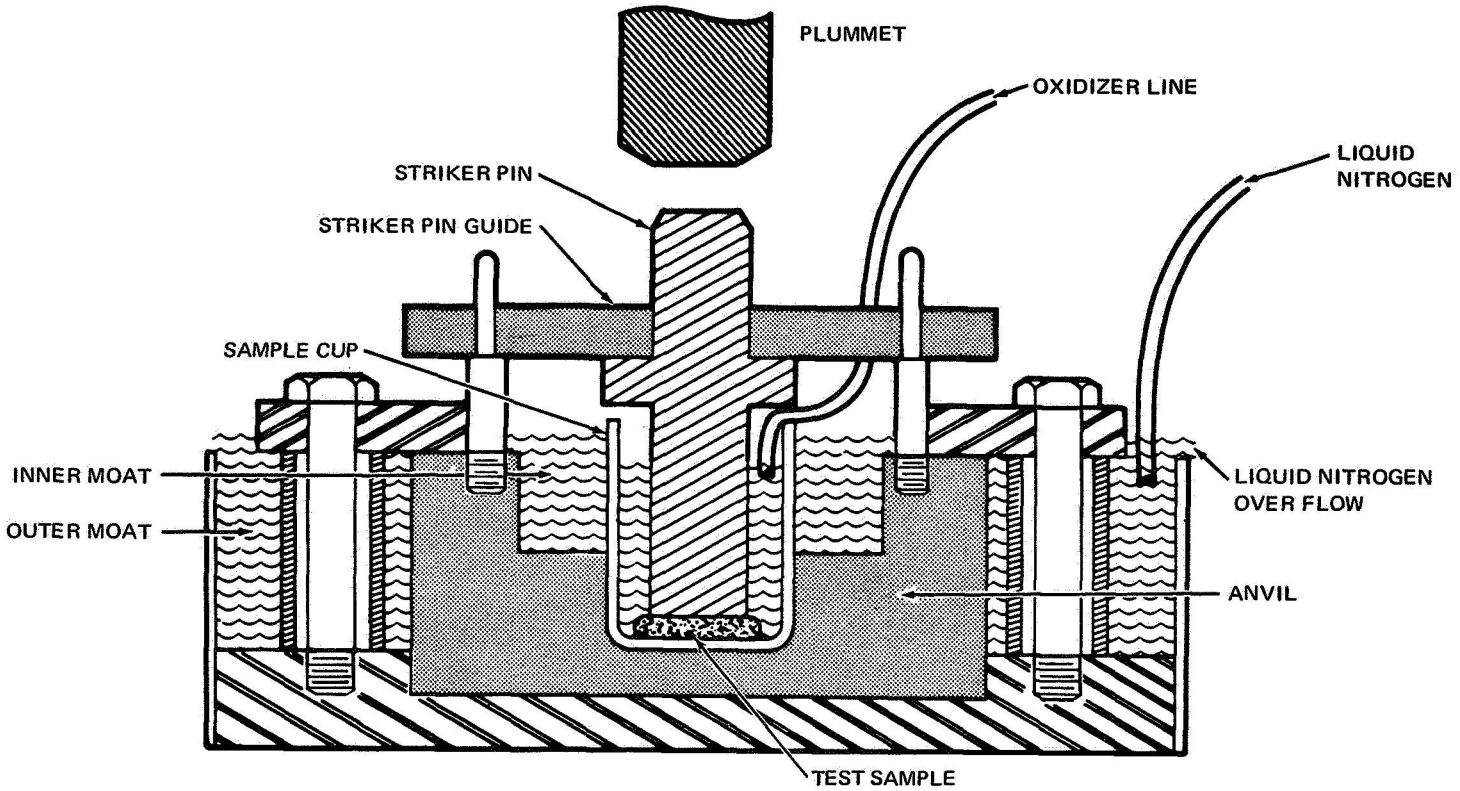

Figure 25. Anvil Assembly of Impact Tester

The trays of parts and samples were then placed in the enclosure under the liquid nitrogen overflow tubing from the moat, the enclosure and door to the testing room closed, and the gaseous nitrogen turned on. Using the remote manipulator, the covers on the trays were opened so that dry gaseous nitrogen had access to the trays. The sweep was continued for 1 hour, then the liquid nitrogen was turned on into the moat. The air around the moat was carefully observed during liquid nitrogen entry to determine whether frost condensed from any water vapor in the enclosure. If frost appeared, the liquid nitrogen was shut off and the enclosure subjected to an additional 1/2 hour sweep with dry gaseous nitrogen, then retested.

When the atmosphere in the enclosure was found to be dry, testing was initiated. The liquid nitrogen supplies were turned on to the anvil moat (overflow to the trays) and to the condenser for the oxidizer. The chilldown was complete when the violent boiling of the liquid nitrogen in the moat and oxidizer control valve jacket stopped. A sample cup containing a stainless steel disk was placed on the anvil, then a striker pin and the guide bar was put in position, using the remote manipulator. Oxidizer was condensed in the stainless steel Liebig condenser, the position of the plummet checked, the liquid oxidizer was caused to flow into the sample cup, the lights in the control room and test enclosure turned off, and the plummet dropped. The anvil area was carefully observed during the time that the impact was delivered, and signs of reaction noted.

A test control blank was tested and no reaction was detected, so the sample cup and striker pin were set aside and a new sample cup with a titanium specimen set in place. A new striker pin was installed, the guide bar replaced, and the impact test carried out. Up to 20 separate impact tests were carried out on the titanium, using a fresh specimen disk and fresh striker pin for each drop.

The final test of each series consisted of another blank test with a stainless steel disk. The liquid nitrogen was then shut off. The gaseous nitrogen sweep was continued until it was safe to enter the test enclosure. The sample cups and striker pins were removed. Each specimen disk, striker pin, and cup were examined visually and by optical microscope for evidence of chemical reaction.

The test series was conducted first with liquid fluorine as the oxidizer, then with liquid oxygen. Since this titanium alloy was found to have unacceptable impact characteristics in the liquid form of both fluorine and oxygen, there was no justifiable reason to test the intermediate gaseous fluorine and oxygen mixtures as had been originally planned and no further testing was attempted.

After completion of the liquid tests, the gaseous tests were conducted. These tests were made in the same manner as the liquid oxidizer tests described above, except that the oxidizers were not condensed from the gaseous state and the condenser and the oxidizer control valve were not chilled with liquid nitrogen. The anvil, cups, samples, and striker pins were chilled as usual.

In the tests, the oxidizer supply manifold was pressurized with gaseous oxidizer at 20 psia (1.38×10^5 pascals). A chilled cup and striker pin were placed on the chilled anvil. The lights were turned off, the oxidizer control valve opened to flow gaseous oxidizer into the cup and the plummet was released about one second after turning on the gas flow.

As in the liquid oxidizer tests, pure oxygen and pure fluorine (0% and 100% fluorine gas) were tested first. The results of these tests are shown on Table13. Because neither propellant was found acceptable during the liquid impact tests, there was no justifiable reason to run intermediate FLOX mixture tests for either in liquid or the gaseous impact tests. This is true even though a difference was noted between the two types of oxidizer on the gaseous impact tests. It should be noted that the fluorine gas tests indicated an acceptable impact sensitivity while the gaseous oxygen was not rated acceptable. However, because only two reactions were detected out of a total of 40 drops for the entire gaseous test program, an attempt to evaluate intermediate FLOX mixture sensitivity would prove meaningless without testing an extremely large number of test samples. This is true because the only intermediate reaction rate which was left (between 0 and 2) was one reaction in 20 drops, and there is no way of separating the potential performance of different FLOX mixtures without testing enough samples to have provided a statistical meaningful number. Because the testing of such a large number of samples was not within the scope of work covered by this contract, and since the material had failed to pass the impact sensitivity tests in the liquid medium, no further impact testing was undertaken.

3.3.1.2 Static Corrosion Tests

The titanium alloy static corrosion tests were conducted in LF_2 (100% FLOX) because no corrosion data existed for this alloy in LF_2, but liquid oxygen corrosion data are available. The results of the Task II contamination studies indicated that a value of less than 0.3% (by volume) of hydrogen fluoride would be expected to exist in a typical flight-stage oxidizer tank using procurement specifications and handling procedures which are presently available. This being the case, a value of 0.3% equivalent volume of aqueous hydrogen fluorine was selected as the optimum level of hydrogen fluorine concentration for those static corrosion tests.

The static corrosion rate of this alloy in LF_2 at -320° F (77.6° K) was studied, using standard rectangular test coupons (3/4 by 3 by 0.020 in. thick) (1.91×10^{-2} by 7.63×10^{-2} by 5.09×10^{-4} m thick) Both unwelded and longitudinally welded coupons were used, and exposures included the gas phase, the liquid phase, and interface layer of the oxidizer. The weld was longitudinal on the test coupon, but this was transverse to the direction of rolling. Two welded and two plain coupons were exposed to each phase for a total of 12 coupons in each test. The oxidizer used was fluorine, and the tests were conducted at -260° F (110.9° K) at the saturation pressure (500 psi (3.45×10^6 pascals)) of the oxidizer. Two exposure durations were tested, 1 day and 21 days.

Coupons were prepared by shearing them from the sheet stock of alloy received from NASA-LeRC and then finish machining to the required dimensions. Welded coupons were prepared by cutting the sheet of titanium alloy into 1-1/2 in. (3.81×10^{-2} m) wide strips, and then butt welding the strips together using Ti-5Al-2.5Sn (ELI) filler rod. The welds were 100% inspected by X-ray. Then the rectangular coupons were cut from the welded stock with the weld longitudinal. A 1/4 in. (6.35×10^{-2} m) diameter hole was drilled near one end of each coupon; this hole is for suspending the

coupons in the test array. The coupons were marked for individual identification after they were manufactured, then cleaned for LF_2 service, using the same procedure used for the impact sample disks made from this alloy, and individually weighed on an analytical balance.

The tests were conducted in stainless steel containers, 3 in. (7.62×10^{-2} m) diameter and 9 in. (2.29×10^{-1} m) internal height. A coupon support jig consisting of a base and a central vertical rod (both of stainless steel) and horizontal support members made of 1/4 in. (6.35×10^{-2} m) diameter aluminum oxide rod at appropriate vertical separations were cleaned for LF_2 service. The cleaned coupons hung from the alumina rods with 1/4 in. (6.35×10^{-2} m) thick aluminum oxide spacers between adjacent coupons. There were two plain and two welded coupons hung so that their upper edges are 3-1/2 in. (8.90×10^{-2} m) from the bottom of the test container; a like number hung so that their mid points are 3-5/8 in. (9.21×10^{-2} m) from the bottom; and a further four specimens hung so that their bottom edges are more than 3-3/4 in. (9.53×10^{-2} m) above the container buttom. The suspension system, with coupons attached are shown in Figure 26.

A significant change was made in the static corrosion testing apparatus based on the test results obtained during the preceding NASw-1351 effort. This change consisted of installing an inert platinum plated aluminum oxide liner in the corrosion test chamber as shown in Figure 27. With the platinum liner, test medium was not exposed to the plain stainless steel chamber walls. This liner was used for the 1 day static corrosion tests to evaluate the influence of the reactivity of the chamber walls on the corrosion rate of the test specimens.

The use of the platinum liner introduced a separate but related variable to the test program. This change was in the location of the aqueous hydrogen fluorine relative to the test specimens. Without the platinum liner installed, it was possible to place the aqueous hydrogen fluorine on the bottom of the test chamber to one side of the test specimens as shown in Figure 26. For testing with the platinum liner, it was necessary to place the aqueous hydrogen fluorine directly under the test specimens, as shown in Figure 27.

It was suspected that the lower reactivity rate of the inert platinum liner would result in a reduction in the amount of hydrogen fluorine which would react with the container walls and would therefore reduce the amount of hydrogen fluorine which would be reacted out of the test solution. If less hydrogen fluorine was removed by the reaction with the container liner, then more hydrogen fluorine would remain in the test solution and would be available for reaction with the test specimens.

The first test run made with the complete platinum liner produced unexpected results. The four samples which were completely submerged in the liquid, immediately above the aqueous hydrogen fluorine, were corroded severely on the lower edges of the test coupons. This corrosive attack was sufficient to cause the complete removal of the identification marks which had been placed on the samples and therefore, prevented an accurate check of the weight change of each specimen as the result of the 24-hour exposure. This test was then rerun with almost identical results. The specimens from this second run are shown in Figure 28. Again the identification

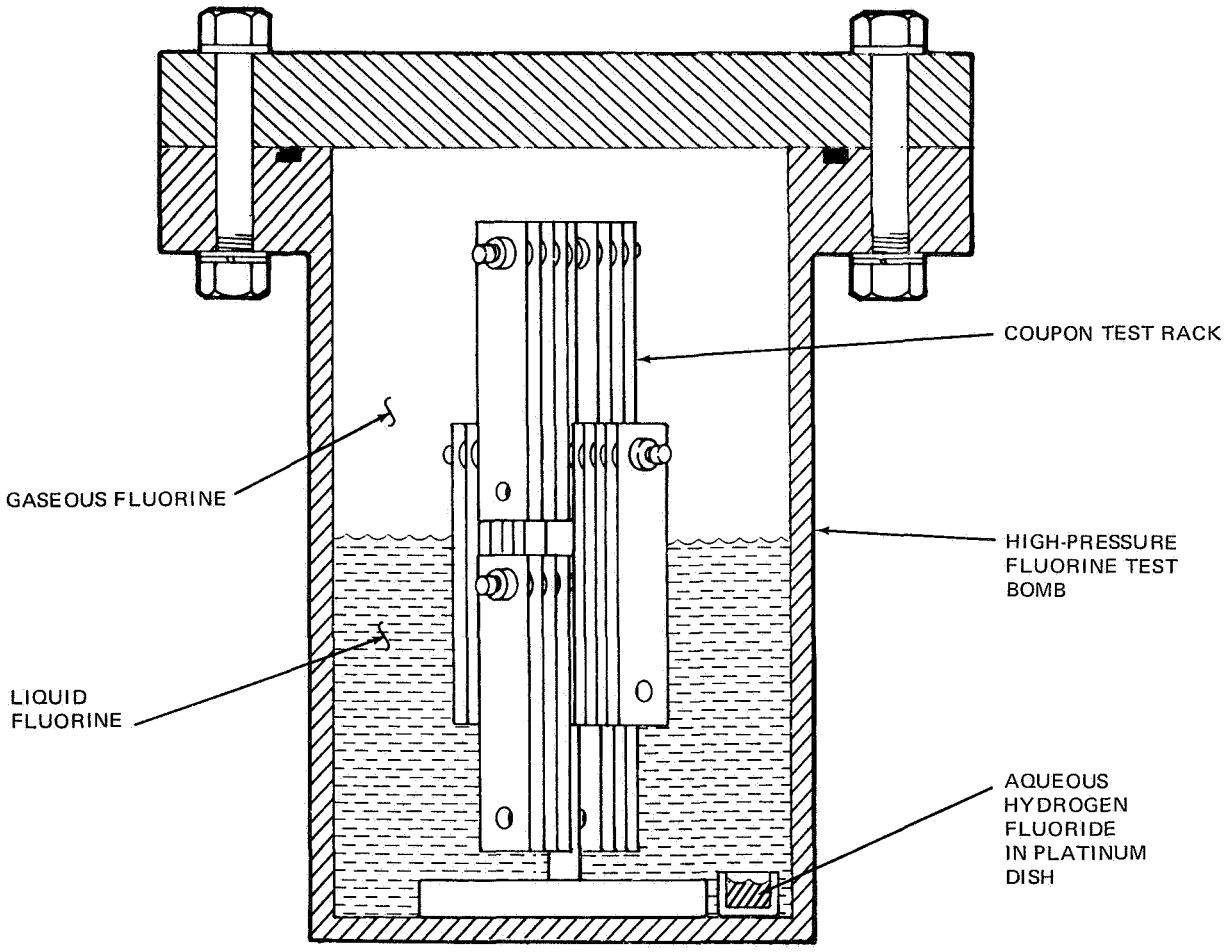

Figure 26. Corrosion Test Chamber

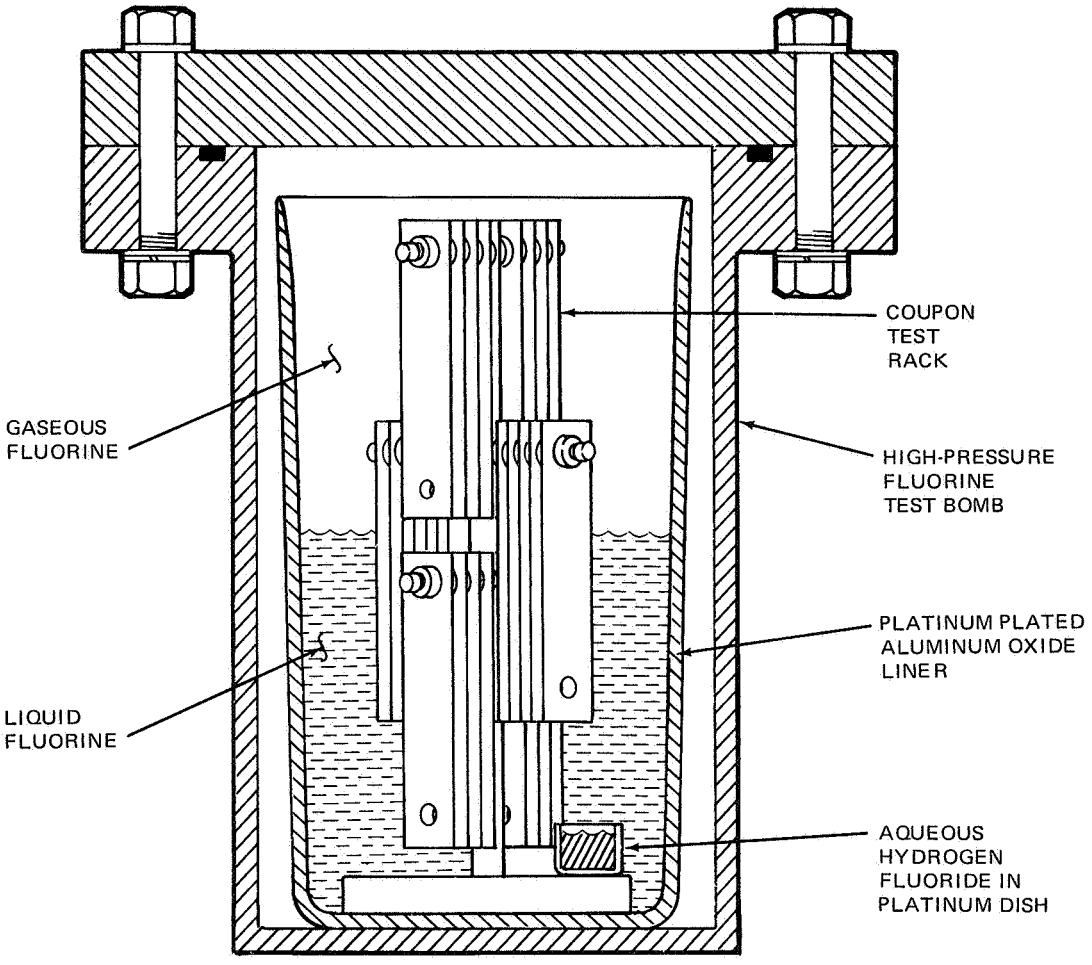

Figure 27. Corrosion Test Chamber With Platinum Liner

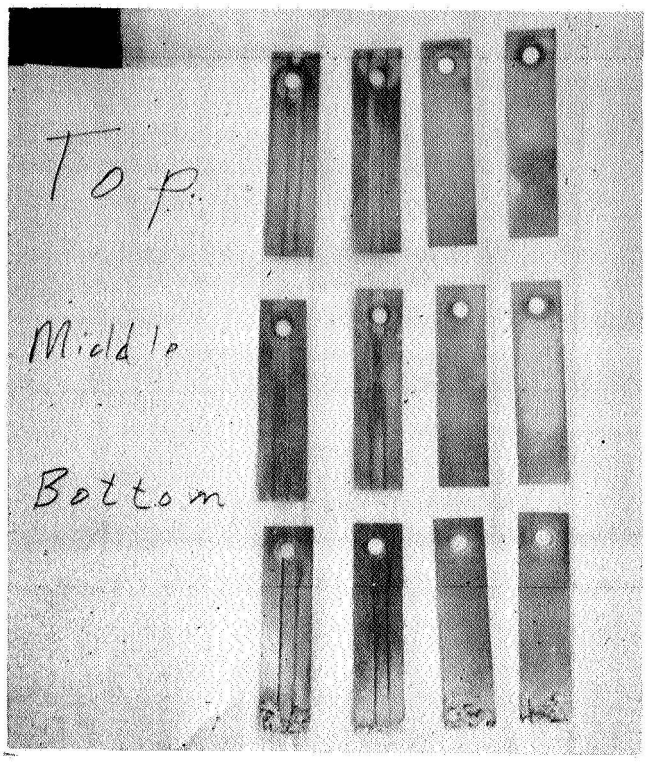

Figure 28. Titanium Samples After Exposure to Fluorine

marks were lost due to the excessive corrosion and no firm analysis could be made. However an approximate analysis was made by weighing the samples on a relative weight basis. The sample that was the heaviest after exposure was assumed to have been the heaviest before exposure. The results of this second test are shown on Table 14.

It should be noted that even with the high rate of corrosion which can be visually observed on the lower specimens, the lower specimens do not show a corresponding corrosion rate on a weight change basis. This would indicate that excessive corrosion can occur with a weight increase, a weight decrease, or with practically no net weight change at all. As a consequence no absolute evaluation can be made based on the results of these 1-day tests. As would be expected, the weight changes for all specimens are higher with this test setup, which has the test specimens directly over the corrosive media, and is somewhat higher on the specimens which are physically closer to the aqueous hydrogen fluorine.

A third test of 21-days duration was then run with new test specimens but in the normal configuration without the platinum liner. The results of this test is shown in Table 15. This combination of tests provided comparisons of both the test procedure using inert chamber liners and without the liners, and also yielded comparative data for the titanium alloy and the aluminum A356 alloy tested on the previous program. The results of these tests indicate that the corrosion rate of the Ti-5Al-2.5Sn (ELI) material is relatively low, approximately the same as for the aluminum A356 alloy.

Table 14

ONE-DAY CORROSION TESTS
TITANIUM IN LIQUID FLUORINE

Temperature = -260°F (110.9°K)
Fluorine with 0.3% Equivalent Volume Aqueous HF
Titanium Alloy Ti-5Al-2.5Sn (ELI)

Non-Welded Specimens

Specimen No.	Phase	Initial Weight (gm) (10^{-2} kg)	Weight Change (gm) (10^{-2} kg)	Corrosion Rate $mg/in.^2$ (kg/m^2)	mpy
1	G	4.1831	0.0100	2.2 (3.41×10^{-2})	11
2	G	4.1699	0.0110	2.3 (3.57×10^{-2})	11
3	G/L	4.1640	0.0131	2.7 (4.18×10^{-2})	13
4	G/L	4.1173	0.0177	3.8 (5.90×10^{-2})	18
5	L	3.8674	0.0170	3.6 (5.58×10^{-2})	18
6	L	4.0808	0.0231	4.6 (7.13×10^{-2})	24

Welded Specimens

7	G	3.4570	0.0110	2.3 (3.57×10^{-2})	11
8	G	3.4517	0.0104	2.2 (3.41×10^{-2})	11
9	G/L	3.5961	0.0194	4.0 (6.20×10^{-2})	20
10	G/L	3.6878	0.0147	3.1 (4.80×10^{-2})	15
11	L	3.9482	0.0334	7.0 (1.08×10^{-1})	33
12	L	3.8352	-0.0075	-1.6 (-2.48×10^{-2})	-8

*G = Gas; L = Liquid

Table 15

21-DAY CORROSION TESTS
TITANIUM IN LIQUID FLUORINE

Temperature = -260°F (110.9°K)
Fluorine with 0.3% Equivalent Volume Aqueous HF
Titanium Alloy Ti-5Al-2.5Sn (ELI)

Non-Welded Specimens

Specimen No.	Phase	Initial Weight (gm) (10^{-2} kg)	Weight Change (gm) (10^{-2} kg)	Corrosion Rate mg/in.^{2} (kg/m^2)	mpy
1	G	4.2146	0.0019	0.40 (6.20×10^{-3})	0.09
2	G	4.1932	0.0013	0.27 (4.18×10^{-3})	0.06
3	G/L	4.0059	0.0018	0.39 (6.04×10^{-3})	0.09
4	G/L	4.1402	0.0009	0.19 (2.94×10^{-3})	0.04
5	L	4.1946	0.0020	0.42 (6.51×10^{-3})	0.10
6	L	4.0571	0.0030	0.63 (9.76×10^{-3})	0.15

Welded Specimens

7	G	3.6548	0.0016	0.33 (5.12×10^{-3})	0.08
8	G	3.6785	0.0020	0.42 (6.51×10^{-3})	0.10
9	G/L	3.8186	0.0023	0.48 (7.44×10^{-3})	0.11
10	G/L	3.7936	0.0016	0.27 (4.18×10^{-3})	0.06
11	L	3.8959	0.0016	0.30 (4.65×10^{-3})	0.07
12	L	3.8138	0.0027	0.57 (8.83×10^{-3})	0.13

*G = Gas; L = Liquid

3.3.2 Polymeric Coatings

3.3.2.1 Test Specimens

This testing program was conducted to evaluate the use of certain thin coatings of Teflon TFE and the proprietary Astrocoat-T coatings in LF_2 service. The Teflon coatings were limited to commercially available materials which consisted of a pure TFE primer coating with a pure TFE enamel final coat. No primers, binding, or coloring agents were permitted. The Astrocoat-T specimens were in-situ polymerized laboratory grade coatings processed by the Materials Research group of the Astropower Laboratory.

The two types of fluorocarbon coatings were deposited on 321 CRES disks coined from a sheet of 0.025-in. (6.35×10^{-4} m) thick material. Each disk was 5/8 in. (1.59×10^{-3} m) in diameter and was drilled with a single 0.032-in. (8.13×10^{-4} m) diameter hole near one edge of the disk. This hole was used to suspend the disk on a mounting wire during the respective coating processes.

The commercial TFE coating was applied by RACO Engineering under the specification listed in Appendix III-3 of the Fluorine Systems Handbook. One coating of TFE Primer 850-201 and one coating of TFE clear enamel 852-2-1 was used on each disk. After receipt of these specimens at the laboratory, they were cleaned by vapor degreasing in Freon TF, washed in detergent and distilled water, rinsed in distilled water, and then vacuum baked at 105°C (378°K) and 1mm Hg (1.33×10^2 pascals).

Specimens coated with the MDAC-WD proprietary in situ polymerized process (Astrocoat-T) were made using the same type of metal disk that was used for the commercial coating process. Because the nature of the Astrocoat-T process, no cleaning was required after completion of the coating process, and none was used for these specimens.

Each test series was scheduled to include a total of 20 impact drops for each test material with a new specimen being used for each drop. The 20 test disks prepared by RACO were tested first. When these specimens were delivered, all of them were not the same color. About half were brown while the other half were blue-gray. An investigation of this color difference revealed that all 20 specimens were processed at the same time by the same operator and that the materials used were from the same source. It was further established that only one can of primer and one can of TFE enamel had been purchased by RACO and all specimens were coated with material from these two cans.

The supplier of the primer and TFE enamel stated that these two color results are common and have no effect on the basic coating. The difference in color is due to the difference in the length of the air-drying time between the first specimens sprayed and the last specimens sprayed. No difference in characteristics of the coatings--other than color--had been reported prior to these tests.

The test specimens used for the erosion tests were fabricated from 0.025-in.-(6.35×10^{-4} m) thick 321 CRES. The specimens were 5/8-in.-(1.59×10^{-3} m) diameter disks with a 0.017-in.-(4.32×10^{-4} m) diameter orifice drilled through the center. A 0.017-in. (4.32×10^{-4} m) radius was machined on the inlet side of the drilled orifice to control the orifice inlet flow. After the specimen disks were fabricated, the Astrocoat-T coating was applied to all surfaces of the disks. Then, optical measurements were made of the final orifice diameter. Since the holes were slightly oversize before coating, a final diameter of 0.017 in. (4.32×10^{-4} m) was obtained after coating.

3.3.2.2 Impact Tests

The testing of the commercial Teflon TFE coating was conducted with specimens of each of the two color groups tested as separate specimen groups. In both cases the number of reactions were higher than the acceptable number.

The open-cup impact tests were conducted with the same test procedure as that used for the Titanium alloy specimens (for the LF_2 portion only). The results of these tests are shown on Table 13. It should be noted that the brown commercial coated specimens were more likely to react than the blue-gray specimens. Four out of eight reactions occurred on the brown specimens, while only two out of ten reactions occurred on the blue-gray specimens.

The processing literature indicates that the 850-201 primer is responsible for the coloration noted and the yellow-orange color of the wet primer turns to a brown or gray-green during the normal air-drying process. This drying process is used to remove the volatile portion of the spray. A 850-202 primer, normally used for aluminum metal coating, would be expected to give a brownish or blue-gray coating (instead of a gray-green as with the 850-207 primer). Whether the 10 specimens in this sample batch were actually gray-green or gray-blue is relative and, pending an identification against a color reference, it is assumed that the 850-201 primer is behaving normally.

The Astrocoat-T specimens were tested with the same equipment and with the same procedure used for the commercial TFE specimens. The identification of a reaction was based on both the operator's visual observance of the test, and the posttest visual examination for reaction residues. The normal drop procedure was followed, with the test chamber lights turned off so that a resulting spark or flash could be observed visually. Each specimen was given a posttest examination to confirm the operator's observation. With the Astrocoat-T specimens, however, the operator was unable to evaluate the drop reaction with certainty. In three cases, the operator visually noted that a very faint spark may have occurred. However, the spark was too faint for positive identification. The posttest examination of these questionable specimens did not reveal any indication of a reaction. On all three specimens, the striker indentation had crossed over the edge of the small hole that was drilled into the specimen for mounting the specimen in the processing chamber. On the other 17 specimens, the striker pin had not overlapped the mounting hole and no indication of a reaction was observed on any of them. To reconfirm the acceptability of the Astrocoat-T coating, an additional 20 specimens were prepared and tested. No reaction was observed

on this series and no deformation was detected across the small mounting hole. Based on these results, the Astrocoat-T coating is nonreactive for impacts in LF_2 at up to a 72 lb-ft (10 kg-m) energy level.

3.3.2.3 Erosion Tests

The Astrocoat-T coating was tested for erosion characteristics. The apparatus used was identical to that used on previous cavitation corrosion tests except for the test specimen configuration. The test setup is shown in Figures 29 and 30. The same test specimen holder was used for these tests; however, the orifice plate was coated with the test material and became the test specimen. The cavitation corrosion test coupon was then omitted from the setup.

After preparing the specimens, the erosion test assembly was attached to the LF_2 flow loop. The test loop was checked for helium leaks at ambient temperature and 700 psi (4.83×10^6 pascal). During this period the differential pressure transducer output was calibrated from 0 to 300 psia (0 to 2.07×10^6 pascals) differential pressure against atmosphere in 50 psia (3.45×10^5 pascals) intervals. The output was recorded on a four-channel Sanborn oscillograph recorder. The Foxboro turbine flowmeter output frequency was also recorded on the Sanborn recorder with a frequency converter calibrated from 200 to 1,400 cps (Hz).

The LF_2 flow test loop was cooled to -320° F (77.6° K) by submerging the complete flow loop in liquid nitrogen, and 600 cc (6. x 10 m^3) of gaseous fluorine was condensed into the flow-loop cavity. The loop was then pressurized to 400 psig (2.76×10^6 pascals) with helium. Upstream helium pressure of 225 ±25 psi ($1.55 \times 10^6 \pm 1.73 \times 10^5$ pascals) was applied to operate the diaphragm pump. The pumping cycle was adjusted by a timer to give an average flowrate of 0.5 gpm ($3.15 \times 10\text{-}5$ m^3/sec). The initial calculated flow velocity through the orifice was 200 fps (6.10×10^1 m/sec) as shown in Table 13. The test was run for 30 min with no erosion attack indicated by the pressure differential data.

After the completion of the first test run, the liquid nitrogen bath was drained and the fluorine vented to a charcoal scrubber. The residual fluorine in the test loop was evacuated and finally the test system was purged with helium gas. The erosion test unit was removed from the flow test loop and the orifice specimen removed. The orifice diameter was optically measured and no change in diameter was detected.

The second test run was then completed using a new test specimen. This test was designed to run for 30 min with a flow velocity of 400 fps (1.22×10^2 m/sec). This increase in velocity was to have been obtained by increasing the system operating pressure with no change in the test-specimen orifice diameter. The system pressure was increased and the 30-minute run was completed. After securing the test system, the test data was analyzed and the flow velocity for this run was 200 fps (6.10×10^1 m/sec). Again no change in pressure drop or erosion damage was detected.

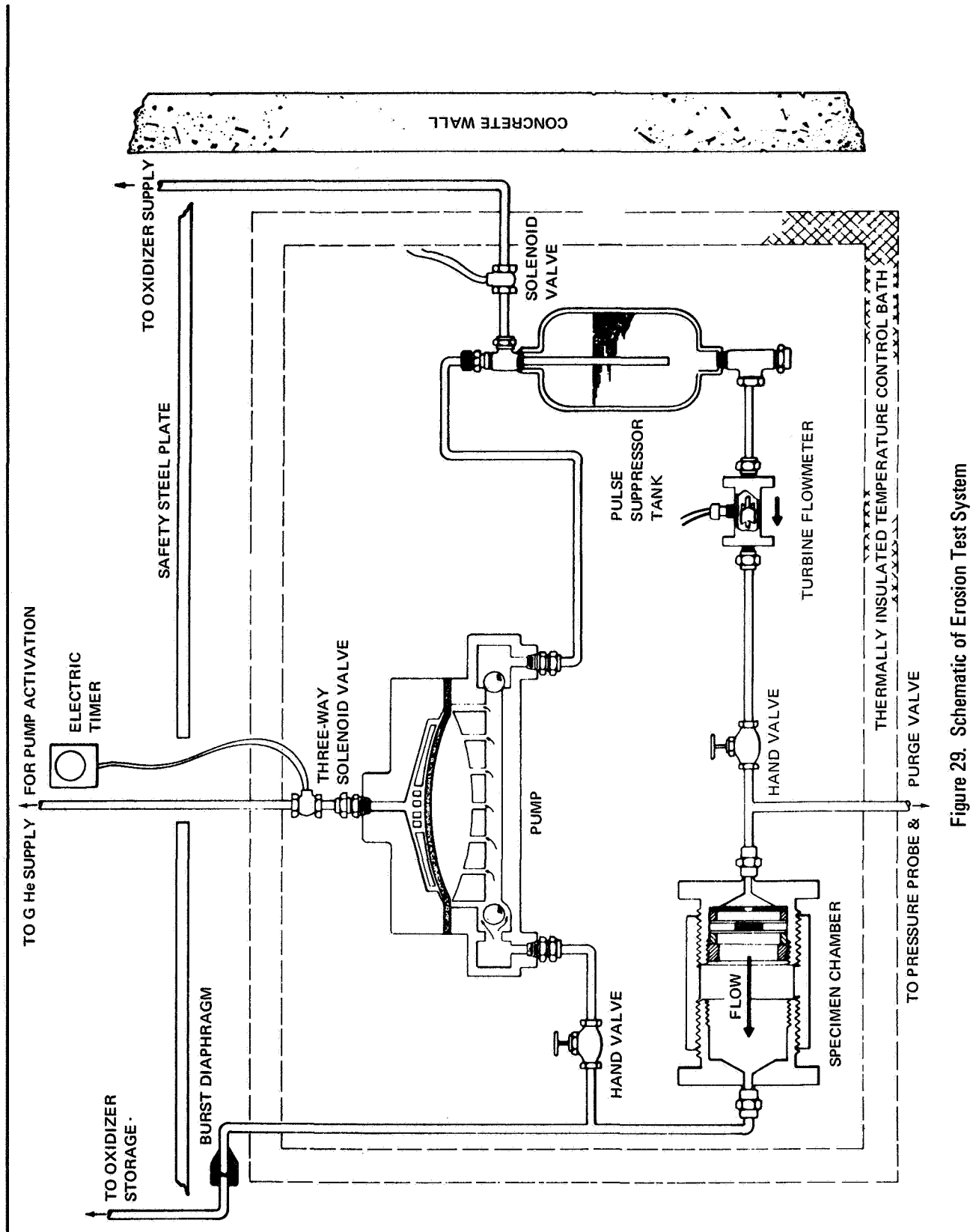

Figure 29. Schematic of Erosion Test System

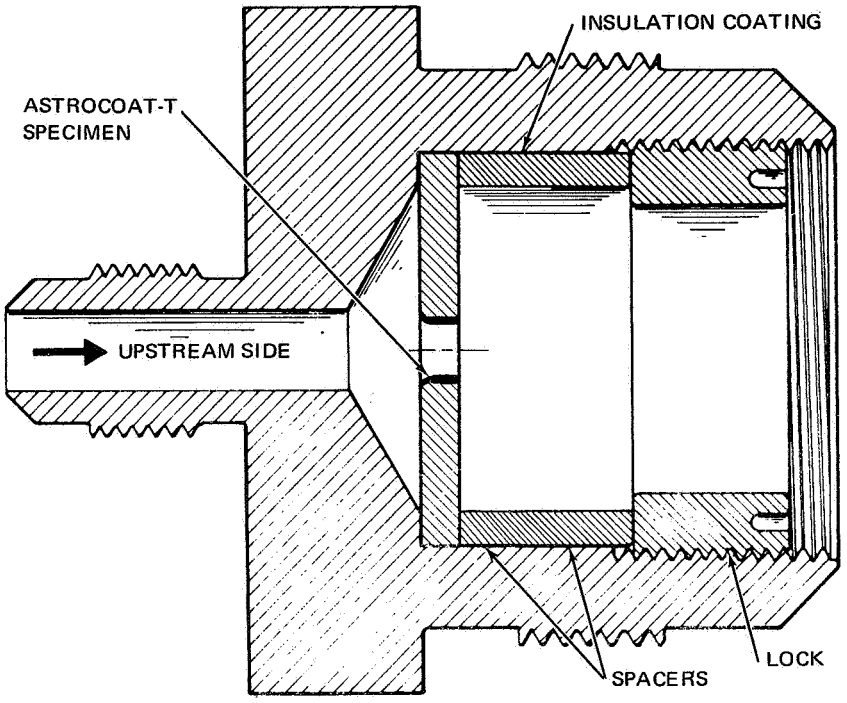

Figure 30. Erosion Test Specimen Holder

It was considered desirable to evaluate the performance of this material at flow velocities higher than 300 fps (9.16×10^1 m/sec) and so the testing effort was continued using still higher system pressures. Two new orifice test specimens were fabricated and coated with the Astrocoat-T coating. To obtain the required velocity, a specific pressure drop must be maintained across the flow orifice. Since the test orifice was already at the smallest practical size, the only available method of increasing the velocity across the orifice was by increasing the overall system pressure.

A check of the limitations on the apparatus system pressure revealed that with certain modification to the helium driving system, the overall system pressure could be increased to 1,200 psig (8.28×10^6 pascals). The diaphragm-type pump used is capable of withstanding pressures in excess of 2,000 psi (1.38×10^7 pascals). However, the driving diaphragm is limited to a differential between the driving pressure and the pump outlet pressure of 400 psid (2.76×10^6 pascals). To operate with a differential pressure of 800 psid (5.52×10^6 pascals) across the pump (and also across the flow orifice) it would be necessary to operate at a pump outlet pressure of 1,200 psig (8.28×10^6 pascals) and a pump inlet of 400 psig (2.76×10^6 pascals). To operate at these high pressures, it was necessary to alter the normal atmospheric vent cycle on the helium drive side, as well as alter the system to prevent the pressure on the helium drive side of the diaphragm from falling below 400 psig (2.76×10^6 pascals).

This modification was made and the third test run was started. After 12 sec of operation (of this 30-min test) the downstream shutoff valve burned through and released the 400 psig (2.76×10^6 pascals) pump inlet pressure. Without the 400 psig (2.76×10^6 pascals) pressure on the pump, the whole system was subjected to the full 1,200 psid (8.28×10^6 pascals) differential pressure for a short time. This burnthrough failure occurred at a valve which was not normally pressurized during testing but was operating at a 400 psig (2.76×10^6 pascals) pressure level for this special test. No visual evidence of erosion damage was detected under a microscope during the posttest inspection of the orifice, although moderate damage was suffered by part of the flow loop. The calculated velocity through the orifice for this short test was a nominal 290 fps (9.14×10^1 m/sec) with the peak at the time of failure being approximately 340 fps (1.07×10^2 m/sec).

The damage to the flow loop was such that further testing could not be undertaken without considerable rework and possible modification to the basic system. Therefore, no further testing was attempted.

3.3.3 General Compatibility Test--Silver Friction Test

The component design analysis conducted under Task I indicate a theoretically suitable all-metal bushing combination for use in fluorine service. This metal combination is silver sliding on steel. The theoretical model analysis indicates that the adhesive forces are such that silver will not adhere to steel under normal conditions. This lack of adhesion is the reason for providing an underplating in the normal silver plating process. The theoretical analysis indicates that a coefficient of friction of 0.40 would be expected for dissimilar metals operating in air and a value of 0.10 to 0.18 with a fairly good lubricant.

To evaluate the silver-steel combination in a fluorine environment, a preliminary test run was conducted at the Gypsum Canyon Test Site (A12) using the frictional-energy test device shown in Figures 31 and 32. This device was used under a separate Air Force contract to evaluate the reactivity of various tankage materials in fluorine. To conduct this test, a frictional-energy test disk was refinished and given a silver plate in the McDonnell Douglas Materials Research Laboratory. During the refinishing, a series of ventilation slots were cut into the test specimen so that the GF_2 exposure of the contact surfaces could be assured. These slots are shown in Figure 33.

After installation of the test specimen in the apparatus, the test section was pressurized with ambient gaseous fluorine and a series of friction runs was conducted up to the capacity of the machine. The results of the tests are shown on Table 16. During the last two tests, the sameples were loaded so that the mechanism could not complete enough travel for a realistic value of friction coefficient to be determined. Posttest inspection of the test sample showed no evidence of galling on the specimen after all five tests. The silver fluoride film was a yellow-green fine-grained coating which transferred from the silver to the 316 CRES in small quantities. This is an acceptable condition for dry film lubrication. The measured coefficients of friction of 0.08 to 0.20 indicate that the fluoride film provides a reasonable measure of lubrication. Therefore, further testing in this area is recommended.

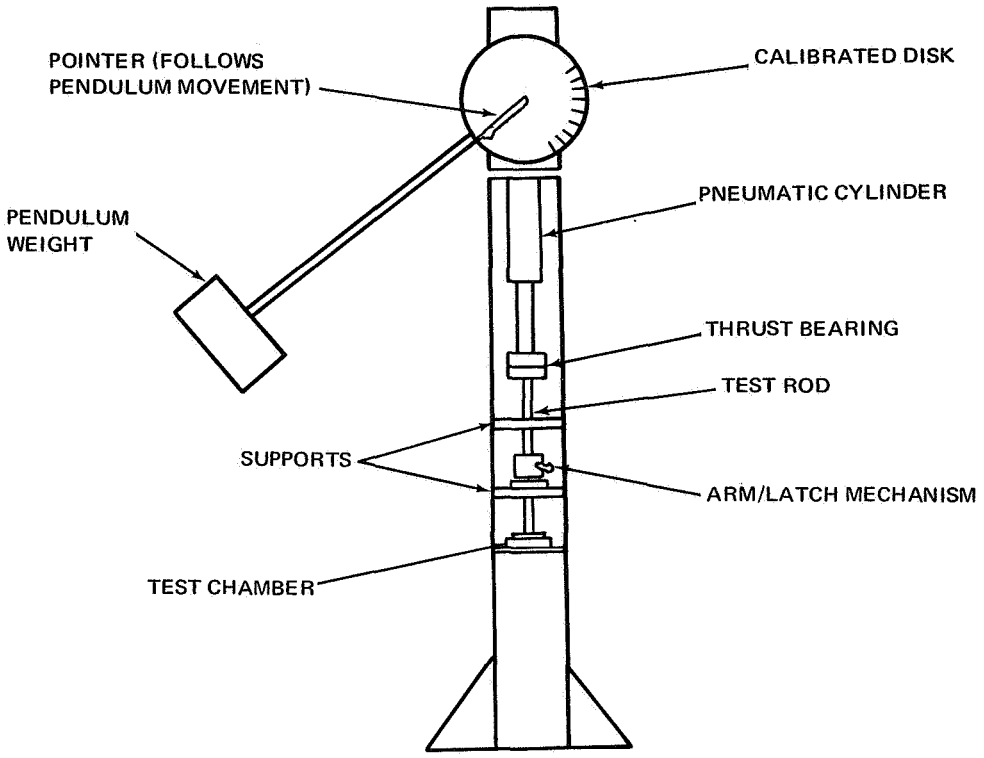

Figure 31. Schematic of Friction Test Apparatus

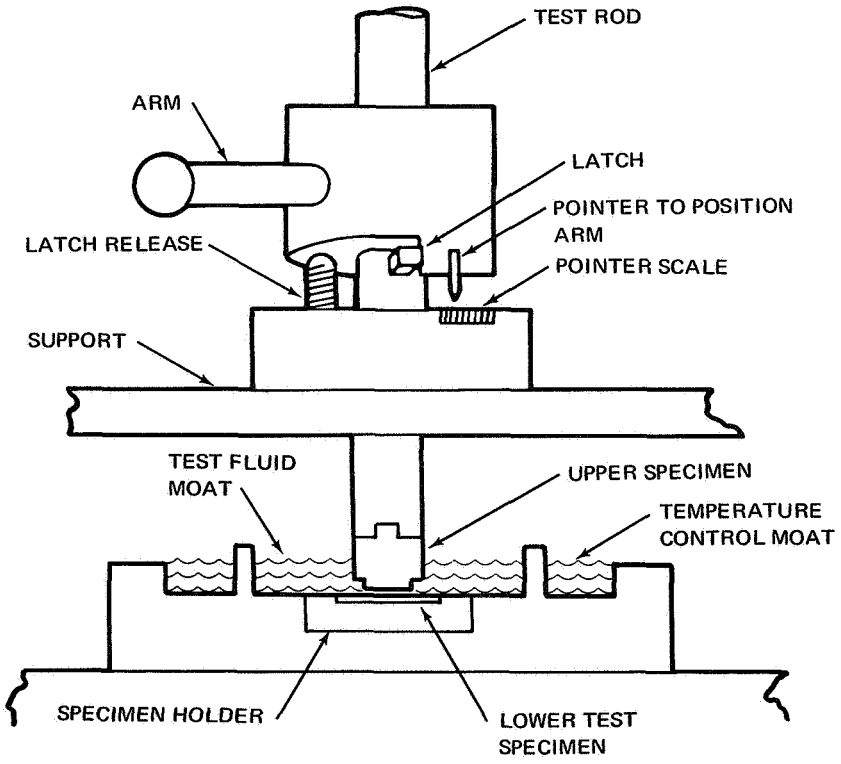

Figure 32. Schematic of Friction Test Specimen Chamber

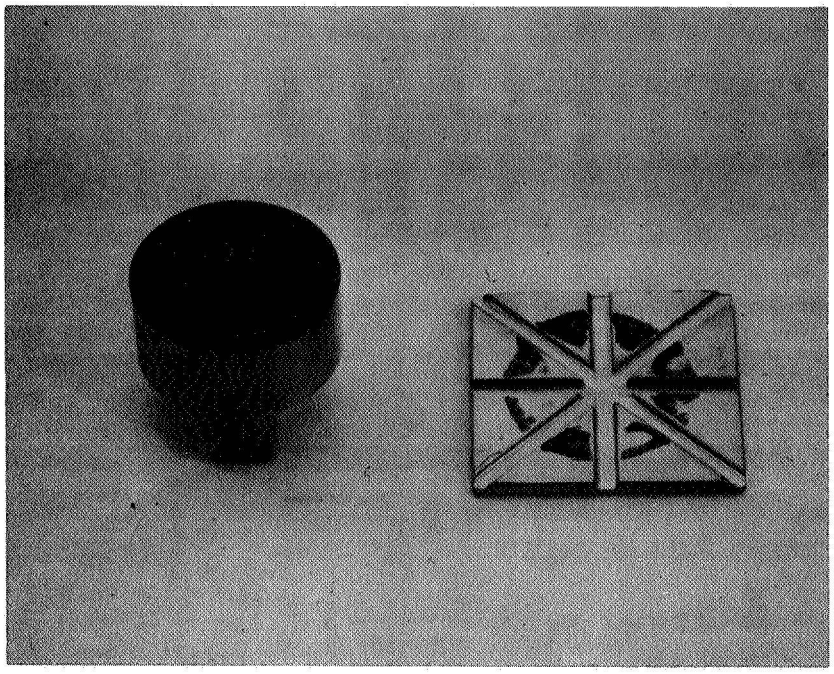

Figure 33. Silver Friction Test Specimens

Table 16

SILVER FRICTION TEST RESULTS

Test No.	Load-psi (pascals)	Coefficient of Friction
1	1,000 (6.90×10^6)	0.20
2	1,180 (8.14×10^6)	0.17
3	1,980 (1.37×10^7)	0.08
4	4,000 (2.76×10^7)	--
5	6,050 (4.18×10^7)	--

4.0 TASK IV: FILTER COMPATIBILITY TESTS

4.1 Introduction

The Task IV effort consisted of a study to determine the availability and suitability of existing propellant filters for fluorine service, and to evaluate by tests at least two types of filter elements. The evaluation tests were conducted at the MDAC-WD Test Facility using both uncontaminated fluorine and fluorine containing controlled amounts of solid particulates and solid hydrogen fluoride as contaiminants. Full-size, 2-in. (5.09×10^{-2} m) line size test items capable of flowrates of 20 lb/sec (9.08 kg/sec) at 50 psi (3.44×10^{5} pascals) supply pressure were to be tested.

The filter rating requirements were studied and a final rating size selected, based on the results of the Task II study and the rocket engine particle size requirements study. The effectiveness of the filters were evaluated on the basis of differential pressure across the filter, durability, and particle removal.

4.2 Summary

A survey was conducted of the various types of filters available that might be considered for a LF_2 propellant feed system. The general types of filters found suitable for this service included:

1. Sintered porous ceramic.
2. Sintered porous metal.
3. Sintered wire mesh.
4. Stacked metal disks.
5. Electrodeposited wire screen.

An investigation of the propellant-feed system filtering requirements of a number of missile and space vehicle systems led to the selection of a target filter rating of less than 70 microns (7.0×10^{-5} m) absolute. The filtration values selected for the actual test hardware were influenced by cost and schedule requirements.

Design proposals were solicited from several potential suppliers. From the proposals received, four filters were selected for compatibility testing: porous sintered aluminum oxide; two rating sizes of porous sintered nickel; and sintered nickel wire mesh.

The filter compatibility tests consisted of a total of 17 LF_2 flow tests in two categories: four short duration tests and 13 extended duration tests. All the candidate filter elements were shown to be compatible with LF_2, and effective in removing deliberately introduced contaminants from the flow stream. In addition, the 25-micron (2.5×10^{-5} m) sintered porous nickel

filter element was successfully operated for long duration tests of over 900 sec and then 10-micron sintered porous nickel element for 800 sec in LF_2 flow.

4.3 Filter Hardware

The initial objectives of this study were to determine the optimal filter rating for LF_2 feed systems, and to evaluate the presently available filters to find hardware suitable for fluorine systems. The propellant feed system filtering requirements for several large missile and space vehicle systems were investigated. As a result, it was tentatively decided to limit the test filters to under 70 microns (7.0×10^{-5} m) absolute. This is the same rating presently specified on most liquid-oxygen systems. A survey of the available liquid-oxygen filters that might be converted to LF_2 was then made. The survey indicated that there were apparently no acceptable candidates, unless the LOX filters were reworked to accommodate suitable filter elements. The filter elements available were predominantly wire-mesh or sintered metal.

Design proposals for test hardware were solicited from five filter manufacturers with emphasis on the design of the filter element and housing, the price, and the delivery schedule. The filter element types considered were sintered porous ceramic (aluminum oxide), sintered porous pure nickel, sintered (pure nickel) wire mesh, stacked (aluminum) disks, and electrodeposited (pure nickel) wire screen. Properly designed, each of the five types of filters should be acceptable for AGE service. The sintered aluminum oxide (Al_2O_3) elements appeared better than metal elements due both to the resistance to LF_2 reaction and to the relatively high resistance to any HF attack that might occur in the filter element.

Design proposals for test hardware were received from the following suppliers:

	Supplier	Filter Type
1.	Aerospace Components Corporation Los Angeles, Calif.	Sintered porous nickel
2.	Coors Porcelain Company Golden, Colo.	Sintered porous ceramic
3.	Vacco Industries El Monte, Calif.	Stacked aluminum disks
4.	Western Filter Col., Inc. Gardena, Calif.	Sintered wire mesh
5.	Western Gold & Platinum Co. (WESGO) Belmont, Calif.	Sintered porous Ceramic

Evaluation of these proposals revealed a need to establish a common interface requirement for the filter housing and all the filter elements. This would permit interchangeability of the filter lements in a single filter housing. Therefore, each supplier was requested to resubmit their proposal to the required design. Revised proposals were received, and the following filters were chosen for testing:

Porous ceramic element: 40-micron (4.0×10^{-5} m) absolute - WESGO Co.

Porous nickel element: 25-micron (2.5×10^{-5} m) absolute - Aerospace Components Corp.

Filter housing and sintered wire mesh element: 60-micron (6.0×10^{-5} m) absolute - Western Filter.

A 10-micron (10^{-5} m) absolute, porous sintered nickel filter element was later added to this list. Mott Metallurgical Corporation, Hartford, Connecticut, which subcontracted to Aerospace Components Corp. to supply the sintered nickel section of the 25-micron (2.5×10^{-5} m) filter, produced the 10-micron element for McDonnell Douglas.

4.3.1 Filter Housing

The standardized filter housing designed and fabricated by Western Filter Co., Inc., is shown in Figure 34. The housing was delivered to McDonnell Douglas in November, 1967. Despite prior radiographic inspection, the housing had a small weld crack. This was repaired and radiographically

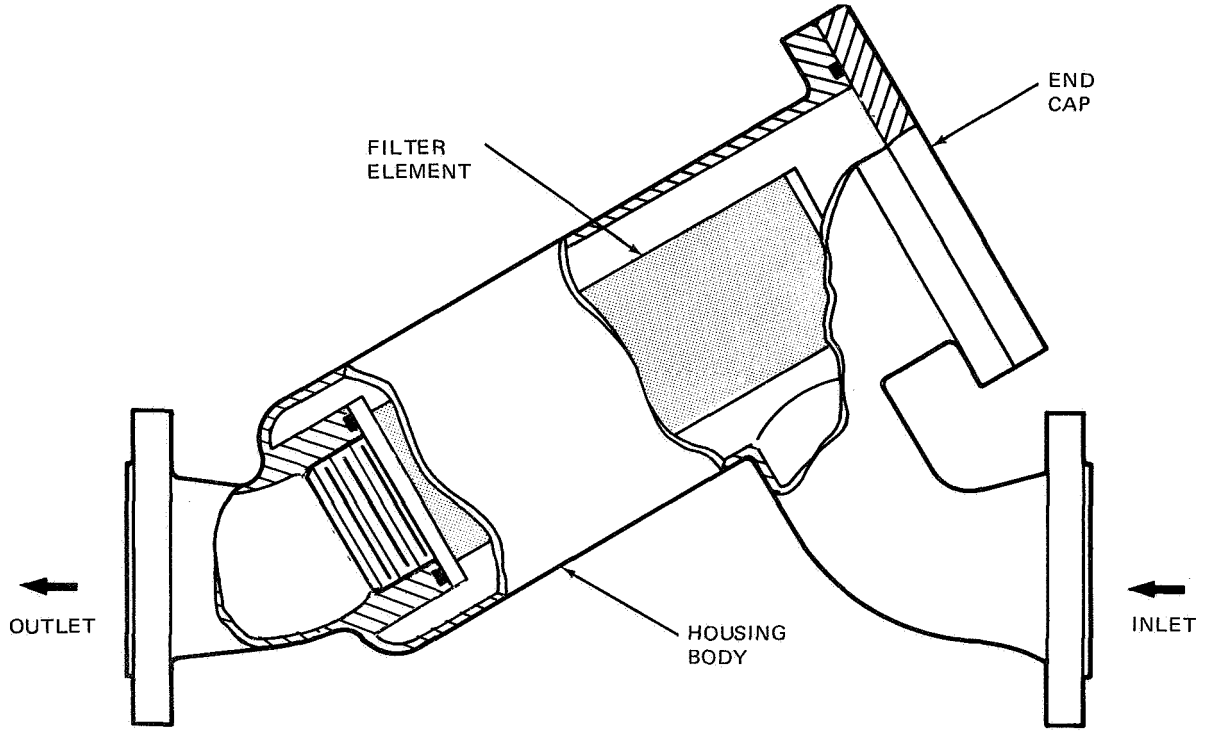

Figure 34. Filter Housing

re-inspected. In addition, the threads on the end of the test backup wire mesh element, and the mating boss on the filter housing, were machined with 12 threads per inch (473 threads per meter) instead of 8 threads per inch (315 threads per meter) as specified. Because of the delay in reworking the housing, Western Filter was allowed to convert the threads on the 25-micron (2.5×10^{-5} m) porous metal filter element to mate with the filter housing.

4.3.2 Sintered Nickel Element

The 25-micron (2.5×10^{-5} m) porous metal filter element was radiographically inspected at Douglas and showed no irregularity in the porous structure. Mott Metallurgical Corp., who made the element for Aerospace Component Corp., reported that the powdered nickel used had 99.9% purity. The mounting threads on the porous metal filter element were converted from 8 threads per inch (315 threads per meter) to 12 threads per inch (473 threads per meter) to mate with the filter housing.

This porous metal element, when assembled by welding, appeared subject to failure due to service and handling. After a preliminary checkout with liquid nitrogen, the porous nickel element developed a circumferential crack at the weld bead on the threaded end. It is not known whether the crack developed due to over-torquing during installation of the elements, cryogenic shock during the flow test, or the strain of removal. However, this filter element was sufficiently strong to endure a torque load to 1,400 lb-in. (1.52×10^2 newton-m) on the body before the checkout, and a liquid nitrogen flowrate of 6.02 lb/sec (2.72 kg/sec), with a differential pressure of 5.6 psid (3.86×10^3 pascals) across the filter assembly. The girth weld on the opposite end and the seam weld running the entire length of the element were not affected. An attempt to reweld the porous metal body of the filter element to the fitting end in an argon chamber using manual TIG welding was not successful. Although an apparently good weld bead could be laid over the edges, the porous body caused local parting of the pieces adjacent to the weld as the part cooled. Tack welding was attempted, but did not remedy this problem.

The use of brazing resulted in some improvement, but the brazing wire (ASTM 73.29, class 2) produced a zinc boiloff onto the sintered nickel element. This boiloff may be due to the temperature used to melt the wire. No hydrogen chamber was available to try to improve the brazing technique.

To alleviate the filter assembly problem, it was decided to eliminate the two girth weld joints altogether. The ends were cut from the sintered-nickel cylinder, and the cylinder was clamped between two metal ends held together mechanically by a tie rod. Figure 35 compares the original configuration and the revised configuration. Except for the sintered porous cylinder which is made of 99.9% pure nickel, all the component parts shown in the figure are stainless steel. The threads on the tie-rod are copper-plated to prevent galling during assembly. Another view of the revised configuration is shown in Figure 36.

Because of the success of this 25-micron (2.5×10^{-5} m) filter element, a 10-micron (10^{-5} m) porous sintered-nickel filter element was procured later in the program. Taking advantage of the experience gained during fabrication and testing of the first element, McDonnell Douglas procured only the sintered nickel cylinder for this element, and installed the nickel cylinder in the filter element assembly shown in Figure 36.

The original welded 25-micron (2.5×10^{-5} m) filter had been supplied by Aerospace Components Corp. However, Aerospace Components had purchased the sintered nickel cylinder, and at their suggestion McDonnell Douglas procured the new one directly from the supplier, Mott Metallurgical Corp.

4.3.3 Ceramic Element

Early in the program, a meeting was held with the Coors Procelain Company of Golden, Colorado, to obtain firsthand knowledge of porous ceramic elements. Technical discussion with Coors personnel revealed the following information:

1. Coors produces a ceramic AD-999 (99.98% pure alumina) most suitable for fluorine usage; however, Coors could not make a filter element for our program within a reasonable time due to material shortage and undeveloped technique in the application of this material to a porous element.

2. Coors ceramic AD-995 (99.5% pure alumina) or its equivalent was the best that could be made into a porous form suitable as a filter element.

3. The mechanical, thermal, and electrical properties of alumina ceramics were available for the solid, non-permeable materials, but the corresponding properties for the porous materials were not available.

4. No thermal shock data were available for porous media. However, Coors subsequently conducted a simple quick immersion test of porous alumina in a liquid nitrogen bath. The material performed acceptably under thermal shock conditions.

5. Coors recommended that we contact Western Gold & Platinum Company (WESGO) in California as an alumina fabricator.

To establish the procedure for preparation of the test filter elements, a series of 10 different porous ceramic sample disks of 99.6% pure aluminum oxide were received from WESGO and evaluated. The disks showed good porosity control, i.e., 45 through 55% voids, but had lower filtration ratings than desired. The filtration ratings were 14 through 37 microns (1.4×10^{-5} through 3.7×10^{-5} m) absolute; the design goal was 70 micron (7.0×10^{-5} m) absolute. The disk materials were tested and were not affected by three 5-min cycles of ultrasonic cleaning, or by immersion in a liquid-nitrogen bath.

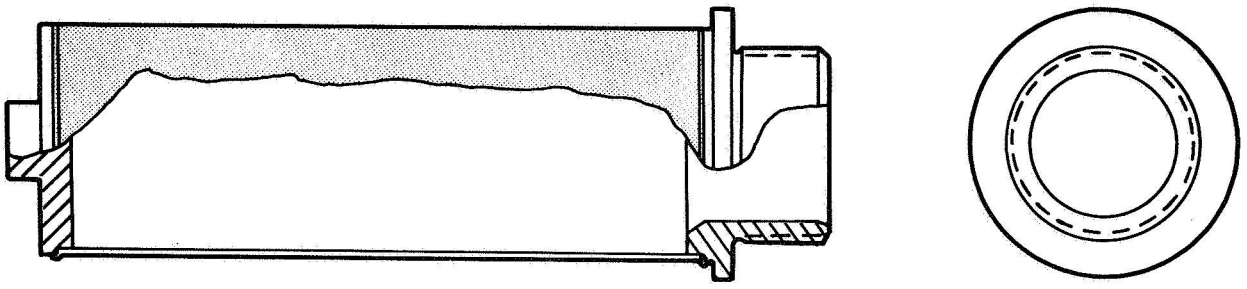

A. WELDED VERSION

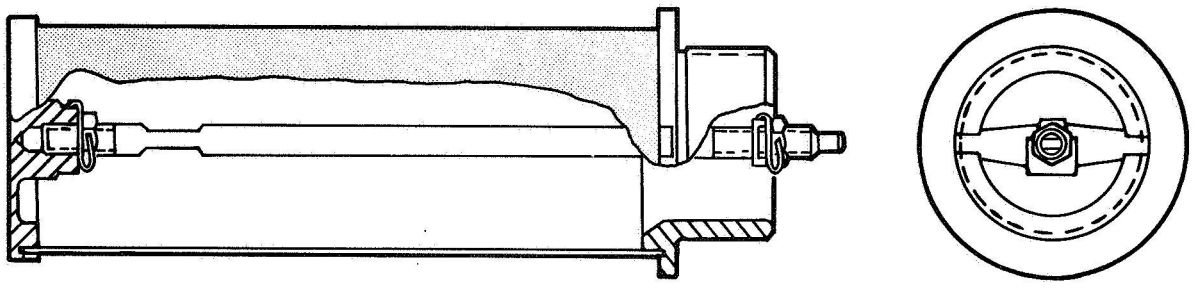

B. BOLTED VERSION

Figure 35. Porous Metal Filter Element

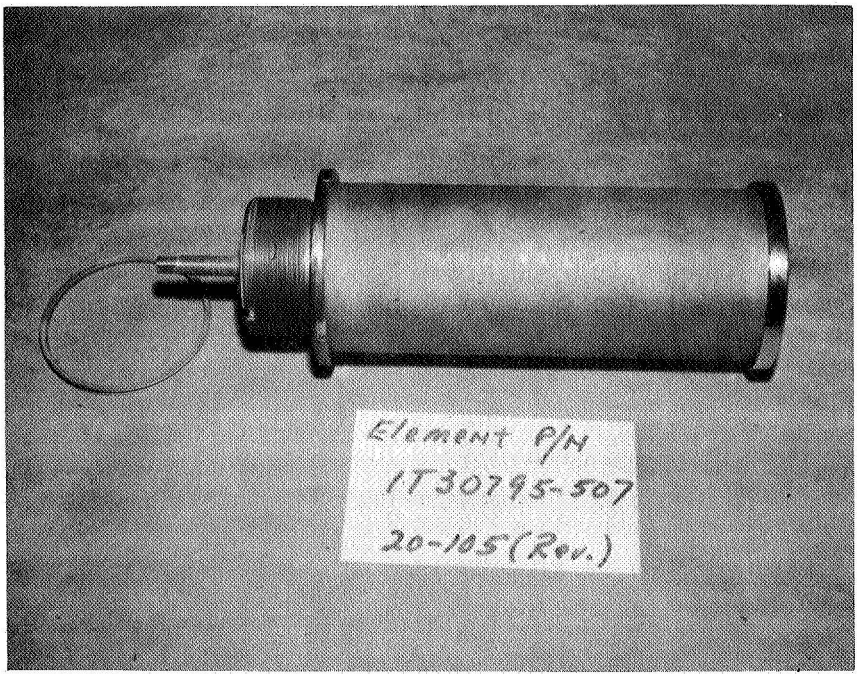

Figure 36. Sintered Nickel Filter Element

WESGO was requested to raise the filter ratings, since the finer pore sizes associated with the lower micron ratings result in relatively high pressure drops. WESGO suggested that the ceiling for the filtration rating of the sintered-ceramic element be extended to 110 microns (1.1×10^{-4} m) absolute, while keeping a porosity of 50% by weight. However, there was difficulty with the porous elements due to sagging of the lower half of the cylinder-shaped element during the sintering operation. Therefore, it was tentatively decided to accept the element in two 4-in. (1.02×10^{-1} m) sections rather than the planned 8-in. (2.03×10^{-1} m) long segment.

The first samples of 4-in. (1.02×10^{-1} m) and 8-in. (2.03×10^{-1} m) elements received from WESGO exhibited insufficient cohesion of the aluminum oxide particles that make up the sintered porous body. Although some improvement was achieved by reducing the porosity from 50% to near 40%, alumina grains still could be removed from the elements by scratching the surfaces with a fingernail. To reduce this lack of cohesion, WESGO increased the binder percentage from 1/2% to near 2%, by adding some silica. The use of silica had been completely avoided previously to optimize the fluorine compatibility of the filter. Since A356 cast aluminum containing 7% silicon is acceptable for LF_2 service, it was assumed that a 2% silicon content in aluminum oxide would not constitute a great risk.

To supplement the WESGO effort, a study was initiated by Douglas to determine the effects of porosity and shape on the mechanical properties of a high purity alumina body. It has been well established that the strength of a ceramic specimen will decrease with increasing porosity. For example, Figure 37 presents the predicted Young's modulus of elasticity and compressive strength as a function of percentage porosity based on the application of Sprigg's equation. (Reference 9) In addition, with a hollow cylindrical piece like this element, the normal practice is to make the length no longer than the diameter. The reason for this limitation is that the product must be placed on its end for furnace firing, and excess body weight could lead to distortion of the lower end during sintering unless elaborate precautionary techniques are used.

The first two acceptable 4-in. (1.02×10^{-1} m) sintered ceramic filter elements received from WESGO had a composition which included 0.7% magnesium oxide (MgO), and 1.3% silicon dioxide, resulting in a marked improvement in surface texture, strength, and machinability. WESGO had also fabricated some sample pieces of porous aluminum oxide which contained 0.3% silicon dioxide. This composition resulted in some improvement to the samples, but not as much as the addition of 1.3% silicon dioxide. Although further increases in silicon dioxide should improve this material even more, it was felt that the physical properties of the 98% alumina filter elements would be adequate for this program. The filter element assembly consisting of the element holder and two 4-in. (1.02×10^{-1} m) alumina cylinders is shown in Figure 38.

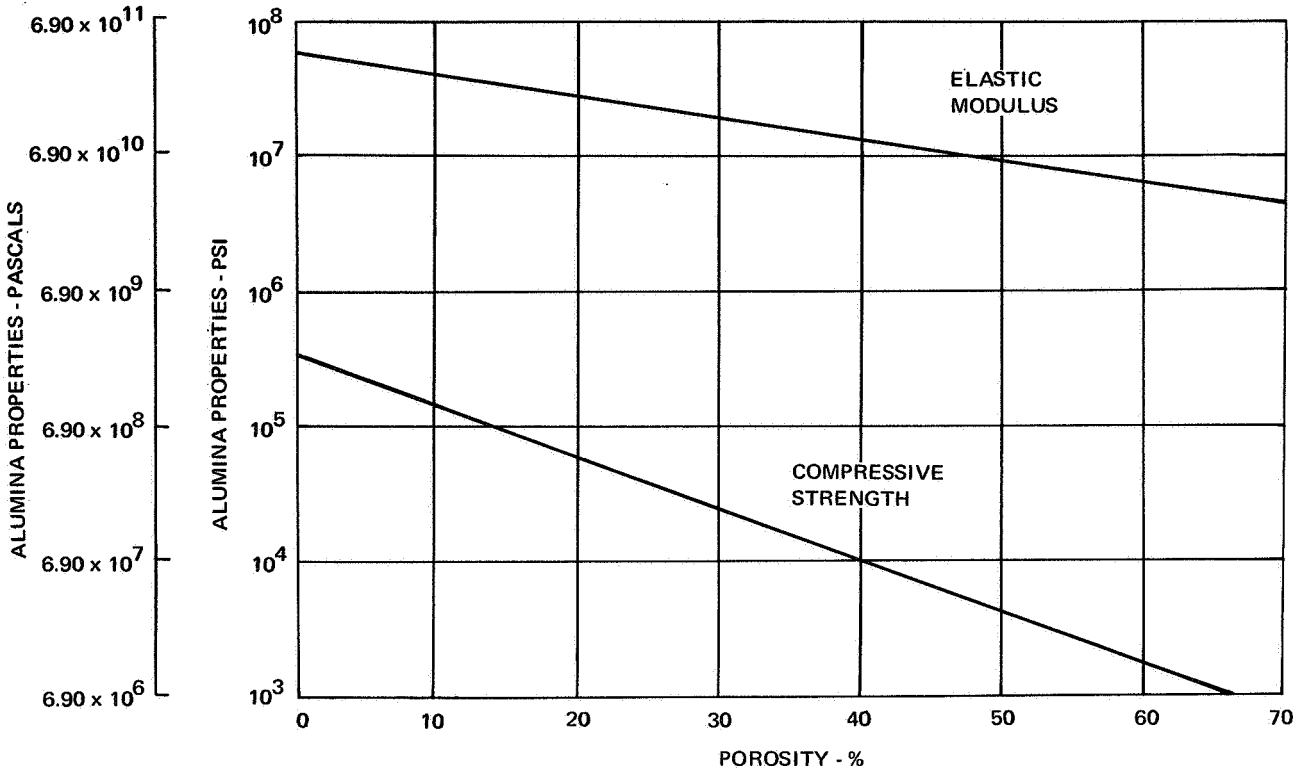

Figure 37. Effects of Porosity on Alumina Properties

The second and final set of two 4-in. (1.02×10^{-1} m) porous ceramic filter sections was received from WESGO 1 month later. These two segments were the results of readjusted isostatic forming pressure and sintering temperature. These data were obtained from further evaluation of the relationship between the dry pressing and isostatic pressing methods. WESGO reported that a good correlation between the two pressing methods was achieved by decreasing the pressure used in the isostatically formed parts. Compared to the first set of segments, the second two segments were more porous, but at the same time more uniform. The surfaces of the new segments were rougher, but they appeared to have adequate bond strength. With the receipt of the second set of segments, the first set was returned to the vendor for enlargement of the internal diameters which interfered with the element holder.

4.3.4 Sintered Wire Element

The sintered-nickel wire-mesh filter element was fabricated by Western Filter Co., Inc., with a filter rating of 60-microns (6.0×10^{-5} m) absolute. The completed filter element, together with the housing-to-element seal, are shown in Figure 39. This wire element was made of high purity nickel and of Dutch weave construction. The element is sintered to increase the strength of the wire mesh and to eliminate entrapment areas which would be difficult to clean properly.

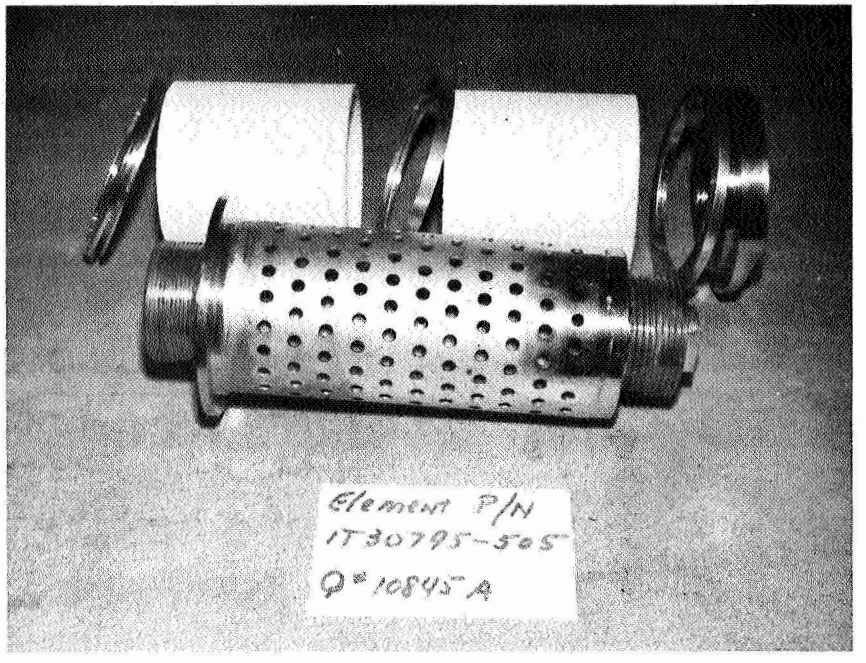

A. DISASSEMBLED

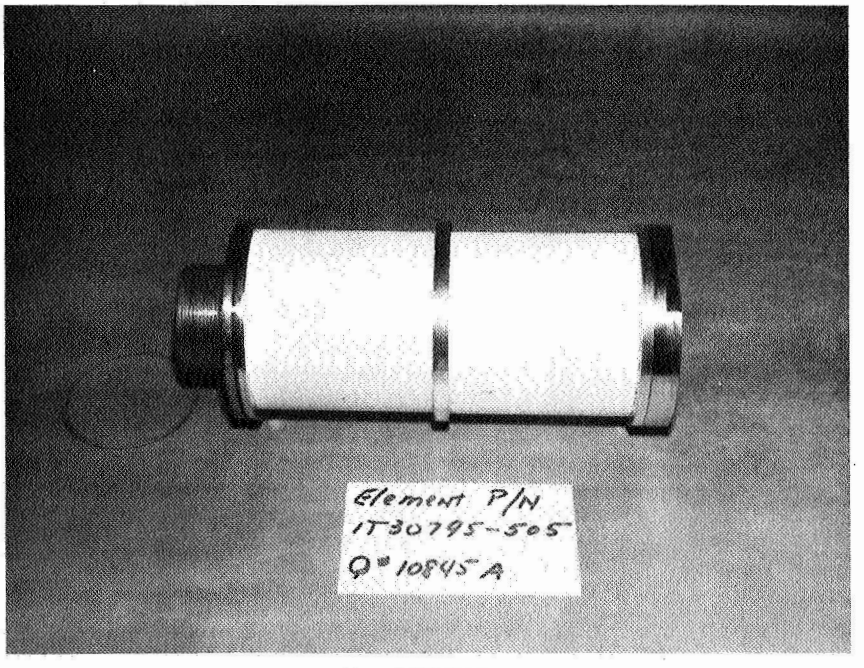

B. ASSEMBLED

Figure 38. Sintered Porous Ceramic Filter Element

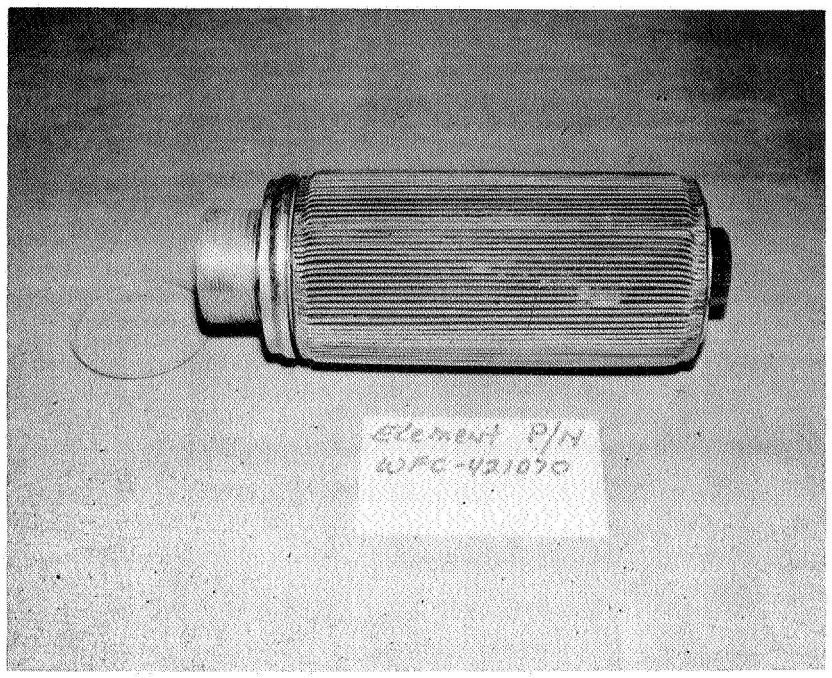

Figure 39. Sintered Wire Mesh Filter Element

4.4 Test Program

The filter compatibility test program was conducted in two phases: short-duration tests and extended-duration tests. The short-duration tests consisted of one run made with deliberately contaminated LF_2 introduced into the filters, and a control flow test made with uncontaminated fluorine. The three filters tested were the 25-micron (2.5×10^{-5} m) sintered porous nickel filter, the sintered porous ceramic filter, and the sintered wire mesh filter. The sintered porous nickel filter was tested twice making a total of four sets of short duration tests. The extended-duration tests consisted of six longer flow tests of the 25-micron (2.5×10^{-5} m) sintered nickel filter assembly to achieve a total flow duration of over 900 sec for this filter, and seven extended-duration tests of the 10-micron (1.0×10^{-5} m) sintered nickel filter procured later in the program.

The test setup is shown in Figure 40, and a schematic of the setup is given in Figure 41. A contaminant isolation test fixutre (CITF) was used to contain the metal test dusts and hydrogen fluoride. This fixture consisted of a burst disk housing welded onto an elbow and flange. The housing contained the metal dust and the hydrogen fluoride. After the housing was pressurized, the burst disk ruptured, and the contaminants passed down through the elbow and into the fluorine flow system. This arrangement virtually eliminated all potential fallout points of the test dusts upstream of the filter. The hydrogen fluoride was maintained in the liquid stage while in the CITF. The hydrogen fluoride subsequently froze upon contact with the LF_2 steam, after the

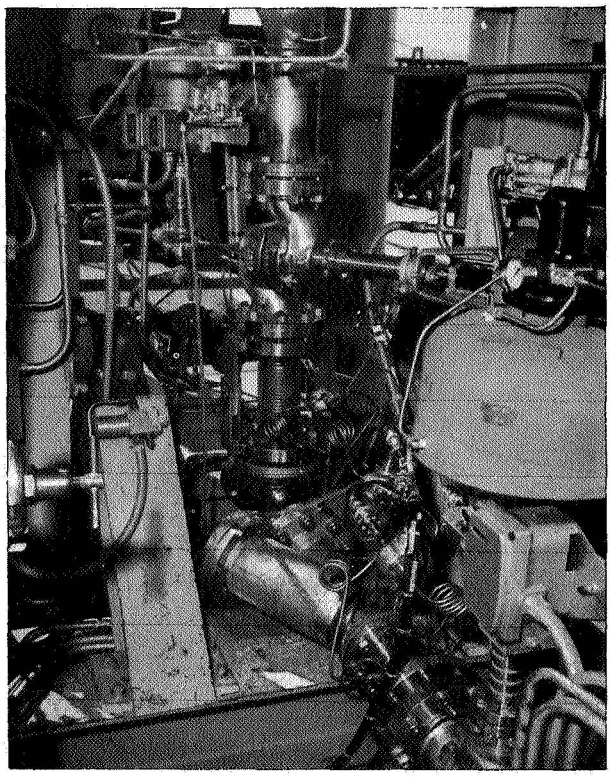

Figure 40. Filter Compatibility Test Setup

aluminum isolation burst disk had been ruptured. A checkout of the assembly using liquid nitrogen in place of the LF_2 stream, verified that the hydrogen fluoride remains in a liquid state inside the CITF during the test period. The CITF can be seen installed in the test system in Figure 42.

The contaminants selected for the evaluation tests were:

2 grams (2.0×10^{-2} kg) of stainless steel particulates at 100 to 150 microns (1.0 to 1.5×10^{-4} m);

2 grams (2.0×10^{-2} kg) of stainless steel particulates at 200 to 500 microns (2.0 to 5.0×10^{-4} m);

2 grams (2.0×10^{-2} kg) of aluminum particulates at 100 to 150 microns (1.0 to 1.5×10^{-2} m); and

2 grams (2.0×10^{-2} kg) of aluminum particulates at 200 to 500 microns (2.0 to 5.0×10^{-4} m).

The hydrogen fluoride was transferred into the contaminant chamber as a liquid from a supply bottle which contained 98.5% pure hydrogen fluoride.

The aluminum and stainless steel test dusts were the same type as the metal test powders used by MDAC Astropower during the passivation study program (Reference 10). Astropower had avoided the use of oil-contaminated metal

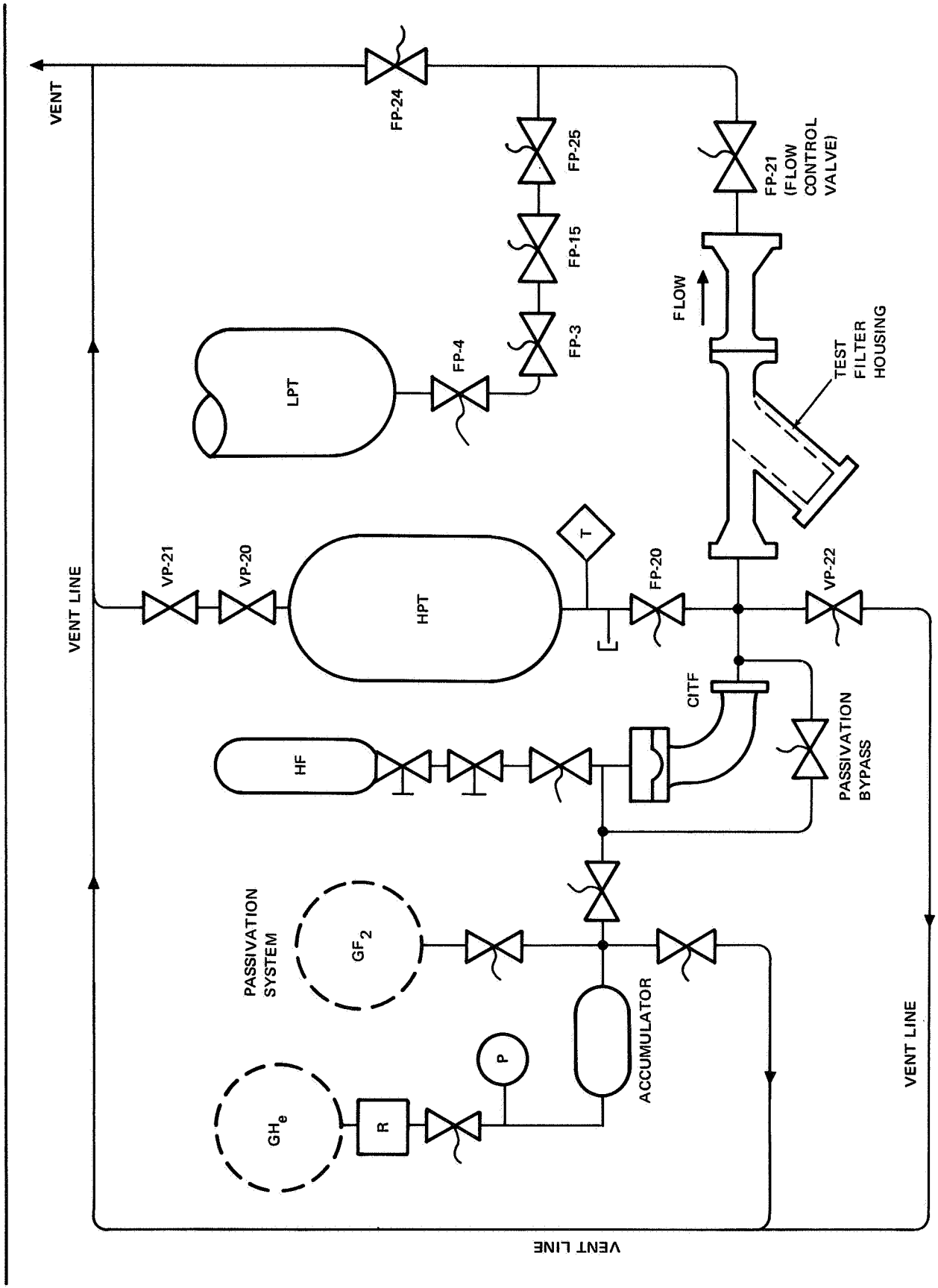

Figure 41. Filter Compatibility Test Schematic

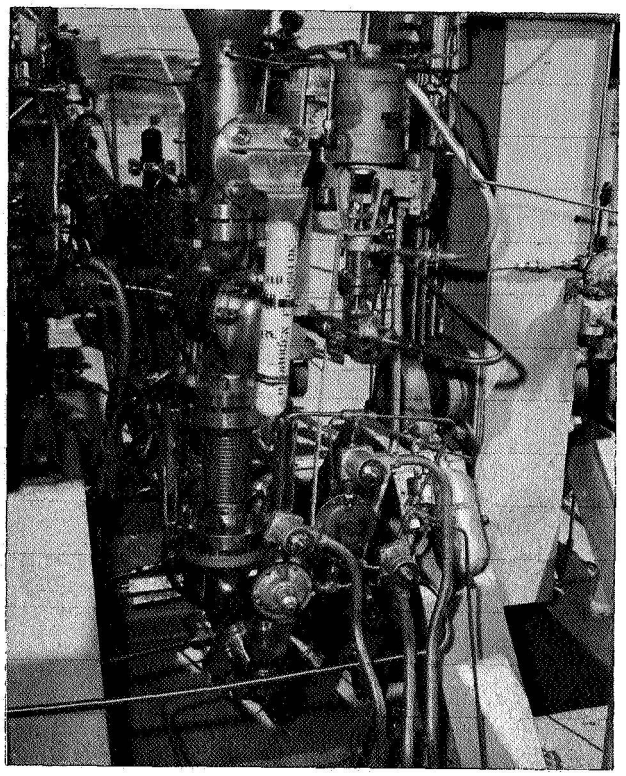

Figure 42. Contamination Isolation Burst Disk Installation

powders by studying the wetable quality of metal particulates in distilled water. All the powders which immediately sank to the bottom were considered oil-free and no cleaning of the test dusts were done. Except for one can of aluminum powder, all the dusts passed this test. The one questionable can of test dust was not used on this test program.

To evaluate the degree of contamination of the LF_2 in the closed-loop test system prior to conducting the filter tests, a separate test was run using a settling trap. Solid contaminants, both metallic and nonmetallic, were found in the trap after the test. Most of the contaminant consisted of small metal-colored particles.

Based on these findings a decision was made by MDAC-WD to warm up and clean the storage tank and other critical parts of the system before testing the filter elements. A boiloff and recondensing cycle was therefore added to the test plan for the filter compatibility tests to insure the cleanliness of the test fluid.

Prior to the filter compatibility tests, the 25-micron (2.5×10^{-5} m) porous metal and the wire mesh filter elements were flow-checked at cryogenic temperature with liquid nitrogen. The porous ceramic element was not checked because it was not yet available. The purpose of this pretest operation was to determine the integrity of the test elements in an inert cryogenic

environment. The test setup included the filter housing, the orifice flowmeter, and three pressure transducers scheduled for use on this program. The maximum liquid-nitrogen flowrate through the filters was limited to 7 lb/sec (3.18 kg/sec). This checkout disclosed the problem areas discussed in Section 4.3.2.

4.4.1 Short-Duration Tests

Three filter elements were tested during the short duration tests. The three elements were:

1. 25-micron (2.5×10^{-5} m) absolute, sintered high-purity nickel filter element supplied by Aerospace Components.

2. Sintered aluminum oxide (Al_2O_3) ceramic filter element supplied by WESGO.

3. Sintered high-purity nickel-wire filter element supplied by Wester Filter Company.

The test results and evaluations of these filter tests are discussed in the following paragraphs and are summarized in Table 17.

4.4.1.1 Sintered Nickel Element

The sintered-nickel filter element tested was originally intended to have a filter rating of 70-microns (7.0×10^{-5} m) absolute. However, the element actually tested had an estimated rating of 18-micron nominal, or 25-micron (2.5×10^{-5} m) absolute. This lower rating was a result of the size of high-purity nickel particles available for fabrication at the time the element was procured. Since the nickel particle size was not expected to affect the compatibility of this filter element, it was decided to test this standard nickel particle size on this program. However, the particle size did affect the welding problem experienced earlier in the program. If this sintered-nickel material were to be used for a 70-micron (7.0×10^{-5} m) service filter, further work would be needed to optimize the welding process for the particle size used.

The procedure for the first test consisted of three separate runs. The three runs were planned for 10 sec duration each and were to be accomplished as close together as possible. The first two runs were completed using distilled LF_2 which has a measured hydrogen fluoride content of approximately 0.02% by weight. These two runs were completed as scheduled and the LF_2 was returned to the storage tank after passing through the filter. During the third run, a premixed quantity of contaminant was scheduled to be released into the flow system after approximately 1.5 sec of clean LF_2 flow. This contaminant was released by rupturing a burst disk which was used to isolate the contaminant chamber. The contaminant chamber contained 8 gm (8×10^{-2} kg) of premixed metal dust and 1.8 in.^{3} (2.95×10^{-5} m^3) of anhydrous hydrogen fluoride.

Table 17

FILTER COMPATIBILITY TEST SUMMARY
SHORT DURATION TESTS

Uncontaminated Fluorine
Less than 0.05% HF

Test No.	Test Filter	Absolute Filter Size microns (m)	Duration (sec)	Average Pressure Drop psid(pascals)	Average Flowrate lb/sec (kg/sec)	Total Flow lb (kg)	Contaminants	Average Resistance Coefficient (K)
1a	Sintered porous nickel	25 (2.5×10^{-5})	23	21.2 (1.46×10^{5})	17 (7.72×10^{0})	390 (1.77×10^{2})	None	33
2a	Sintered ceramic	40 (4.0×10^{-5})	19	19.5 (1.35×10^{5})	20 (9.08×10^{0})	383 (1.74×10^{2})	None	21
3a	Sintered nickel wire	60 (6.0×10^{-5})	20	3.6 (2.48×10^{4})	26 (1.53×10^{1})	520 (2.36×10^{2})	None	2
4a	Sintered porous nickel (rerun)	25 (2.5×10^{-5})	28	18.5 (1.28×10^{5})	17 (7.72×10^{0})	460 (2.09×10^{2})	None	29
				Contaminated Fluorine				
1b	Sintered porous nickel	25 (2.5×10^{-5})	10	34.7 (2.40×10^{5})	7 (4.13×10^{0})	70 (3.18×10^{1})	(1)	303
2b	Sintered ceramic	40 (4.0×10^{-5})	10	18.5 (1.28×10^{5})	16 (7.27×10^{0})	160 (7.27×10^{1})	(2)	30
3b	Sintered nickel wire	60 (6.0×10^{-5})	10	2.0 (1.38×10^{4})	22 (9.98×10^{0})	220 (9.98×10^{1})	(2)	2
4b	Sintered porous	25 (2.5×10^{-5})	28	25.5 (1.76×10^{5})	13 (5.90×10^{0})	383 (1.74×10^{2})	(2)	60

(1) 8 gm (8×10^{-2} kg) of metal dust and 1.8 $in.^3$ (2.95×10^{-5} m^3) of HF

(2) 8 gm (8×10^{-2} kg) of metal dust and 0.8 $in.^3$ (1.31×10^{-5} m^3) of HF

The third run of the first test was completed without apparent difficulty, but the results were somewhat unexpected. The differential pressure across the filter showed the same characteristic rise at the start of flow as seen during the first two cycles. However, this pressure rise did not subside after reaching a peak as on the previous runs. The pressure drop across the filter should have stablized at a lower steady-state value before the scheduled time of introduction of the contaminants.

This third run was conducted with the filter outlet routed to the overboard vent system just prior to the start of the run (see Figure 41). This change in the LF_2 flow path downstream of the filter element resulted in a significant reduction in the absolute pressure at the filter outlet. The overboard vent system pressure was slightly higher than one atmosphere, while the storage tank ullage pressure was approximately 27 psia (1.87×10^5 pascals). This change in back pressure may have caused the filter differential pressure to remain at a peak during the start of the contaminant injection portion of the cycle.

A second possible explanation of the higher filter differential pressure before the scheduled injection of the contaminant is that the burst disk ruptured prematurely and released the hydrogen fluoride into the flow stream before the scheduled time.

The net result of this third test run was that the filter element was contaminated to such an extent that the flowrate was lower than desired. A careful examination of the recorded test data did not reveal the cause of the unusually high plugging of the filter element. Posttest inspection of the element showed no detectable damage as a result of this plugging. Based on the results of the first test, the following conclusions were reached:

1. The amount of hydrogen fluoride injected into the flow system should be reduced to prevent plugging of the filter element with hydrogen fluoride ice. This was accomplished by reducing the volume of the contaminant cavity from 1.8 to 0.8 $in.^3$ (2.95×10^{-5} to 1.31×10^{-5} m^3).

2. The burst disk lockup pressure should be monitored after each flow cycle to verify that premature rupture has not occurred.

3. The sintered nickel element test should be rerun, with the LF_2 flow during the third cycle returned to the storage tank rather than vented overboard.

After inspection, the filter element was back flushed at low pressure, and the contaminant flushed out was analyzed for quantity and composition. The results of this analysis indicated that the element had filtered out about 1 gm (1.0×10^{-2} kg) of the metal particles together with an unknown quantity of hydrogen fluoride ice. The remainder of the injected metal particles were found in the upstream side of the filter housing and in the flow passage on the upstream side of the filter. The flow loop downstream of the filter was inspected for particles but no evidence of contaminant of any type was found.

An absolute evaluation of the filter differential pressure could not be obtained, apparently because of the lower downstream absolute pressure due to the overboard venting. The higher-than-expected time delay between runs may have influenced this problem, also. However, it is significant that 460 lb (2.09×10^2 kg) of LF_2 passed through the filter in 30 sec without evidence of deterioration of the element. This is more significant when it is noted that during the last 10 sec, flow was accomplished with the element in a plugged condition and operating at a pressure differential of at least 34 psi (2.34×10^5 pascals).

4.4.1.2 Sintered Aluminum-Oxide Element

The sintered aluminum-oxide filter element was tested during the second test series and was found compatible with the test environment. The element tested was the last of a number of experimental elements which were prepared by WESGO to get a porous specimen of high-purity Al_2O_3 with sufficient strength to be useful as a filter element. Several changes were made by WESGO in the sintering temperatures, length of parts, particle size, and binder additions in an attempt to optimize the parts.

The test part, which consisted of two 4-in. (1.03×10^{-1} m) porous ceramic sections, was found LF_2-compatible and had sufficient strength to withstand the pressure differential imposed. However, there was still a noticeable tendency for particles to flake off during handling and assembly of the unit. Additional development will be required to obtain a porosity rating of 70 microns (7.0×10^{-5} m) while providing adequate mechanical strength with this element.

The changes to the test procedure discussed above were incorporated in this test. In addition, the overall time required for the test was kept to a total of 86 sec (for 30 sec of flowing). The detail changes for this test were:

1. The hydrogen fluoride quantity was reduced to 0.8 $in.^3$ (1.31×10^{-5} m^3)

2. The burst disk pressure rating was increased to 90 psid (6.20×10^5 pascals) (from 70 psid (4.83×10^5 pascals)) and pressure checks were made between the three runs to verify that the disk had not failed prematurely.

3. Overboard venting of the third cycle was eliminated, and all three cycles were completed with the fluorine being returned to the system storage tank.

These changes in test procedure eliminated the pressure differential problem encountered previously. The measured flowrate for this test was checked against the facility propellant weight measuring system and good agreement was obtained on all runs.

Back-flushing the filter element produced about 1 gm (1.0×10^{-2} kg) of solids. This material was analyzed and consisted primarily of the test dust injected into the system. A small quantity of Al_2O_3 particles was also found

in the analysis. A check of the system downstream of the filter revealed a few contaminant particles of aluminum dust. No Al_2O_3 particles were found downstream of the filter. There is no way of determining whether these aluminum dust particles had passed around the seals on the elements, or were residual particles left over from the first test. However, the quantity was so small that little significance was placed on their presence.

4.4.1.3 Sintered Nickel Wire Element

Because the first two tests were completed ahead of schedule, it became feasible to run the backup element design. This element was an alternate design to the first two elements and was supplied by Western Filter as a part of the filter housing assembly which they fabricated for this effort. This element was made of wire mesh of high-purity nickel which had the woven wires sintered together. The element was supplied with a rating of 60-microns (6.0×10^{-5} m) absolute because no wire of 70-micron (7.0×10^{-5} m) absolute design size was available on an off-the-shelf basis.

The test was run without difficulty and the results are summarized in Table 17. As expected, the relative differential pressure of the filter was much lower for this element than for the first two filter elements due to both the wire-mesh size and the shortness of the flow passage through the wire mesh.

Posttest inspection of the filter element revealed no evidence of damage. Back-flush of the element produced about 1 gm (1.0×10^{-2} kg) of particulate from the 8 gms (8.0×10^{-2} kg) of dust injected. While this element may have a somewhat lower filtering efficiency than the other two tested, it appears completely compatible with fluorine under the conditions tested.

4.4.1.4 Sintered-Nickel Element (Rerun)

Utilizing the remaining program time available, a retest was made of the sintered-nickel element. The test procedure was the same as that used on tests 2 and 3, except that greater flow time was desired. To accomplish the longer flow time, it was necessary to eliminate the fluorine distillation and to run the test with the propellant that was in the storage tank. Analysis of the propellant indicated an hydrogen fluoride level of 0.05% by weight during the tests.

The test cycles were also altered in that the original three 10-sec runs were replaced with two 30-sec runs. The contaminant level was unchanged, and the time of injection was 10 sec after the start of the second-run cycle. The overboard vent system had been eliminated for this test and the data are comparable with tests 2 and 3.

The data from this test were in good agreement with the expected values, and are shown in Table 17. The filter element was inspected after this test and no detectable change was found. The back-flushing procedure produced the characteristic 1 gm (1.0×10^{-2} kg) of contaminant dust and no other impurities.

4.4.2 Extended Duration Tests

Two porous sintered-nickel filter elements were tested during the extended-duration tests. The first was the 25-micron (2.5×10^{-5} m) absolute filter procured at the start of the filter test program; the second was a 10-micron (1.0×10^{-5} m) absolute filter obtained after successful testing of the first.

The extended-duration tests were conducted in the same test setup as the short duration tests. The significant difference between the two test series is in the flow times for the various runs. The extended-duration test procedure specified the following events:

1. A series of uncontaminated tests of approximately 250 sec, or until 5,000 lb (2.27×10^3 kg) of LF_2 have flowed through the filter.

2. A 1-week hold period to simulate a normal field condition. During this hold period, the filter assembly remained in the transfer line. The transfer line and the filter, together with the rest of the flow loop, was inerted with a helium purge and then isolated from the atmosphere by a low-pressure blanket purge.

3. After a minimum hold of 1 week, a second 5,000-lb (2.27×10^3 kg) flow cycle was conducted. During this flow cycle, contaminant was injected into the system after approximately 2,500 lb (1.14×10^3 kg) of LF_2 passed through the filter.

The test results and evaluations of the extended-duration filter tests are discussed in the following paragraphs.

4.4.2.1 25-Micron Filter

The 25-micron (2.5×10^{-5} m) sintered-nickel filter element was subjected to six extended-duration flow tests. During these tests 9,970 lb (4.52×10^3 kg) of LF_2 was filtered in a total flow time of 849 sec. Posttest inspection and evaluation revealed that the element and housing are still in serviceable condition after the completion of the test series.

The individual tests in this test series are summarized in Table 18. This table includes both the short and long duration tests on this filter element. These cumulative performance data show that the total flow of LF_2 through this one test sample was 11,273 lb (5.10×10^3 kg) over a total flow time of 938 sec.

An indication of the flow performance of the filter is given by the average resistance coefficient (K) of the element during a test. Resistance coefficient (K) is a measure of the pressure loss through a component of a fluid flow system in terms of velocity head. It is defined by the relationship

$$K = h_L / \frac{v^2}{2g} = 0.447 \rho \Delta P \left(\frac{A}{\dot{w}} \right)^2$$

Table 18

SINTERED NICKEL FILTER ELEMENT CUMULATIVE TEST SUMMARY

25-MICRON ABSOLUTE

(2.5×10^{-5} m ABSOLUTE)

Test No.	Duration (sec)	Average Flowrate lb/sec (kg/sec)	Average Pressure Drop psid (pascals)	Total Flow lb (kg)	Contaminants	Average Resistance Coefficient (K)
Short Duration Tests						
1a	23	17 (7.72×10^{0})	21.2 (1.46×10^{5})	390 (1.77×10^{2})	None(1)	33
1b	10	7 (3.17×10^{0})	34.7 (2.49×10^{5})	70 (3.17×10^{1})	(2)	303
4a	28	17 (7.72×10^{0})	18.5 (1.28×10^{5})	460 (2.09×10^{2})	None	29
4b	28	14 (6.35×10^{0})	25.5 (1.76×10^{5})	383 (1.74×10^{2})	(3)	60
Long Duration Tests						
1	143	11 (4.99×10^{0})	13.5 (9.32×10^{4})	1,630 (7.39×10^{2})	None	45
2	151	11 (4.99×10^{0})	19.4 (1.34×10^{5})	1,630 (7.39×10^{2})	None	73
3	136	12 (5.45×10^{0})	25.0 (1.72×10^{5})	1,640 (7.44×10^{2})	None	73
4(4)	120	14 (6.35×10^{0})	18.7 (1.29×10^{5})	1,650 (7.48×10^{2})	None	42
5	129	13 (5.90×10^{0})	21.0 (1.45×10^{5})	1,695 (7.69×10^{2})	None	52
6	170	10 (4.54×10^{0})	24.7 (1.70×10^{5})	1,725 (7.82×10^{2})	(3)	104
Total	938			11,273 (5.12×10^{3})		

(1) Contains less than 0.05% HF (by weight)

(2) 8 gms (8×10^{-2} kg) of metal dust and 1.8 $in.^3$ (2.95×10^{-5} m^3) of HF

(3) 8 gms (8×10^{-2} kg) of metal dust and 0.8 $in.^3$ (1.31×10^{-5} m^3) of HF

(4) Conducted after 13 day (1.12×10^{6} sec) hold period

where

h_L = head loss, ft (m)

v = average fluid velocity, fps (m/sec)

g = gravitational constant, ft/sec^2 (m/sec^2)

ρ = fluid density, lb/ft^3 (kg/m^3)

ΔP = pressure loss, psid (pascals)

A = flow area, $in.^2$ (m^2)

w = weight flowrate, lb/sec (kg/sec)

From Table 18 it can be seen that initially, the new filter element had a resistance coefficient of about 30 when flowing uncontaminated fluorine for short durations (Test 1a and 4a). Test 1b was the first contaminated test and it was determined that the hydrogen-fluoride addition was too great, causing excessive blockage of the filter element as seen by the K-factor of 303. Test 4b shows the results of the reduced contamination addition on filter performance; the resistance coefficient averaged 60 for the test.

The long-duration filter tests began with test number 1. A sufficient quantity of metal dust had become embedded in the filter during the initial tests to permanently affect its performance. This appears as a shift in average K-factor from around 30 to around 45. The second and third long-duration tests which followed test 1 in quick succession shown an increase in K-factor to 73. However, during test 4, after a 13-day hold at ambient conditions, the filter element exhibited a resistance coefficient of 42. The results of tests 5 and 6, which quickly followed test 4, again show the temporary increase in resistance seen during tests 2 and 3. The final test (No. 6) was the first contaminated test to be conducted as a part of the extended-duration test series.

These test results show that during repeated LF_2-transfer cycles the flow resistance of the filter increases. This is apparently due to progressive plugging of the filter element. The results also show that the flow resistance decreases after a hold at ambient conditions. Thus, the filter was catching a quantity of frozen particles which boiled off during hold periods at ambient conditions. These particles were probably frozen hydrogen fluoride which were stirred up from the bottom of the storage tank during the testing.

Each long-duration flow test was accomplished by flowing approximately 1,700 lb (7.71×10^2 kg) of LF_2 from the test tank to the storage tank. In each of the two long-duration tests series, the initial tests were made with fluorine that was transferred to the test tank from an undisturbed storage tank. During the flow test, the fluorine was returned to the storage tank, disturbing any settled hydrogen fluoride particles in the bottom of the storage tank. The test fluid for the second and third tests was then transferred from the storage tank to the test tank, and from there through the filter.

Posttest inspection of the filter revealed that a number of white plastic particles had been caught by the filter element and were distributed over the outer surface of the element. Several of these particles had washed into the gap between the element body and the two end caps. At several locations on each end cap, the plastic had reacted with the fluorine and burn marks appear on the stainless steel end caps as shown in Figure 43. No corresponding marks appear on the nickel element which has better heat-transfer characteristics than the stainless steel end caps. No permanent damage was observed on any of the parts.

Chemical analysis of the plastic revealed that all samples were of TFE Teflon which is used on the stem seals of the facility valves.

While this occurrence was not a planned part of the test run, it does show the acceptable performance of this filter-element material under representative conditions of operation.

4.4.2.2 Ten-Micron (1.0×10^{-5} m) Filter

The 10-micron (1.0×10^{-5} m) sintered-nickel filter element was subjected to seven extended-duration flow tests. During these tests, 11,560 lb (5.25×10^{3} kg) of liquid fluorine was flowed in a total of 800 sec. Posttest inspection and evaluation revealed that the element and housing were in excellent condition after the completion of the test series. The tests of this series are summarized in Table 19.

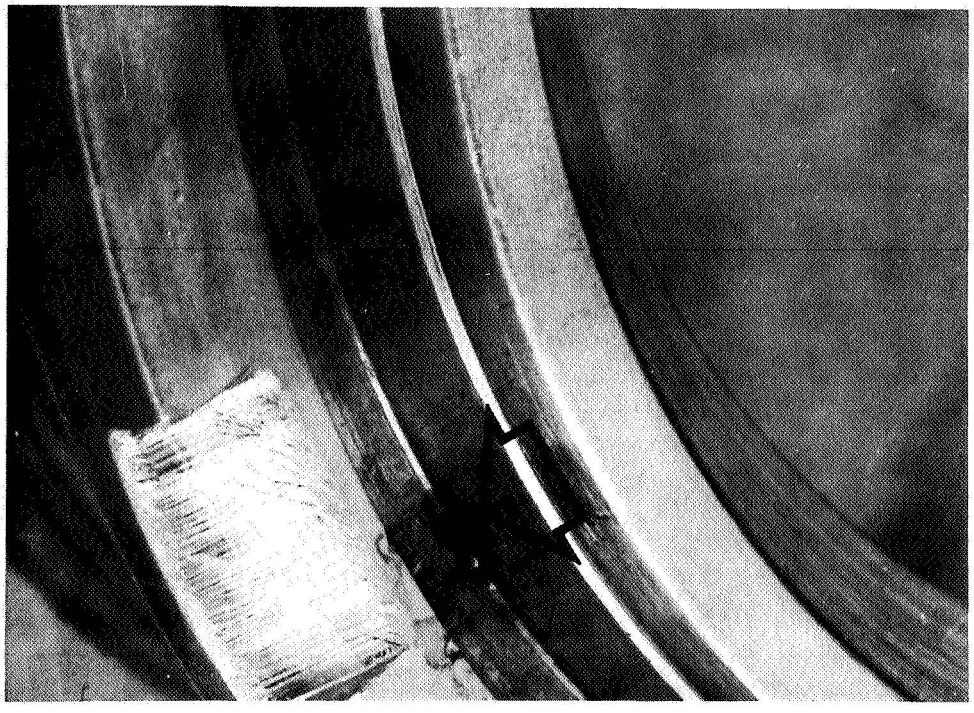

Figure 43. Sintered Nickel Element End Cap

Table 19

SINTERED NICKEL FILTER ELEMENT CUMULATIVE TEST SUMMARY

10-MICRON ABSOLUTE

(1.0×10^{-5} m ABSOLUTE)

Test No.	Duration (sec)	Average Flowrate lb/sec kg/sec)	Average Pressure Drop psid (pascals)	Total Flow lb (kg)	Contaminants	Average Resistance Coefficient (K)
Long Duration Tests						
7	89	18 (8.16×10^{0})	9.7 (6.70×10^{4})	1,565 (7.11×10^{2})	None(1)	13
8	96	17 (7.72×10^{0})	8.9 (6.14×10^{4})	1,565 (7.11×10^{2})	None	14
9	99	16 (7.27×10^{0})	8.9 (6.14×10^{4})	1,630 (7.39×10^{2})	None	14
10	110	14 (6.35×10^{0})	6.9 (4.76×10^{4})	1,550 (7.04×10^{2})	None	15
11	110	15 (6.81×10^{0})	7.4 (5.10×10^{4})	1,620 (7.36×10^{2})	None	15
12	104	16 (7.27×10^{0})	8.2 (5.66×10^{4})	1,680 (7.63×10^{2})	None	13
13	192	10 (4.54×10^{0})	30.6(2) (2.11×10^{5})	1,950 (8.85×10^{2})	(3)	16 to 569(2)
Total	800			11,560 (5.25×10^{3})		

(1) Contains less than 0.05% HF (by weight)

(2) After contamination

(3) 8 gms (8.0×10^{-2} kg) of metal dust and 1.2 $in.^3$ (1.97×10^{-5} m^3) of HF

The extended-duration tests were conducted in the same test setup shown schematically in Figure 41. The 10-micron (1.0×10^{-5} m) sintered-nickel element was received from the supplier, inspected, and cleaned ultrasonically and freon flushing, followed by a distilled-water rinse and oven-drying for 12 hours (overnight). After cleaning, the unit was installed in the filter housing and then installed in the fluorine flow loop.

The first series of long-duration tests (tests 7, 8, and 9), was completed with a transfer of 4,760 lb (2.16×10^3 kg) of liquid fluorine in a total run time of 284 sec. The results of these tests are given in Table 19. Nothing unusual was detected during the running of the three individual tests which constitute this test series except that the resistance coefficient of the filter was lower than expected. From Table 19, the resistance coefficient for the first three tests are about 14 as compared to a value of 42 to 73 for the 25-micron (2.5×10^{-5} m) element.

Since the 10-micron (1.0×10^{-5} m) element would be expected to have had a higher flow resistance, it was suspected that the element might have loosened in the housing and allowed some of the fluorine flow to bypass the filter element. To check on this possibility, the end cap was removed from the housing and a visual inspection made of the element assembly. No loosening or damage of the element could be observed without removal of the element. The filter element was therefore removed from the housing and taken into the clean room for a detailed inspection.

No damage or loosening of the filter element assembly could be detected after a complete inspection, but it was noted that the retaining nut on the central tie bolt which holds the assembly together had lost its retaining torque. Attempts to retorque the nut were unsuccessful since the stainless-steel spring assembly would deform when the nut was tightened. To eliminate this problem, a heavy spring backup plate was fabricated and cleaned, and reassembled in the element assembly. With the backup plate, the normal torque value of 40 lb-in. (4.35×10^0 N-m) was obtained on the retaining nut. This modification was completed in one afternoon and the element was reassembled into the flow loop for the 7-day hold period.

The second test series (tests 10, 11, and 12) of the extended-duration tests was completed as scheduled, except that the contamination was not injected into the LF_2 flow as originally planned. Because of uncertainty as to the cause of the low; pressure drop, it was decided to complete the first test of the series and determine the performance of the element under noncontaminated conditions. If the measured filter differential pressure appeared to be a reasonable value, the contamination would be released as originally planned. If, on the other hand, the ΔP was still found unusually low, the test would be completed for the full duration without the release of the contamination. The realtime data on this test run indicated that the pressure drop was still very low, so the test series was completed without contamination, yielding a total LF_2 transfer of 4,850 lb (2.20×10^3 kg) in 323 sec. The filter ΔP and flowrate were almost exactly the same as on the earlier test series.

After completion of this test series, the complete filter assembly was removed from the flow loop and returned to the clean room. Disassembly and inspection revealed that the element appeared undamaged and would be acceptable for further testing. To evaluate the possibility that liquid was bypassing the filtering part of the element by flowing between the element and the end caps, a water flow test was made on both the 10-micron (1.0×10^{-5} m) element and the 25-micron (2.5×10^{-5} m) element. In both cases, the element exhibited uniform flow through the filter element and no indication of excessive end flow was detected.

During the water flow tests, it was noted that the 10-micron (1.0×10^{-5} m) element was longer than the previously tested 25-micron (2.5×10^{-5} m) element. This was due to the area that was sacrificed when the original 25-micron (2.5×10^{-5} m) unit was changed from the welded design to the bolted design. To counteract any effect from this difference in length, the 10-micron (1.0×10^{-5} m) element was trimmed down to the same length as the 25-micron (2.5×10^{-5} m) unit. The length of this element was originally 8.5 in. (2.16×10^{-1} m), then changed to 7.75 in. (1.97×10^{-1} m).

Based on the water-flow test results, it was decided to return the 10-micron (1.0×10^{-5} m) unit to the fluorine flow loop and conduct a single-flow cycle with contaminant injection.

This test was completed successfully with no indication of contaminant passing through the filter. The uncontaminated portion of the test stabilized at a pressure differential of 14.6 psi (1.01×10^5 pascals) with a flowrate of 20 lb/sec (9.08×10^0 kg/sec), indicating a resistance coefficient of 16. This increase in resistance was expected due to the shortened length of the filtering element. When the contamination was injected, the pressure differential increased to 30.6 psi (2.11×10^5 pascals) and the flowrate decreased to a level too low to give a reading on the flow-measuring orifice. The filter was not completely plugged, and so the remaining LF_2 was transferred through the element. Based on a time-versus-weight measurement, a flowrate value of 5 lb/sec (2.27×10^0 kg/sec) was established for the final filter flow. This test transferred 1,950 lb (8.85×10^2 kg) of LF_2 in a run-time of 192 sec.

Because the degree of filter plugging on this test was higher than had been expected, a complete recheck of the contaminant injection system was made. It was determined that during the reinstallation of this system for the last test, an extra piece of tubing was installed between the hydrogen fluoride bottle and the injection burst disk. This extra length of tubing increased the hydrogen fluoride volume to 1.2 in.^{3} (1.97×10^{-5} m^3) from the specified 0.8 in.^{3} (1.31×10^{-5} m^3). While this change produces a test condition which was more severe than had been planned originally, it does improve the confidence level for the compatibility of this type of filter element.

The filter assembly was disassembled and inspected. No deterioration of the element was detected and no contaminant was found in the system downstream from the filter. The excellent performance of the 10-micron (1.0×10^{-5} m) sintered nickel element makes it a prime candidate for future filtering requirements.

At the conclusion of the testing portion of this task, an investigation was made into the difference in measured differential pressure for the two sintered nickel elements. A check with Mott Metalurgical Corporation, the fabricator of the two elements, revealed that the 10-micron (1.0×10^{-5} m) element had been bubble tested as requested and was within the specified 10-micron (1.0×10^{-5} m) range. As discussed previously, this element had been ordered directly from Mott, while the 25-micron (2.5×10^{-5} m) element was obtained from Aerospace Component Corporation, which accomplished the original assembly of the welded-construction, sintered-nickel element. The request for a bubble test on the 25-micron (2.5×10^{-5} m) element was apparently lost and no record of the bubble rating for this element is available. Visual inspection of the nickel particle size used in the 25-micron (2.5×10^{-5} m) element indicate that it is close to the predicted 25-micron (2.5×10^{-5} m) rating.

4.5 Conclusions

It can be concluded from the results of this effort that suitable materials and acceptable design techniques are available to produce full-size filters suitable for use in LF_2 service. Materials with high thermal heat conductivity and high-ignition temperatures are preferable for use in the critical filter elements.

High-purity nickel has the highest ignition temperature of the common metals recommended for LF_2 service (see Reference 1) and a thermal conductivity which is four times greater than for the 300 series CRES. This combination of properties makes the high-purity nickel the preferred material for metal filter elements.

Aluminum oxide (Al_2O_3) is a ceramic which is already in a completely oxidized state and is therefore highly resistant to reaction with either LF_2 or hydrogen fluoride. (It should be noted that this high-purity sintered Al_2O_3 is a high density, hard, nonabsorbent form of Al_2O_3 and has completely different mechanical properties than the specially prepared activated absorbent alumina which is used for fluorine scrubber service.)

The sintered nickel, sintered Al_2O_3, and the sintered-nickel wire elements were all found compatible with LF_2 when used in filter service. While the objectives of this task did not include optimization of filter mechanical design, the test results obtained can be useful for design selection. For service requiring high mechanical reliability without requiring a high filtration efficiency, the sintered-nickel wire element would be recommended due to its simplicity of construction and ease of handling. For applications requiring a high filter efficiency, the sintered-nickel element with welded construction would be recommended. The sintered Al_2O_3 design is compatible with LF_2 and will have a high filter efficiency. However, the problem of obtaining an acceptable seal between the element and the housing requires special consideration. This special consideration would probably be justified for the design of a filter which would be exposed to high concentrations of aqueous hydrogen fluoride due to the high inertness of this material.

5.0 TASK V: EXPLOSIVE VALVE COMPATIBILITY TESTS

5.1 Introduction

The need for shutoff valves capable of providing extremely low leakage rates for long-duration deep-space vehicles has created an interest in explosively actuated valves. These single-function valves are capable of obtaining low leakage rates because of the high degree of plastic deformation obtained on valve closure. Some question as to the feasibility of the valves for fluorine has been raised because of the effects of heat generated by this plastic deformation and because of the leakage of the propellant gases into the fluorine.

Task V consisted of evaluating explosively actuated shutoff valves suitable for fluorine. The study encompassed small valves in the line-size range of 1/4 to 3/8 in. (6.35×10^{-3} to 9.52×10^{-3}m)and large valves in ranges up to a 2-in. (5.08×10^{-2}m) line size. Six valve manufacturers submitted designs which included the normally open (N/O) and normally closed (N/C) configurations; these designs were evaluated for liquid and gaseous fluorine. Complete valve assemblies from four different suppliers, and explosive actuators (squibs) from three other suppliers were evaluated. Valve testing was limited to the small size range and included LF_2 and gaseous fluorine tests.

The valves supplied by three manufacturers were found to be compatible with LF_2 and gaseous fluorine. Valves from a fourth supplier were found to be compatible with gaseous fluorine but not with LF_2. The results of the evaluation of the failure in LF_2 of the valves from the fourth supplier were inconclusive, and additional testing is needed to isolate the exact cause of failure.

5.2 Summary

The compatibility of fluorine with valve designs submitted by the following six suppliers of explosive valves was studied:

1. Pyronetics Inc., Santa Fe Springs, Calif.
2. Conax Corporation, Buffalo, N.Y.
3. Pyrodyne Division of William Wald Corp., Santa Monica, Calif.
4. Pelmec Division of Quantic Industries, San Carlos, Calif.
5. Holex Corp., Hollister, Calif.
6. Wallace O. Leonard Inc., Pasadena, Calif.

A total of 25 design configurations were submitted. These designs represented valves readily available and potentially suitable for fluorine use. Many of the valve designs were similar to those of other suppliers.

Twelve valve configurations were selected for testing. These valves represented important design criteria for fluorine service which could not be readily analyzed as to their fluorine performance. The two basic designs were

incorporated into a test matrix containing a series of four tests with four valves being tested for each test. A valve failure on the third test required a rerun of test 3. The final test matrix is shown in Table 20.

The evaluation tests were designed to provide answers to several component variables which do not lend themselves to an analytical solution. These variables are the effects of:

1. Gas blowby into the fluorine
2. Ignition effects of metal shearing
3. Ignition effects of frictional heating
4. Leakage characteristics of various mechanical designs

During this test series two valves of one type (Conax 18300600) failed completely and two other designs (Conax 1802-087 and Pyrodyne 9163) were found to be somewhat unsatisfactory.

For larger sizes of valves and for critical applications of small valves the keyhole and swaged tube configurations appear to offer the greatest margin of safety and would be recommended for most applications. The use of mechanical gas seals which are compatible with LF_2 is considered to be acceptable for LF_2 service.

No difference was found in operation of the aluminum or CRES versions of acceptable valve designs. With proper attention to detail design considerations all of the valves tested should be capable of acceptable performance in LF_2 service.

The exposed-pin configurations were found to be unacceptable with the present clearances on the interference fit sealing arrangement when used in cryogenic service. A change in the design of the interference fit between the exposed pin and trigger housing and the addition of a low friction plated surface on the pin are recommended as potential design modifications. Gold and silver plating are recommended for this service.

Additional tests were conducted to evaluate the compatibility of fluorine with explosive squibs. Although these squibs are not exposed to fluorine under normal operation, accidental exposure could occur. The squibs tested were taken from valves that were supplied for testing or that were ordered separately for these tests. Three squib types were identified and subsequently tested during this program. They were manufactured by the following:

1. Pelmec Div., Quantic Industries, San Carlos, Calif.
2. Hi Shear
3. Holex, Inc., Hollister, Calif.

Table 20

EXPLOSIVE VALVE TEST

Test No.	Test Medium	Manufacture	Model No.	Type	Remarks
1	LF_2	Pyronetics	1300 Quad	N/C	Standard design with aluminum cup seal
				N/O	Standard design with aluminum cup seal
				N/C	Standard design with bal seal
				N/O	Standard design with bal seal
2	GF_2	Conax	1802-087-08	N/C	17-4 in 310 CRES body
			1801-045-08	N/O	17-4 in 310 CRES body
			1802-087-07	N/C	17-4 in 2024-T4 AL body
			1801-018-01	N/O	17-4 in 2024-T4 AL body
3	LF_2	Conax	18300600	N/C	Con-o-cap AL body
		Pyrodyne	9163	N/O	Copper plated cork - 304 CRES body
		Conax	1802-087-08	N/C	17-4 in 310 CRES body
			1801-045-08	N/O	17-4 in 310 CRES body
4	LF_2	Pelmec	1200	N/C	Standard design CRES in CRES
			1485	N/O	304 CRES swaged tube type
		Conax	1802-087-08	N/C	17-4 in 310 CRES body
		Pyrodyne	9163	N/O	Copper plated cork - 304 CRES body
5	LF_2	Conax	1802-087-07	N/C	17-4 in 2024-T4 AL body
			1801-045-08	N/O	17-4 in 310 CRES body
			18300600	N/C	Con-o-cap AL body
			1801-018-01	N/O	17-4 in 2024-T4 AL body

All of the squibs were found satisfactory for fluorine when acceptable cleaning procedures were used. Two squibs failed explosively during testing; however, it was found that external incompatible materials (nylon or Krytox) were the likely cause of failure.

5.3 Discussion

5.3.1 Evaluation Study and Component Selection

A survey of explosive valves available was completed at the outset of the Task V effort. Engineering data were received from several explosive valve manufacturers. From these data, the following five suppliers were identified who had valves which appeared to be potential candidates for use with fluorine:

1. Pyronetics, Inc.
2. Conax Corp.
3. Pyrodyne Div., William Wald Corp.
4. Pelmec Div., Quantic Industries
5. Holex, Inc.

None of these suppliers had existing valves designed for fluorine. However, each of them had valves which appeared suitable for evaluation testing with minor modification. This testing was conducted to evaluate the design variables critical to successful operation. The variables evaluated were:

1. Squib gas blowby into the fluorine stream.
2. Heating from metal shearing during valve actuation.
3. Heating from friction during valve actuation.
4. Material compatibility of the materials used in valve construction.
5. Sealing ability of the valves before and after operation.

The valve designs were selected for testing on the basis of which could provide the most information on these critical design variables.

5.3.1.1 Squib Gas Blowby Into the Fluorine Stream

Valve damage or complete failure caused by the reaction of hot burned gases with the fluorine propellant is possible when explosive valves are used with fluorine. It is expected that an explosive reaction would occur if the fluorine is exposed to the hot burning gases from the squib assembly. The products of combustion of oxidizer-rich propellant would be expected to react less violently with fluorine than the products of combustion of fuel-rich propellant. Mixture ratios of the squib charges used in the valves studied were not available from the explosive-valve suppliers. All powder charges studied were of the detonating type (fast burn) when operated at the combustion pressures obtained in explosive valve service. With detonating-type powders, it would be expected

that small amounts of gas leakage could be tolerated in the valve because the narrow leak paths through the metal parts would tend to quench the residual heat of combustion of the completely burned gases. A large leak rate would prevent the quenching effect of the metal parts and could only be tolerated if the temperature of the fluorine is low enough to quench the heat of the gases. The sealing method used to seal the propellant charge then becomes an important consideration.

The valves studied in this program utilized three of the four common methods of sealing the burned gases of the squib propellant from the fluorine stream. The four common methods, in order of increasing seal leakage are:

1. Diaphragm/Bellows
2. Interference
3. Mechanical fit

Valves incorporating all of these methods were considered on this program. The diaphragm seal was used on the Pelmec 1485 valve and consisted of a stainless steel (CRES) tube which separates the fluorine stream from the squib-actuation portion of the valve (see Figure 44). This design provides zero leakage of the burned gases during all normal operations.

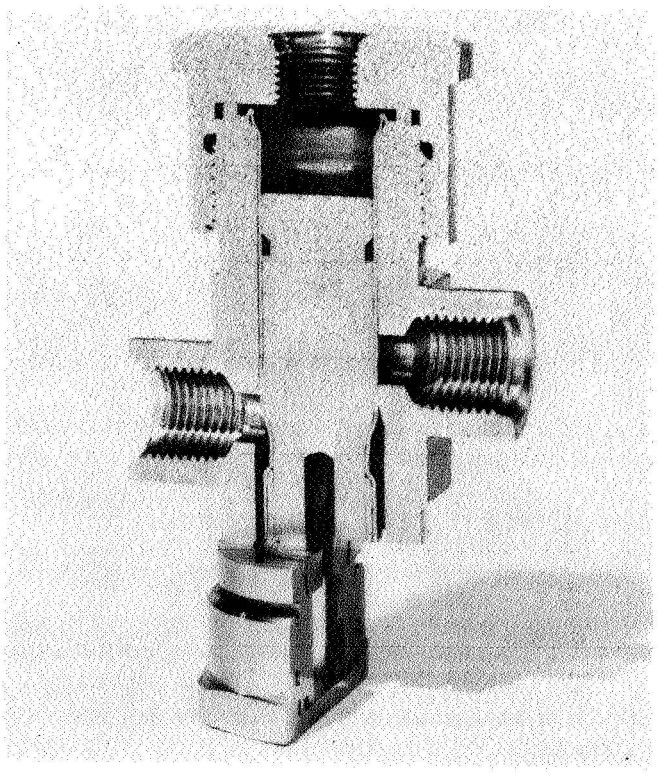

U. S. PATENT 3,422,832

Figure 44. Pelmec 1485 Expandable Tube Valve

The bellows seal was studied on some proposed valve designs of the Pyrodyne Co., but these designs were for large valves; (1-1/2 to 2 in.) (3.81×10^{-2} to 5.08×10^{-2} m) therefore, they were not considered to be available for this program. The bellows seal would be expected to provide zero leakage, no supplier was found who proposed a bellows seal for the small 1/4-in. valve. It would be expected that the diaphragm seal and the bellows seal would provide similar performance.

The interference-fit method of sealing the squib gases was used by Conax, Pyrodyne, and Pelmec. The Conax version is shown on Figure 45, the Pyrodyne on Figure 46, and the Pelmec on Figure 47. The Conax Corp. considered the design details of their interference-fit seal proprietary information and no design details were made available to this program. In general, the Conax design uses a piston which has an interference fit with the mating cylinder and which is integral with various types of actuating pins.

The Pyrodyne design uses a tapered gold-plated plug in the shape of a cork which is fitted with a light interference to the cylinder. The gold plating is used to provide a gas-tight seal before firing and to provide some lubrication for the plug during the firing cycle.

The Pelmec 1200 valve design uses an interference fit on the ram as a primary seal and a rubber O-ring as a secondary seal. The interference fit is so designed that an increasing interference is obtained as the ram travels down the bore, displacing considerable metal as it does so. The displaced metal is allowed to flow into a relief cavity provided for this purpose. The secondary

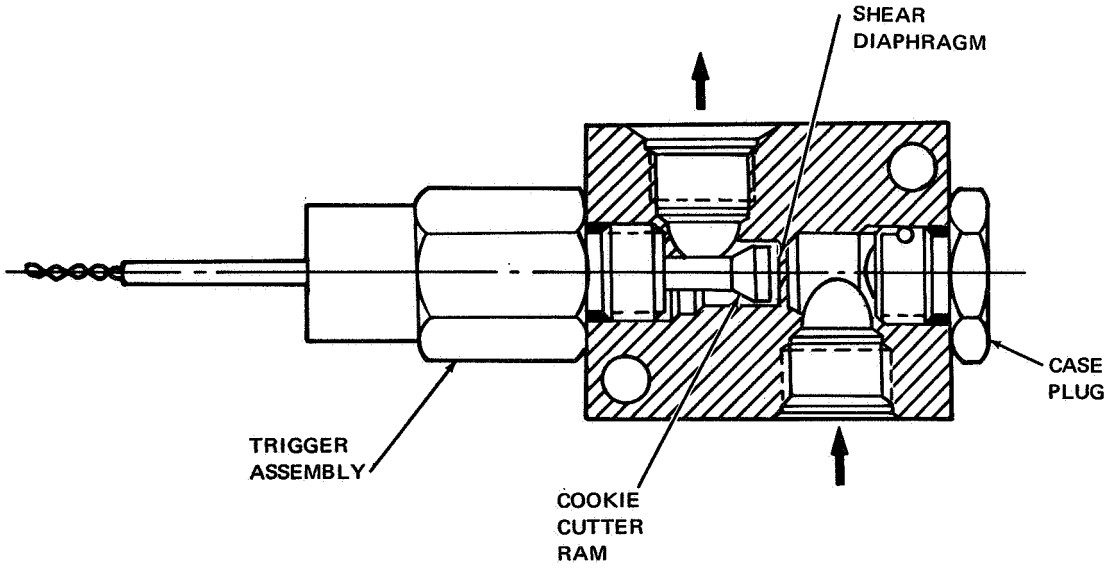

Figure 45. Conax 1802 Valve

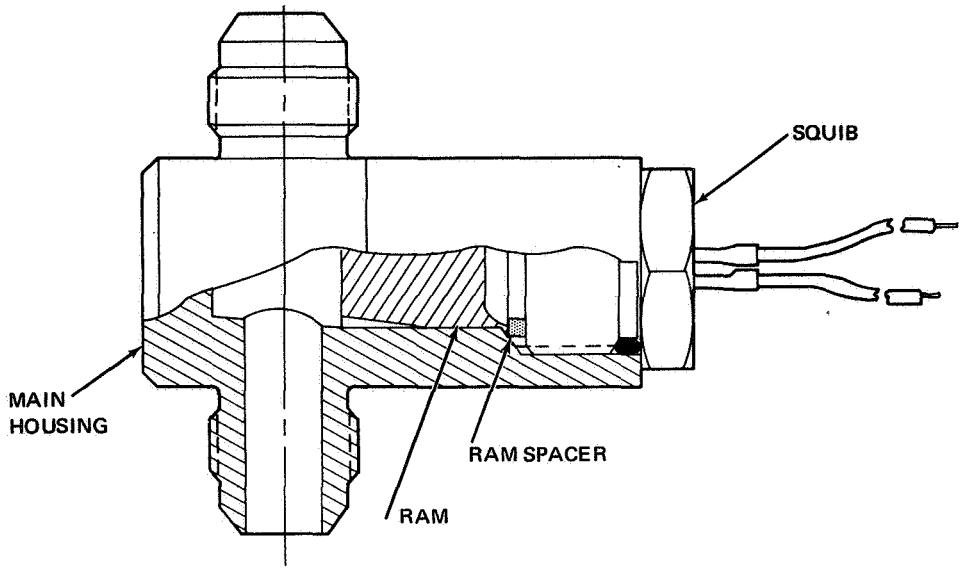

Figure 46. Pyrodyne 9163 Valve

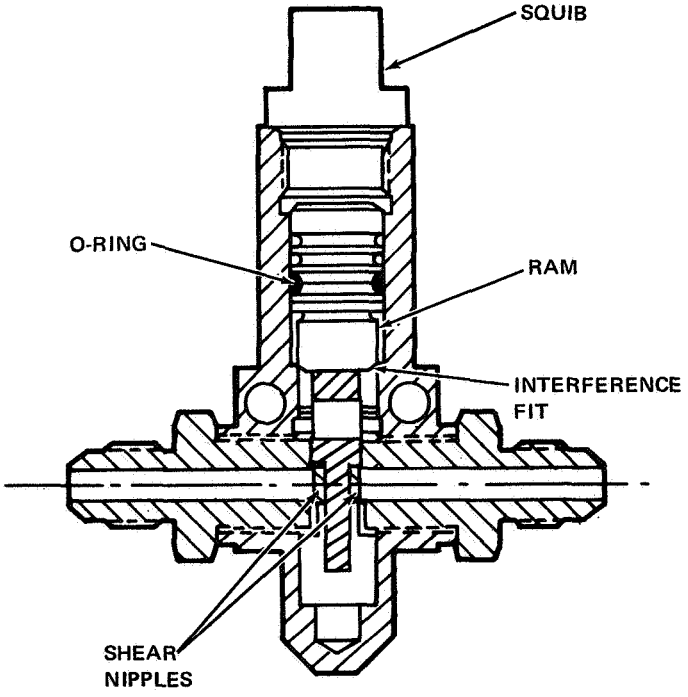

Figure 47. Pelmec 1200 Valve

O-ring provides a positive seal for the gases which may pass through the primary seal.

The mechanical seal method was used by Pyronetics. The valve tested incorporated a conventional spring-loaded Teflon seal in one arrangement and a metal-cup seal in a second configuration (Figure 48). The conventional spring-loaded Teflon seals were supplied by the Bal-Seal Engineering Company and represent a conventional Pyronetics valve arrangement. The metal-cup seal was a special configuration developed for fluorine. The cup seals evaluated on this program were coated by MDAC-WD with the proprietary Astrocoat-T coating.

Several additional valve designs were submitted by various manufacturers which used rubber O-rings as a form of primary seals, but because rubber is incompatible with fluorine, these designs were eliminated from further consideration.

5.3.1.2 Heating From Metal Shearing During Valve Actuation

In evaluating the valve designs, great importance was given to the elimination of hot spots that may prove to be ignition sources. The heat generated during the shearing action that occurs on almost all explosive valves was considered to be a potential source of component failure. Critical in this area are the ignition temperature of the material in fluorine, the heat conductivity of the mating materials, and the total heat generated. The first two items are governed by the material selected and the last by the amount of plastic deformation, and the total energy expended to complete the shearing operation. The material combinations found in the available valves were CRES on aluminum, CRES on CRES, aluminum on aluminum, and gold plate on CRES.

Two different shearing processes are used to form the sheared surfaces in the various valves. In one case, the shearing is accomplished in a progressive manner which is similar to the operation of a guillotine. The test fluid can flow onto the raw shear area as the shearing operation is taking place. The second case is not progressive. No area is exposed to the test fluid until the entire opening is made. This action is like a cookie cutter where the cut is started on the back side of the diaphragm and completes the final shearing on the surface exposed to the fluid.

The Conax valve 18300600, shown in Figure 49, was unique with respect to shear area. In this design, the aluminum nipple is sheared off with a CRES ram but the action is such that the CRES ram does not contact the shearing surface as it does on other valves. The CRES ram does strike the aluminum nipple, and therefore some secondary shearing may occur at the point of impact.

All of the valves studied were of the progressive type except for the Conax 1802-087-08 and the 1802-087-07 valves, which were of the cookie cutter type. The valves of interest of the various types are shown on Table 21.

The normally closed (N/C) valves are generally more sensitive to the metal shearing problem because these valves open on actuation and permit fluorine to flow over the newly sheared surfaces. The normally open (N/O) valves, on the other hand, are less critical because they isolate the flow when actuated, and the newly sheared surfaces are not in contact with the test fluid. Because

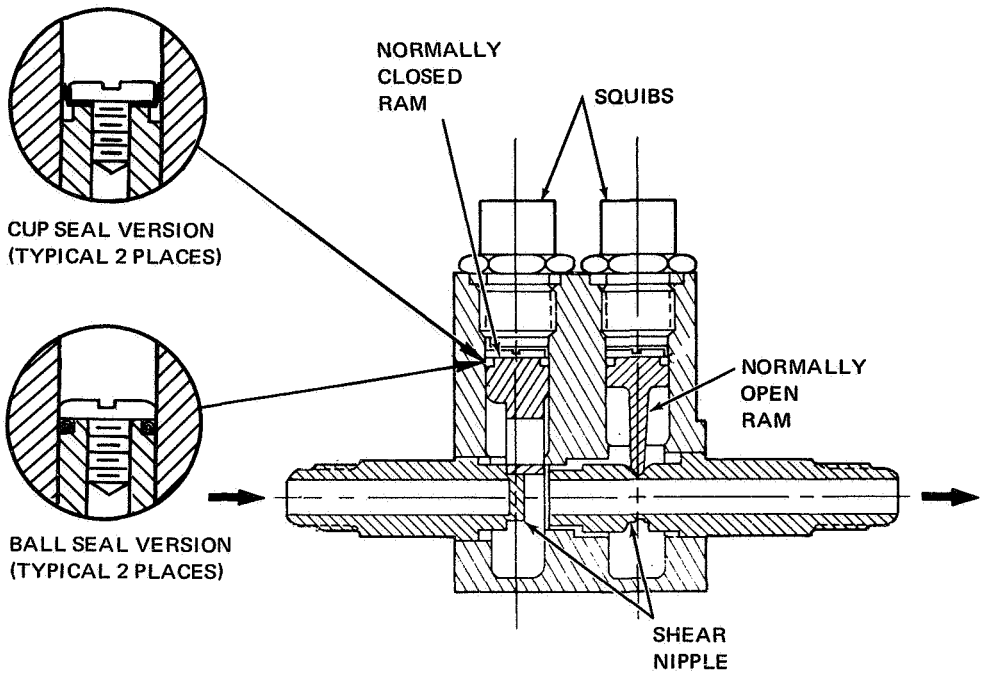

Figure 48. Pyronetics 1300 Valve

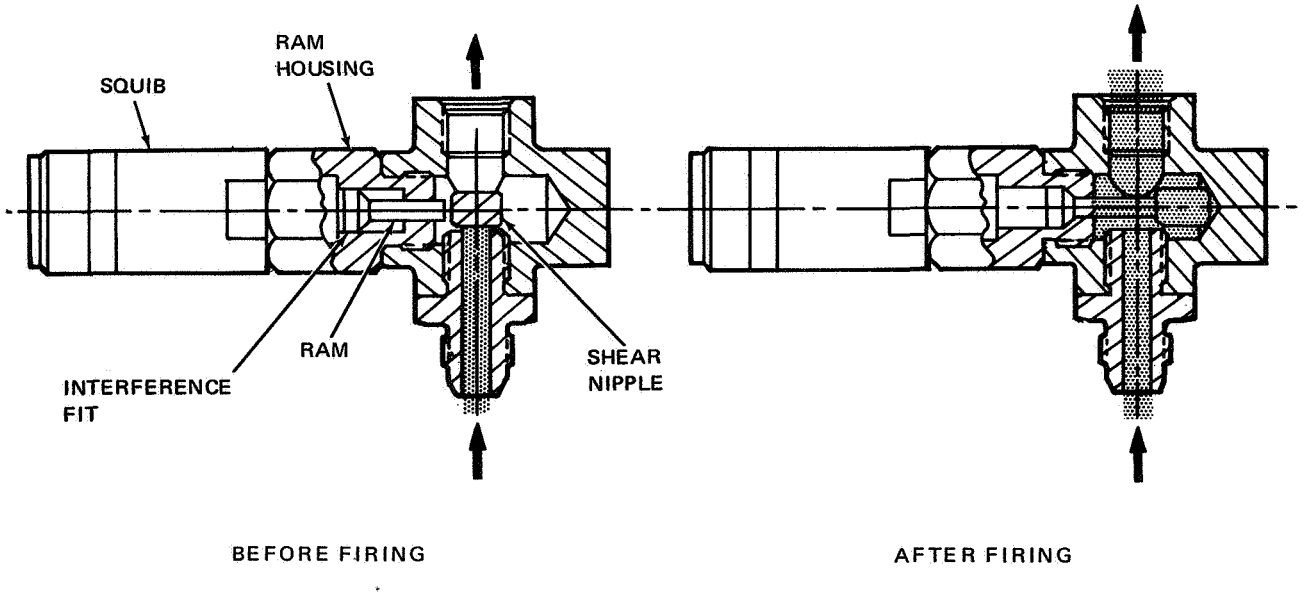

Figure 49. Conax Con-O-Cap (18300 600) Valve

Table 21

MECHANICAL DESIGN FEATURES

	Keyhole	Exposed Pin	Blade	Cork	Swaged Tube	Cookie Cutter
Normally Open (N/O) Valves						
Pyronetics N/O 1300			X			
Conax 1801-045				X		
1801-018				X		
Pelmec 1485					X	
Pyrodyne 9163				X		
Normally Closed (N/C) Valves						
Pyronetics 1300	X					
Conax 1802-087		X				X
18300600		X				
Pelmec 1200	X					

they isolate the flow when actuated, and the newly sheared surfaces are not in contact with the test fluid. Because of this difference in sensitivity to shear action, it was desirable to test a N/C valve for each of the material combinations. This was done with the Pyronetics 1300, Conax 1802-087-08 and the Conax 18300600 valves.

The total energy released in the shearing operation is a function of the design of the shearing elements and the energy produced by the explosive charge. These variables are not readily evaluated by analytical methods and no attempt was made to do so in this limited program. Instead, the final test matrix was designed to include as many of these configurations as possible.

5.3.1.3 Heating From Friction During Valve Actuation

The design variable of friction heating is related to the heating caused by shearing in all cases except with interference-fit sealing. The valves with interference-fit sealing may encounter additional heating from friction generated by the movement of critical parts. It would be expected that the tighter the interference fit, the greater the amount of heat generated by friction. Five designs were studied which appeared to provide different degrees of frictional heating. These five are ranked in order of estimated heating, from least heating to most.

1. Pyrodyne 9/63 – gold plate on CRES
2. Conax 1802-087-08 CRES on CRES on CRES

3. Pelmec 1200 CRES on CRES

4. Conax 1802-087-07 CRES on aluminum

5. Conax 18300600 CRES on aluminum on aluminum

The two variables considered in estimating the heating of the valves were the tightness of the intereference fit and the coefficient of friction of the mating surfaces. The gold-plated surface on the Pyrodyne valve was considered to yield the lowest frictional heating of the valves in this category due to a small improvement in coefficient of friction. The coefficient of friction was considered minor as compared with the change in interference fit which occurs at cryogenic temperatures. The Pyrodyne valve has a conventional one-piece CRES housing, with the gold-plated CRES ram on the inside.

The Pelmec 1200 has the tightest fitting ram of any of the valves tested and would be likely to generate the greatest amount of frictional heat. However, this valve is designed with a pierced ram, and the surfaces subjected to frictional heating are not directly exposed to the fluorine.

The Conax valves are more complicated due to the fact that they have removable trigger assemblies. On the Conax valves the ram is CRES on all versions and the frictional heating surface is exposed to fluorine in the N/C versions. The rams are installed with an interference fit into a trigger housing which may be made of CRES or aluminum. The trigger assembly is then installed into a valve housing which may be made of CRES or aluminum. The Conax valve with the least change of interference fit on chilldown would be the 1802-087-08 valve which has the CRES ram in a CRES trigger housing in a CRES main valve housing (see Figure 45). The 18300600 Con-O-Cap valve is the worst combination because it has a CRES ram installed in an aluminum trigger housing, which is then installed in an aluminum main housing. Valves of all of these types were incorporated into the test matrix to evaluate the overall effects of frictional heating.

5.3.1.4 Sealing Ability of the Valves

Several areas of sealing ability were considered in the valve selection. The N/C valves must prevent port-to-port leakage before firing and must not leak externally after firing. The N/O must provide external-leakage control before firing and exhibit no port-to-port leakage after firing. All of the valves studied have the theoretical capability of providing acceptable leakage control for the areas mentioned. The only area where a problem may be expected is where the thermal distortion of material caused by cryogenic temperature cycling may produce some degree of leakage. This problem would only occur where the material selection is limited by the constraint of off-the-shelf hardware. Given the time to optimize the material selections for LF_2 service, all of the valves studied should provide adequate leakage control.

In addition to the above tests, the valve designs were evaluated for ease of cleaning, inspection and passivation. It was found that the difficulties encountered in these areas were not normally caused by the design differences between the different manufacturers but rather by the nature of explosive valves in general. A N/C valve with double shear nipples can only be cleaned,

inspected and passivated through the squib port because both the inlet and outlet fittings are solid-metal diaphragms. Because the single shear nipple N/C valve does have access through the outlet port, it is somewhat more convenient to handle but even in this case the completely assembled valve cannot be processed because of the sealing required of the ram assembly. The N/O valves vary more in the ease of cleaning than do the N/C valves. The solid-nipple type of valve, such as the Pyronetics 1300 has all of the drawbacks listed for double nipple N/C valves. The plug type of N/O valves such as the Pelmec 1485, Pyrodyne 9163 and the Conax 1801 series are all relatively easy to clean and passivate. The Pelmec 1485 is a swaged tube and plug design which is easy to clean by flushing with cleaning fluid but is impossible to inspect after the tube is welded in place.

The passivation process for most of these valves must be controlled carefully or omitted entirely. This restriction is caused by the possibility of applying a high enough back pressure to the ram assemblies in such fashion that they move out of position. This problem is more severe during system leak checks where the technique of pressure decay versus time would normally be utilized. Except for the upstream port of the N/C valves, all other openings should be subjected to vacuum tests rather than pressure tests. Under these conditions, it is recommended that the N/O valves and the downstream side of the N/C valves be leak checked by measuring the ability to retain a vacuum condition and then passivated by bringing the pressure back to ambient with pure GF_2.

The tight interference-seal valves, such as the Conax design, are not as sensitive as the other valves to high downstream pressures and are therefore least sensitive to this problem.

The overall comparisons for the valves studied are shown on Table 22.

5.3.2 Explosive Valve Test

The results of the design evaluation study provided the basis for selection of the valves tested on this program. The final component selection was incorporated into a test matrix which originally included four separate tests. Each of these tests evaluated two N/C and two N/O valves. As a result of the failure of a Conax 18300600 valve on the third test, the original test matrix was revised to permit a rerun of the test 3 valves but with the combination of valves rearranged so that some of the rerun valves were in test 4 and some of them in test 5. The final test matrix contained a total of five tests and is shown in Table 20. It should be noted that some of the valves tested were selected as mating components for the testing of critical valve designs and were not units selected to provide primary information.

The testing effort was conducted in three separate areas. These include leakage tests, compatibility tests of squibs with LF_2 and compatibility tests of valves with gaseous fluorine and LF_2. The following sections describe the details of these tests.

5.3.2.1 Leakage Tests

The valves that were functionally tested during this program were given pretest and post-test leakage tests. These tests were conducted using helium gas at 50 psig (3.45×10^5 pascals) and at ambient and cryogenic temperature.

Table 22
COMPARATIVE VALVE DATA

Manufacture	Model	Nominal Size (in.)	Type	Material	Squib	Connector	Comments
1. Pyronetics*	1300	3/8	2 N/O	2219 Al Body, 304 Ram	Hi Shear PC 27		Guillotine Type - One TFE Ball Seal, One Cup Seal
Pyronetics*	1300	3/8	2 N/C	2219 Al Body, 304 Ram	Hi Shear PC 27		Keyhole Type Guillotine, One Ball Seal. One Cup Seal
2. Pyronetics	1222	1 1/2	1 N/O, 1 N/C	6061 Body, 303 Ram, TFE Seals	3544		Swinging Pin Type, Wedge Shear to Open, Cork to Close
3. Pelmec	1410	3/8	N/O				
4. Pelmec	1100-02	1/4	N/C	304 Body & Ram, O Ring Seal		PT 02-8-4PW	Keyhole Type - Double Shear Nipples, Double Guides
5. Pelmec *	1200	3/8	N/C	304 Body & Ram, O Ring Seal	#1287		Keyhole Type - Double Shear Nipples, Double Guides
6. Pelmec *	1485	3/8	N/O	304 Body & Ram, O Ring Seal			Swaged Tube Type Cork
7. Pyrodyne *	9163	1/4	N/O	304 Body - Gold Plated 304 Ram			Tapered Cork Style Interference Fit Seal Tapered Cork N/O
8. Pyrodyne	9037	1 1/2	1 N/O & 1 N/C	All CRES w/Bellow Seal			Design Only - Not Built - Keyhole Type Single Shear - N/C
9. Pyrodyne	9165	2	1 N/O & 1 N/C	7075 Al Body, CRES Ram w/Bellow Seals			Design Only - Not Built - Similar to 9037 w/Al Body
10. Pyrodyne	8112	1/4	2 N/O & 2 N/C	7075 Al Body, Cupper Ram - O Ring Seals			Keyhole Type Single Shear Nipple - Tapered Cork Ram
11. Holex	R 7592	1/4	N/C	304L Body & Ram w/Bal Seal		PT 06-8-4S	Keyhole Type-Double Shear Nipple
12. Holex	R 7352	1/4	N/O	316L Body & Ram w/O Ring Seal	5022	MS3116-8-4S	Tapered Cork Type Designed for Hydrazine
13. Conax *	18300600	3/8	N/C	2024 Body, Trigger Assy, 17-4 Ram			Con-O-Cap (Reusable) Style, Exposed Pin, Single Nipple, Interference Fit Seal
14. Conax *	1802-087-07	3/8	N/C	2024 Body, 303 Trigger Assy, 17-4 Ram	Integral		Diaphragm Type - Cookie Cutter - Exposed Pin, Interference Fit Seal
15. Conax *	1802-087-08	3/8	N/C	304 Body, 303 Trigger Assy - 17-4 Ram	Integral		Same as -07 w/CRES Body
16. Conax *	1801-045-08	3/8	N/O	304 Body, 303 Trigger Assy - 17-4 Ram	Integral		Exposed Pin Type Cork - Interference Fit Seal
17. Conax *	1801-018-01	1/4	N/O	2024-T4 Body, 303 Trigger Assy - 17-4 Ram	Integral		Similar to -045-08, Except w/Alum Body.
18. Conax	1801-036	2	N/O	310 Body, 303 Trigger Assy - A286 Ram	Integral	CB3101A-14S-6P	Similar to -045-08 Except in 2" Size w/Refiring Kits Available.
19. Conax	18303200	2	N/C	2024 Body & Trigger Assy, 17-4 Ram			Similar to 18300600 Except in 2" Size
20. Conax	1807-005	3/8	2 N/O	2219 Al Body, 304 Trigger Assy - 17-4 Ram	Integral	MS27478YE8-3P	CTF Quad Valve With Non-Std Mounting - Similar to 1801-018-01
Conax	1807-005	3/8	2 N/C	2219 Al Body, 304 Trigger Assy - 17-4 Ram	Integral	MS27478YE8-3PA	CTF Quad Valve With Non-Std Mounting - Similar to 18300600
21. W.O. Leonard	1073A	1/4	N/C	17-4 Body, Slide, O Ring Seal	1073A-24	10-104758-2P	Squib Actuated Pilot Type GN_2 Release Valve w/Burst Diaphragm

*Tested.

No special test setup was required for these tests. The tests were accomplished by connecting the gaseous helium supply to the valve at one port and then connecting a Vecco leak detector to the port which was of interest. The Vecco leak detector failed during the early part of the test program, and it was necessary to send this leak detector to the instrument shop for repair and recalibration. During this interim period the test effort was continued using the water displacement method of leak detection. The Vecco was returned during the test effort and all critical post-test measurements were made with the recalibrated instrument.

The test procedure for the leakage tests consisted of connecting the pressurization lines and the detector lines to the test valve and taking an ambient temperature leak reading. Where more than one reading was required the remaining ambient temperature tests were completed. When the last ambient check was made, the valve housing was submerged in a liquid nitrogen bath to a depth that covered the valve housing below the electrical squib area. The electrical squib area was not covered even in those cases where the squib had been replaced with a leak check fitting.

The N/C valves were checked first with the pressure applied at the inlet port and the leakage measured at the outlet port. No leakage was detected on any N/C valve when measured across the inlet nipple or diaphragm. The next measurement taken was with pressure applied to the squib port and the leakage measured at the outlet port. This reading was taken to determine the leakage across the ram seal. The results of these tests are shown on Table 23. The possibility of pressurizing the rams so that they would move from their original position was considered in the design of these tests. The only valve which could be disassembled to the point that the ram position could be measured was the Pyronetics model 1300. Ram positions were determined before and after the leakage tests to insure that the ram position had not changed.

The Conax trigger assemblies are made as a single unit that contains the squib and the ram assembly. There is no way to separate the squib assembly on these valves and therefore no readings of ram-seal leakage are possible.

No reading was taken on the Pelmec 1200 because of its construction. There is no way to verify the position of the ram without a complete disassembly of the valve and it was not feasible to conduct this type of disassembly at the test site.

The posttest leakage measurements were made with the equipment used for the pretest checks. A N/C valve is opened when actuated and therefore the inlet and outlet ports are not separated. The only reading possible with a fired N/C valve is the external leakage around the ram seal. The Pyronetic valve was the only valve where this measurement could be made (for the reasons given above). No leakage was detected with the leak detector in the posttest condition.

The N/O valves were leak checked in the same manner as the N/C valves except in reverse order. The pretest leakage measurement consisted of external readings taken across the ram seal (at the squib port). The results of these tests are shown on Table 24. The Pyrodyne 9163, the Pyronetics 1300, and the Pelmec 1485 were tested for seal leakage before test. The

Table 23

LEAKAGE RATES OF NORMALLY CLOSED EXPLOSIVE VALVES

	70°F (249.3°K)			-320°F (77.6°K)		
	External Leakage		Internal Leakage	External Leakage		Internal Leakage
	Pretest	Posttest	Pretest	Pretest	Posttest	Pretest
#1 Pyronetics 1300 - Cup Seal	300 CCM	0	0	50 CCM	–	0
Ball Seal	1 CCM	0	0	720-1200 CCM	–	0
2 Conax 1802-087-08	–	–	0	–	–	0
1802-087-07	–	–	0	–	–	0
3 Conax 18300600	–	X	0	–	X	0
1802-087-08	–	X	0	–	X	0
4 Pelmec 1200	–	–	0	–	–	0
Conax 1802-087-08	–	–	0	–	–	0
5 Conax 1802-087-07	–	X	0	–	X	0
18300600	–	X	0	–	X	0

X = not measured due to valve failure.

Table 24

LEAKAGE RATES OF NORMALLY OPEN EXPLOSIVE VALVES

	70° F (294.3° K)			-320° F (77.6° K)		
	External Leakage		Internal Leakage	External Leakage		Internal Leakage
	Pretest	Posttest	Posttest	Pretest	Posttest Ext	Posttest
Pyronetics 1200 Cup Seal	0	0	0	0	0	0
Ball Seal	0	0	0	0	0	0
Conax 1801-045-08	-	-			-	
1801-018-01	-	-			-	
Pyrodyne 9163*	0(1 ccm)		-	0		-
Conax 1801-045-08*	0	0	-	-	-	-
Pelmec 1485	0	0	1.5×10^{-6} ccs	0	0	2.3×10^{-6} ccs
Pyrodyne 9163	-	0	3.7×10^{-2} ccs	-	0	9×10^{-2} ccs
Conax 1801-045-08	-	-	5.2×10^{-9} ccs	-	-	6.9×10^{-9} ccs
1801-018-01	-	-	3.4×10^{-9}	-	-	2.7×10^{-9}

*Pyrodyne 9163 and Conax 1801-045-08 did not fire on test No. 3 and were reused on test No. 5.

Pyrodyne 9163 originally had an undetectable leakage across the ram seal, but because of an accident the leakage was greater when the valve was tested. This valve was inadvertently reassembled without the ram spacer ring after the original leakage measurements were made. During the flow loop pressure checks, the ram in this valve was moved from the original position. The ram was then returned to the proper depth and a quick recheck was made with the valve installed in the flow loop. This check was made at ambient temperature using a water displacement setup. The leakage was then found to be detectable but less than could be readily measured.

The posttest through-leakage rates were measured in the normal manner. The values obtained on the Pelmec 1485 and the Pyrodyne 9163 were higher than would be expected. The warmup cycle at the end of the test and the rechilling of these valves may have produced thermal effects which would cause a shift in the sealing member. This would account for some of the high leakages.

5.3.2.2 Squib Compatibility Tests

The compatibility of unfired squibs was evaluated by exposing the sealed end of the squib to pressurized gaseous fluorine and LF_2. This was accomplished by installing the squibs in a special fixture (see Figure 50).

This fixture was fabricated by joining two blind 2-in. (5.08×10^{-2}m) line-size standard flanges together. An undercut cavity provides an LF_2 chamber of approximately 2-in. (5.08×10^{-2}m) in diameter and 0.5 in. (1.27×10^{-2}m) in depth. One of the two flanges has four holes tapped with 1/2 x 20 UNF3A threads to allow installation of four squibs at one time for testing. However,

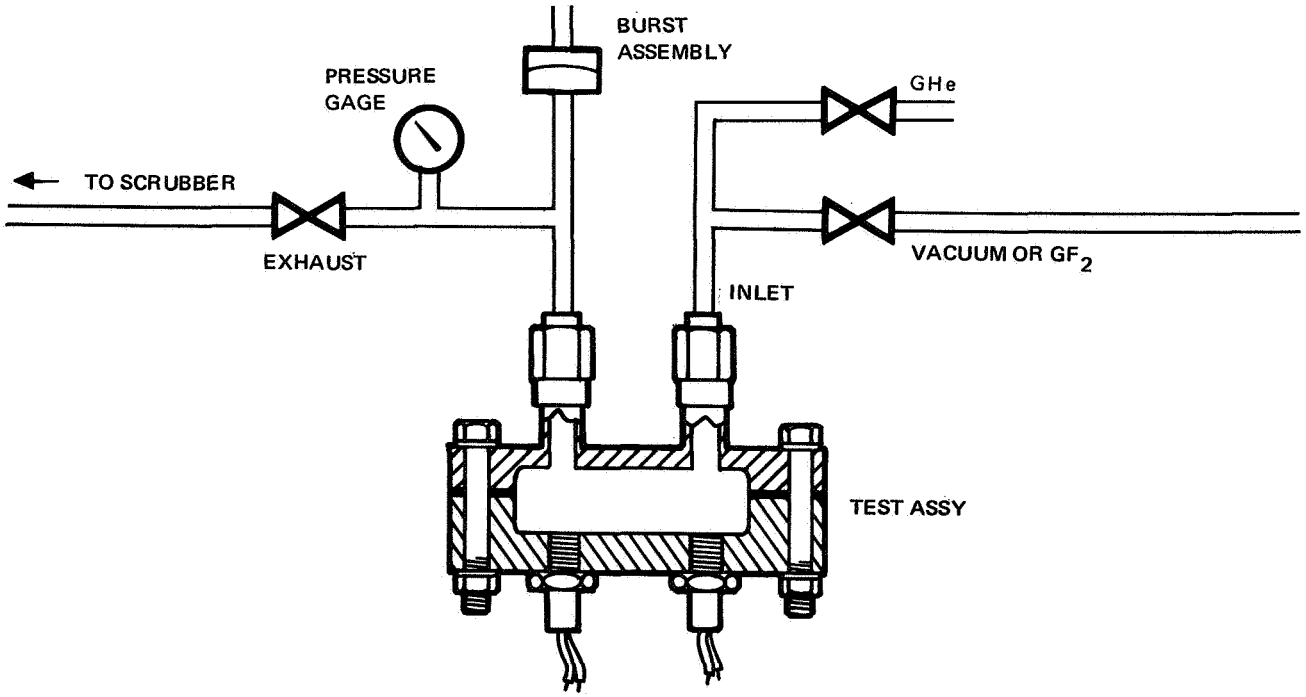

Figure 50. Squib Test Setup

the first squib was tested as a single test item with three of the test holes plugged. The flange with the test specimens is mounted on the bottom of the test fixture so that the liquid fluorine runs down into this lower half and rests directly on the test specimen.

The test specimen and the plugs were installed with gold-plated metal seals supplied by RACO Engineering Co. of Santa Monica. The test sequence started when the system was helium leak checked and then passivated for 30 min using gaseous fluorine at 50 psig (3.45×10^5 pascals). After the passivation process, the gaseous helium pressure was increased to 400 psig (2.76×10^6 pascals) and the system was locked up for 60 min. After this 60-min hold period, the system was purged and evacuated and then pressurized with gaseous fluorine at 100 psi (6.90 x 10 pascals). The cryostat was then filled with LN_2, condensing the gaseous fluorine in the test chamber to liquid. Additional gaseous fluorine was condensed into the test fixture until the test cavity was approximately half full of liquid fluorine. The volume of fluorine condensed was determined by pressure decay in the gaseous fluorine supply bottle. When the desired LF_2 was obtained, the gaseous fluorine supply valve was closed, and the LF_2 pressurized to 400 psig (2.76×10^6 pascals) with gaseous helium.

The system was then locked up at 400 psig (2.76×10^6 pascals) for 60 min. After this hold period, the pressurizing gas was vented to the scrubber and the liquid nitrogen was allowed to boil out of the cryostat. When the LN_2 was completely gone, the fluorine was allowed to boil off at a controlled 400 psi (2.76×10^6 pascals) until the system would hold 400 psi (2.76×10^6 pascals) without venting. A 60-min hold period was then made with gaseous fluorine. After this hold period the system was purged with helium, evacuated, purged again, and the test specimen was removed.

The Holex R6170 squib assembly was the first unit tested. This squib has a hermetically sealed explosive charge. The seal is effected by a metal end cover soldered to the main housing. The complete end cover had been coated with a red plastic film (for identification) when the squib was received from the supplier. The supplier indicated that this plastic film was soluble in acetone and could be removed without difficulty. This did not prove to be correct, and it became necessary to scrape the plastic coating from the end cover by hand. While scraping this film from the first squib, the seal diaphragm was accidentally punctured, and this assembly had to be scrapped. The spare squib was successfully cleaned by scraping off the plastic film, washing in acetone, rinsing with distilled water, and finally, rinsing with Freon. The squib was then installed into the squib test fixture.

The test was then conducted without difficulty and the specimen removed for inspection. No damage was observed at the sealing point of the squib after this test. A slight discoloration of the solder was observed, but this would not normally be expected to affect the operation of the squib (see Figure 51).

The second test was conducted using two squibs. They were a Pelmec 1287 and a HiShear PC 33. The Pelmec squib was removed from the Pelmec Model 1485 valve. The HiShear squib was obtained from Pyronetics, Inc., and is the same style squib as used on the Pyronetics Model 1300 Quad valve tested on the first valve compatibility test.

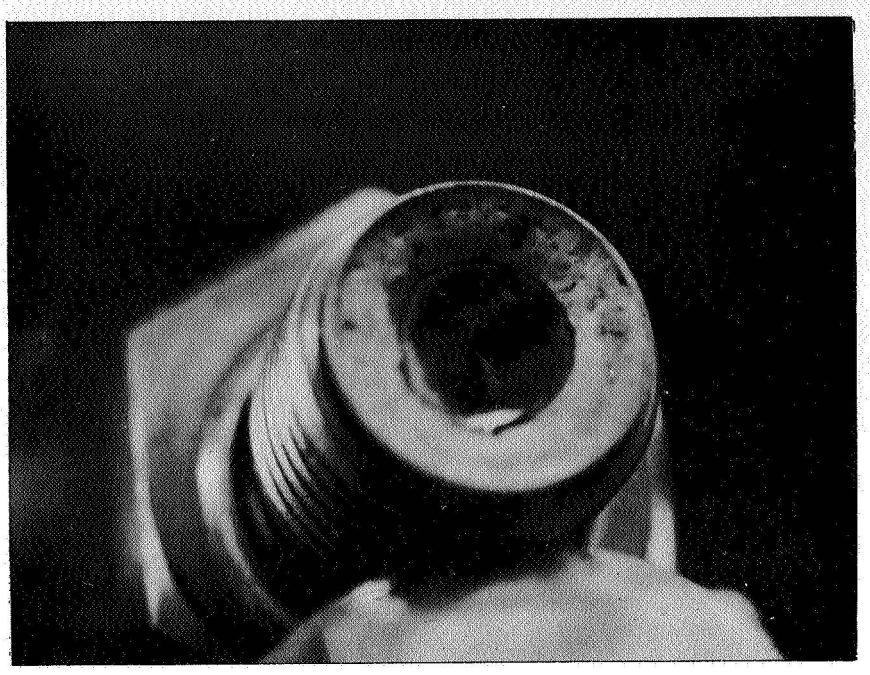

Figure 51. Holex R6170 Squib After Test

The PC 33 is identical to the PC 27 used on the first valve test except that it has a 1/2-in. (1.27×10^{-2}m) thread instead of the 5/8 in. (1.59×10^{-2}m) thread. The smaller thread size permitted installation into the squib test fixture without remachining the squib mounting holes.

Both squibs were cleaned by brushing with a wire brush and flushing with Freon. The Pelmec 1287 unit was found to have a nylon thread locking device. This nylon ball was removed and extensive cleaning in the ball socket area was conducted. Both squibs were installed in the test fixture using a small quantity of Krytox grease for lubrication.

The squibs were passivated at 50 psig (3.45×10^5 pascals) in GF_2 without difficulty and were removed for inspection after the passivation process. No component deterioration was observed. The squibs were then reinstalled, and the compatibility test started. The squibs both failed after 15 min of the scheduled 60-min hold at 400 psig (2.76×10^6 pascals) in LF_2. The reaction which occurred when the squibs ignited was sufficient to blow both squibs out of the test fixture and through the liquid nitrogen jacket. One squib was found in the test bay along with the liquid nitrogen jacket fragments while the second squib was found to have traveled over the barricade and into the test bay adjacent to the one used for this test.

A posttest inspection of the two squibs revealed that the Pelmac 1287 had burned through the threaded section at the location of the nylon-threat lock

socket (see Figure 52). It appears that this burn-through occurred from the outside and into the inside of the explosive-charge chamber. Once the LF_2 entered the explosive charge chamber, the LF_2 reacted with the explosive charge with such force that the HiShear squib was ignited. This reaction appears to have been caused by an incompatible material remaining on the exterior of the threaded portion of the squib housing in the vicinity of the nylon-thread lock cavity. Because the material which caused the reaction could not be isolated, the test was repeated with the following changes:

1. A new Pelmec 1287 squib was taken from stock before the nylon ball had been deformed into the threaded area.

2. No Krytox grease was used on the remaining tests in this test series. The Krytox grease used was taken from a supply which had successfully passed the 72 lb-ft (10 kg-m) impact test in LF_2 and was considered to be acceptable for this test.

The squib test rerun was completed in two separate tests. The Pelmec 1287 squib was tested separately from the HiShear PC 33. No difficulty was encountered on either of the rerun tests. It appears that the basic squib designs are compatible with fluorine; however, special attention is required to prevent contamination of the external surfaces of the squibs.

5.3.3 Fluorine Flow Tests

5.3.3.1 Test Setup

The fluorine flow tests were completed in a series of five tests which are shown on the text matrix, Table 20. The testing was conducted in a special

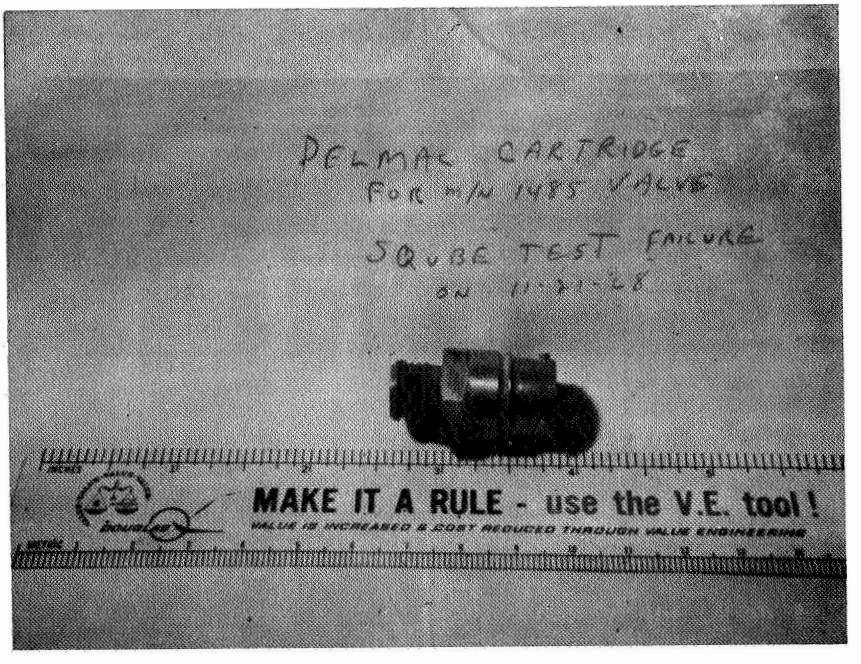

Figure 52. Pelmec 1287 Squib After Test

flow loop which was installed at the Gypsum Canyon Test Site (A12). The flow loop consisted of a storage tank and a receiver tank that were mounted on a steel frame and that was readily removable from the cryostat. The test valves were mounted between the two tanks and were used to control the transfer of fluorine from the storage tank to the receiver tank. The test arrangement is shown on Figure 53. The fluorine used for each test was taken from a gaseous fluorine bottle, passed through an HF scrubber and condensed into the storage tank. After each test, the flow loop was warmed up and the LF_2 boiled off through a vent line connected to a charcoal scrubber. No attempt was made to recover the fluorine used for these tests.

5.3.3.2 Test Procedure

The complete test procedure used for the flow tests and the relative position of each test valve was designed to prevent accidental overpressurizing of the N/C valves from the downstream side. The upstream side was leak checked under pressure while the downstream side was leak checked by using a vacuum decay technique. The upstream side of the loop was passivated at 50 psig (3.45×10^5 pascals) with GF_2, and the downstream side was passivated at 0 psig (0 pascals) gaseous fluorine. The upstream and downstream sides were determined by the location of the two N/C explosive valves.

5.3.3.3 Flow Tests

The first valve test was conducted using the Pyronetics 1300 valve module containing four separate valves. This Quad arrangement consisted of two N/C valves and two N/O valves. Prior to the LF_2 flow tests, the valve was given the pretest leakage check.

The valve assembly was then recleaned by Freon rinsing and installed in the fluorine flow loop as shown in Figure 54. During the test, the LN_2 level was maintained so that the valve bodies were submerged, but the squibs were above the liquid level. The flow portion of the test was conducted by condensing 5 lb (2.27×10^0 kg) of LF_2 into the supply tank, and sequentially actuating the tests valves to control the transfer of the LF_2 into the receiver tank.

No difficulty was encountered with the Pyronetics Model 1300 valve during this test, and posttest inspection revealed no indication of any internal reactions. However, the outlet fitting of valve 4 showed evidence of a minor gas leak. This leak apparently occurred only during the firing of the valve, when the valve body was disturbed. Motion pictures taken during the test showed that the entire valve assembly shakes noticeably each time a squib fires. This valve displacement is large enough to identify the portion of the test cycle which is occurring.

The very rapid rise of the downstream pressure on the firing of valve 1 resulted in the loss of the downstream pressure gage and the downstream pressure transducer. The indicator needle was pegged and bent on a 1000-psig (6.90×10^6 pascals) pressure gage even though the system operation pressure was 400 psig (2.76×10^6 pascals). The upstream pressure transducer failed electrically during the first valve sequencing and did not function for the remainder of the test. The pressure differential transducer worked properly, and the ΔP across the flow orifice was sufficient to provide the necessary basis for evaluating the test results.

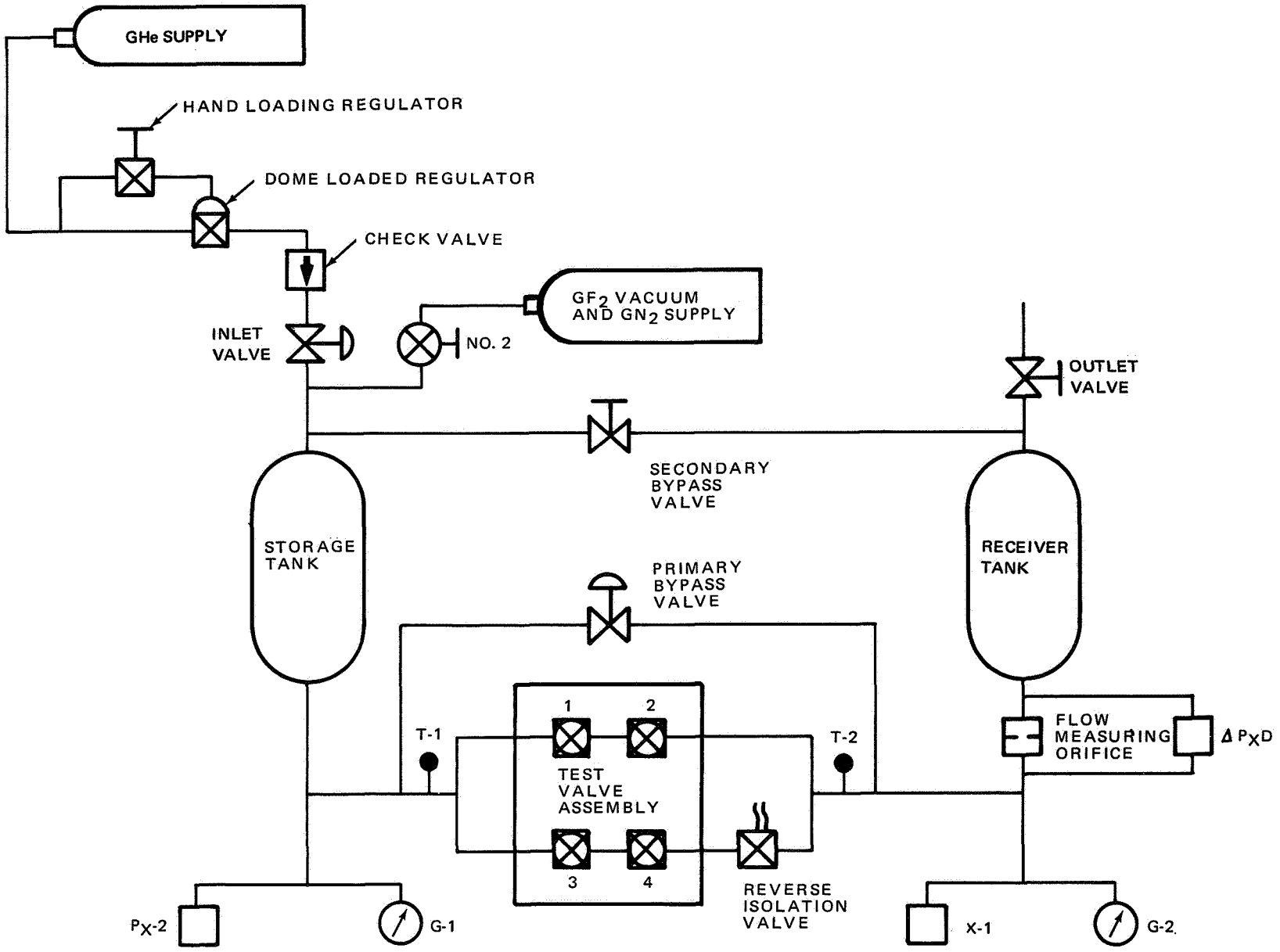

Figure 53. Explosive Valve Flow Test Schematic

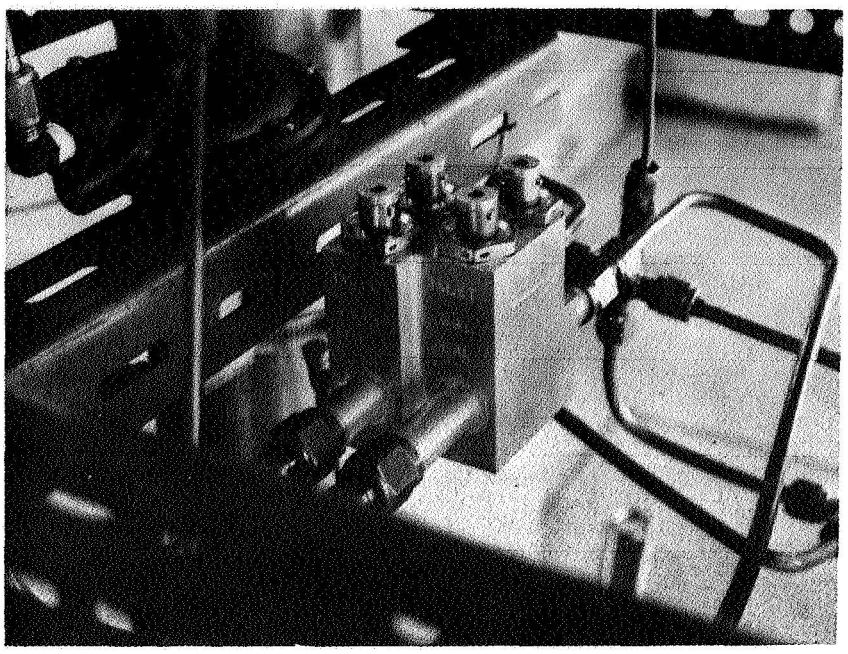

Figure 54. Pyronetics 1300 Valve in Flow Test Setup

After the test was completed, the remaining LF_2 was transferred through the bypass valve and the flow orifice into the receiver tank while recording the ΔP readout. By ratioing the flow time during the test to the flow time required to complete the posttest transfer, it was determined that approximately 2 lb (9.08×10^{-1} kg) of LF_2 were transferred during the test, while approximately 3 lb (1.36×10^{0} kg) remained in the supply tank to be bypassed. For a valid fluorine compatibility test, it is necessary to establish that LF_2 was still flowing through the system and not GHe pressurant when the valve closed. With 3 lb (1.36×10^{0} kg) of fluorine remaining in the supply tank at the end of the test, the valve could not have been flowing helium during this test; therefore, this was a valid test.

The posttest helium-leakage check was performed with a mass spectrometer, and no leakage was detected across any of the plastically deformed ram members. After the leakage test, the valves were sectioned by cutting off the outer half of each valve component as shown in Figure 55. Visual inspection of the sectioned valve revealed no signs of valve deterioration.

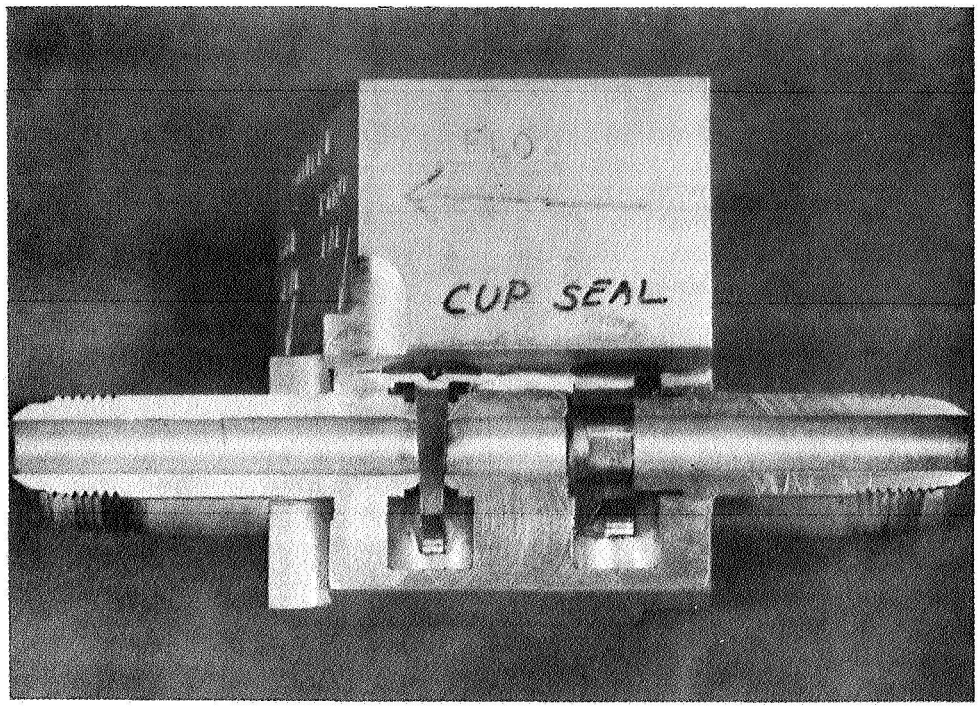

Figure 55. Section of Pyronetics 1300 Valve After Test

The second flow test was run with ambient gaseous fluorine and was conducted using the following four valves supplied by Conax Corporation, Buffalo, N. Y.:

No. 1 – Conax 1802-087-08 (N/C)

No. 2 – Conax 1801-045-08 (N/O)

No. 3 – Conax 1802-087-07 (N/C)

No. 4 – Conax 1801-018 (N/O)

These valves were selected to evaluate specific design and material combinations and hence not specifically designed for F_2 service. Valve 1 is a normally closed valve with a ram made from A286 CRES and a 310 CRES valve body. Sealing of the propellant gases is provided by an interference fit of the ram with the body of the valve. This interference fit can cause high frictional loads and subsequent heat generation that could cause the parts to exceed the ignition temperature of the metal in fluorine. The squib assembly is made integral with the ram assembly and cannot be removed from this valve. Valve 2 is the mating normally open valve for valve 1 and has the same material and design features. Valve 3 is also identical to valve 1, except that the main valve housing is made from 2024-T4 aluminum.

Valve 4 is a normally open valve with an A286 CRES ram, and a 2024-T4 body combination, but it is not in the same design series as valve 2. This valve was one of six which were supplied by NASA from a previous program. While this valve is configured differently from valve 2, the basic design is similar to it, and design features are common to both valves.

These four valves all have the integral squib and trigger assembly, and therefore, no provisions were available for measuring the ram-seal leakage in the before-fired condition. The two normally closed valves were checked for port-to-port leakage, and no leakage was detected.

These Conax valves were supplied in off-the-shelf configurations, and special processing was needed on all. This processing consisted of removing all threaded fittings from the valve bodies and then removing the standard rubber O-rings and nylon ball self-locking devices. After removing the nylon balls, the fittings and threads were cleaned by brushing and by chemical cleaning. The valves were reassembled using gold-plated RACO seals in place of the standard O-rings. Where thread galling appeared to be a problem, a very light coating of Krytox lubricant was spread on the threads. The Krytox grease was taken from tubes which had previously been used for ABMA impact-sensitivity tests where this grease was found to be acceptable at the 72-lb-ft (10 kg-m) impact energy level. The valve bodies and fittings were all cleaned by Freon rinsing before reassembly into complete components.

The test sequence for the gaseous fluorine tests was the same as for the LF_2 tests, except the test medium was gaseous fluorine at a nominal 100 psig (6.90×10^5 pascals). The gaseous fluorine pressure is limited because of the response of the gaseous fluorine regulators which are used in the fluorine supply system of the test facility. The supply regulator is operated with the adjusting handle turned all the way in, yet the system pressure will vary from approximately 100 psig (6.90×10^5 pascals) down to about 60 psig (4.14×10^5 pascals) during the system flow sequence.

The valve test sequence was completed without difficulty. However, when the posttest hold period was started, it was found that the system was leaking at a high rate. It was not feasible, therefore, to attempt the 60-min (3.6×10^3 sec) posttest hold period. After the system was inerted, it was found that valve 2 was leaking at the static seal between the trigger assembly and the valve body. The motion pictures taken of this test indicate that this leak started when the valve was actuated.

This leakage caused some discoloration in the valve body in the vicinity of the seal but no other apparent damage. Because this static seal was not a part of the basic test, it would appear that all four valves are compatible with gaseous fluorine.

The third test was an LF_2 test of the following valves:

No. 1 — Conax 18300600 (N/C)

No. 2 — Pyrodyne 9163 (N/O)

No. 3 — Conax 1802-087-08 (N/C)

No. 4 — Conax 1801-045-08 (N/O)

Valve 1 was a standard off-the-shelf Conax Con-O-Cap design with replaceable shear, squib, and trigger assemblies. This valve has a 17-4 PH CRES ram in a 2024-T4 Al body and has essentially the same features as the previously tested Conax valves. However, this valve is different in that it has no nylon-thread locking balls.

Valve 2 was supplied by Pyrodyne Corporation, Santa Monica, and incorporated several special features. This valve has a tapered cylindrical ram of goldplated 17-4 PH CRES which is installed in a 304 CRES housing with a light interference fit. When the valve is actuated, the ram is driven across the flow stream, sealing both the inlet and outlet passages.

Valves 3 and 4 were supplied by Conax, and are identical to those used in the gaseous fluorine test run. They were included in this run to evaluate the design in LF_2. No leakage was indicated through the three Conax valves prior to test.

The pretest leak check across the ram of the Pyrodyne valve indicated no detectable leakage. However, during the preliminary system leak check the ram was inadvertently pressurized from the reverse side and forced out of its proper position. This occurred because the ram spacer ring was inadvertently omitted by the test crew after the helium leak check across the ram was completed. After consulting with the supplier of the valve, it was decided to replace the spacer, return the ram to its original position, and recheck the leakage around the ram. The recheck showed that the movement of the ram had effected the leakage across the interference fit. However, the leakage was so small that reworking the ram was not considered necessary.

These four valves were cleaned as before and installed in the flow loop as shown in Figure 56. The test started with the same procedure as used on the first LF_2 flow test. No problems were encountered until after the passivation and condensing of LF_2. When the 400 psig (2.76×10^6 pascals) hold was attempted, the valves and downstream system held the vacuum as specified, but the upstream system would not hold 400 psig (2.76×10^6 pascals) pressure. The upstream system would hold 350 psig (2.42×10^6 pascals), but leakage was indicated at 400 psig (2.76×10^6 pascals). Because the upstream system ends at the blind inlet fittings of the two normally closed valves, it was apparent that the cause of this leakage was not located within any of the four test valves, and the decision was made to continue the test at the 350 psig (2.42×10^6 pascals) pressure level.

The pressure control regulator was readjusted to 350 psig (2.42×10^6 pascals) and the arming and firing sequence started. When valve 1 was actuated, a violent reaction was audible, followed by intermittent sounds of reaction. However, none of the subsequent reaction sounds occurred at the preselected times for valve actuations. The sequencer was allowed to continue for the full 10 sec. It was determined on posttest inspection that the failure of valve 1 resulted in the burning of the squib lead wires which led to the other three valves, and none of these three valves operated.

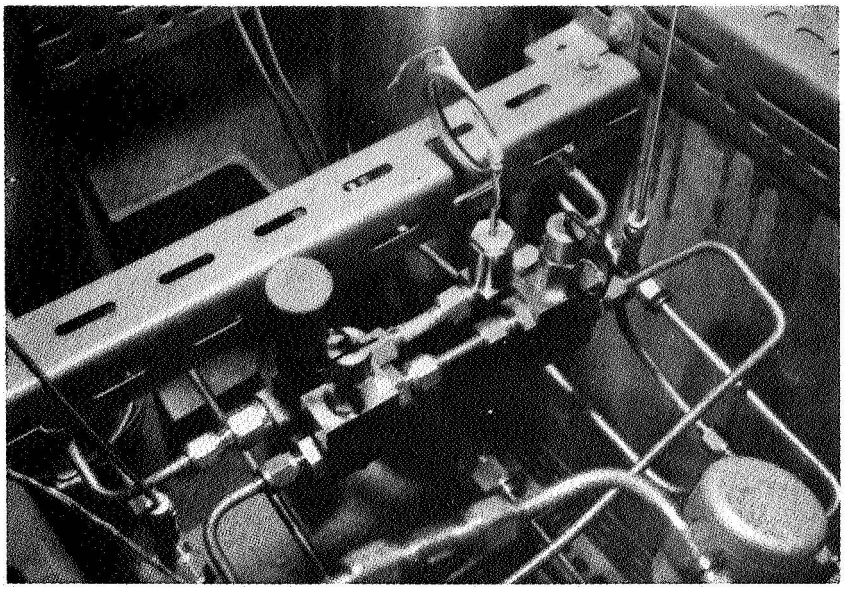

A BEFORE TEST

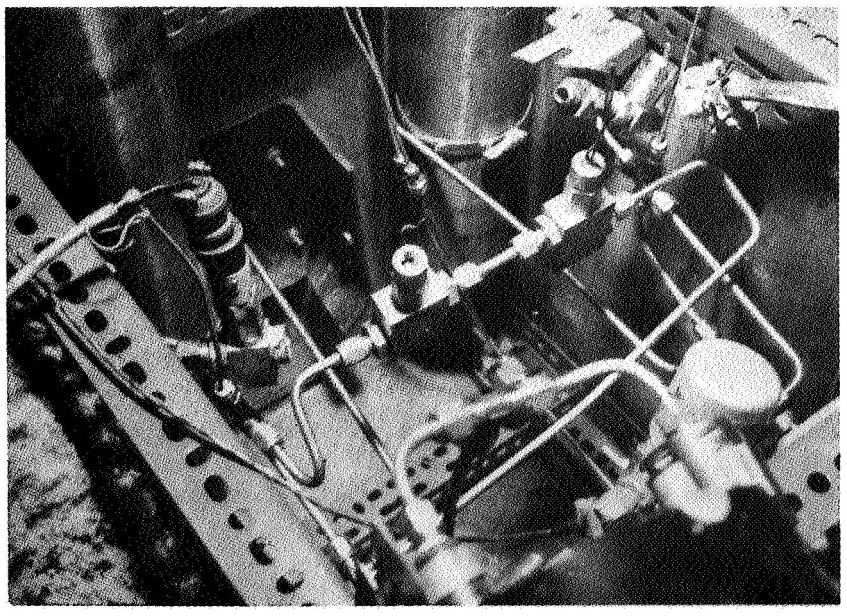

B AFTER FAILURE

Figure 56. Test Apparatus for Test 3: Before and After

The gaseous helium supply was shut off because the helium was leaking from the test loop at a rapid rate. This loss of the test system integrity prevented purging of the flow loop, and therefore, it was not possible to inert the flow loop. The concentration of fluorine was too high to allow personnel to enter the test area and release the liquid nitrogen. Therefore, it was necessary to shut off the liquid nitrogen supply and let the system warm to ambient conditions.

After the fluorine vapors had dispersed, a visual inspection was made of the test installation. It was found that a reaction had occurred in valve 1. This reaction heated the valve body so that the outlet fitting blew out of the housing and 5 lb (2.27×10^0 kg) of liquid fluorine had dumped into the liquid nitrogen bath. This failure left the flow loop open, resulting in complete loss of control of the LF_2 transfer.

Posttest inspection revealed that valve 1 failed internally because of an LF_2 reaction as shown in Figure 57. The 17-4 PH ram was still intact and the shear button was still in the valve. The button appears to have been burned on one side. However, the rest of the button appears normal. The ram does not appear to have reacted with the LF_2. The threaded area of the housing where the outlet fitting was connected was melted and the threads in the housing completely reacted. The threads on the outlet fitting show little or no damage. The exact point of origin of the reaction was not determined. Valve 2 suffered slight damage to the sealing portion of the inlet fitting which

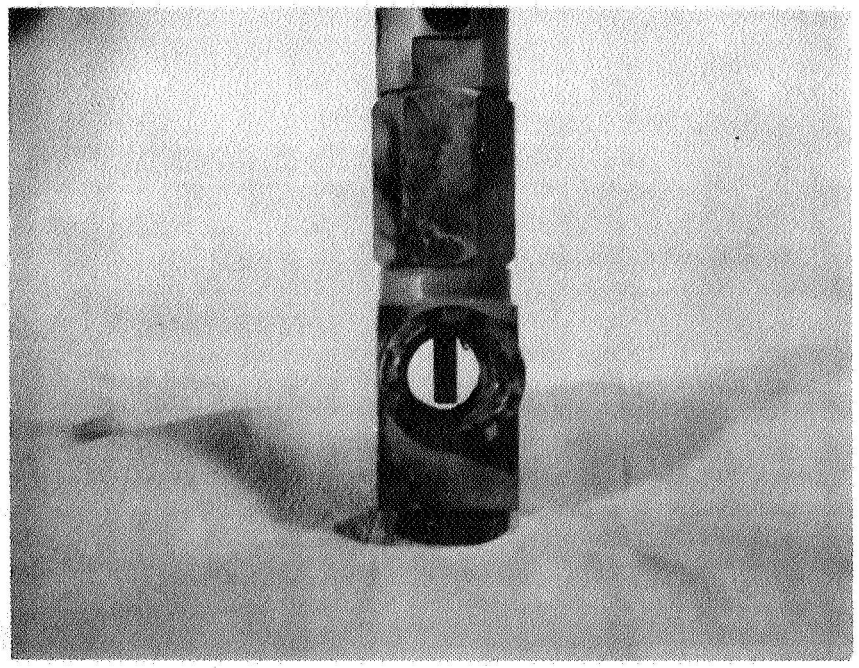

Figure 57. Conax Con-O-Cap (1800 600) Valve After Test 3

is integral with the housing. This damage was repaired and the valve retested. Valve 3 was damaged extensively by a burn-through even though the valve was not actuated. See Figure 58. This burn-through started from the inlet side of the main flow cavity, and out through a plug in the bottom of the valve housing. This plug closes the access hole in the body needed to perform the machining of the main closure element. This burn out occurred on the upstream side of the valve.

Inspection of the closure of valve 3 revealed that the shear diaphragm had been plastically deformed to a concave shape, and was pressed up against the ram. This deformation indicates that high pressure or high temperature conditions existed upstream of this valve during the test. Valve 4 was found to be undamaged.

The mechanism of failure of valves 1 and 3 was not completely identified. Two possibilities account for the failure which occurred. The first possibility is that valve 1 failed during operation because of either frictional heating or propellant gas blow by and an LF_2 reaction followed. This reaction then produced enough heat to soften the aluminum valve body and caused the failure of the outlet fitting joint. The reaction would also have produced a pressure rise which reflected back upstream into the connecting manifold and thence to the upstream side of valve 3. This reflected pressure wave would then have caused an LF_2 reaction in the threads of the body plug and deformed the main element diaphragm. The reaction would have caused the burn-through of the housing plug which was observed.

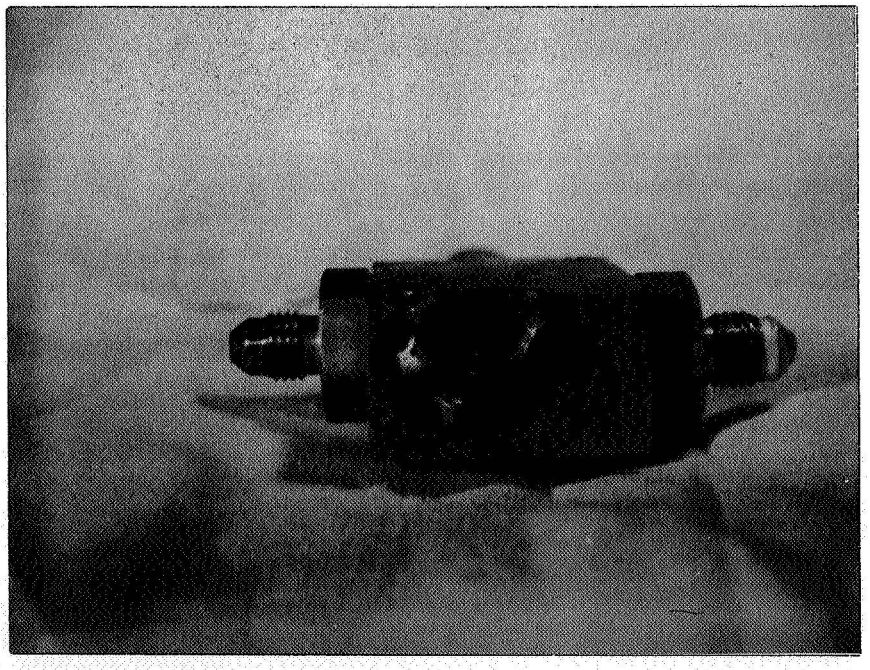

Figure 58. Conax 1802 Valve After Test 3

The second theory is that valve 3 failed first and damaged valve 1. Such a reaction is assumed to have started in the threaded section of valve 3 when the system pressure was increased to 400 psig (2.76 x 10^6 pascals). This reaction started a burn-through of the plug. Because of the side-by-side mounting of these two valves, it could have been possible for the escaping LF_2 to have flowed through the liquid nitrogen bath and impinged on the housing of valve 2. This impingement of hot metal and LF_2 would have started an external reaction on valve 1 which would have heated the metal to the point of thread failure when the valve was actuated.

Detailed inspection of the test hardware and evaluation of the motion pictures of the test failed to give a clear indication as to which of these theories was valid. Inspection of the Con-O-Cap valve did not produce positive indication that an LF_2 reaction in the ram and nipple area had occurred. The ram was unburned and the nipple was still in the housing. On the other hand, the films taken during the test failed to indicate the presence of an external reaction in the LN_2 bath near either of the valves in question. It is even possible that both of these failure mechanisms occurred at about the same time and jointly produced the results observed.

Posttest inspection also revealed that the welds of the cryostat were broken by the LF_2 reaction, and repair of the system was required before further testing could be conducted.

The valves for test 4 included the two Pelmec valves which were originally scheduled for this test, a new Conax 1802-087-08, and the reworked Pyrodyne 9163 which had been installed on test 3, but which had not fired after the failure of the Conax Con-O-Cap (18300600) valve.

The new Conax 1802-087-08 valve was delivered from the supplier as requested without the nylon-ball thread lock. The nylon ball had been removed from this valve before the valve was assembled. This procedure ensured that no nylon particles were entrapped in the threaded areas.

The Pyrodyne valve had a small amount of corrosion damage on the sealing surface of the inlet fitting during the running of test 3. This damage was repaired by the supplier by remachining the inlet fitting to provide a smooth seal surface.

All of the valves for test 4 were cleaned at the test site and leak checked as specified in the test plan. The test sequence proceeded in the normal manner until the final leak check was made. This check was made at 400-psig (2.76 x 10^6 pascals) pressure with LF_2 on the upstream side of the N/C valves. It was found that the system would hold 350 psig (2.41 x 10^6 pascals) pressure, but would not hold 400 psig (2.76 x 10^6 pascals). This was the same difficulty which had been encountered on test 3. Because test 3 had been continued at the 350-psig (2.41 x 10^6 pascals) pressure level with subsequent failure of the first valve to actuate, it was decided to stop test 4 and determine the reason for the failure of the system to hold pressure at the 400-psig (2.76 x 10^6 pascals) level. The condensed LF_2 was boiled off through the charcoal scrubber, and the system was inerted with helium and

inspected for component malfunction. It was found that the actuator seal on the pneumatic bypass valve was defective and needed replacement. This defect allowed the system pressure to open the external bypass-valve poppet and permit flow from the upstream side of the test setup to the downstream side. It did not result in external leakage of LF_2. The seal was replaced and the test started again.

A check of all valves in the test loop was made at the start of the rescheduled test, and it was found that the electrical solenoid on the secondary isolation valve had failed. This solenoid was replaced without removing the valve housing from the flow loop and because of the nature of the repair it was not necessary to repassivate the system. The LF_2 was then recondensed into the system and test 4 was completed without further difficulty. The 2-hour hold period after the valves had all fired was completed with no indication of pressure decay (indicating a no-leak condition). The posttest inspection indicated that all four valves had operated in a normal manner.

The fifth test consisted of a combination of four Conax valves including the second 18300600 Con-O-Cap which had been purchased for this program, one 1802-087-07 N/C valve, and two N/O 1801-045-08 and 1801-018-01 valves which were available for this test. The pretest arrangement is shown in Figure 59. The 1801-045-08 valve was salvaged from test 3, and the 1801-018-01 was one of several valves which had been supplied by the NASA program office. The N/C 1802-087-07 valve was a new unit which was ordered for this test and which had not been contaminated with the nylon thread locks.

No difficulty was encountered during pretest checkout or test sequence prior to valve operation. The valves were sequenced during the test in the order they are listed in Table 20. The first two valves functioned as scheduled. However, the Con-O-Cap valve 3 again failed explosively just as this type of valve failed on test 3. Explosions were heard at the time of firing of both valves 3 and 4. Considerable external leakage of LF_2 occurred during this failure, and inerting the system was difficult. The posttest inspection revealed that the electrical squib and the ram were blown out of the trigger assembly of the Con-O-Cap valve as shown in Figure 59b. The external plumbing on the upstream side of the test loop was found to have failed in a number of places. The tubing failed by burning through at all points where a bend was present in the original tubing. Valve 4 (1801-018-01) was found to be in good shape even though an explosion was heard at the time the valve was fired.

After disassembling the test setup, the following conditions were found. The Con-O-Cap valve 3 (18300600) had extensive burning on the valve housing and on the ram as shown in Figure 60. The threads on the squib assembly had failed under shear loads but were not burned in the manner that would have been expected.

Valve 1 (1802-087-07) was found to have extensive internal burning, even though the valve had cycled properly and the valve parts were intact. Valve 2 (1801-045-08) and valve 4 (1801-018-01) appeared to be undamaged.

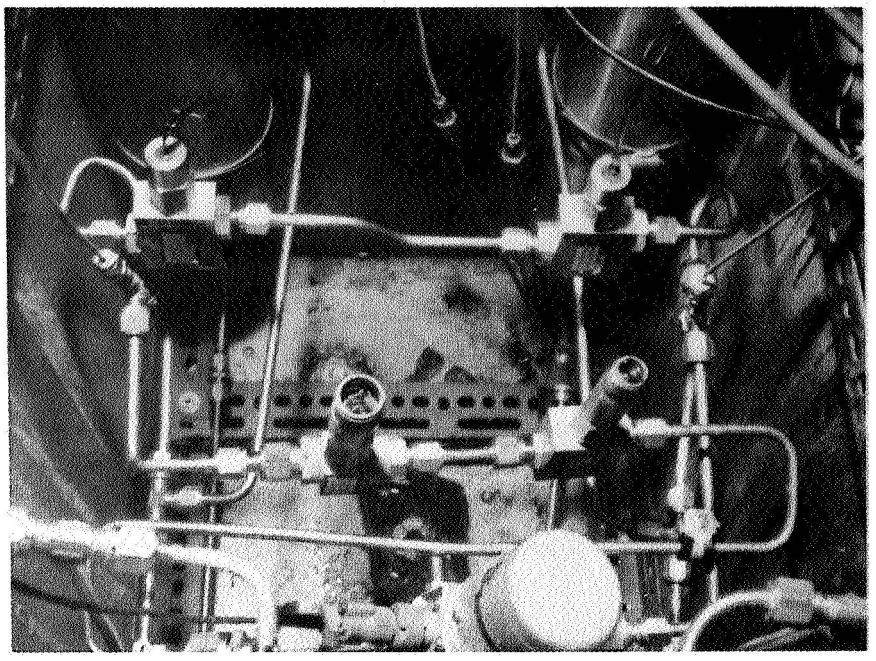

A. BEFORE TEST

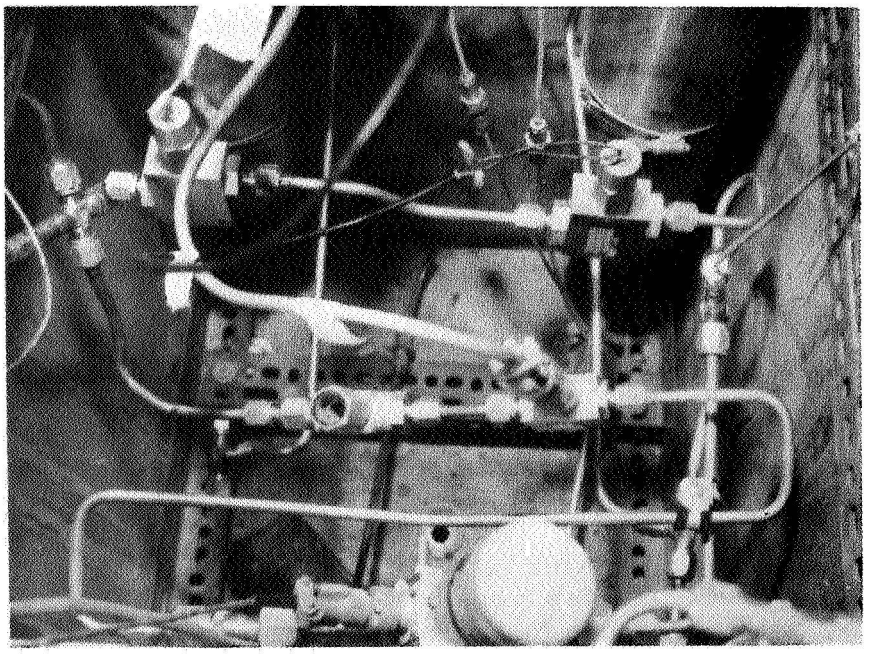

B. AFTER TEST

Figure 59. Test Apparatus for Test 5 Before and After

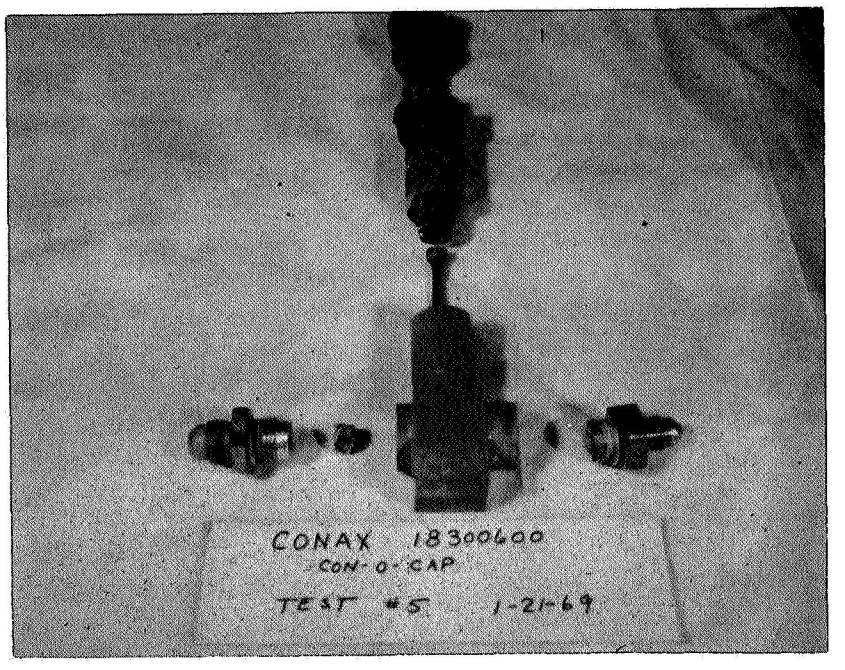

Figure 60. Conax 18300 600 Valve After Test 5

When the high-speed movies of the test were reviewed, it was determined that the first external failure occurred when valve 3 fired. This failure occurred at the inlet fitting of valve 1, and not in the trigger assembly of valve 3. The vapors from the LN_2 bath obscured the test setup at the time valve 4 fired, but it is possible that the squib and ram blew out of valve 3 when valve 4 fired. This would explain the explosion heard when valve 4 fired, even though valve 4 was found to be in good condition. It would appear that both external failures occurred from the effects of shock waves generated by the action of valves located downstream from where the external failures occurred.

5.4 Conclusions

5.4.1 Burned Gas Blowby into the Fluorine

Three different methods of providing a seal between the squib cavity containing the burned gases and the fluorine flow passage of the valves were tested. No failures were encountered with values using mechanical seal or with the swaged tube type seal. Since the pretest leakage checks on valves using mechanical seals revealed leakage rates of up to 20 ccs (2.0×10^{-6} m^3/sec) and these same valves were tested successfully it is concluded that moderate burned gas blow can be tolerated in explosive valves used in fluorine service. The valves which incorporated the interference fit sealing arrangement were less predictable. Some of the valves using interference

fit seals were tested successfully and others failed repeatedly. The Conax Con-O-Cap valves failed twice with explosive reactions. The amount of burned gas blowby experienced by this valve design is unknown but it may have been very high under the test conditions. Since this valve is also subject to functional heating problems, no single specific cause of valve failure could be isolated from the test data available and additional testing in this area is indicated.

5.4.2 Ignition Effects of Metal Shearing

The generation of heat due to the shearing action which occurs on almost all explosive valves during actuation was considered to be a potential source of component failure. The possible combinations of materials which are common in the various valve designs were tested on this program.

It can be concluded that the shear area phenomenon is not critical under the conditions tested. The unsuccessful Conax Con-O-Cap valves were inspected and in both cases the shear nipple and ram were found to have survived the failure. The condition of the nipples and rams are such that it is not possible to determine the extent that the shearing area may have contributed to the failure. However, the frictional heat area of the rams were found to have been damaged to a greater extent than was the shear areas and thus it is less likely that the shear area phenomenon was the cause of failure. This is covered more fully in Section 5.4.3.

5.4.3 Ignition Effects of Frictional Heating

The frictional heating effects are separated from the heating effects of the shearing action because these two effects may occur in different areas. The frictional heating effects which are considered on this program are limited to the heat generated by movement of parts which incorporate the interference fit seal provision. This discussion will be concerned with the entire family of Conax valves, the Pelmec 1200, and the Pyrodyne 9163 valve.

The generation of heat under conditions of sliding with an interference fit will be controlled by the amount of interference which exists during the actual test run, and the degree of lubrication which is available to reduce the coefficient of friction.

The degree of interference fit of the ram in the various valves at the time of testing is unknown due to the change in dimensions with the change at the test temperatures. The Conax 1802 series valves have CRES trigger assembly housing while the Con-O-Caps have aluminum housings. The shrinking effect on the aluminum Con-O-Caps would be expected to result in a tighter fit under cryogenic conditions than would be expected with the 1802 valves. Both Con-O-Cap valves (18300600) failed explosively during the LF_2 tests at -320°F. The failed valves show the effects of high temperature and high pressure. The ram shank is susceptible to frictional heating when the pin bends during operation and this frictional contact area was found to have been reduced in diameter as compared to the portion of the ram which was not subjected to friction. This reduction in area appears to have been caused

by reaction of the metal with LF_2. The 1802-087-07 valve which operated in LF_2 during the test 5 shows the same area reduction and effects of high heat as was observed on the Con-O-Cap valves but the reaction was not of the explosive type.

It was noted on posttest inspection that the ram shank on the 1802 valve showed a reduction in area on the portion of the ram that would contact the lower guide bushing if bending of the pin occurred, however, this reduction in area appears to be somewhat less than was observed on the Con-O-Cap valves. This would indicate that either less bending of the pin occurred in the 1802 valve than occurred on the Con-O-Cap valve or that the pin was operating with a greater side clearnace on the 1802 valve. Since less bending and greater side clearnaces would both be normal for this valve, it is not possible to use this information to assist in isolating the principal cause of failure on the Con-O-Cap design.

Based on the test data available, it appears that the failure of the Conax N/C valves was caused by a combination of frictional heating of the ram in the trigger assembly and excessive burned-gas leakage into the LF_2. This condition can be improved by modifying the interference fit design and by plating the ram with a coating which will produce less frictional heating and which is compatible with LF_2. Potential coating materials are gold, silver, and Astrocoat-T. The gold plating feature was evaluated on the Pyrodyne 2163 valve, however, because this valve was an N/O valve, it is not possible to evaluate the reduction in frictional heat from the present test series.

5.4.4 Leakage Characteristics of Various Mechanical Designs

All of the valves tested appear to have the potential of controlling port-to-port leakage to an acceptable level ($<10^{-11}$ ccs of GHe) if optimized for cryogenic service. The valves tested were selected from existing designs and were not necessarily designed for operation at cryogenic temperatures. The pretest and posttest leakage rates for the N/C valves tested are shown on Table 23. The leakage rates for the N/O valves are shown on Table 24. A change in the material selection used on some of the N/O valves should be made to minimize the thermal distortion experienced on these valves during the thermal cycling which occurred on this test program. With the change in material it is concluded that these valves would have acceptable leakage rates without changing the basic valve designs.

Appendix A
EMPIRICAL METHOD FOR METAL-TO-METAL SEAL LEAKAGE CALCULATION

A. 1 INTRODUCTION

Metal-to-metal seals are commonly used in applications where it is necessary to handle corrosive chemicals that are not compatible with rubber or plastic seal materials. With the increased use of metal-to-metal seals, the term zero leakage has come to mean a defined maximum allowable leakage. As a result of this usage, a requirement for reliable techniques for calculating leakage through metal-to-metal seals has arisen. The method of leakage calculation described here is based upon the work of G. F. Tellier of Rocketdyne (Reference 3).

When observed microscopically, real sealing surfaces are characterized by surface irregularities, or asperities, which appear as alternate ridges and furrows, following the direction of the finishing operation. For very smooth surfaces such as those produced by lapping, it can be assumed that these irregularities are fairly uniform. The peak-to-valley (PTV) height of these uniform irregularities therefore provides a convenient measure of the roughness of the surface finish. A more common measure of surface finish roughness is the arithmetic average (AA) or the older root mean square (RMS). The difference between the AA and RMS roughness values is that the RMS method weights the larger asperity heights and therefore gives a greater roughness value than the AA method for a given surface. However, both AA and RMS roughness values will approach the same value for a fine finish. The PTV asperity height is approximately three times the arithmetic average value for a given surface.

A. 2 DISCUSSION

A typical metal-to-metal seal configuration in Figure 61 depicts a valve closure consisting of a flat, circular poppet and seat with annular flow through the sealing surfaces. For analytical purposes, this model can be further simplified so that the seal can be represented mathematically by two parallel flat plates as shown in Figure 62.

To calculate leakage through a real seal, theoretical leakage through the simplified, flat-plate model of the seal is first calculated. An empirical correction factor is then applied to the theoretical leakage to provide a realistic estimate of the actual leakage. This empirical correction factor accounts for the fact that the seat and poppet of the closure under study are not flat plates, but rather plates with irregular surfaces that are being elastically deformed by the stress applied to the closure.

Before theoretical leakage can be predicted for a particular seal, it is first necessary to identify the flow regime represented by the sealing situation. For normal seals, four flow regimes are possible: turbulent, laminar, transition, and molecular. The criteria that identify the dominant flow regimes are shown in Table 25.

The turbulent flow regime is characterized by relatively large flow passages and high velocities and flowrates. Because of the high flowrates associated with turbulent flow, this regime will be considered only as an upper limit for seal evaluation. The numerical procedure that follows will be concerned only with leakage flowrates equivalent to those encountered in laminar flow or below.

The laminar flow regime is characterized by small flow passages and relatively low fluid velocities and flowrates. The effects of viscosity are prominent in this flow regime. The laminar regime is the most important regime for the analysis of most metal-to-metal seals.

In the molecular flow regime, the dominant effect is the kinetic motion of the test fluid molecules. Molecular flow occurs when the mean free path of the gas molecules exceeds the hydraulic diameter of the flow path cross-section.

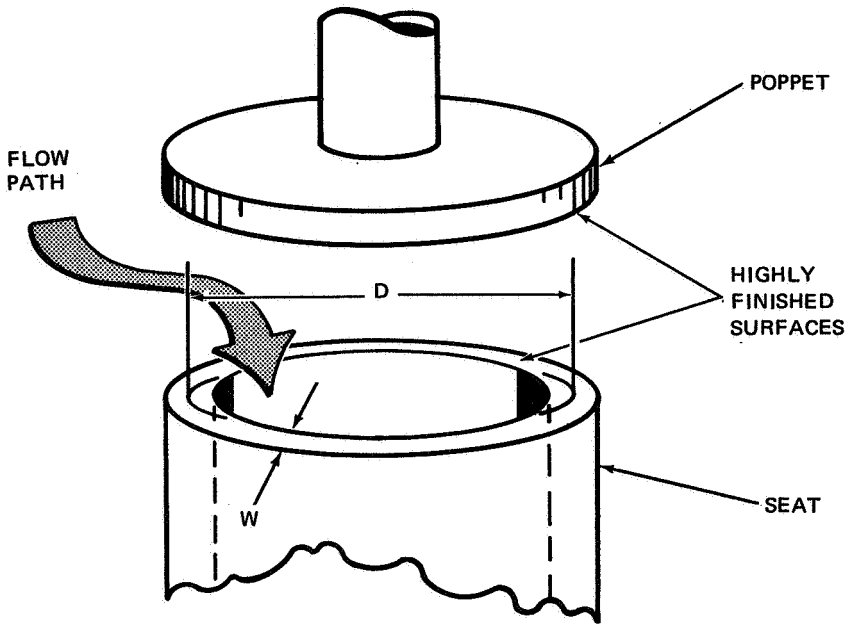

Figure 61. Schematic of Typical Seal

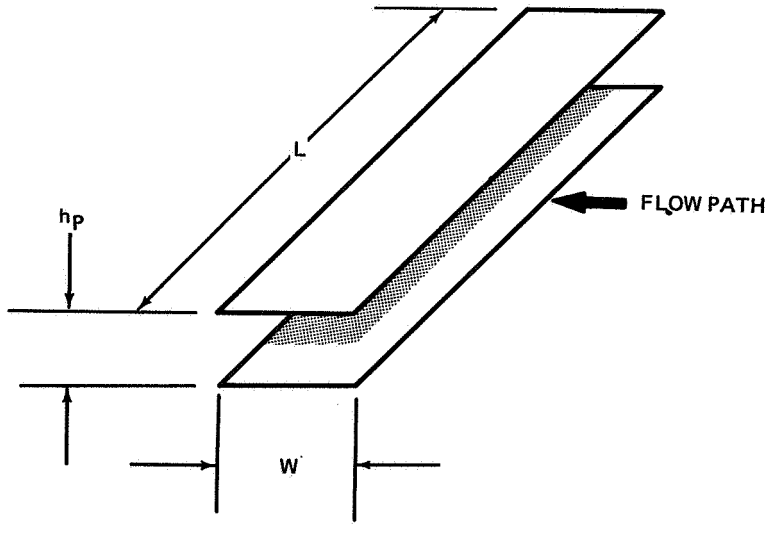

Figure 62. Flat Plate Seal Model

Table 25

CRITERIA FOR LEAKAGE FLOW REGIMES*

Flow Regime	Criteria	
	Reynolds Number	Knudsen's Number
Turbulent	>1,200	---
Laminar	<2,100	<0.01
Transition	---	0.01 to 1.0
Molecular	---	>1.0

*After Marr (Reference 4)

When the mean free path is considerably less than the hydraulic diameter of the flow path, however, the flow is laminar. The criterion for identifying molecular flow is Knudsen's number, which is the ratio of the mean free path to the hydraulic diameter of the flow path. Mean free path is a measure of the kinetic energy of the molecules of the working fluid. At cryogenic temperatures, the mean free path is generally small enough so that molecular flow becomes negligible.

A. 3 CALCULATIONS

The numerical procedure consists of first calculating values for laminar and molecular flow, Reynolds number, and Knudsen's number as described in Subsection A. 3. 1. The computed numbers are then compared with the values given in Table 25, and a judgment is made as to the flow regime in which the seal is operating. The resultant theoretical flowrate will be either the laminar flow value for the laminar regime, the molecular value for the molecular regime, or the sum of laminar and molecular for the transition regime. The empirical correction factor is then found by the procedure given in Subsection A. 3. 2.

All the formulas given in Subsections A. 3. 1 and A. 3. 2 are expressed in terms of weight flowrates in pounds per second. Consistent use of these units throughout the calculations avoids confusion in terms. Flowrates may subsequently be transformed to other units by means of the conversion formulas given in Subsection A. 3. 3.

A. 3. 1 Theoretical Leakage

The following equations for theoretical leakage flowrate are based upon flow through parallel flat plates. The geometry of the seal model is shown in Figures 61 and 62. For a circular seal as shown in Figure 61, the length of the seal (L) is given by the expression

$$L = \pi \overline{D} \tag{A-1}$$

where:

$\overline{D}$ = mean seal diameter, in.

The seal width (W) is equivalent to the contact width of the real seal. For the flat-plate separation height (h_p), the average asperity height (h) of the real surfaces should be substituted, or for convenience, a value of three times the AA surface roughness of the seal and poppet may be used.

A. 3. 1. 1 Laminar Liquid Flow

Theoretical weight flowrate for laminar liquid flow can be calculated from Equation A-2

$$\dot{w} = \left(\frac{L}{W}\right) \frac{(h_p \times 10^{-6})^3 \rho (P_1 - P_2)}{144 \mu} \tag{A-2}$$

where:

$\dot{w}$ = flowrate, lb/sec

L = seal length, in.

W = seal width, in.

h_p = flat-plate separation distance, microinches

ρ = density, lb/ft^3

P_1 = inlet pressure, psia

P_2 = outlet pressure, psia

μ = viscosity, $lb\text{-}sec/ft^2$

= (lb/ft-sec)/g

= centipoises/1,488g

Reynolds number for liquid flow is given by Equation A-3 or A-4

$$Re = \frac{1}{6g} \cdot \frac{(h_p \times 10^{-6})^3}{W} \cdot \frac{\rho(P_1 - P_2)}{\mu^2} \qquad (A\text{-}3)$$

$$Re = \frac{0.746}{L\mu} \cdot \dot{w} \qquad (A\text{-}4)$$

A.3.1.2 Laminar Gas Flow

Laminar gas flowrate calculations follow the same procedure as the laminar liquid calculations, but use the following equations

$$\dot{w} = \left(\frac{L}{W}\right) \frac{(h_p \times 10^{-6})^3}{2} \frac{(P_1^2 - P_2^2)}{\mu RT} \qquad (A\text{-}5)$$

where:

R = gas constant, ft-lb/lb/°R

T = inlet gas temperature, °R

The gas flow is assumed to be isothermal for the low flowrates through seals. Reynolds number for gas flow is given by Equation A-6.

$$Re = \frac{12}{g} \cdot \frac{(h_p \times 10^{-6})^3}{W} \cdot \frac{(P_1^2 - P_2^2)}{\mu^2 RT} \qquad (A\text{-}6)$$

or by Equation A-4.

A. 3. 1. 3 Molecular Flow

Theoretical weight flowrate for molecular flow can be calculated from Equation A-7

$$\dot{w} = 6.05 \times \left(\frac{L}{W}\right) \frac{(h_p \times 10^{-6})^2 (P_1 - P_2)}{\sqrt{RT}} \qquad (A\text{-}7)$$

Knudsen's number is defined by the following relationship

$$K_N = \frac{\lambda}{D_H} \qquad (A\text{-}8)$$

where:

λ = mean free path, in.

D_H = hydraulic diameter, in.

For flat plates, where $h_p << L$, hydraulic diameter may be approximated by

$$D_H = 4(A/P)_{Flow} = 2h_p \qquad (A\text{-}9)$$

where:

A_{Flow} = flow area, $in.^2$

P_{Flow} = flow perimeter, in.

The equation for mean free path as given by Maxwell is

$$\lambda = 1.66 \times 10^{-23} \frac{T}{P_1 \sigma^2} \qquad \text{(A-10)}$$

where:

T = temperature, °R

P_1 = pressure, psia

σ = molecule diameter, in.

Molecule diameter is a complex statistical function of the molecular activity of the working fluid. However, an approximate relationship for molecule diameter is given in Perry (Reference 11). This equation is of the form

$$\sigma = aM^{-2/3} \qquad \text{(A-11)}$$

where:

a = empirical constant

M = molecular weight

Substituting this relation into Equation A-10, it is possible to develop a formula for mean free path as a function of molecular weight. Figure 63 shows a plot of this formula for one temperature and pressure. Superimposed on this curve are the measured values of mean free path for some common gases. The measured values plotted on this figure are tabulated in Table 26. The equation for the curve in Figure 63 is given below in engineering units

$$\lambda = 6.02 \times 10^{-7} \frac{T}{P_1 M^{2/3}} \qquad \text{(A-12)}$$

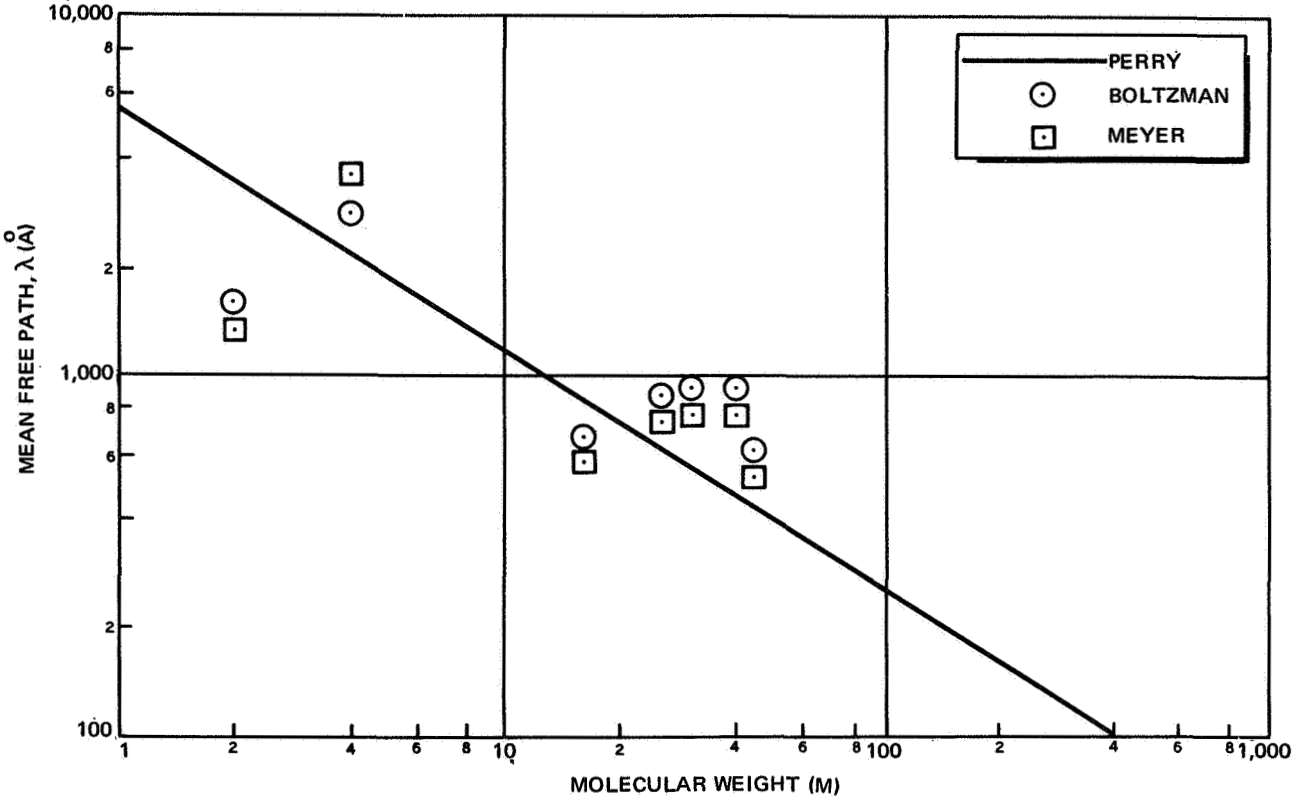

Figure 63. Mean Free Path as a Function of Molecular Weight

where:

λ = mean free path, in.

T = temperature, °R

P_1 = pressure, psia

M = molecular weight, lb/lb-mol

A.3.2 Actual Leakage

Actual leakage flowrate can be calculated by Equation A-13

$$\dot{w}_{actual} = K \cdot \dot{w}_{theoretical} \qquad \text{(A-13)}$$

Table 26

MEAN FREE PATH FOR SOME COMMON GASES*

T = 20°C
P = 750 mm Hg

Gas	Molecular Weight	Mean Free Path (Å) Boltzman	Meyer
Hydrogen (H_2)	2.02	1,744	1,540
Helium (He)	4.00	2,745	3,310
Ammonia (NH_3)	17.08	660	583
Carbon monoxide (CO)	28.01	923	816
Nitrogen (N_2)	28.01	929	821
Oxygen (O_2)	32.00	993	878
Argon (Ar)	39.95	998	873
Carbon dioxide (CO_2)	44.01	615	544

*Reference 12

where:

K = empirical correction factor

$w_{theoretical}$ = resultant seal flowrate calculated as described in Subsection A.3.1, lb/sec

Values for the empirical correction factor are plotted in Figure 64 as a function of apparent seat stress. This figure is based upon a series of leakage tests reported by Tellier. Apparent seat stress is given by Equation A-14.

$$S = F/A \qquad \text{(A-14)}$$

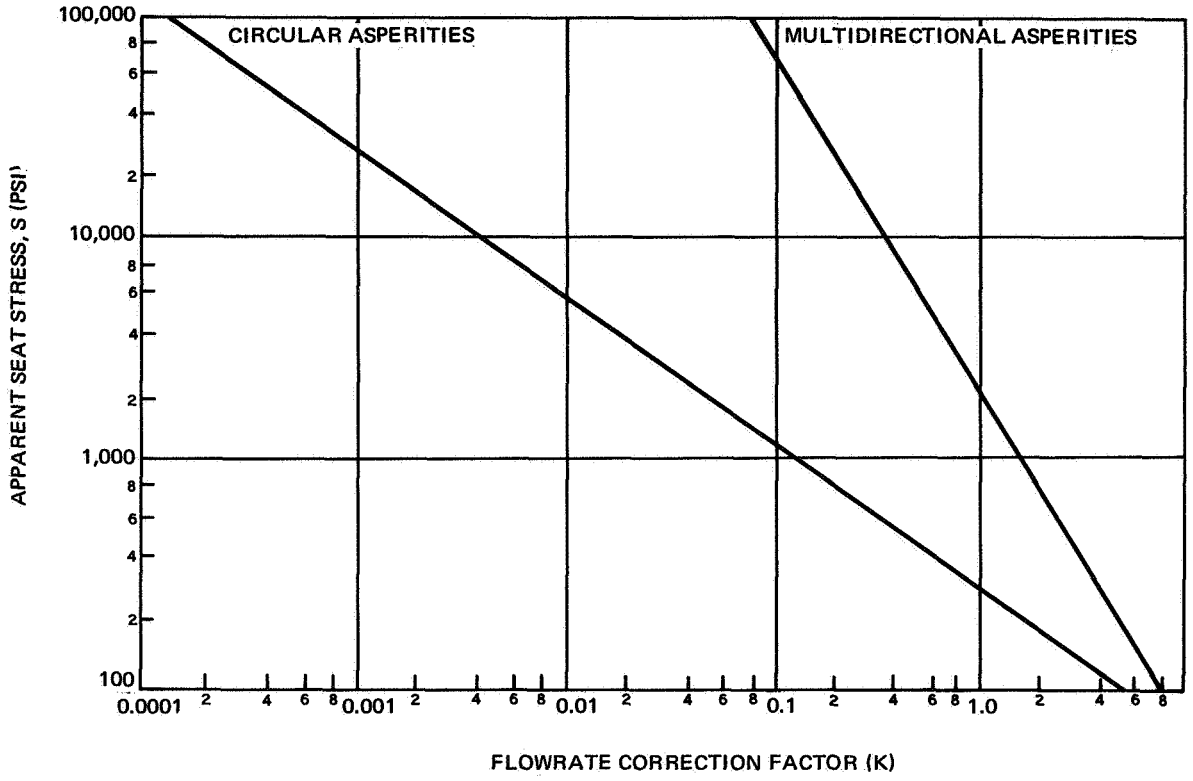

Figure 64. Empirical Flowrate Correction Factor for Leakage Flow

where:

F = sealing force, lb

A = seal area, $in.^2$

For the flat-plate model, the seal area is

$$A = L \cdot W \qquad (A\text{-}15)$$

The correction factors in Figure 64 are shown for two conditions of surface finish. The first finish condition consists of surface irregularities which are circular and concentric. These circular asperities will always be at right angles to the leakage flow direction. The second finish condition is one in which the seat and poppet have each been lapped unidirectionally. When the two pieces are put together, the asperities will cross each other at some random angle, resulting in multidirectional asperities. Tellier's tests have

shown that a marked difference in the performance of these two classes of seals will occur, as indicated in the figure.

The proper use of the empirical correction factor given in Figure 64 requires a number of important assumptions. It is assumed that the sealing surfaces under consideration have uniform surfaces, and that the finish is uniform on both the poppet and the seat. It is also assumed that the surfaces to be studied exhibit no anomalies such as scratches, pits, bumps, or gross waviness. If these anomalies do exist, they will completely dominate the leakage situation, and the use of the correction factor will not provide valid results.

A. 3. 3 Conversion Formulas

The following conversion formulas are helpful in converting flowrates from pounds per second to other common units.

ρ = density, lb/ft^3

M = molecular weight, lb/lb-mole

1. Liquids

   Gallons per Minute:

   $$gpm = 448.6\ (lb/sec)/\rho$$

   Pounds per Minute:

   $$lb/min = 60\ (lb/sec)$$

2. Gases

   Standard Cubic Inches per Minute

   $$scim = 4.01 \times 10^7\ (lb/sec)/M$$

Standard Cubic Centimeters per Second

$$\text{std cc/sec} = 1.095 \times 10^{7} \text{ (lb/sec)/M}$$

Standard Cubic Centimeters per Minute

$$\text{std cc/min} = 6.575 \times 10^{8} \text{ (lb/sec)/M}$$

Standard Cubic Centimeters per Hour

$$\text{std cc/hr} = 3.94 \times 10^{10} \text{ (lb/sec)/M}$$

Appendix B
VALVE CLOSURE SELECTION CRITERIA

Before a valve closure design can be selected, several critical design parameters must be considered. The design parameters that were considered to be of major importance for a liquid fluorine service valve closure include the following:

B. 1 FLOW RESISTANCE

Flow resistance is one major factor to be considered in the selection of the valve closure. A comparison of the relative resistance of several types of closures is shown graphically in Figure 65. This comparison is based on data published by the valve industry. The resistance coefficient, or K-factor, shown in this figure is a measure of the pressure loss through a component of a fluid-flow system in terms of velocity head. The K-factor is defined by the relationship

$$K = h_L / \frac{v^2}{2g} = 0.447 \, \rho \Delta P \left(\frac{A}{\dot{w}}\right)^2$$

where:

h_L = head loss, ft

v = average fluid velocity, fps

g = gravitational constant, 32.17 ft/sec^2

ρ = fluid density, lb/ft^3

ΔP = pressure loss, psid

A = flow area, in.^{2}

$\dot{w}$ = weight flowrate, lb/sec

The values of the resistance coefficients plotted in Figure 65 are for wide-open valves only. As shown in the figure, a great variation in flow resistance is possible with any given valve type. For this reason, the values in the figure should be considered comparative only. Where pressure loss is critical, flow test data should be acquired for particular configurations and specific fluid-flow conditions before precise performance estimates are attempted.

B. 2 SEALING ABILITY

Sealing ability is another major factor to be considered in the selection of a valve closure. The selection of the valve closure for LF_2 or gaseous fluorine use is influenced to a very great extent by the restrictions placed upon the sealing materials that may be used. At present, there are no rubber or

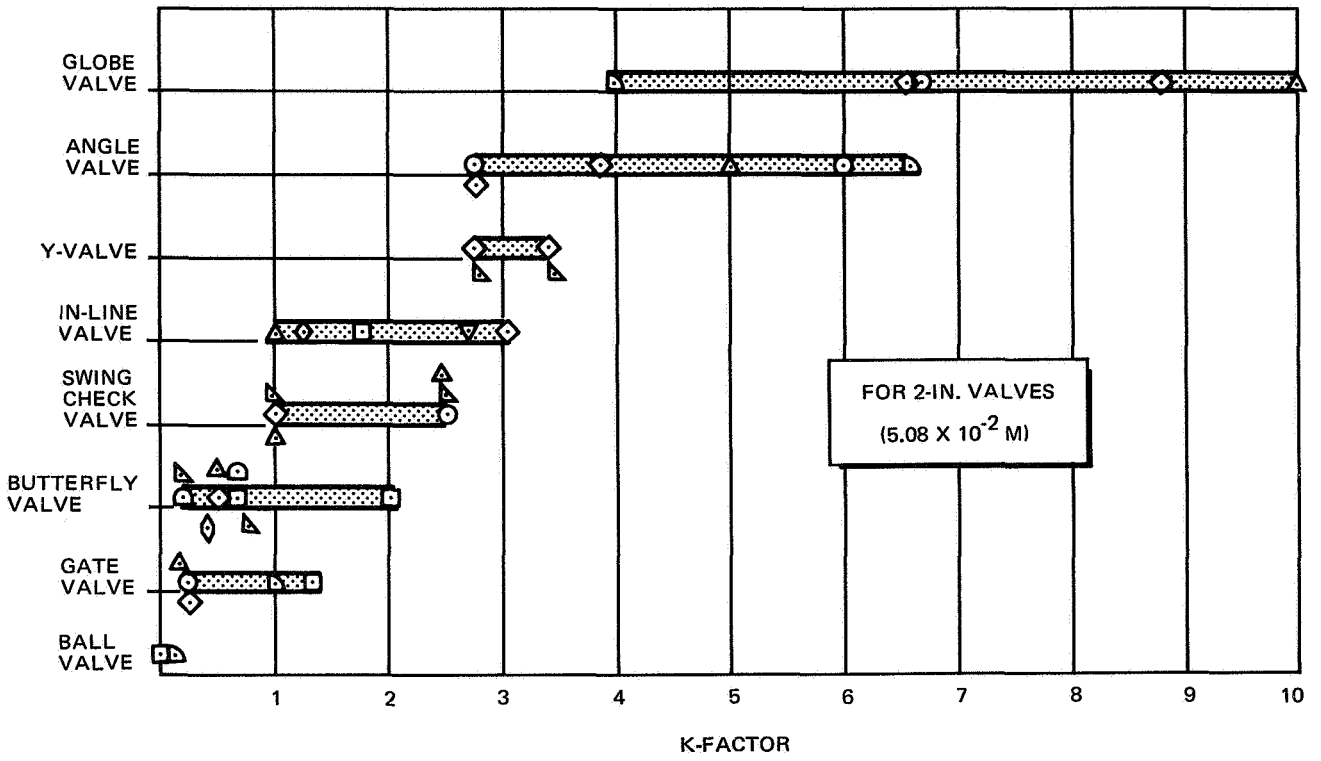

Figure 65. Valve Flow Resistance Comparison

plastic materials that are recommended for use in direct exposure to fluorine. Therefore, the valve closure must rely upon a metal-to-metal sealing interface, and minimizing leakage through the all-metal surfaces becomes a dominant design consideration. Some of the closure types commonly used by valve manufacturers will be found unsuitable for low-leakage applications when resilient rubber or plastic inserts are prohibited.

The sealing ability of a metal-to-metal closure depends on (1) the uniformity of contact between two sealing surfaces, (2) the surface finish of the mating surfaces, (3) the dimensions of the sealing surfaces, and (4) the loading, or seating stress, between the two surfaces. The effects of these variables on closure leakage are discussed in the following paragraphs. Further information on seal leakage is in Appendix A.

B. 2. 1 Surface Contact

To prevent gross leakage through a closure, intimate contact between the two mating surfaces must be obtained. This intimate contact requires that the shapes of the mating surfaces be exactly matched, and that the two surfaces be perfectly aligned. If either of these requirements is not met, leakage through the seal will be found to be many orders of magnitude greater than anticipated.

B. 2. 2 Surface Finish

The second variable of importance is the surface finish of the mating surfaces. The sealing lands of the closure must be given highly finished mating surfaces

to provide good sealing ability. These surface finishes must be maintained throughout the useful life of the valve.

B. 2. 3 Sealing Dimensions

The leakage through a closure is directly proportional to length of seal exposed to the working fluid, and is inversely proportional to the width of the seal, all other factors being equal.

B. 2. 4 Sealing Stress

The final parameter affecting the sealing ability of the metal-to-metal closure is the sealing stress between the two mating surfaces. This stress, usually called apparent seat stress, is defined by the relationship

$$S_{app} = F/A$$

where:

Sapp = apparent seat stress, (psi)

F = force pressing sealing surfaces together, lb

A = apparent contact area of seal, $in.^2$

The apparent contact area of the seal is defined as

$$A = L \cdot W = \pi \cdot D\, W$$

where:

L = seal length, in.

W = seal width, in.

D = mean seal diameter (for circular sealing surface only), in.

From these relationships, it can be seen that increased apparent seat stress can be developed either by increasing the loading on the closure, or by reducing the contact area of the closure. In practice, the contact area for metal-to-metal closures is usually established by the selection of a closure diameter, and a typical seat width of from 0. 010 to 0. 060 in. Seat widths narrower than this range tend to be susceptible to sealing surface anomalies, while widths greater than this range require excessive loading forces.

B. 3 BALL VALVES

The ball valve family is characterized by rotation of a pintle, plug, or ball, through the fluid stream to interrupt the flow. The movable element of the closure may be either spherical, cylindrical, or conical, or it may be a segment of a sphere or cylinder as in the so-called visor or eyelid designs.

As shown in Figure 65, the ball valve closure is very attractive in terms of pressure loss. When fully open, the ball valve creates no expansions or contractions of the flow stream, and causes no change in flow direction. As a result, the flow resistance of the ball valve is close to zero. However, the ball valve appears less attractive in terms of sealing ability.

The sealing interface of the ball valve closure is a complex shape generated by the intersection of the flow path with the rotating member. To provide the valve with adequate sealing ability for most uses, it is necessary to match the shapes of the two sealing elements within a few microinches. A fit of this kind can be obtained by lapping the two parts together.

Another adverse condition in the ball valve closure is the rotary sliding motion of the ball across the seat. This scrubbing action is particular undesirable with metal-to-metal sealing surfaces. The relative motion occurring during normal service cycles of the valve may cause rapid degradation of the finish of the sealing surfaces allowing the valve to exceed its design leakage rate.

In the ball valve closure, seating stress is usually generated by spring loading the stationary seat against the rotating ball. The seating stresses required for satisfactory metal-to-metal sealing will be higher than those normally used with rubber or plastic seals. However, this arrangement could provide adequate sealing stress if properly designed.

B.4 GATE VALVES

The gate valve family includes all valves in which interruption of the flow is achieved by translation of a gate or blade through the flow stream. The gate valve is often specified where minimum valve length is a requirement, as the gate or blade valve can provide the minimum length-to-diameter ratio of any closure.

The blade or gate valve can be designed to create no expansions or contractions of the flow stream, and to cause no changes in flow direction. Sometimes, for simplicity, a gap in the flow path is left when the gate rises, and the fluid must cross this gap as a jet. The greater the length of the gap, the more pressure drop is introduced.

Because the sealing surfaces of the gate valve are flat, the possibility of providing intimate contact between the metal-to-metal sealing surfaces is better with the gate valve than with the ball valve; however, the gate valve is subject to degradation of the sealing surface due to sliding of the gate across the seat. Seating stress is generated in the classical gate valve closure by wedging of the gate into the seat. With the blade valve closure used in the aerospace industry, the seating stress is obtained by spring loading the stationary seat against the translating blade.

B.5 BUTTERFLY VALVES

The butterfly valve consists of a flat circular butterfly, or disk, that rotates through 90 degrees to vary the flow stream from full to zero flow. The butterfly valve causes no change of direction to the flow stream, and can be designed to cause only a small obstruction in the flow path. Therefore, the flow resistance of the butterfly valve can be kept quite low.

Because of the rotary motion of the butterfly disk with respect to the seat, the sealing surface of the disk is always spherical. With metal-to-metal mating surfaces, the seat is normally conical, thus eliminating any problem of matching radii between the two mating surfaces.

Obtaining high degrees of surface finish on spherical and conical surfaces is relatively easy with rotary lapping equipment.

To provide the required seating stress, and to alleviate the scrubbing action ordinarily associated with valves having rotary motion, the butterfly disk is usually mounted a fraction of an inch off center with respect to the seat. Therefore, as the disk rotates open, it also translates away from the seat so that scrubbing of the disk on the seat is minimized. However, it is impossible to eliminate all of the scrubbing and some degradation of the sealing surfaces may occur after repeated valve cycling.

B. 6 POPPET VALVES

The poppet valve closure consists of a poppet (a disk on a stem) which moves in an axial direction, makes contact with a stationary seat, and interrupts the flow of a fluid.

The flow performance of the poppet closure is dependent upon the body styles in which it is mounted. Poppet valves are generally classified as in-line valves, angle valves, Y-valves, or globe valves. For clarity, the following definitions and examples are given.

B. 6. 1 In-line Valve

The flow stream flows in a straight path through this valve. The poppet of the in-line valve is buried in an island mounted on struts in the center of the flow stream. It is usual for the valve actuator to be contained in this central housing. The flow stream of a typical in-line valve enters the valve inlet, flows through the valve closure, expands slightly and flows over the actuator housing and the poppet, contracts slightly and passes out through the valve outlet. This valve configuration provides the lowest potential flow resistance of the poppet valve family.

B. 6. 2 Angle- or Y-Valve

Angle- or Y-valves turn the flow through angles of up to 90 degrees from the original path to allow the valve actuator to be situated outside of the flow stream. In practice, the name "angle valve" is reserved for a valve that turns the flow 90 degrees, and "Y-valve" is the name given to valves that turn the flow through angles of less than 90 degrees.

Because of the change of direction imposed on the flow path, the angle valves have higher flow resistances than the in-line valves. When selecting the angle valve, the valve designer trades a higher pressure loss for the inherent simplicity of design that is possible by placing the valve actuator outside the flow stream.

B. 6. 3 Globe Valve

The globe valve utilizes an S-shaped flow path (two 90-degree bends) to provide a poppet valve with in-line inlet and outlet ports, and with the actuator mounted outboard of the flow stream. These valves are commonly used for laboratory or test facility equipment where the emphasis is on ruggedness and durability rather than light weight and high performance. Globe valves are rarely used for airborne systems where weight and performance are important.

The combinations of poppet and seat shapes that are usually selected for valve closures are shown in Figure 66. All of the shapes shown can be shaped and finished with normal tooling, and all the appropriate combinations can be mated without difficulty.

The relative motion of the opening poppet with respect to the seat is translation of the poppet away from the seat along its centerline. The seating stress for the poppet closure is applied through the poppet stem or shaft. The valve actuator is usually mounted directly to the poppet shaft. Wedging of the poppet into the seat is possible with all the poppet-and-seat combinations of Figure 66, except the flat-on-flat combination. Wedging depends upon the contact angle between the poppet and seat, and the seating stress between the two. The flat-on-flat combination, which exhibits a contact angle of 90 degrees between the poppet and seat, cannot wedge. However, as the contact angle of the closure is reduced, its tendency to wedge will increase. Wedging should be avoided if possible because it can lead to scoring and galling of the mating parts.

SEATS \ POPPETS	FLAT 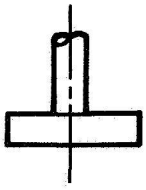	CONICAL 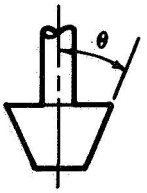	SPHERICAL 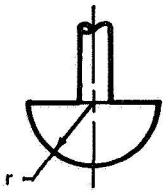
FLAT 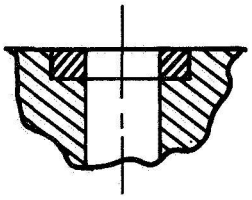	GOOD ANNULAR CONTACT	FAIR LINE CONTACT	FAIR LINE CONTACT
CONICAL 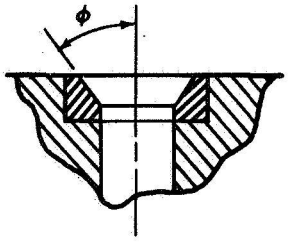		GOOD CONICAL CONTACT ($\theta = \phi$)	GOOD CONICAL CONTACT
TOROIDAL 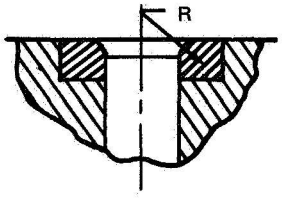		GOOD CONICAL CONTACT	GOOD CONICAL CONTACT
SPHERICAL 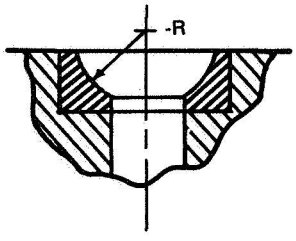		*A special case of this combination is shown in reference (7)*	GOOD SPHERICAL ZONE CONTACT

Figure 66. Seat and Poppet Combinations

Appendix C

PRELIMINARY DESIGN STUDY, BUTTERFLY VALVES

This appendix is extracted from Liquid Fluorine Design Study Program Final Report, AE-10821-R, AiResearch Manufacturing Company of Arizona, dated 7 June 1968. This document is the final report for the "Fluorine Component Design Study Program", Douglas Purchase Order A67-7037. This report presents the results of a study program leading to the design of a 2-in.-line-size butterfly shutoff valve for use with liquid fluorine or FLOX. The general design criteria and, specifically, the butterfly disk, seal, and seal loading mechanism used in this study program were derived from the previous design study program conducted under NASA Contract NASw1351.

Described in this appendix are the design, fabrication and assembly methods and quality control criteria for each of two valve designs which were developed in the study program.

3. DESIGN

3.1 Description

The objective of this study program was the design of a fail-safe-closed, 2-in.-line-size butterfly shutoff valve for liquid fluorine, liquid oxygen, or mixtures of the two. This section describes the designs of two valves which meet these requirements. The two valves, while having identical performance capabilities, differ in external configuration and in the method used to apply actuation force to the butterfly disk. The two valve designs are illustrated in Drawings L-395678-1 and -2.*

The two valves presented have been designed with special attention given to the following areas which are discussed in detail:

1. Valve and actuator housing
2. Butterfly disk and main shutoff seal
3. External seals
4. Butterfly shaft and bearings
5. Butterfly shaft seal and actuator linkage

---

*Valves shown in figures 6 and 7.

3.1.1 Butterfly Valve and Actuator Housing

The flow housings for both valves are machined forged billets of 6061 aluminum alloy. Castings were not used because of the need for specially graded castings and the potential problem of porosity and contamination in the casting. Because the quality requirements for castings used in fluorine are extremely restrictive, the casting rejection rate would be very high. The resulting high cost per casting, in addition to the tooling costs required for castings, would also tend to rule out their use. Weldments were also avoided because of the potential problem of cracks, porosity, and contamination in the weld joint.

Both valves have been made modular in design. This feature permits assembly of the actuator separate from the valve and will also permit removal of the actuator from the valve for servicing or adjustment, without disassembly of the entire valve or removing the valve from the system.

The actuator housings have been provided with dual purge ports for initial purging and to permit removal of fluorine seepage past static seals. In the event of a bellows shaft seal failure, the purge ports would also permit disposal of the fluorine leakage without letting it escape to the surrounding atmosphere and endanger personnel and equipment.

3.1.2 Butterfly Disc and Main Shutoff Seal

With only very minor exceptions, the configuration used on both valves for the butterfly disc, and its mating seal with integral loading bellows, is identical to the components developed under Contract NASw1351. The significant changes are: (1) reduction in size from three-inch to two-inch diameter, (2) reduction in loading bellows spring rate, and (3) setting the seal contact diameter equal to the bellows mean diameter.

The inside diameter of the seal bellows was selected to provide an open-position valve flow area very nearly the same as the inlet tube area. To reduce the loss in seal/butterfly disc contact force as a

result of assembly tolerances and deflection of parts under load, the spring rate of the seal loading bellows was reduced as much as practical. After consultation with Hydrodyne Inc, the minimum practical spring rate for the loading bellows was determined to be 812 pounds per inch. To attain the desired leakage limit, a butterfly disc-seal force of 115 pounds is required to be exerted by the loading bellows. Because of the low bellows spring rate, bellows stops have been provided in the valve body housing to limit bellows travel during valve actuation.

The seal contact diameter has been made equal to the mean diameter of the loading bellows. This permits application of valve inlet pressure to either side of the butterfly disc without resulting in an appreciable change in seal/butterfly disc contact force.

Two approaches have been considered to provide a closed-position stop for the valve butterfly; a fixed stop integral with the butterfly disc, and an adjustable butterfly disc stop in the valve body.

In Drawing L-395678-1, a fixed closed-position stop is incorporated directly on the butterfly disc to reduce downstream deflection of the disc during application of upstream pressure while closed. The closed position of the butterfly disc, relative to its seal, is determined by the fixed stop on the disc contacting a fixed pad within the valve body. The use of this fixed closed-position stop will necessitate close tolerances on its related dimensions and/or matched assembly parts to arrive at the proper closed position. Because the closed position is set during assembly of the unit, it can not be readily readjusted in the field. To accomplish a change in closed position the valve would have to be removed from the system and disassembled. Before use, the valve would again require recleaning and fluorine repassivation. Once the proper closed position adjustment is achieved, a wide variation in inlet pressure may be tolerated without resulting in a significant shift in the closed position of the disc.

Another feature of the fixed stop is that the closed position can not change during operation because of improperly secured position stops.

In Drawing L-395678-2, the closed position of the butterfly disc relative to its seal is determined by an adjustable stop in the valve body that is contacted by a fixed pad on the butterfly disc. This infinitely adjustable stop permits adjustment of butterfly disc position for minimum leakage and also restricts downstream deflection of the disc during application of upstream pressure while closed. This position adjustment capability will permit a greater latitude in fabrication tolerances and ease of assembly and adjustment of the valve. The closed position is set during assembly and is not readily readjusted unless the valve is removed from the system and partially disassembled. Before reuse, the valve would once again require recleaning and fluorine repassivation. Once adjusted to the proper closed position, a wide variation in inlet pressure may be tolerated without resulting in a significant shift in the closed position of the butterfly disc.

3.1.3 External Seals

External seals for containment of the liquid fluorine flow media are uncoated Inconel "X" bellows-type Hydrodyne seals. To assure compliance with the external leakage requirements of the specification, and in the interest of safety, dual external static seals have been used. With only minor modification to the valve body, special ports connected to the area between the dual seals could be provided for collection, detection, and removal of possible static seal leakage. The "bellows" characteristic of the seals is expected to permit disassembly and reassembly of sealing surfaces without requiring rework of the sealing surface.

The helium purge static seals are made of a filled TFE. In addition to containment of the purge gas, these gasket-type seals also act as thermal insulators to minimize conduction of cryogenic temperatures from the valve body to the pneumatic actuator cylinder. Static seals used to contain helium actuation gas are TFE "O" rings.

3.1.4 Butterfly Shaft and Bearings

Two butterfly shaft configurations have been considered; a one-piece through shaft, and stub shafts in the valve body engaging lugs on the butterfly disc.

The valve in Drawing L-395678-1 uses a one-piece butterfly shaft. The butterfly disc is splined to the shaft, and the shaft rotates in spherical bearings in the valve body. The use of the one-piece shaft through the valve body has the disadvantage of reducing flow area and creating turbulence in the flow stream. However, use of the continuous shaft through the valve to support the butterfly disc provides a rigid mounting for the disc, thus reducing disc displacement to a minimum during application of operating pressures.

The valve detailed on Drawing L-395678-2 uses stub shafts fixed to the valve body. The butterfly disc contains spherical bearings that engage the stub shafts in the body. The two-piece shaft configuration provides a maximum flow area through the valve with a minimum of turbulence induced in the flow stream. However, the two shafts do not provide the rigidity of a single through-shaft, and may permit a very limited amount of displacement of the butterfly disc upon application of upstream pressure. Comparing the shaft area shown on Drawing L-395678-1 with that on Drawing L-395678-2, it is noted that the two-piece shaft configuration will require twice the number of external static shaft seals as the one-piece shaft configuration.

Based on the data and recommendations contained in a bearing report prepared by the AiResearch Bearings Group (Appendix I) spherical bearings were selected for mounting the butterfly shaft. On Drawing L-395678-1, an alternate configuration is shown using full-ball-complement ball bearings. Because of the larger bearing O.D. required for ball bearings, their use in the bearing arrangement shown on Drawing L-395678-2 would not be practical.

Centering of the butterfly disc within the center of the seal is accomplished on both valve configurations by applying shims between a shoulder on the shaft and the shaft spherical bearings. Differences in expansion between the valve body housing and the butterfly shaft and disc will be accommodated by installing the necessary number of shims on the butterfly shaft to provide 0.008/0.009 inch end play of the butterfly disc.

Because of the limitations imposed by the liquid fluorine flow media, available lubrication material for the butterfly shaft and actuator linkage bearings is severely limited. Consideration was given to the use of either calcium fluoride or a fluorocarbon dry film called "Astrocoat-T". Based on available data, the use of "Astrocoat-T" would be the more suitable lubricant material, with a coefficient of friction of approximately 0.2 compared to approximately 0.4 for calcium fluoride. In the event of unforeseen difficulties, calcium fluoride should be used as an alternate lubricant. To prevent a catastrophic failure in the event of leakage past the actuator shaft seal bellows, the use of lubricants on bearings in the immediate vicinity of the bellows will be restricted to a fluorine-compatible lubricant.

3.1.5 Butterfly Shaft Seal and Actuator Linkage

Because of the extreme hazards resulting from fluorine leakage, it is imperative that measures be taken to provide a zero leakage hermetic seal on the valve actuator shaft. To meet this requirement, both valves employ a single-ply formed-convolution bellows on the actuator shaft. Two basic bellows motions have been employed, axial (extending and retracting) and rocking.

Drawing L-395678-1 illustrates use of the axial movement of a bellows. A relatively long bellows is needed to accommodate the necessary actuator stroke. Direct actuation of the valve is accomplished with the use of two actuator bearing joints, only one of which is required to operate in the liquid fluorine environment. The rocking motion of a bellows is used in the

design shown on Drawing L-395678-2. This type of bellows motion requires a less severe deflection and will, therefore, permit a longer service life than the axially deflected bellows of the previous design. Using the rocking motion of the bellows to transmit actuation force to the butterfly disc, as illustrated, requires the use of four actuator bearing joints, two of which are required to operate in liquid fluorine. In both valve designs the bellows are out of the direct flow stream when the valve is in the open position. This will prevent obstruction of flow through the valve and, most important, it will reduce the corrosion rate of the bellows by preventing the protective fluoride coating on the bellows from being removed by the flow stream.

Spherical bearings were not used in the actuator linkage because of space limitations. Their size would result in a much greater restriction in flow area than journal type bearings. For this reason journal bearing pinned joints have been used in all actuator linkage joints.

3.2 Analysis

3.2.1 Flow/Pressure Drop

To be assured of compliance with the pressure drop requirements at rated flow as specified in the requirements in Section I, the pressure drop was calculated for the valve . In determining the minimum flow area thru the two valves, and its location, both valves were found to be very nearly the same. The location of the flow restriction occurs where the end of the butterfly disc extends into the butterfly seal bellows in both valves.

Valve pressure drop ΔP is given by:

$$\Delta P = \frac{\rho v^2 f L}{2g \times 144 \times D} = 0.000108 \rho v^2 \left(\frac{fL}{D}\right)$$

ΔP = Valve pressure drop, psi

ρ = fluid density, lb/ft^3

v = fluid velocity at minimum flow area, ft/sec

$= q/A$

q = rate of flow, ft^3/sec

A = valve minimum flow area, ft^2

$\frac{fL}{D} = K$ = Resistance coefficient

A coefficient (K) of 0.28 is used. This selection of coefficient was determined from test data obtained from AiResearch valves of similar design and sizes. Except for extreme conditions of flow, there will not be a significant change in coefficient with a variation in flow.

$$\Delta P = 1.08 \times 10^{-4} \rho v^2 K$$

$$\rho = 96.7 \text{ lb/ft}^3$$

$$v = q/A = 0.2/0.0191 = 10.49 \text{ ft/sec}$$

$$K = 0.28$$

$$\Delta P = (1.08 \times 10^{-4})(96.7)(10.49)^2(0.28) = 0.32 \text{ psi}$$

The calculated pressure drop of 0.32 psi is well within the specified target value of 5.0 psi.

3.2.2 Material Selection

A detailed material selection for each of the two valves was made from data contained in a fluorine-compatible materials report prepared by the AiResearch Materials Engineering Group. This complete report is contained in Appendix II. The resulting material selections are summarized below.

Highly stressed parts in the valve body in contact with the fluorine are stainless steel. The butterfly disc and actuator linkage pins are "S" monel and the actuator shaft or linkage, shaft seal bellows, butterfly shaft, butterfly seal, and seal bellows are Inconel 718. The valve body is 6061 aluminum alloy. The actuator housing, cylinder, and lightly loaded actuator parts are aluminum alloy. The actuator piston, springs, and other heavily loaded parts are stainless steel. Static and dynamic actuator seals are TFE plastic. Valve-to-actuator thermal insulators are filled with TFE. The valve static seals containing the fluorine media are Inconel X.

For a detail part-material breakdown for both valves, refer to Drawings L-395678-1 and -2.

3.2.3 Stress Analysis

To assure the structural integrity of critical valve components, stress analyses were made of the areas of concern. The components and areas studied and the analyses are presented in the following outline. The actuator shaft bellows and the butterfly seal loading bellows are not included in the following outline as the supplying vendor assumes responsibility for their compliance with the design requirements.

Symbols used in the analyses are defined as follows.

F	Material property, allowable stress tensile, shear, ultimate, yield indicated by subscripts
E	Young's Modulus
G	Shear Modulus
t	Thickness
I	Moment of inertia of cross section
c	Distance from neutral axis to outer fiber
p	Pressure
P	Force
M	Moment
f	Calculated Stress
δ	Calculated Deflection

SPRING SECTION

d	Wire Diameter
D_M	Mean Coil Diameter
n_a	Number of Active Coils
f_N	Surge Frequency
K	Spring Rate
S.I.	Spring Index
W.F.	Wahl Factor
L	Free Length

Since the maximum ambient temperature is 140F, creep and stress rupture will not be a factor. All of the materials used exhibit increased strength at cryogenic temperatures while retaining good ductility, and all are generally acceptable for cryogenic use. Thus, for purposes of stress analysis, only yield and ultimate strengths at 140F need be listed.

Materials	F_{Tu} (psi)	F_{Ty} (psi)
"S" Monel	120,000	80,000
Inconel 718	180,000	150,000
CRES 347	85,000	40,000

The shear yield strength will be taken equal to 1/2 F_{Ty}.

It will be assumed that the pressure conditions of paragraph 2. must be withstood with metal temperatures equal to the maximum ambient temperature of +140F.

STRESS CALCULATIONS FOR PART 395678-1

Item 18, Butterfly Shaft (Inconel 718)

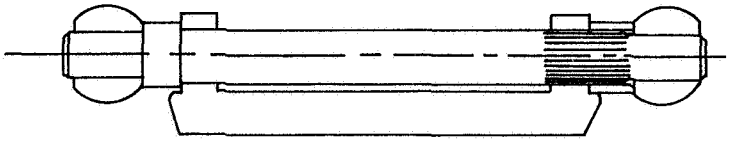

Plate Load - $\frac{\pi}{4}(2.5)^2(p) = 4.91p$

Operating, 491 pounds
Proof, 1230 pounds
Burst, 1840 pounds

$\frac{1230}{150} = 8.2$; $\frac{1840}{1.4 \times 180} = 7.3$ Proof Critical

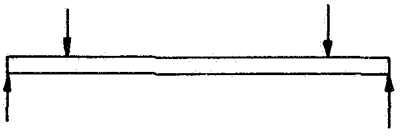

$M = 0.5\ (\frac{1230}{2}) = 307.5$ lb-in.

$f_B = \frac{32(307.5)}{\pi(0.28)^3} = 142{,}800$ psi

Item 4, Butterfly Disc ("S" Monel)

Disc Diameter 2.15 in.

For deflection, treat as a plate supported at the ends of a diameter.

δ_1 (center) $= 0.269\ \frac{p(1.075)^2}{D}$; δ_2 (edge) $= 0.371\ \frac{p(1.075)^2}{D}$

$D = \frac{24.2 \times 10^6\ (0.22)^3}{12(1 - 0.3^2)} = 2.36 \times 10^4$

$\delta_1 = 0.269\ \frac{100\ (1.075)^2}{2.36 \times 10^4} = 0.00152$ in.;

$\delta_2 = 0.371\ \frac{100\ (1.075)^2}{2.36 \times 10^4} = 0.0021$ in.

Deflections are tolerable for seal.
Check for stress:

$\frac{250}{80} = 3.125$; $\frac{375}{120} = 3.125$

Proof and burst condition is equally critical

$$f = \frac{250(2.15)^3}{\pi^2} \quad \frac{6}{(2.15)(0.22)^2} = 14{,}550 \text{ psi plate bending}$$

Actuator Lug

Actuator Force $P = \frac{\pi}{4}(1.25)^2 p = 1.228p$

Operating, 614 pounds
Proof, 736 pounds
Burst, 920 pounds

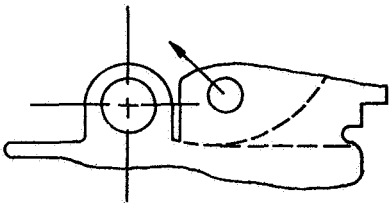

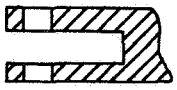

Use fitting factor of 1.3

$$f = 1.3 \frac{736}{2(0.2 \times 0.05)} = 47{,}900 \text{ psi}$$

Shaft Lugs

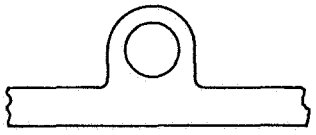

$$f = 1.3 \frac{615}{2(0.2 \times 0.08)} = 25{,}000 \text{ psi}$$

Item 21, Actuator Linkage Pins ("S" Monel)

$$f_s = 1.3 \frac{736}{2 \times \frac{\pi}{4}(0.15)^2} = 27{,}100 \text{ psi}$$

Item 5, Actuator Piston Shaft End (CRES 347)

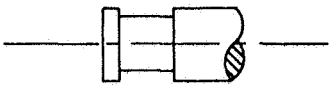

Peripheral load $\frac{736}{\pi(0.32)} = 1005$ lb/in.

$m = 1005 \left(\frac{0.32 - 0.28}{2}\right) = 20.1 \frac{\text{lb-in.}}{\text{in.}}$

$f = \frac{6\ (20.1)}{(0.08)^2} = 18{,}800$ psi

Direct Shear

$f_s = \frac{756}{\pi(0.28)(0.08)} = 10{,}750$ psi

Item 33, Actuator Shaft Ends (Inconel 718)

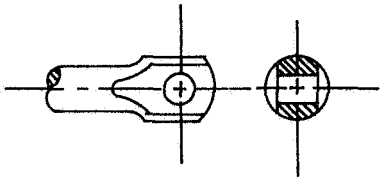

$\frac{920}{180} = 5.11$; $\frac{736}{150} = 4.91$

Burst is critical

$f = 1.3 \frac{920}{2(0.2 \times 0.06)} = 49{,}800$ psi

Item 13, Actuator Spring (inner) (Inconel 718)

$d = 0.222$ in., $D_M = 1.902$ in., $n_a = 7.5$, $G = 11 \times 10^6$

$F_{SPL} = 101{,}200$ psi $\quad F_{SY} = 121{,}500$ psi

$f_N = 14{,}040 \frac{0.222}{(1.902)^2(7.5)} = 115$ cps

$K = \frac{11 \times 10^6\ (0.222)^4}{8(1.902)^3(7.5)} = 64.9$ lb/in.

S.I. $= \frac{1.902}{0.222} = 8.57$

$$W.F. = \frac{8.32}{7.57} + \frac{0.615}{8.57} = 1.1697$$

$$f_S = 1.1697 \frac{8P\ (1.902)}{\pi (0.222)^3} = 518P$$

Load at loaded length, 160 pounds

Stack load = 160 +6.49 (0.88) = 217 pounds

f_S = 82,900 psi at loaded length

f_S = 112,000 psi stacked

Item 14, Actuator Spring (outer) (Inconel 718)

d = 0.250 in., D_M = 2.65, n_a = 6.5

$$f_N = 14{,}040 \frac{0.250}{(2.65)^2 (6.5)} = 77 \text{ cps}$$

$$K = \frac{11 \times 10^6\ (0.25)^4}{8(2.65)^3\ (6.5)} = 44.4 \text{ lb/in.}$$

$$S.I. = \frac{2.65}{0.25} = 10.6$$

$$W.F. = \frac{10.35}{9.6} + \frac{0.615}{10.6} = 1.137$$

$$f_S = 1.137 \frac{8P\ (2.65)}{\pi (0.25)^3} = 491P$$

Load at loaded length, 170 pounds

Stack load 170 + 44.4 (0.88) = 209.1 pounds

f_S = 83,500 psi at loaded length

f_S = 102,500 psi stacked

STRESS CALCULATIONS FOR PART 395678-2

Item 16, Butterfly Disc ("S" Monel)

$\frac{250}{80} = 3.125$, $\frac{375}{120} = 3.125$ Burst and proof equally critical

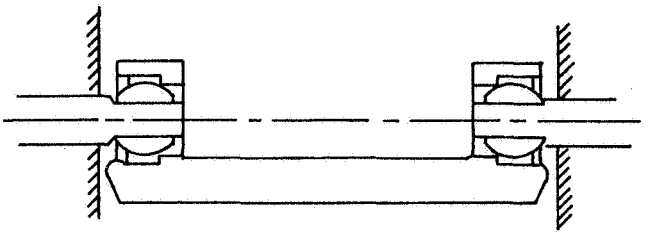

Calculate deflection treating this as a plate supported at the ends of a diameter

δ_1 (center) $= 0.269 \frac{p R^4}{D}$; δ_2 (edge) $= 0.371 \frac{p R^4}{D}$

$$D = \frac{24.2 \times 10^6 (6.22)^3}{12(1 - 0.3^2)} = 2.36 \times 10^4$$

$$\delta_1 = 0.269 \frac{100(1.075)^4}{2.36 \times 10^4} = 0.00152 \text{ in.}$$

$$\delta_2 = 0.371 \frac{100(1.075)^4}{2.36 \times 10^4} = 0.0021 \text{ in.}$$

$$f = \frac{250(2.15)^3}{\pi^2} \quad \frac{6}{2.15(0.22)^2} = 14{,}550 \text{ psi}$$

Shaft Lugs

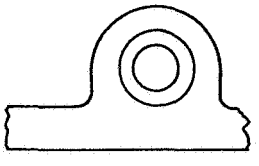

$$1/2 \left(\frac{\pi}{4}\right)(2.5)^2 (250) = 614 \text{ pounds}$$

$$f = 1.3 \frac{614}{0.35(0.06)} = 38{,}000 \text{ psi}$$

Actuator Lug

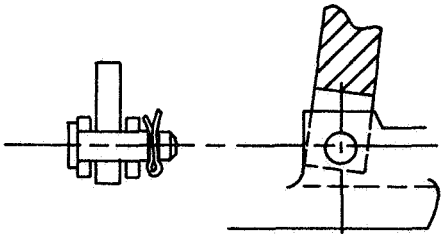

$\frac{600}{80} = 7.5 \qquad \frac{750}{120} = 6.25$

Proof pressure in actuator is critical

Force at plate $\left[\frac{\pi}{4}(1.17)^2(600) - 250\right] \frac{1.89}{1.3} = 572$ pounds

$f = 1.3 \frac{572}{2(0.12)(0.09)} = 34{,}400$ psi

Item 20, Actuator Linkage Pins ("S" Monel)

$f_S = 1.3 \frac{572}{2(\frac{\pi}{4})(0.16)^2} = 18{,}600$ psi at plate

Pivot Pin Force $\frac{\pi}{4}(1.17)^2(600) - 250 + 572 = 967$ pounds

$f_S = 1.3 \frac{967}{2(\frac{\pi}{4})(0.16)^2} = 31{,}400$ psi

Piston Pin Force $\frac{\pi}{4}(1.17)^2(600) - 250 = 395$ pounds

$f_S = 1.3 \frac{395}{2(\frac{\pi}{4})(0.16)^2} = 12{,}900$ psi

Item 15, Link Ends (Inconel 718)

Force at plate 572 pounds (proof)

At burst conditions, $P = \left[\frac{\pi}{4}(1.17)^2(750) - 250\right] \frac{1.89}{1.3} = 806$ pounds

$\frac{572}{150} = 3.81 \qquad \frac{806}{180} = 4.49$ Burst condition is critical

At plate, $f = 1.3 \frac{806}{4(0.06)(0.08)} = 54{,}600$ psi

At pivot

$$M = 1.3 \times 806 = 1050 \text{ lb-in.}$$

$$I/C = \left[\frac{0.32(0.36)^3}{12} - \frac{0.32(0.18)^3}{12}\right] \frac{1}{0.18} = 0.00605$$

$$f = \frac{1050}{0.00605} = 173{,}500 \text{ psi}$$

Item 18, Butterfly Stub Shafts (Inconel 718)

$$\frac{250}{150} = 1.67 \qquad \frac{375}{1.7 \times 180} = 1.225 \qquad \text{Proof is critical}$$

$$M = 0.24\ (615) = 147.5 \text{ lb-in.}$$

$$I/C = \frac{\pi}{32}\ (0.24)^3 = 0.001355 \text{ in.}^3$$

$$f = \frac{147.5}{0.001355} = 109{,}000 \text{ psi}$$

Item 6, Actuator Spring (inner) (Inconel 718)

$$F_{Sy} = 121{,}500 \text{ psi}$$

$d = 0.192$ in., $D_M = 1.90$ in., $n_a = 9.5$, $G = 11 \times 10^6$ psi

$$f_N = 14{,}040 \frac{0.192}{(1.90)^2(9.5)} = 78.6 \text{ cps}$$

$$K = \frac{11 \times 10^6\ (0.192)^4}{8(1.9)^3(9.5)} = 28.6 \text{ lb/in.}$$

$$S.I. = \frac{1.9}{0.192} = 9.9$$

$$W.F. = \frac{9.65}{8.9} + \frac{0.615}{9.9} = 1.083 + 0.0621 = 1.1451$$

$$f_S = 1.1451 \frac{8P\ (1.9)}{\pi(0.192)^3} = 783P$$

Load at loaded length, 90 pounds

Load when stacked, 90 + 1.75 x 28.6 = 140 pounds

f_S at loaded length, 69,500 psi

f_S at stacked height, 108,000 psi

Item 7, Actuator Spring (outer) (Inconel 718)

$d = 0.25$ in., $n_a = 8$, $D_M = 2.55$ in.

$$f_N = 14{,}040 \frac{0.25}{(2.55)^2(8)} = 67.5 \text{ cps}$$

$$K = \frac{11 \times 10^6 (0.25)^4}{8(2.55)^3(8)} = 40.5 \text{ lb/in.}$$

$$\text{S.I.} = \frac{2.55}{0.25} = 10.1$$

$$\text{W.F.} = \frac{9.85}{9.1} + \frac{0.615}{10.1} = 1.082 + 0.061 = 1.143$$

$$f_S = 1.143 \frac{8P\ (2.55)}{\pi(0.25)^3} = 475P$$

Load at loaded length, 160 pounds

Load when stacked, 160 + 40.5(1.65) = 227 pounds

f_S at loaded length, 76,000 psi

f_S at stacked height, 107,900 psi

3.2.4 Actuation Torque Requirements

The required pneumatic actuation and fail-safe spring force output was calculated using butterfly seal data and other information obtained under Contract NASw1351.

The opening torque required was determined as follows:

Butterfly seal material - Inconel 718

Butterfly disc material - "S" Monel

Contacting surface finishes - 4 to 8 micro inches

Friction coefficient - 0.14

Axial bellows load - 115 lb

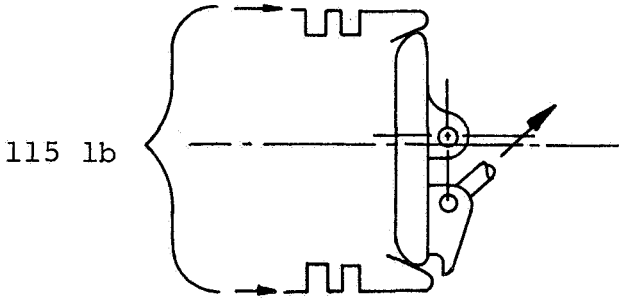

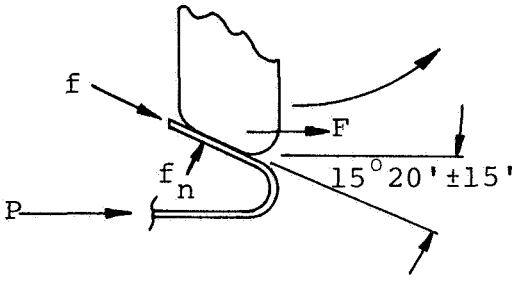

P = Bellows Force

f_n = Seal Normal Force

f = Seal Friction Force

F = Disc Force

$$f_n = \frac{P}{\sin 15^\circ 5'} = \frac{115}{\sin 15^\circ 5'} = 442 \text{ pounds}$$

$$f = uf_n = (0.14)(442) = 61.8 \text{ pounds}$$

$$F = \frac{f}{\cos 15^\circ 5'} = \frac{61.8}{\cos 15^\circ 5'} = 64 \text{ pounds}$$

Torque required by butterfly disc seal friction,

Butterfly disc gauge dia. = 2.290 in.

R = 1.145 in.

$T_D = RF = (1.145)\ (64) = 73.3$ in.-lb.

Torque required by pressure acting against butterfly disc offset.

Butterfly Disc Area = 4.12 $in.^2$

Butterfly Disc Offset = 0.040 to 0.0005 in.

Disc Differential Pressure = 100 psi

$T_p = (4.12)\ (100)\ (0.0405) = 16.7$ in.-lb.

Torque consumed by butterfly shaft bearings and equivalent torque consumed by the actuator linkage bearings is expected to approximate 10 in.-lb.

$T_B = 10$ in.-lb.

The minimum actuator output at the actuator shaft must be capable of providing the following torque to the butterfly disc to open the valve.

$$T_T = T_D + T_P + T_B = 73.3 + 16.7 + 10.0 = 100 \text{ in.-lb.}$$

This opening torque will be considerably higher than the required closing torque because the dynamic coefficient of friction between the disc and seal will be approximately one-half of the opening static friction coefficient. Also, the inertia of the blade and actuator assembly will assist in closing the valve. To be assured of adequate closing torque, the fail-safe mechanism for each valve has been designed to provide a closing torque equal to the opening torque requirements.

To determine the valve torque requirements resulting from flow, a review was made of test data from a valve of very similar design and size. It was determined that the hydrodynamic torque resulting from flow through the valve at the specified rate would be negligible. A dynamic torque curve of a 3-inch butterfly valve of very similar design is shown in Figure I.

The fail-safe spring force and actuator bore size required for each valve is determined as follows:

Part 395678-1

Fail-safe spring forces:

Torque required = 100 in.-lb

Close piston minimum moment arm = 0.36 in.

Minimum spring force required:

$$F = \frac{\text{Torque}}{\text{Arm}} = \frac{100}{0.36} = 278 \text{ pounds}$$

To overcome actuator friction, a minimum spring force of 310 pounds is required. To provide this spring force within the package, two springs are employed, nesting one within the other.

To overcome the spring force and also have an output adequate to operate the valve, an actuator output of approximately 560 pounds is desired (Actuator pressure = 500 psig).

Minimum actuator piston area required = $\frac{560}{500} = 1.12 \text{ in.}^2$

Actuator piston dia. = 1.250 in.

Actuator piston shaft dia. = 0.375 in.

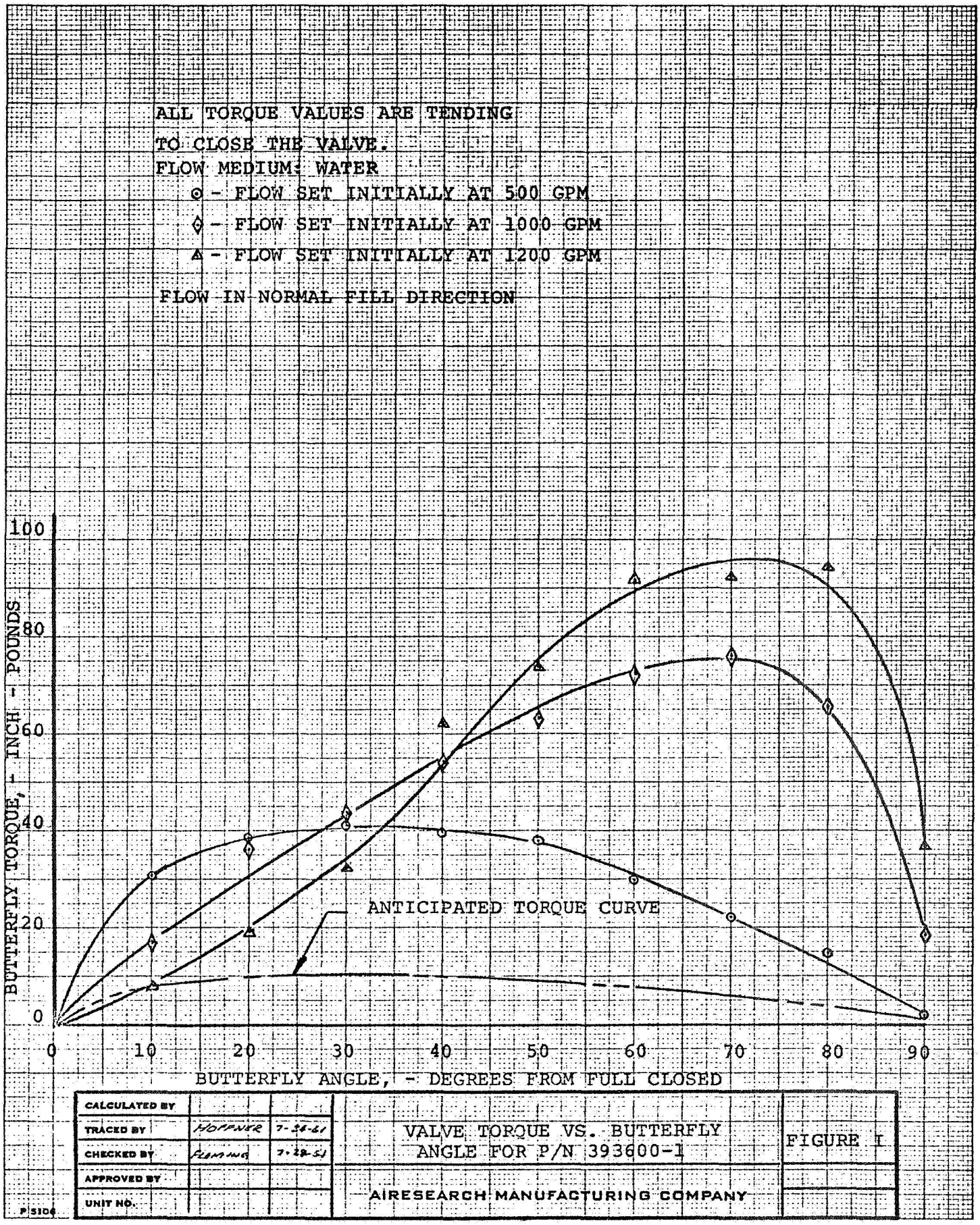

CALCULATED BY			VALVE TORQUE VS. BUTTERFLY ANGLE FOR P/N 393600-1	FIGURE 1
TRACED BY	HOFFNER	7-28-61		
CHECKED BY	[illegible]	7-28-61		
APPROVED BY			AIRESEARCH MANUFACTURING COMPANY	
UNIT NO.				

P 5106

Part 395678-2

Fail-safe spring forces:

Torque required = 100 in.-lb.

Close position minimum equivalent moment arm = 0.79 in.

Minimum spring force required

$$F = \frac{\text{Torque}}{\text{Arm}} = \frac{100}{0.79} = 127 \text{ pounds}$$

To overcome actuator friction, a minimum spring force of 160 pounds is required. One spring is capable of supplying this force within the given package. An additional operational margin of safety can be obtained by nesting a second spring within the first. The resultant combined spring force is 250 pounds.

To overcome the spring force and also have an output adequate to operate the valve, an actuator output of approximately 500 pounds is desired (Actuator pressure = 500 psig).

Minimum actuator piston area required = $\frac{500}{500} = 1.00 \text{ in.}^2$

Actuator piston dia. = 1.13 in.

4. MANUFACTURING

No unique fabrication processes are required for the fabrication of either of the two butterfly valves presented in this report. The important concern during fabrication is application of sufficient control to ensure a minimum degree on contamination of material being fabricated.

Both valves presented are very similar in design configuration and the same fabrication processes will be used for both valves. Because of possible cracks, porosity, and contamination problems, no castings or weldments are to be used in fabrication. The valve body, actuator housings, valve adapters, and the butterfly disc are machined from large billets. All other parts are machined from smaller diameter bar and plate stock. In securing the raw stock from a supplier, it is not possible to be assured that the surface of the material has not been contaminated with a foreign material. To prevent this surface contamination, special material handling at the mill and by the supplier would be required which would not prove to be economically feasible. To be assured of removal of surface defects and contamination, all parts should have a minimum of 0.188 inch stock surface removal before starting machining of actual part dimensions. This material must not be removed with less than three consecutive cutting passes over the surface to prevent imbedding the contaminants into the fresh machined surface. All machining operations are to be listed on the routing sheet in detail. At each operation the cutting tool material shall be recorded and the type of coolant used, if any.

The only coolants permitted are Hocut S5, Cincool T-10, and Pems 1755. No cutting oils of any type are permitted to be used. The cutting tool materials should be limited to high-speed tool steel and/or carbide-tipped and ceramic-tipped tools. No grinding or honing operations will be permitted because of surface-imbedded impurities resulting from the process.

Heat-treatment, stress relieving, and normalizing of any part will be done in the premachined condition or in an atmospheric controlled furnace. If any of these operations are performed, they must be recorded on the routing sheet accompanying the part. Floor inspection will follow each

operation as it is performed and will be recorded on the part routing sheet. Any purchased parts must be certified to comply with the fabrication requirements that have been discussed.

After fabrication, all parts shall be identified by only one of two methods. The part may be electro-etch identified on a non-functional surface or, if size or material will not permit etch identification, the part may be bagged and tagged.

After all fabrication processes are complete and prior to any assembly operations, all parts shall be cleaned per Component Control Document "D" and its referenced documents in Appendix III.

5. ASSEMBLY

After completing the preassembly cleaning and inspection requirements of Component Control Document "D", each valve can be assembled per the following applicable assembly instructions.

5.1 L-395678-1 Valve Assembly Instructions

5.1.1 Purpose - These instructions outline the assembly procedure and adjustments for the subject valve. The attached assembly record shall be completed for each unit assembled.

5.1.2 PROCEDURE

All parts shall be cleaned per the applicable cleaning document and all assembly procedures should be completed in a MIL-STD-209 Class 100 or MSFC-STD-246 Class III clean room.

Assembly of the valve shall be accomplished in the following sequence. Refer to Drawing L-395678-1 during assembly.

5.1.2.1 Actuator Assembly

5.1.2.1.1 Install Item 10 piston shaft seal in Item 3 actuator body. Refer to drawing and note proper location and orientation of the seal within the body.

5.1.2.1.2 Install Item 11 seal retainer over the piston shaft seal with the reduced O.D. end of the retainer against the shaft seal.

5.1.2.1.3 Insert Item 38 teflon sleeve into Item 12 guide until it bottoms out in the bottom of the bore.

5.1.2.1.4 Install the guide and sleeve assembly in the actuator body over the previously installed seal and seal retainer. With the guide positioned as shown in the drawing, secure with proper length screws and washers.

5.1.2.2 Piston Subassembly

a. Install Item 6 expander ring in the Item 5 piston groove per the drawing.

b. Place Item 7 backup ring on the piston over the previously installed expander ring. Orient as shown on the drawing.

c. Position Item 8 piston ring over the Item 7 backup ring with the one cut through the piston ring located 90° relative to any one of the two cuts through the backup ring. The groove in the piston ring O.D. should be facing the end of the piston.

d. Install the Item 9 piston ring in its mating groove in Item 8 piston ring. Position the one cut through the Item 9 piston ring 180° relative to the one cut through the Item 8 piston ring.

5.1.2.2.1 Carefully install Item 5 piston with its seal in the cylinder bore of the Item 3 actuator body. Bottom the piston in the cylinder bore using care not to permit rotation of the piston.

5.1.2.2.2 Place Item 39 seal in the groove around the cylinder bore in the end of the actuator body.

5.1.2.2.3 Position Item 23 cover over the actuator bore opening and secure with screws and washers.

5.1.2.2.4 Place the actuator assembly on a table with the open end up.

5.1.2.2.5 Place Item 13 and 14 springs inside the actuator body assembly.

5.1.2.2.6 Place Item 17 spring retainer over the springs with the flat surface up.

5.1.2.2.7 Place a spring compressing assembly tool over the spring retainer and fully compress the springs.

NOTE: While compressing the springs, be certain both springs are in full contact with the face of the retainer and are not partly resting on the separating ring.

5.1.2.2.8 Place Item 15 clevis retainer, spherical end down, over the protruding end of the piston shaft and let it rest against the spring retainer.

5.1.2.2.9 Engage the two halves of the Item 16 actuator clevis with the groove in the end of the actuator piston shaft protruding through the spring retainer as shown on the drawing.

The parting line between the two clevis halves is to be aligned with the actuator pressure inlet port centerline on the opposite end of the actuator body assembly.

5.1.2.2.10 While holding the actuator clevis halves in position, carefully remove the spring compressing tool. During removal of the tool, the I.D. of the clevis retainer Item 15 should be guided over the outside of the clevis halves, thus locking them together on the shaft.

The actuator assembly is now complete and should be set aside for later mating with the valve assembly.

5.1.2.3 Valve Assembly

5.1.2.3.1 Install Item 33 bellows and actuator rod assembly on the Item 1 valve body with Item 29 and 30 seals positioned between the bellows flange and valve body as illustrated on the drawing. The Item 33 bellows assembly should be oriented so that the flat sides of the actuator rod ends are parallel to the valve body centerline. Secure with Item 44 screws.

5.1.2.3.2 Place Item 19 spacer in the bottom of the butterfly shaft bearing bore in the Item 1 valve body and install Item 32 bearing in place bottoming out all parts.

5.1.2.3.3 Place a protective soft plastic cover over the sealing surface on the O.D. of the Item 4 butterfly disc.

5.1.2.3.4 Insert the Item 4 butterfly disc into the Item 1 valve body flow passage through the larger end opening with the disc positioned as shown by the dashed disc outline on the drawing.

5.1.2.3.5 Secure the Item 33 actuator rod to the butterfly disc center lug with an Item 21 pin. Place an Item 45 washer over the end of the pin and secure pin and washer with an Item 46 cotter pin.

5.1.2.3.6 Insert Item 18 butterfly shaft, splined end first, into the opening in the side of the valve body and engage the lugs on the butterfly disc.

5.1.2.3.7 Place Item 20 spacer on the end of the butterfly shaft, as illustrated on the drawing, and install Item 35 shims to obtain the butterfly disc position within the valve body bore as shown on the drawing. Continue insertion of the shaft, engaging the shaft splines with the splines in the butterfly disc lug and insert the shaft end into the previously installed Item 32 bearing.

5.1.2.3.8 Install the remaining Item 32 bearing on the end of the butterfly shaft.

5.1.2.3.9 Place Item 19 spacer on top of the bearing as shown.

5.1.2.3.10 Position Item 24 and 31 seals in their groove around the butterfly shaft opening and bottom Item 2 shaft cover against the seals and valve body.

5.1.2.3.11 Install Item 36 shims as required to obtain 0.008/0.009 inch end play of the butterfly disc. The shaft cover is then secured with screws and washers.

5.1.2.3.12 The butterfly disc is manually rotated to its farthest open position and is secured in this position by placing a TFE block between butterfly disc and the valve body.

5.1.2.3.13 Place Item 22 thermal gasket on the actuator mounting flange of the valve body.

5.1.2.3.14 The completed actuator assembly is positioned over the valve body with the actuator inlet port facing the valve body. The clevis on the end of the actuator assembly is placed over the flats on the actuator shaft end extending from the valve body. Secure the two assemblies together with an Item 21 pin. Place an Item 45 washer over the end of the pin and secure pin and washer with an Item 46 cotter pin.

5.1.2.3.15 Remove the protective soft plastic cover from the sealing surface of the butterfly disc and rotate the disc to the closed position.

5.1.2.3.16 Place proper length screws with protective washers through the actuator flange and engage the threads in the valve body. Tighten the screws uniformly, pulling the actuator down evenly onto the valve flange.

5.1.2.3.17 During assembly sequence 5.1.2.3.18, apply and maintain full actuator pressure of 500 psig on the actuator.

CAUTION: Make certain all fingers and tools are clear of the valve interior during actuation of the butterfly disc.

5.1.2.3.18 Install Item 34 butterfly seal with Item 28 static seal under the disc seal flange as illustrated in the drawing. Secure the disc seal with flat head screws.

5.1.2.3.19 Release the actuator pressure while exercising due caution.

AIRESEARCH MANUFACTURING COMPANY OF ARIZONA
A DIVISION OF THE GARRETT CORPORATION
PHOENIX, ARIZONA

PART 395678-1

ASSEMBLY RECORD

DATE: _____

UNIT SERIAL NUMBER: _____

ASSEMBLED BY: _____

VALVE BODY SERIAL NUMBER: _____

BUTTERFLY DISC SERIAL NUMBER: _____

BUTTERFLY SEAL SERIAL NUMBER: _____

BUTTERFLY DISC END PLAY: _____ (0.008 inch to 0.009 inch)

BUTTERFLY CLOSE POSITION WITH
ZERO UPSTREAM PRESSURE: (Record on Fig.)

BUTTERFLY CLOSE POSITION WITH
100 PSIG UPSTREAM PRESSURE: (Record on Fig.)

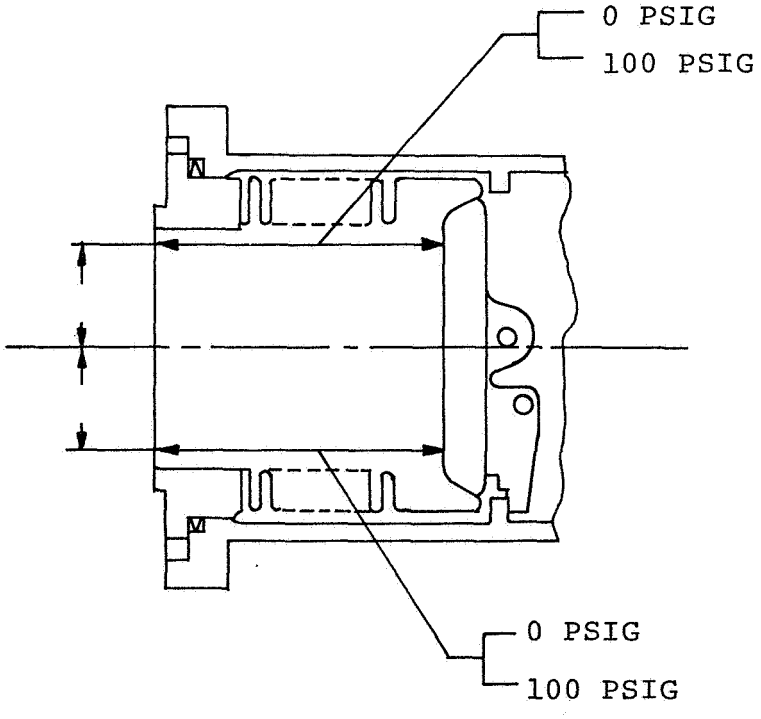

5.2 L-395678-2 Valve Assembly Instructions

5.2.1 Purpose - These instructions outline the assembly procedures and adjustments for the subject valve. The attached assembly record shall be completed for each unit assembled.

5.2.2 PROCEDURE

All parts shall be cleaned per the applicable cleaning document and all assembly procedures should be completed in a MIL-STD-209 Class 100 or MSFC-STD-246 Class III Clean Room.

Assembly of the valve shall be accomplished in the following sequence. Refer to Drawing L-395678-2 during assembly.

5.2.2.1 Actuating Cylinder

5.2.2.1.1 Press Item 12 bushing into its mating bore in the Item 3 actuator body. Press bushing in until end of bushing is flush with external recessed surface as indicated on the drawing.

5.2.2.1.2 Place actuator body assembly, Item 3, on table with the open end up.

5.2.2.1.3 Place springs, Items 6 and 7, inside the Item 3 body assembly.

5.2.2.1.4 Place Item 5 spring retainer on top of the springs with the smaller O.D. of the retainer nesting down inside Item 6 spring.

5.2.2.2 Piston Subassembly

a. Install Item 25 expander ring on Item 17 piston per drawing.

b. Install Item 24 backup ring over the previously installed expander ring. Orient as shown on the drawing.

5.2.2.2 (contd)

c. Install Item 23 piston ring over the Item 24 backup spring. The groove in the seal O.D. should be facing the shaft end of the piston.

NOTE: Cut through piston ring should be aligned 90° to one of the two cuts through the backup ring.

d. Install Item 22 piston seal in its mating groove in Item 23 piston ring per the drawing.

NOTE: Cut through piston seal should be located 180° relative to the cut through the Item 23 piston ring.

5.2.2.2.1 Insert the shaft of the Item 17 piston subassembly through the hole in the Item 5 spring retainer and through the Item 12 bushing in the actuator housing until the shoulder on the piston shaft contacts the spring retainer. The side flats on the end of the shaft shall be positioned parallel with any one side of the square on the end of the actuator.

5.2.2.2.2 Place Item 11 gasket in position on the end of Item 4 actuator cover.

5.2.2.2.3 Using care not to damage the piston seals, install the actuator cylinder, which is an integral part of the Item 4 actuator cover, over the piston. Slide the cylinder over the piston until it bottoms out in the bottom of the cylinder bore.

NOTE: The common centerline of the two ports on the Item 4 cover shall be oriented to be parallel with the flats on the sides of the piston shaft end. The actuator cover mounting holes should also be aligned with the matching holes in the actuator body before engaging the piston seals and should not be rotated.

5.2.2.2.4 Place two full-length threaded screws, of sufficient length to pass through the cover and engage the matching threads in the actuator body, through two opposing holes in the cover. These two screws are to be tightened simultaneously and equally until the cover is bottomed on the actuator body.

5.2.2.2.5 Install two washers and screws of proper length in the two remaining opposing holes and secure.

5.2.2.2.6 Remove the two long screws previously used for assembly and replace with proper length screws and washers and secure.

The actuator assembly is now complete and should be set aside for later mating with the valve assembly.

5.2.2.3 Valve Assembly

5.2.2.3.1 Place a protective soft plastic cover over the sealing surface on the O.D. of the butterfly disc.

5.2.2.3.2 Install an Item 30 bearing in each lug of the butterfly disc, Item 16. Bearing is to be bottomed in its mating bore.

5.2.2.3.3 Insert the disc into the Item 1 valve body flow passage through the larger end opening, with the disc surface containing the lugs parallel with and facing the opening in the side of the valve flow passage for the actuator linkage. The single lug perpendicular to the edge of the disc is to be closest to the valve body flange opening through which the disc was inserted.

5.2.2.3.4 Item 31 seals are placed in their proper position on the Item 18 stub shafts as indicated on the drawing, and the Item 32 seals are installed in the proper recess in the valve body.

5.2.2.3.5 While the disc is being held in position, the two stub shafts are installed engaging the Item 30 bearing bores and bottomed against the seals in the valve body.

5.2.2.3.6 With the use of the shims indicated on the drawing in Section D-D, the butterfly disc is to be positioned in the center of the valve body bore with 0.008/0.009 inch end play equally spaced about the valve centerline. The stub shafts are then secured with screws and washers.

5.2.2.3.7 Install the butterfly disc stop, Item 21, as shown in Section A-A.

5.2.2.3.8 With the butterfly disc held firmly against the stop, the stop shall be rotated until the entire face of the disc is parallel with the face of the large bolt flange within ±0.001 inch.

5.2.2.3.9 Install Item 33 and 34 static seals as indicated in Section A-A.

5.2.2.3.10 Attach one end of Item 15 link to the end of Item 13 bellows assembly lever with an Item 20 pin as shown on the drawing. Place a washer over the end of the pin and secure washer and pin with a cotter pin.

5.2.2.3.11 Using care not to disturb the position of the butterfly disc stop, the Item 13 bellows assembly is installed in the valve body as shown with the linear pivot centerline aligned perpendicular to the valve centerline.

5.2.2.3.12 Place Item 8 thermal gasket over the bellows assembly flange and place the Item 2 actuator adapter over the bellows assembly and gasket with the actuator cylinder mounting flange oriented directly over the large flange on the valve flow body. Secure these parts with the proper screws and washers.

5.2.2.3.13 Attach the free end of Item 15 link to the butterfly disc with an Item 20 pin. Place a washer over the end of the pin and secure washer and pin with a cotter pin. Check movement of lever and butterfly disc rotation for freedom of movement.

5.2.2.3.14 Install the previously assembled actuator on the valve assembly with Item 10 gasket installed between the two assemblies as shown. Orient the actuator ports as shown on the drawing. Secure with the proper screws and washers.

5.2.2.3.15 Slowly apply pressure to the actuator port until the actuator shaft is fully extended. While the shaft is extending be sure the end of the shaft is guided into the slot in the end of the actuator lever passing through the bellows.

5.2.2.3.16 Secure the actuator lever to the end of the actuator piston shaft with an Item 20 pin. Place a washer over the pin end and secure washer and pin with a cotter pin.

NOTE: Maintain full actuator pressure of 500 psig on the actuator during assembly sequence of 5.2.2.3.16 and 5.2.2.3.17.

5.2.2.3.17 Carefully remove the soft plastic protective cover from the butterfly disc.

5.2.2.3.18 Install the Item 14 butterfly seal with Item 35 static seal under the butterfly seal flange as illustrated in Section A-A of the drawing and secure with the proper flat head screws.

5.2.2.3.19 Release actuator pressure, letting the valve close.

CAUTION: Make sure tools and all fingers are clear of valve interior.

5.2.2.3.20 Install actuator cover and gasket, Items 19 and 9 respectively, and secure.

5.2.2.3.21 Install valve adapters and Items 33, 34, 35, and 36 static seals as illustrated in Section A-A of the drawing.

5.2.2.3.22 The valve assembly is now complete and shall be cleaned per the applicable cleaning specification.

After assembly per the preceding outline, the valve shall be cleaned and packaged per the requirements of Component Control Document "D" in Appendix III.

AIRESEARCH MANUFACTURING COMPANY OF ARIZONA
A DIVISION OF THE GARRETT CORPORATION
PHOENIX, ARIZONA

PART 395678-2

ASSEMBLY RECORD

DATE: _____

UNIT SERIAL NUMBER: _____

ASSEMBLED BY: _____

BUTTERFLY DISC SERIAL NUMBER: _____

BUTTERFLY SEAL SERIAL NUMBER: _____

BUTTERFLY DISC END PLAY: _____ (0.008 inch to 0.009 inch)

BUTTERFLY CLOSE POSITION WITH
ZERO UPSTREAM PRESSURE: (Record on Fig.)

BUTTERFLY CLOSE POSITION WITH
100 PSIG UPSTREAM PRESSURE: (Record on Fig.)

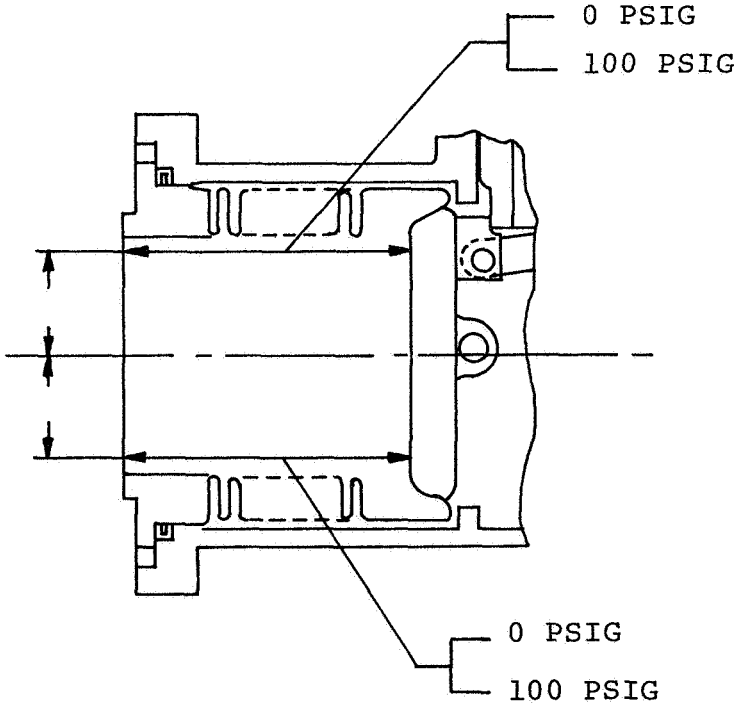

6. INSPECTION AND DOCUMENTATION

The butterfly valve configurations depicted on Drawings L-395678-1 and L-395678-2 are very similar in design and the fabrication, cleaning, and inspection problems to be encountered will be identical for both valves. Therefore, the data presented is equally applicable to both valves.

Because of the highly reactive nature of fluorine, extreme care must be taken in the handling of raw material to be used for fabrication of parts used in fluorine. Additional care must also be taken during fabrication, inspection, and assembly to prevent contamination of parts during these phases of production. To be assured of maintaining the necessary cleanliness level, complete process control and documentation must be maintained throughout all phases of the production of the valves. This includes the raw material as well as all intermediate operations and the final assembly.

Surface inspection of raw material or parts shall be limited to either visual or eddy-current methods. For internal material inspection, ultrasonic or radiographic inspection is to be used. The method to be used will depend primarily on part geometry and defect orientation. In some instances, more than one method may be required to adequately inspect a part.

Determination of chemical composition and physical properties of the raw material shall be obtained from coupons removed from the same piece of raw stock from which the part is to be fabricated. The raw material chemical composition and physical properties must be determined in accordance with applicable ASTM standard procedures and should be determined upon receipt at the fabricators receiving and inspection department.

All finished parts are to be 100 per cent dimensionally inspected. All blueprint dimensions, finishes and special characteristics of parts that will operate in contact with the fluorine media are to be measured and permanently recorded.

TABLE I

INSPECTION REQUIREMENTS

Application	Dimensional Inspection	Physical Properties	Chemical Properties	Surface Inspection	Internal Inspection
Wrought Metals	1	1	1	1	1
Forgings	1	1	1	1	1
Teflon	1, 2, 3	1		1, 2, 3, 4	
Weldments	1, 2, 3	1	1	1, 2. 3	1, 2, 3
Machined Surfaces	1, 2, 3			1, 2. 3, 4	
Formed Parts	1, 2, 3	1	1	1, 2, 3, 4,	1

NOTE: 1. Receiving and Inspection
2. In-Process Inspection
3. Final Inspection
4. Clean Room Inspection

At no time during the manufacturing phase should any repair of material and/or component defect be performed without the written authorization of the cognizant engineer. Any authorized repair will be followed by all of the necessary approved inspection methods which will assure that the integrity and cleanliness of the item being repaired have not been harmed in any way.

Table I, Inspection Requirements, lists the inspection requirements that are to be accomplished with the use of the applicable inspection techniques mentioned above.

All component parts should have a complete itemized history. To be assured of proper documentation, the following documentation outline should be adhered to for each component part. The data should be given in sufficient detail to provide a concise background for analysis and evaluation. Purchased parts should be certified by the supplier as complying with the applicable portion of the following documentation outline.

Raw Material

(a) Lot number

(b) Heat number (where applicable)

(c) Batch number (where applicable)

(d) Rough forming processes

(e) Heat treatment (where applicable)

(f) Cleaning procedures

(g) Repair methods (when approved and where applicable)

(h) Date of manufacture

(i) Name of manufacturer

Receiving and Inspection

(a) Chemical analysis

(b) Mechanical properties, such as tensile strength, etc.

(c) Physical inspection, method and materials used, and results including the following:

  (1) Dimensional

  (2) Porosity

  (3) Inclusions

  (4) Cracks

Manufacturing

(a) Manufacturing process or processes used, such as saw, lathe, and mold

(b) In-process inspection methods, materials, and results

(c) Coolants (where applicable)

(d) Mold-release materials used (where applicable)

(e) Cutting and/or forming-tool materials, such as high-speed steel, carbide-tipped

(f) Heat treatment (where applicable), including stress-relieving and normalizing

(g) Mechanical properties (where applicable)

(h) Repair methods (when approved and where applicable)

(i) Date of manufacture

(j) Precleaning methods and materials

(k) Name of manufacturer

Post-Manufacture

(a) Precleaning methods and materials

(b) Fluorine level cleaning methods and materials

(c) Fluorine clean inspection methods and materials

(d) Assembly procedure and materials (where applicable)

(e) Leak-check procedure, materials, and results

(f) Functional checkout procedure, materials, and results (where applicable)

(g) Preservation and/or packaging

(h) Shipping and handling procedure

(i) Fluorine clean certification date

(j) Leak-check certification date

(k) Functional checkout certification date

The documentation information listed above should be maintained in a step-by-step sequence. This information should be assembled and maintained in a manner to permit concise traceability of a component from the raw-material production phase through the finished form or any intermediate portion. This information must indicate all foreign materials, such as solvents and cutting tools, that contact the component being documented, and the methods by which the contact was made. To document an itemized history of each valve part, a routing sheet must accompany each part during all phases of the fabrication process and remain with its respective part until the part is assembled into a valve. At that time the routing sheet will enter the valve documentation package.

The documentation should also indicate component operational cycles, such as leak and/or functional tests, performed during manufacture to allow evaluation or prediction of operational life. This information should be in sufficient detail to record the operating regime and environment.

Appendix D

PRELIMINARY DESIGN STUDY, POPPET VENT-AND-RELIEF VALVES

This appendix is extracted from Fluorine Vent and Relief Valve PN 5680002 and PN 5680003, Engineering Design Report EDR 5670099, Systems and Advanced Components Division Parker Aircraft Company, dated 7 May 1968. This document was prepared for the McDonnell Douglas Corporation by Parker Aircraft and is the final report under Purchase Order No. DAC-A67-7038. This document reports the development, by Parker Aircraft, of the design for a practical vent and relief valve for fluorine service.

In order to portray the evolution of the design from evaluation of the problem through the various development phases to detailing of the final valve configuration, the report is divided in two parts:

PART I - SELECTION OF THE DESIGN CONCEPT
PART II - DETAILED DESIGN

Described in this appendix are the design, manufacturing, and assembly procedures for the two valve designs which were developed in the study program.

PART II - DETAILED DESIGN

1.0 INTRODUCTION

1.1 Based on the design concept selected in Part I of this report, a detailed design was created. This part of the report first describes the selected design, then presents details of the design analyses. Manufacturing and assembly procedures are outlined.

1.2 The steps leading to the final detail design were:

1. Calculating the time response of the valve, using an appropriate mathematical model.

2. Optimizing the design by altering the values of design parameters:

   a. to obtain good response

   b. to permit practical design elements (e.g. bellows, springs).

3. Verifying compliance with specified performance by calculating the response of the valve, over a full range of operating conditions, for the finally selected design parameters.

These first three steps result in a list of design parameters, such as spring rates, effective areas maximum strokes, seat diameters, etc., which define the properties that the design elements must possess if the valve is to meet the performance requirements. These parameters must next be translated into actual hardware designs.

4. Final decisions are made on how to handle each mechanical detail. This involves decisions such as pistons vs bellows, vs diaphragms, static seals vs welds, etc. Of course such details had already been visualized to guide the preliminary design work.

5. Each of the design elements must be analyzed in detail. For example, the design parameters require a certain spring rate, effective area, maximum pressure, and

stroke, for the power bellows (main valve actuator). Materials limited the permissible stresses. It was necessary to calculate the required material thickness, span, mean diameter, and number of convolutions, for the type of bellows which had been selected for use. These calculations were made for every significant element of the valve.

6. A scale layout of the valve was prepared, showing all mechanical details.

7. The detailed design was reviewed with Parker manufacturing personnel. Manufacturing processes were determined. Design changes were made where manufacturing could be simplified without adversely affecting the part or its function. Particular attention was focussed on those manufacturing procedures which would have to be performed in a specific way due to the valve's intended fluorine service.

2.0 DESCRIPTION OF THE FLUORINE VENT AND RELIEF VALVE

2.1 General - There are two models of this valve. Type 1 (PN5680002) is recommended for flight use. Type 2 (PN5680003) is recommended for test and prototype work, where convenience of modification is important. Reduced prints of the assembly drawings of these valves are reproduced on the following pages.

2.2 How it Operates - The valve has two modes of operation. See figure 20 for a schematic diagram of the valve.

1. Vent Mode - The main valve is held normally closed by a spring preload force, plus the force of any inlet pressure acting on the main valve. To open the valve (vent the tank) pressure is applied to the vent actuator bellows from an external pressure source. This exerts a downward force, which overcomes the upward force holding the valve closed. The valve then opens. To reclose the valve the pressure is vented from the vent mode actuator.

2. Relief Mode - The main valve will open automatically if the tank pressure exceeds a preset value. This is accomplished by means of a pilot valve, and a large

REVISIONS				
E.C.O. NO.	SYM	DESCRIPTION	DATE	APPROVAL

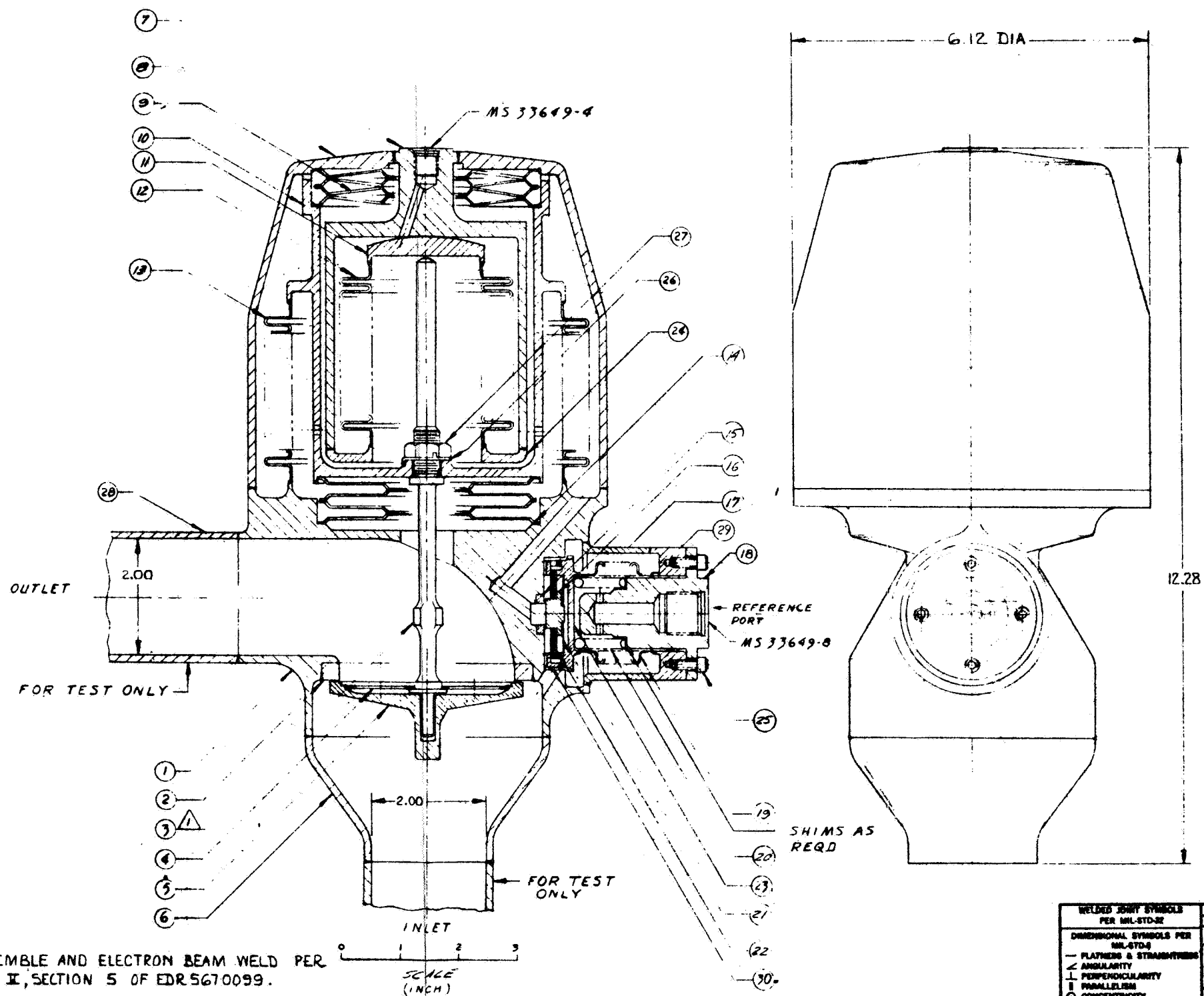

2. ASSEMBLE AND ELECTRON BEAM WELD PER PART II, SECTION 5 OF EDR5670099.

1 THREADS BRUSHED COPPER COATED

NOTES: (UNLESS OTHERWISE SPECIFIED)

ITEM NO.	DWG SIZE	QTY REQD	PART OR IDENTIFYING NO.	NOMENCLATURE OR DESCRIPTION	MATERIAL	MATERIAL SPECIFICATION	HEAT TREAT	FINISH	FABRICATION PROCESS
30		1		PLATE, STOP	INCONEL 718				LATHE & MILL
29		1		FLANGE, BODY	INCONEL 718				LATHE & MILL
28		1		PORT-OUTLET					TUBING
27		1		NUT	CRES				PURCH.
26		1		WASHER, TAB	CRES				PURCH.
25		4		SCREW	CRES				PURCH.
24		1		LOWER VENT HOUSING	INCONEL 718				LATHE
23		1		STOP	321/347	QQ-S-763			LATHE & MILL
22		1		COMPENSATOR-TEMPERATURE	NI. CR. Fe ALLOY				LATHE
21		1		BELLEVILLE	321/347	QQ-S-763			STAMPING
20		1		SPRING	STEEL				PURCH.
19		1		BELLOWS-PILOT	321/347	QQ-S-763			TUBING, FORMED
18		1		PLUG	321/347	QQ-S-763			LATHE & DRILL
17		1		BODY-PILOT	INCONEL 718				LATHE
16		1		POPPET-PILOT	321 CRES	QQ-S-763			LATHE
15		1		SEAT-PILOT	INCONEL 718				LATHE
14		1		FLEXURE-LOWER	321/347	QQ-S-763			STAMPING
13		1		BELLOWS-POPPET	321/347	QQ-S-763			TUBING, FORMED
12		1		BELLOWS-VENT	321/347	QQ-S-763			TUBING, FORMED
11		1		CAP-VENT	INCONEL 718				LATHE
10		1		HOUSING-POPPET BELLOWS	INCONEL 718				LATHE, MILL & DRILL
9		1		FLEXURE-UPPER	321/347	QQ-S-763			STAMPING
8		1		HOUSING-OUTER	INCONEL 718				LATHE OR SPINNING
7		1		HOUSING-VENT	INCONEL 718				LATHE & DRILL
6		1		POPPET-INLET	INCONEL 718				LATHE OR SPINNING
5		1		POPPET-MAIN	321 CRES	QQ-S-763			LATHE
4		1		GUIDE	321/347	QQ-S-763			STAMPING
3		1		STEM	321/347	QQ-S-763			LATHE & MILL
2		1		SEAT-VALVE MAIN	INCONEL 718				LATHE & HAND LAP
1		1		HOUSING MAIN	347	CASTING			LATHE & JIG BORE
				ASSEMBLY					

LIST OF MATERIAL

WELDED JOINT SYMBOLS PER MIL-STD-22
DIMENSIONAL SYMBOLS PER MIL-STD-9
FLATNESS & STRAIGHTNESS
ANGULARITY
PERPENDICULARITY
PARALLELISM
CONCENTRICITY
TRUE POSITION
ROUNDNESS
SYMMETRY
(MMC) MAXIMUM MATERIAL CONDITION
(RFS) REGARDLESS OF FEATURE SIZE

NEXT ASSY	USED ON
APPLICATION	

UNLESS OTHERWISE SPECIFIED
DO NOT SCALE DRAWING
DIMENSIONS ARE IN INCHES
TOLERANCES
FRACTIONS ± 1/32 | DEC (.XX) ± .03 | DEC (.XXX) ± .010 | ANGLES ± 0°30'
TOLERANCES OF HOLES SPECIFIED "DRILL" PER ANSI B94.11
MUST CONFORM TO RMS 1—1
MACHINED SURFACE 125/ PER MIL-STD-10
CLASSIFICATION OF CHARACTERISTICS
CD PER SPI-622-8 & MIL-STD-889
REV 125

SIGNATURES		DATE
DR BY	CALLISON	9/11/67
DESGN BY		
CHK BY	E.J.	9-11-67
PROJ ENG		
APPD BY		

Parker Aircraft — LOS ANGELES, CALIFORNIA — DIVISION OF PARKER-HANNIFIN CORP.

TITLE: FLUORINE VENT AND RELIEF VALVE (TYPE I) WELDED

SIZE	CODE IDENT NO.	DWG NO.
D	92003	5680002

SCALE FULL | UNIT WT ACTUAL CALC | LBS | SHEET 1 OF 2

5680002

REVISIONS					
E.C.O. NO.	SYM	DESCRIPTION	DATE	APPROVAL	

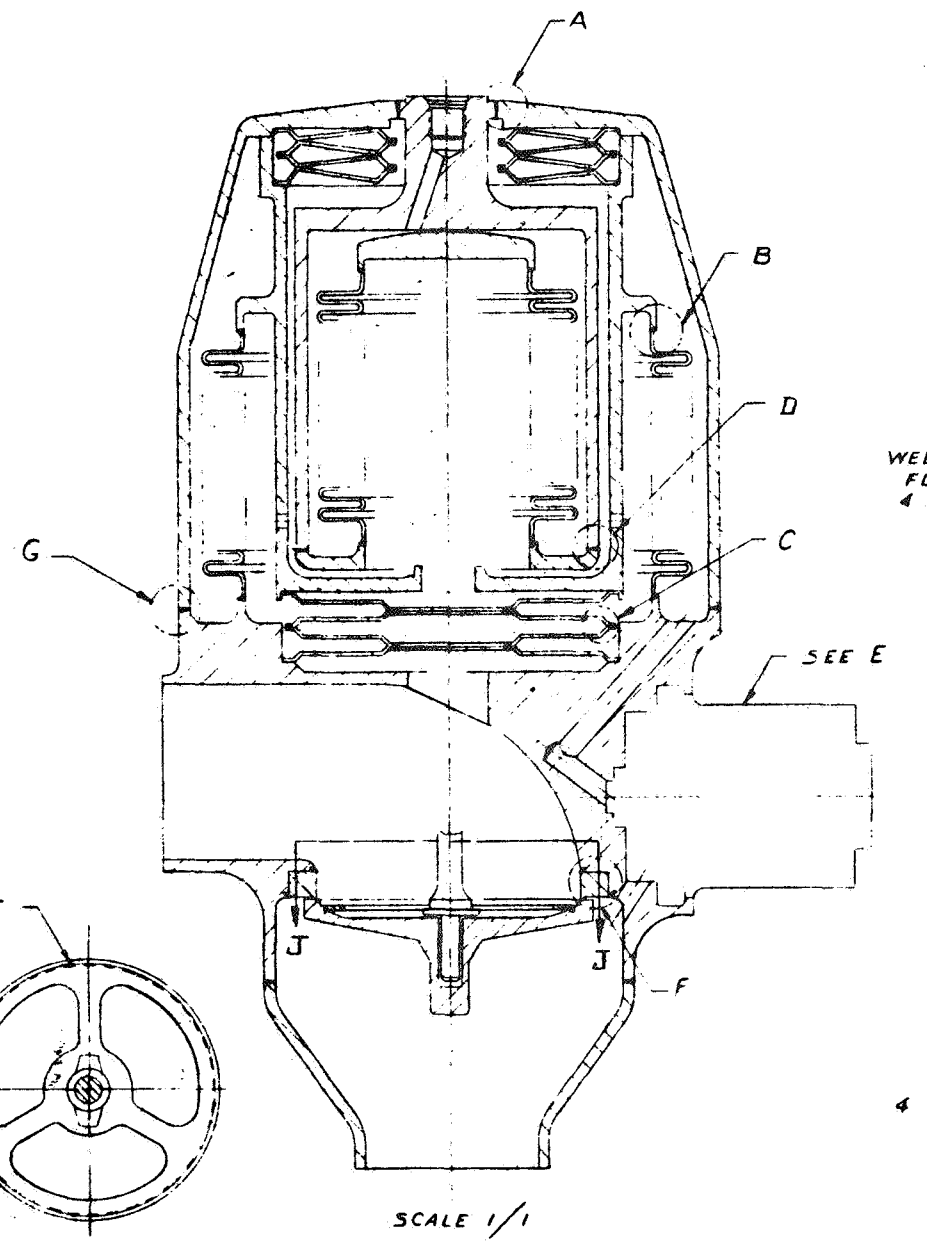

SCALE 1/1

VIEW J-J

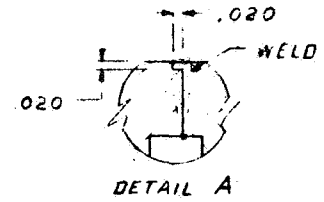

DETAIL A

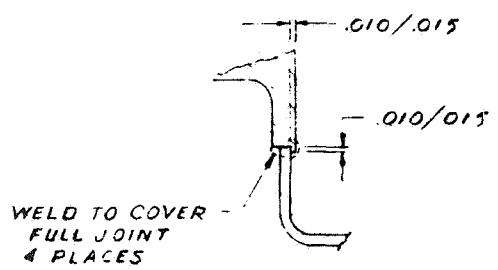

DETAIL B

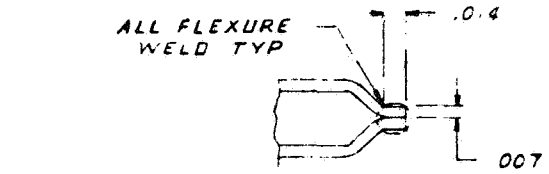

DETAIL C

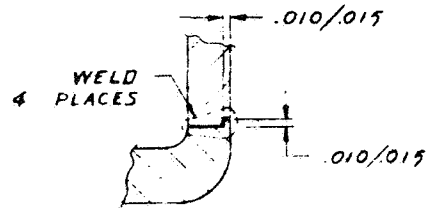

DETAIL D

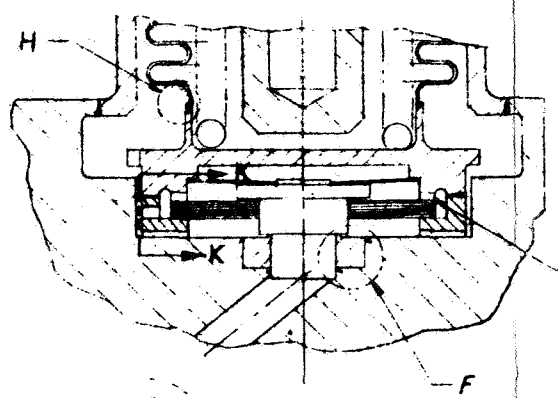

VIEW K-K
TO SHOW FLOW SLOTS

DETAIL E
SCALE 2/1

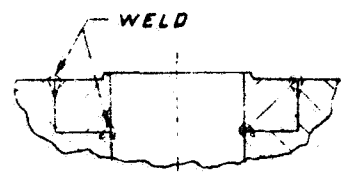

SEAT PRESS FIT TO BODY
2 SEATS

DETAIL F

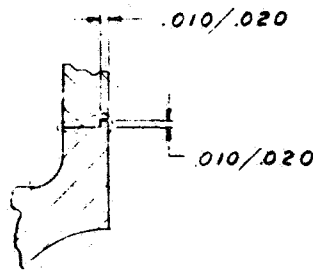

DETAIL G

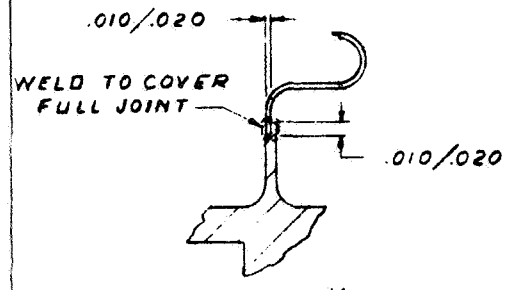

DETAIL H

ITEM NO.	DWG SIZE	QTY REQD	PART OR IDENTIFYING NO.	NOMENCLATURE OR DESCRIPTION	MATERIAL	MATERIAL SPECIFICATION	HEAT TREAT	FINISH	FINISH SPECIFICATION

LIST OF MATERIAL

NEXT ASSY	USED ON
APPLICATION	

WELDED JOINT SYMBOLS PER MIL-STD-22

DIMENSIONAL SYMBOLS PER MIL-STD-8
- FLATNESS & STRAIGHTNESS
- ANGULARITY
- PERPENDICULARITY
- PARALLELISM
- CONCENTRICITY
- TRUE POSITION
- ROUNDNESS
- SYMMETRY
- (RMC) MAXIMUM MATERIAL CONDITION
- (RFS) REGARDLESS OF FEATURE SIZE

UNLESS OTHERWISE SPECIFIED
DO NOT SCALE DRAWING
DIMENSIONS ARE IN INCHES
TOLERANCES
FRACTIONS ± 1/32 | DEC .XX ± .03 | DEC .XXX ± .010 | ANGLES (DEG) ± 0°30'
TOLERANCES OF HOLES SPECIFIED "DRILL" PER ANSI B94.11
MUST CONFORM TO RA 1 — 1
MACHINED SURFACE 125 PER MIL-STD-10
CLASSIFICATION OF CHARACTERISTICS
CR — PER SPI-6024-6 & MIL-STD-105
REF 125

SIGNATURES		DATE
DR BY	G Young	8/19/68
DSGN BY		
CHK BY	E Fisher	8/20/68
PROJ ENG		
APPD BY		

Parker Aircraft — LOS ANGELES, CALIFORNIA — DIVISION OF PARKER-HANNIFIN CORP.

TITLE: FLUORINE VENT & RELIEF VALVE (TYPE I) WELDED

SIZE	CODE IDENT NO.	DWG NO.
D	92003	5680002

SCALE 3/4 NONE UNIT WT ACTUAL CASE LBS SHEET 2 OF 2

NOTES (UNLESS OTHERWISE SPECIFIED)

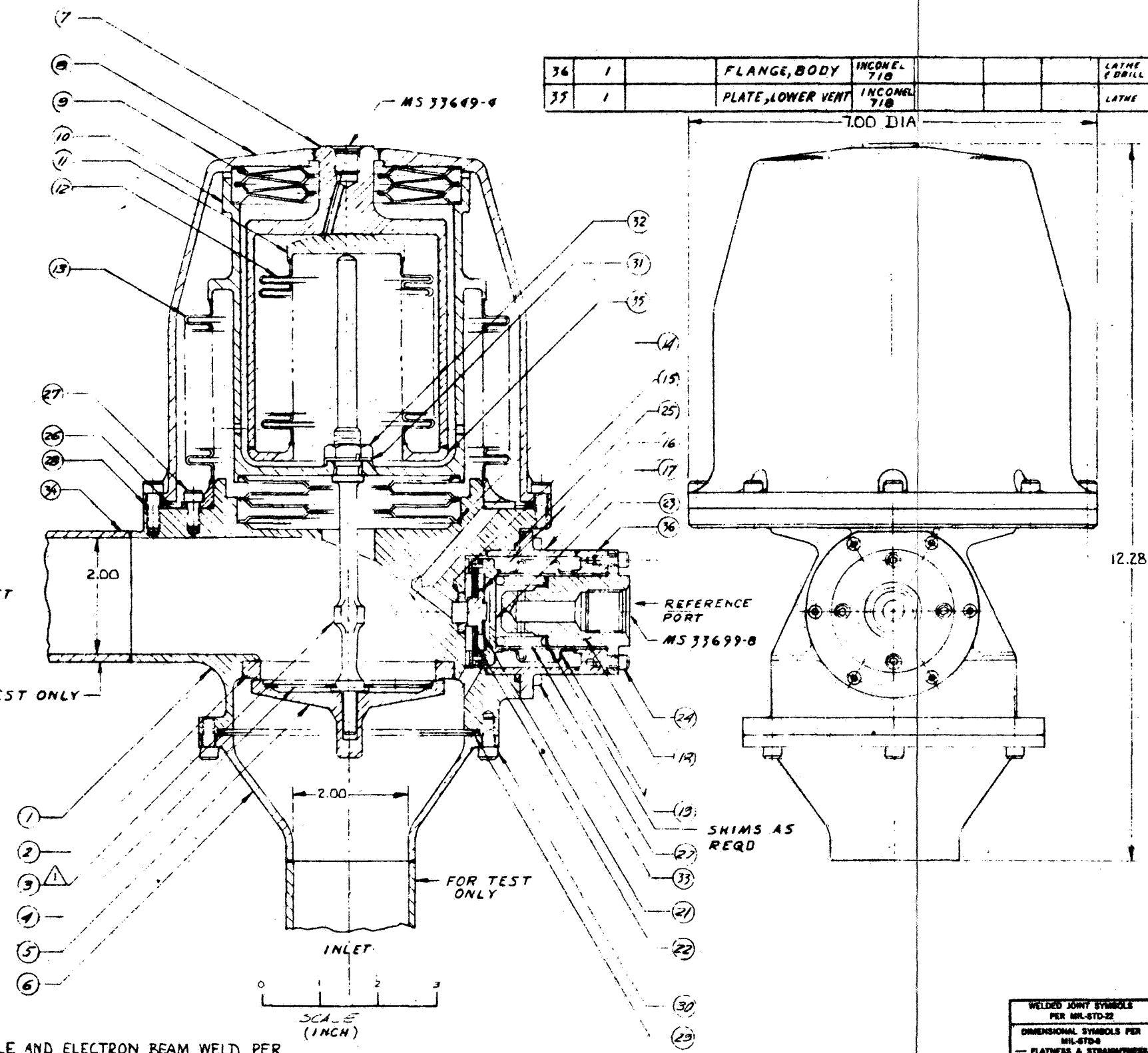

36	1		FLANGE, BODY	INCONEL 718					LATHE & DRILL
35	1		PLATE, LOWER VENT	INCONEL 718					LATHE

ITEM NO.	DWG SIZE	QTY REQD	PART OR IDENTIFYING NO.	NOMENCLATURE OR DESCRIPTION	MATERIAL	MATERIAL SPECIFICATION	HEAT TREAT	FINISH	FABRICATION PROCESS
36				PORT, OUTLET					TUBING, FORMED
33		6		SCREW	CRES				PURCH.
32		1		NUT	CRES				PURCH.
31		1		WASHER, TAB	CRES				PURCH.
30		6		SCREW	CRES				PURCH.
29		1		SEAL	COPPER PLATE				PURCH.
28		8		SCREW	CRES				PURCH.
27		6		SCREW	CRES				PURCH.
26		1		SEAL	COPPER PLATE				PURCH.
25		1		SEAL	COPPER PLATE				PURCH.
24		4		SCREW	CRES				PURCH
23		1		STOP	321/347	QQ-S-763			LATHE & MILL
22		1		COMPENSATOR TUBE	N/CE TO MFR				LATHE
21		1		BELLEVILLE	321/347	QQ-S-763			STAMPING
20		1		SPRING	STEEL				PURCH
19		1		BELLOWS-PILOT	321/347	QQ-S-763			TUBING FORMED
18		1		PLUG	321/347	QQ-S-763			LATHE & DRILL
17		1		BODY-PILOT	INCONEL 718				LATHE
16		1		POPPET-PILOT	321 CRES	QQ-S-763			LATHE
15		1		SEAT-PILOT	INCONEL 718				LATHE
14		1		FLEXURE-LOWER	321/347	QQ-S-763			STAMPING
13		1		BELLOWS-POWER	321/347	QQ-S-763			TUBING, FORMED
12		1		BELLOWS-VENT	321/347	QQ-S-763			TUBING, FORMED
11		1		CAP-VENT	INCONEL 718				LATHE
10		1		HOUSING-POWER BELLOWS	INCONEL 718				LATHE, MILL & DRILL
9		1		FLEXURE-UPPER	321/347	QQ-S-763			STAMPING
8		1		HOUSING-OUTER	INCONEL 718				LATHE OR SPINNING
7		1		HOUSING-VENT	INCONEL 718				LATHE & DRILL
6		1		PORT-INLET	INCONEL 718				LATHE OR SPINNING
5		1		POPPET-MAIN	321 CRES	QQ-S-763			LATHE
4		1		GUIDE	321/347	QQ-S-763			STAMPING
3		1		STEM	321/347	QQ-S-763			LATHE & MILL
2				SEAT-VALVE, MAIN	INCONEL 718				LATHE & HAND LAP
1				HOUSING-MAIN	347	CASTING			LATHE & JIG BORE
				ASSEMBLY					

LIST OF MATERIAL

2. ASSEMBLE AND ELECTRON BEAM WELD PER PART II, SECTION 5 OF EDR5670099.

⚠1 THREADS BRUSHED COPPER COATED

NOTES (UNLESS OTHERWISE SPECIFIED)

REVISIONS				
E.C.O. NO.	SYM	DESCRIPTION	DATE	APPROVAL

NEXT ASSY	USED ON
APPLICATION	

WELDED JOINT SYMBOLS PER MIL-STD-22

DIMENSIONAL SYMBOLS PER MIL-STD-8
— FLATNESS & STRAIGHTNESS
∠ ANGULARITY
⊥ PERPENDICULARITY
∥ PARALLELISM
◎ CONCENTRICITY
⊕ TRUE POSITION
○ ROUNDNESS
⌯ SYMMETRY
Ⓜ (RMMC) MAXIMUM MATERIAL CONDITION
Ⓢ (RFS) REGARDLESS OF FEATURE SIZE

UNLESS OTHERWISE SPECIFIED
DO NOT SCALE DRAWING
DIMENSIONS ARE IN INCHES
TOLERANCES
FRACTIONS ±1/32 DEC (.XX) ±.02 DEC (.XXX) ±.010 ANGLES (DEG) ±0°30'
TOLERANCES OF HOLES SPECIFIED "DRILL" PER AND 18387
MUST CONFORM TO ES 1-1
MACHINED SURFACE 125 PER MIL-STD-10 ▽
CLASSIFICATION OF CHARACTERISTICS PER SPI-5224-5 & MIL-STD-105
REF 125

SIGNATURES		DATE
DR BY	S. CARLSON	3/11/68
DSGN BY		
CHK BY	E. Johnson	3-14-68
PROJ ENG		
APPD BY		

Parker Aircraft — LOS ANGELES, CALIFORNIA — DIVISION OF PARKER-HANNIFIN CORP.

TITLE: FLUDLINE VENT AND RELIEF VALVE, (TYPE II)(BOLTED)

SIZE	CODE IDENT NO.	DWG NO.
D	92003	5680003

SCALE FULL | UNIT WT ACTUAL CALC | LBS | SHEET 1 OF 2

5680003

REVISIONS				
E.C.O. NO.	SYM	DESCRIPTION	DATE	APPROVAL

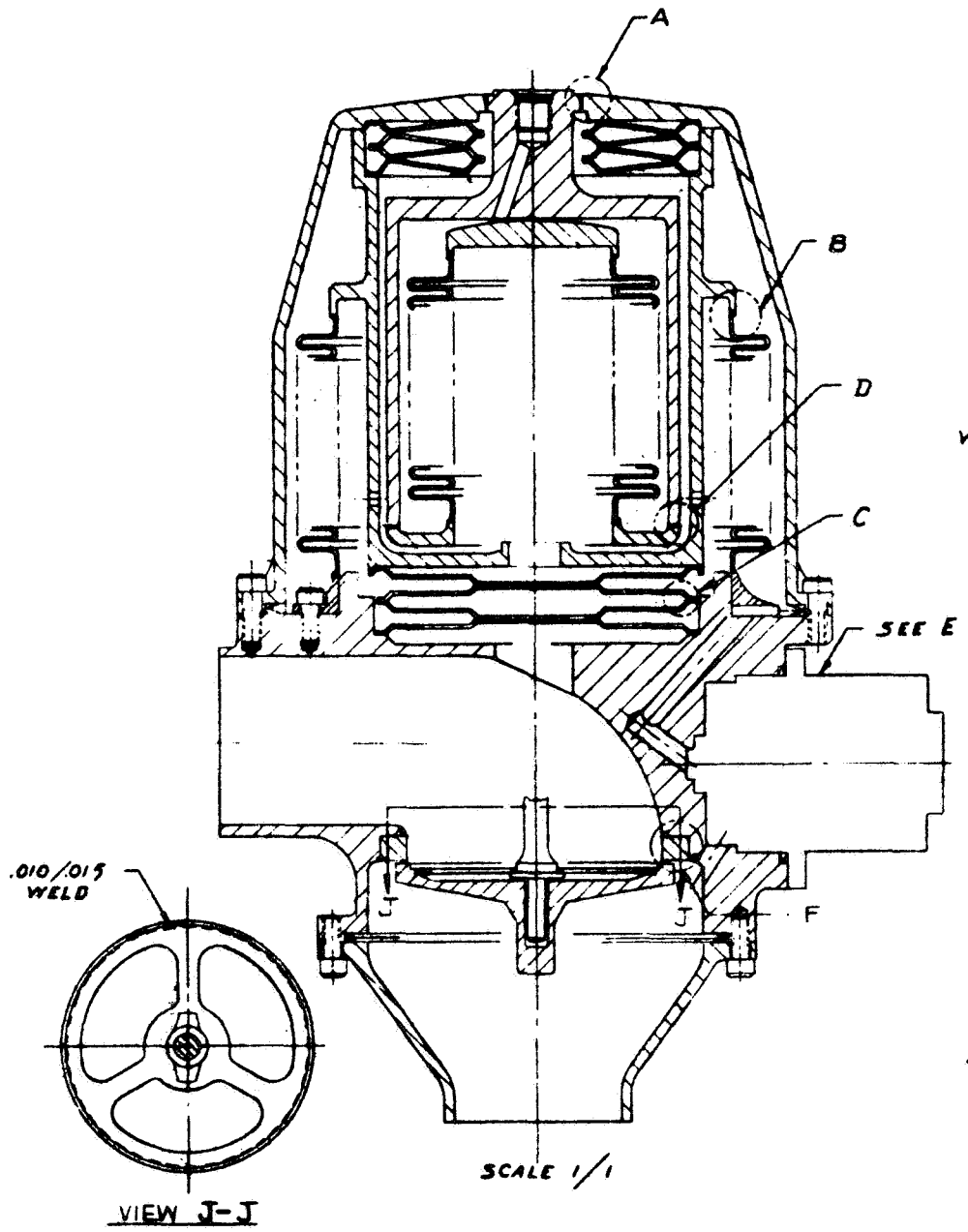

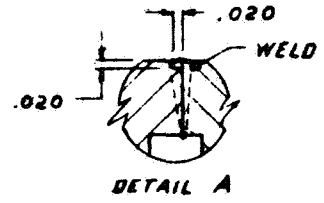

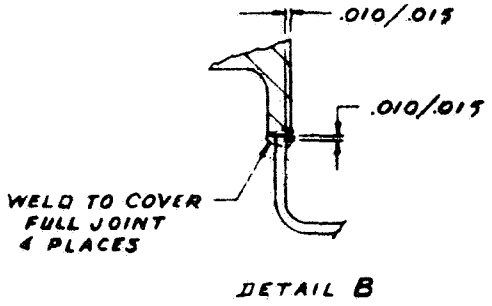

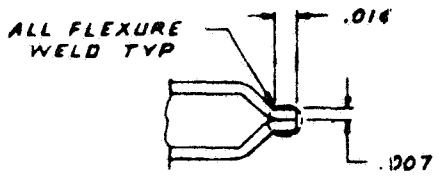

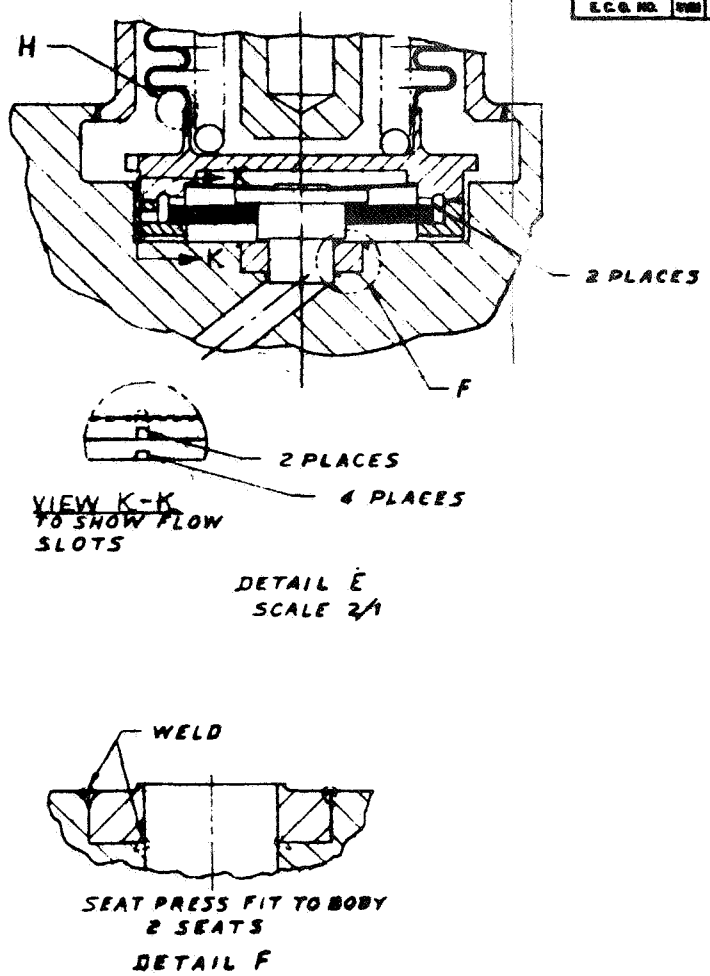

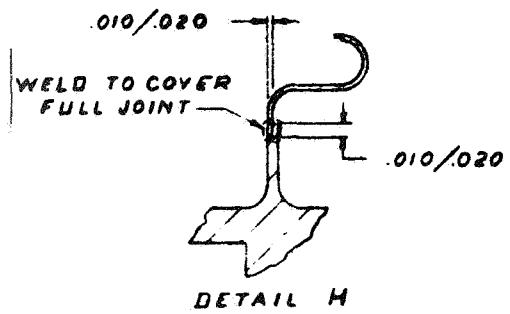

NOTES (UNLESS OTHERWISE SPECIFIED)

ITEM NO.	DWG SIZE	QTY REQD	PART OR IDENTIFYING NO.	NOMENCLATURE OR DESCRIPTION	MATERIAL	MATERIAL SPECIFICATION	HEAT TREAT	FINISH	FINISH SPECIFICATION

LIST OF MATERIAL

NEXT ASSY	USED ON
APPLICATION	

WELDED JOINT SYMBOLS PER MIL-STD-22

DIMENSIONAL SYMBOLS PER MIL-STD-8
- FLATNESS & STRAIGHTNESS
- ANGULARITY
- PERPENDICULARITY
- PARALLELISM
- CONCENTRICITY
- TRUE POSITION
- ROUNDNESS
- SYMMETRY
- (M)MC) MAXIMUM MATERIAL CONDITION
- (RFS) REGARDLESS OF FEATURE SIZE

UNLESS OTHERWISE SPECIFIED
DO NOT SCALE DRAWING
DIMENSIONS ARE IN INCHES
TOLERANCES
FRACTIONS ± 1/32 DEC ± .030 DEC [MM] ± .8 ANGLES ± 0°30'
TOLERANCES OF HOLES SPECIFIED "DRILL" PER ANSI B94.7
MUST CONFORM TO ES 1-1
MACHINED SURFACE 125 PER MIL-STD-10
CLASSIFICATION OF CHARACTERISTICS
PER SPI-6004-5 & MIL-STD-105
REF 125

	SIGNATURES	DATE
DR BY	G Hong	10 APR 68
DSGN BY		
CHK BY	E Stahl	11 APR 68
PROJ ENG		
APPD BY		

Parker Aircraft — LOS ANGELES, CALIFORNIA — DIVISION OF PARKER-HANNIFIN CORP.

TITLE: FLUORINE VENT & RELIEF VALVE (TYPE II) (BOLTED)

SIZE	CODE IDENT NO.	DWG NO.
D	92003	5680003

SCALE 3/4 & 1/1 | UNIT WT | NEXT ASSY | LBS | SHEET 2 OF 2

5680003

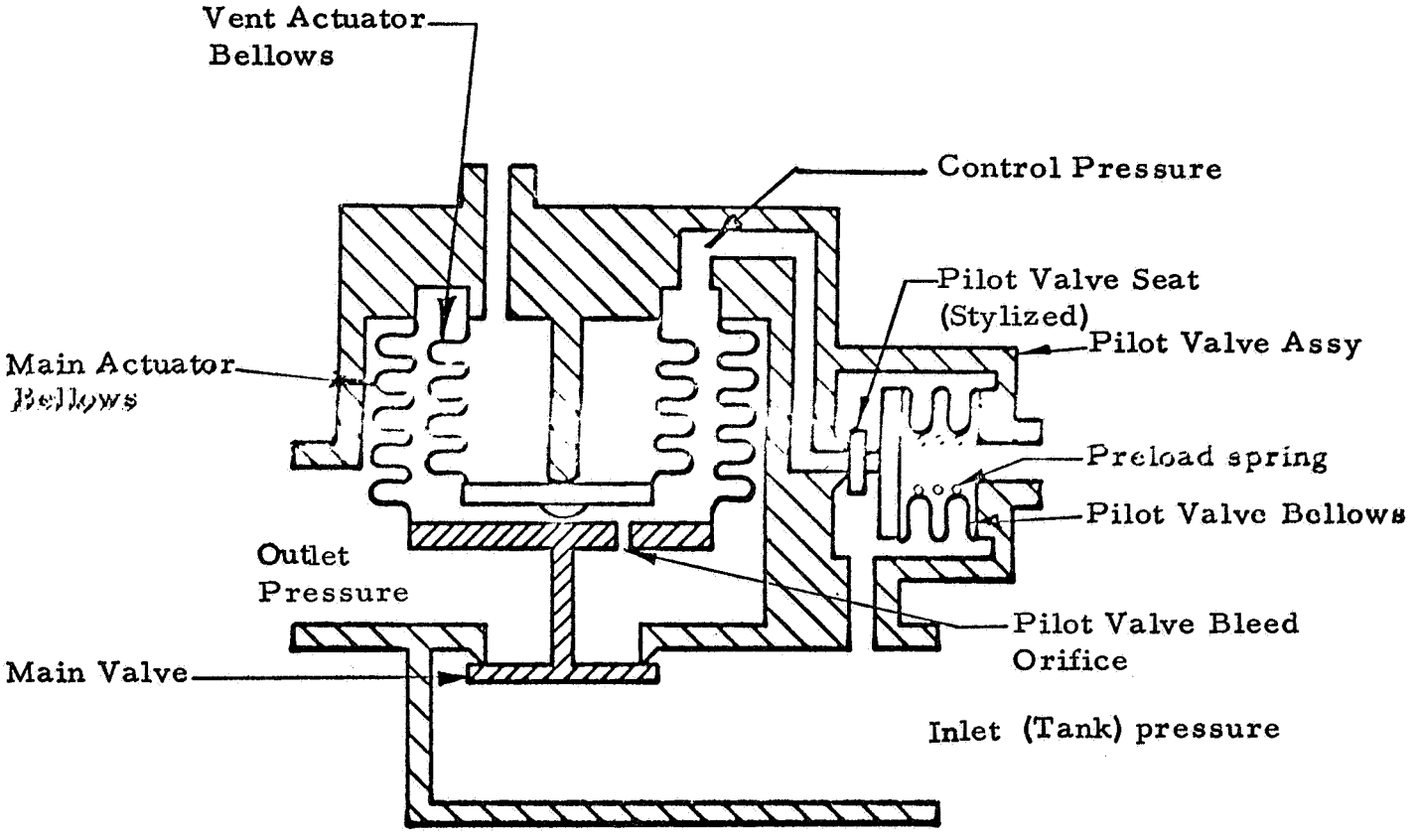

Figure 20. Schematic Diagram of the Fluorine Vent and Relief Valve

effective area actuator, called the power bellows, which uses tank pressure as a source of power. Inlet pressure acts on the pilot valve bellows, creating a force acting toward the right. This force is opposed by the spring preload force. When tank pressure reaches the preset value it overcomes the spring preload force and causes the pilot valve bellows to deflect to the right. This opens the pilot valve and admits gas from the tank into the power bellows. When pressurized, the power bellows exerts a downward force on the main valve, forcing it open. Control pressure is decreased by flow through the large bleed orifice between the main actuator bellows and the valve outlet.

2.2.1 An insight into how the valve operates may be gained from figure 21. This is a graph of tank, control, and outlet pressures vs time. Pilot and main valve positions are also plotted vs time. At the point marked, "2 lb/sec", GF_2 instantly starts flowing into the tank. The tank pressure begins to rise, and when it exceeds the preset cracking pressure of the pilot valve, the pilot valve opens. After opening of the pilot valve, the control pressure begins to build up. When control pressure builds up sufficiently it exerts enough force to open the main valve. Opening of the main valve begins to let substantial quantities of gas out of the tank, and slows the rate of rise of tank pressure. The rise of tank pressure is arrested, and steady state conditions are achieved, when the main valve is open far enough to let 2 lb/sec out of the tank (equalling the flow rate into the tank).

Note that as the main valve opens, back pressure at the valve outlet builds up. Since outlet pressure acts on the same bellows as the control pressure, a matching increase in control pressure occurs.

2.2.2 At the point marked on the graph (figure 21) the 2 lb/sec flow into the tank is suddenly removed. The tank pressure begins to decline, because the main valve is open. As the tank pressure declines, the pilot valve moves toward the closed position. This allows the control pressure to decline by bleeding off through the large orifice (located between control pressure and outlet pressure). When control pressure declines sufficiently, it is unable to hold the main valve open and the main valve recloses. It will be noted from (figure 21) that it is not necessary for the pilot valve to close all the way in order to lower control pressure enough to reclose the main valve. Thus, under the conditions of this example, the main valve closes before the tank pressure has fallen enough to reseat the pilot valve completely. As long as the pilot valve is open, tank pressure will continue to fall, although at a relatively slow rate, due to the small size of the pilot valve. Tank pressure will bleed down to a value sufficient to reseat the relief valve. This is perfectly normal, since as long as tank pressure exceeds the preset cracking pressure the valve is supposed to let gas out of the tank, through either or both valves.

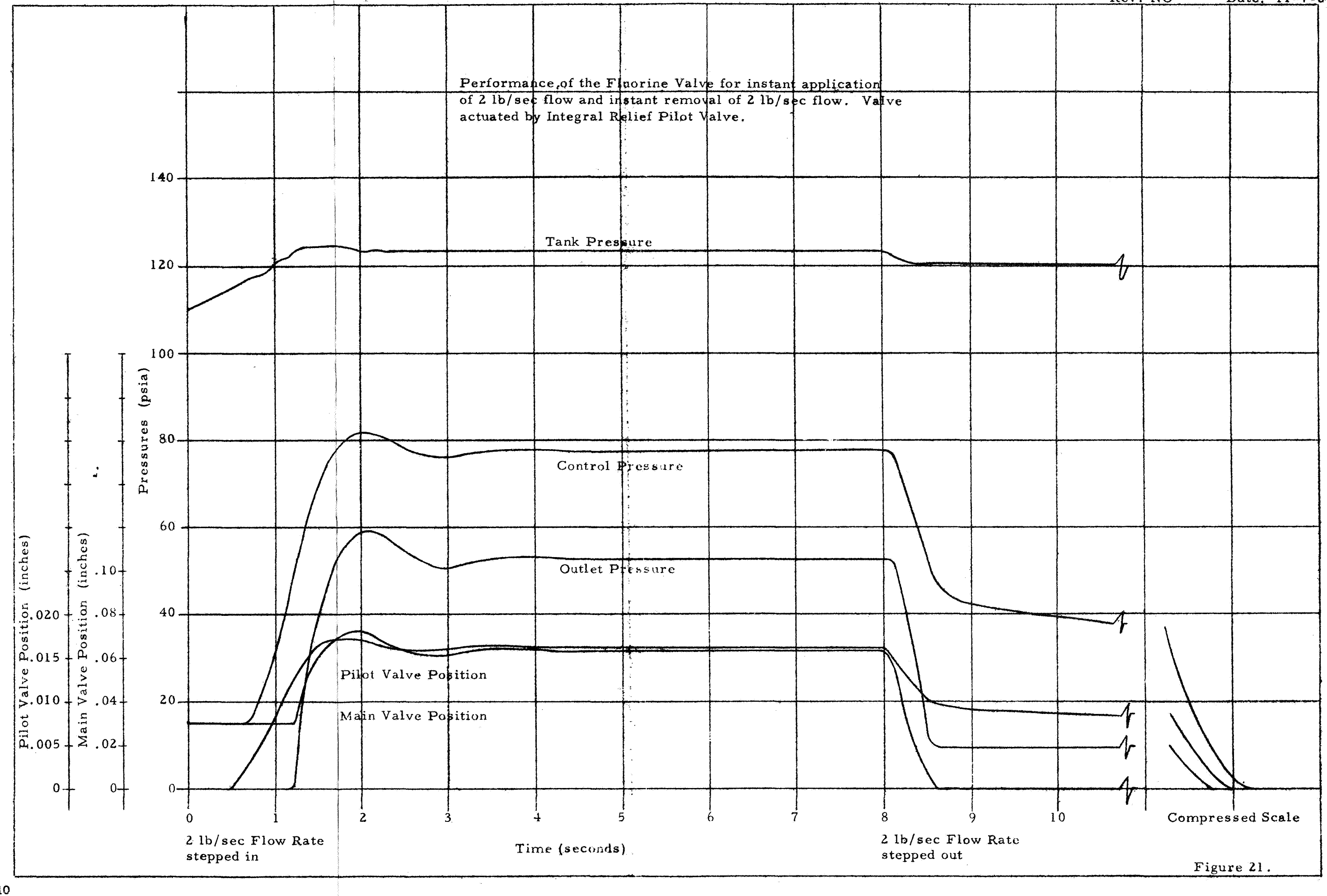
Performance of the Fluorine Valve for instant application of 2 lb/sec flow and instant removal of 2 lb/sec flow. Valve actuated by Integral Relief Pilot Valve.
Tank Pressure
Control Pressure
Outlet Pressure
Pilot Valve Position
Main Valve Position
Pressures (psia)
Pilot Valve Position (inches)
Main Valve Position (inches)
140
120
100
80
60
40
20
0
.020
.015
.010
.005
0
.10
.08
.06
.04
.02
0
0 1 2 3 4 5 6 7 8 9 10
Compressed Scale
2 lb/sec Flow Rate stepped in
Time (seconds)
2 lb/sec Flow Rate stepped out

Figure 21.

2.3 Details of Construction - Parker Drawings 5680002 and 5680003 (reproduced on the preceding pages) show all parts of the assembly, and all significant mechanical details. The drawings are largely self-explanatory, but the following brief description is presented to assist in drawing interpretation.

2.3.1 General - The valve is of all-metal construction. No plastics or elastomers are used. The metals used have been selected for fluorine compatibility. There are no sliding parts in the valve, sliding contact has been completely eliminated. Thus lubrication is unnecessary, galling cannot occur, and sticking and jamming is impossible. The Type 1 valve uses all-welded static seals which virtually eliminates static seal leakage problems. The Type 2 valve uses pressure energized metal seals, which permit easy disassembly of the valve. Parker recommends that Type 1 valves be used unless there is a real need for convenience of disassembly, as in experimental or prototype applications.

2.3.2 Body - The valve can easily be provided with ports of any type desired by the user. The valve is illustrated with tube stubs on the inlet and outlet. Typically these tube stubs are fitted with flared tube fittings for use during manufacturing and acceptance test. They are then cut off by the customer prior to installation in a vehicle having welded or brazed tube connections.

2.3.2.1 It is particularly advantageous to mount the valve directly on the propellant tank, in other words to have the inlet port open directly into the tank, with an opening of 3 inches diameter. Where this is not practical, the valve may be used with the 2-inch inlet line illustrated, but long inlet lines may alter the valve response from that illustrated in this report.

2.3.2.2 From a valve designer's viewpoint, the pressure drop specified was smaller than preferred. It has resulted in a large diameter valve seat, and a large valve actuator, in order to meet the specified flow capacity despite the handicap of a small port size. The specified maximum pressure drop is only 9% of the inlet absolute pressure. Even a modest increase in the 10 psi pressure drop specified, -say to 20 psi-, would allow the valve and body diameter to be reduced about 50% resulting in a valve of more pleasing appearance, and lighter weight.

2.3.3 Main Valve Seat - A flat faced poppet valve is used. The poppet (5) is attached to the actuator shaft (3) by means of a three-legged, sheet metal flexure guide (4). The guide resists radial deflection but permits tilting motion required for seat alignment and axial motion required to allow the actuator assembly to bottom out on its own positive stop.

Tilting of the poppet is limited by the controlled clearance between the end of the shaft (3) and the bore in the poppet (5). When the valve is open, the pressure forces acting on the poppet hold the poppet securely bottomed out on the shaft.

Low leakage requires perfect alignment, adequate seat stress, and maintenance of surface quality. These are obtained as described below:

2. 3. 3. 1 Alignment -

a. Concentricity - Because of the flat sealing surfaces close concentricity is not necessary.

b. Normality - If poppet and seat are not perfectly parallel at the instant of contact, the force exerted at the contact point will cause the poppet to pivot, and become perfectly parallel to the seat. The pivoting is permitted by controlled clearance between poppet (5) and shaft (3). The pivot point is approximately in the plane of the seat, to minimize scuffing of the sealing surfaces.

2. 3. 3. 2 Seat Stress - When the valve is closed, the full force of inlet pressure acts on the valve seat and develops the sealing stress. Thus the maximum sealing stress is developed at maximum inlet pressure, (which is the condition requiring the maximum).

2. 3. 3. 3 Surface Quality - High initial surface quality is obtained by conventional flat lapping methods. The surface quality may easily be inspected by interference microscope. Surface quality is maintained despite the cycling because:

a. The seat does not absorb impact loads due to deceleration of the actuator - the actuator overtravels to its own positive stop.

b. There is virtually no sliding contact between seat and poppet, as the two surfaces mate, so that galling of seating surfaces is eliminated.

2. 3. 4 Main Valve Actuator - The means of actuating the main valve, and guiding its motion, does not involve any sliding contact. This completely eliminates problems such as sticking, galling or fluoride film removal. Friction forces are virtually eliminated.

2. 3. 4. 1 The main valve actuator consists of a formed metal bellows (13), a housing (10), and a stem (3). The assembly is axially guided by flexures (9) and (14), located at opposite ends of the housing (10). The axial guides are short bellows sections, which never have any pressure differential across them. The bellows sections inherently have low spring rates in the axial direction, but resist radial deflection. Consequently, the valve and actuator assembly moves freely in the intended axial direction, but is prevented from moving radially. The use of two axial guides, spaced a considerable distance apart, prevents any titling motion of the assembly.

2. 3. 4. 2 The bellows (13) is arranged so that it is subjected only to external pressure, (i. e. external pressure greater than internal). This makes it impossible for the bellows to "squirm" (fail due to elastic instability). This is quite important, since low spring rate large deflection bellows have low squirm pressures and are impractical for internal pressure.

The bellows is installed with a small deflection in compression, which provides a normally-closed spring bias force to the assembly. In the unpressurized state, this spring force holds the housing (10) against a positive stop on outer housing (9). The elastic deflection of the flexure guide (4) allows the poppet (5) to simultaneously bottom out against the valve seat.

2. 3. 5 Vent Actuator - The vent actuator allows the main valve to be opened by application of an externally supplied pneumatic pressure. Typically, this is done to vent the tank to permit filling it with propellant.

2. 3. 5. 1 The vent actuator consists of a formed metal bellows (12) welded to the housing (7) containing a port for application of pressure from an external source. The free end of the bellows is welded to the cap (11). The bellows is installed with a small initial deflection in compression, such that the cap (11) is held bottomed out against the housing (7) when the assembly is unpressurized.

When the housing is pressurized from an external source the bellows (12) deflects downward, and the cap (11) pushes downward on the stem (12) of the main valve actuator assembly. The entire vent actuator and main actuator assembly is deflected downward until the valve is full open. A positive stop for the full open position is provided by housing (11) bottoming

out on the main housing (1).

Removal of the externally supplied pressure causes the actuators to return to their normal positions, reclosing the main valve.

2.3.5.2 Note that the design is such that the vent actuator does not move at all when the relief pilot valve is actuating the main valve via the power bellows. (13). This is because the vent actuator has a high spring rate bellows that would be difficult to actuate with the sometimes low pressure differentials available in the relief mode of operation. The high spring rate of the vent actuator is to be expected because it must resist higher pressures, and thus is made of thicker material.

2.3.6 Relief Pilot Valve - The relief pilot valve provides a means for automatically opening the main valve, should tank pressure exceed a preset value. The pressure setting is easily adjustable in both Type 1 and Type 2 valves. Changes in pressure setting are made by removing four bolts, removing plug (18) and then changing the shims for spring (20). These parts are located in a portion of the valve that is never in contact with fluorine.

2.3.6.1 The pilot valve is simple in principle, consisting merely of a pressure sensing bellows (19), loaded by a coil spring (18), and capable of lifting poppet (16) off the seat when the tank pressure exceeds the preset value (i.e. when pressure force on the bellows equals spring force). The bellows senses gauge pressure (the difference between tank pressure and atmospheric pressure). Users commonly desire to simulate altitude conditions, for test, by pulling a vacuum on the atmospheric pressure side of the bellows. An MS33649 atmospheric pressure port is provided for convenience.

2.3.6.2 Several accessories are provided for the pilot valve. First, the pressure setting would change with temperature* without the temperature compensator formed by the thermostat metal discs (22). Second, to minimize leakage, the pilot valve develops a high seat stress a few psi below the crack pressure (because the seat diameter is much smaller than the bellows diameter). To prevent the excessive seat stresses that would otherwise be developed when the unit is unpressurized, the pilot valve is equipped with an overtravel device consisting of spring (23), and the loose fit between poppet (16) and disc (22). Both temperature compensator and overtravel device are explained in the following paragraphs.

* The calibration of all pressure sensing instruments changes with temperature.

2.3.6.3 When the unit is unpressurized, the poppet (16) is held down against the seat by spring (21), while the bellows end fitting (23) rests against a positive stop on the valve body. Thus the positive stop against the body supports the large force of spring (20) (minus the small force of spring (23)). The valve poppet is loaded against its seat only by the force of spring (23). When the tank pressure rises to near the cracking pressure, bellows force exceeds spring preload force and the bellows end fitting moves to the right (on the drawing). After moving a few thousandths of an inch, the compensator discs (22) engage poppet (16) and lift it off the seat. The temperature compensator discs are made of thermostat metal. This material consists of a layer of high coefficient of thermal expansion material bonded to a layer of low coefficient of expansion material. As temperature decreases the inner edge of the disc deflects to the right an amount proportional to the temperature decrease. At low temperatures the spring (20) puts out a higher force than at room temperature, at any given deflection, because the modulus of elasticity of the spring material increases as the temperature decreases. (This effect is dominant over ordinary thermal expansion effects which are also present.) The deflection of the thermal compensator causes the poppet to be lifted from the seat with a lesser amount of compression of the spring (20). Thus while the spring force at a given deflection is more, the spring deflection is reduced to compensate for the force increase, and the net force remains essentially constant over the operating temperature range.

2.3.6.4 Another important detail is the proof pressure stop, consisting of the post-like projection on plug (18). This stop prevents excessive deflection of the pressure sensing bellows when the proof pressure is applied to the unit.

2.3.6.5 An essential part of the pilot valve is the bleed orifice between control pressure and outlet pressure. This orifice is located in the side of housing (10). There are two such orifices in parallel. The pilot valve of course, can only admit gas to the control chamber. The orifice lets gas out of the control chamber. Therefore the pilot valve and the orifice act together to determine the control pressure. Since the bleed orifice is so large (about equal to the flow area of a 1/4-inch fitting) it will not clog.

2.3.6.6 It should be noted that the pilot valve meets all the criteria for low valve seat leakage, namely:

1. Alignment - The free floating, flat seat is self aligning.

2. Seat Stress - The pilot bellows area is selected to develop an adequate seat stress when the tank pressure

is at the minimum reseat value.

3. Preservation of Surface Quality - There is essentially no sliding contact of the valve with respect to its seat, nor does the valve seat absorb the impact loads due to deceleration of the bellows and spring. Thus a long seat life is assured.

3.0 VALVE PERFORMANCE

3.1 The performance of the valve is presented in this section.

3.2 Calculation of Valve Response as a Function of Time - When a flow suddenly occurs into the propellant tank, the valve must open rapidly enough to prevent objectionable overshoot in tank pressure. Similarly, when this flow into the propellant tank is suddenly stopped, it is important that the relief valve reclose rapidly enough to prevent an objectionable undershoot in tank pressure. When the valve is flowing, it is preferable that it "modulate" (maintain a stady-state position) rather than "limit cycle" (continuously oscillate) since limit cycles may seriously reduce the life of the valve cause alarming noises, and cause undesirable shifts in pressure setting.

3.2.1 Such matters were taken into consideration in arriving at this design concept. Since response calculations, even with electronic computers, are relatively time consuming, in the evolution of the design concept, experience rather than calculation was used as a guide as to probable response.

In this phase of the program, the response was calculated. A mathematical model of the vent and relief valve was formulated. It is presented in Appendix A. The mathematical model is a set of simultaneous differential equations which incorporate those laws of physics which are responsible for the essential features of valve response. These include the flow of gas through the main valve, pilot valve, pilot orifice, and outlet line, the force balance equations of the main valve and pilot valve, and the dynamic equations for changes in state of the fluid in the tank, the control chamber and the outlet line. The equations are nonlinear, and all limit stop effects are included. The equations were solved simultaneously to obtain the response of the valve as a function of time.

3.2.2 Two cases were considered:

1. Relief Mode Operation - In this mode of operation, a step function flow was assumed to occur into the

propellant tank at time t= 0. After the valve responded, and steady-state conditions were reached, the flow was stepped out, and the calculation was continued until steady-state conditions were reached, or closely approached.

2. Vent Mode of Operation - When venting the tank in order to fill it, the response time for opening and closing the valve is probably immaterial. However, a pressure switch and solenoid valve are sometimes used to provide an alternate means of overpressure protection. They are connected so as to open the valve via the vent mode actuator should pressure become too high, and to reclose the valve when pressure declines. An idealized pressure switch and solenoid valve were assumed, in order to calculate valve performance in this mode. The opening and closing response of the vent actuator must be relatively fast in order to permit this mode of operation.

3.2.3 Appendix A presents the mathematical model used. The equations used for these calculations are fairly standard for work in this specialized field. They are essentially those of Dr. J. L. Shearer, who wrote several pioneer papers in this field, and later explained dynamic analysis of fluid controls at great length in his book (with Reethof and Blackburn) Fluid Power Control (Reference 8 of Part I). A more recent book containing similar material is Andersen's The Analysis and Design of Pneumatic Systems. Those interested in the derivation of the equations used are therefore referred to these books.

3.2.4 The response calculation presented are not valid in the acoustical frequency range. Calculation in this frequency range would require a host of highly speculative assumptions as to the exact lengths, diameters, and other details of upstream and downstream piping. The results would be worthless unless the user duplicated the assumed piping in detail, which would not normally be feasible.

Necessary equations for acoustical frequency response of piping are available in standard references wellknown to those working in the field of fluid system automatic controls. Considerable experience and judgement is necessary in such analyses. As a general rule, if piping is kept short and as large in diameter as possible there will be little difference between the performance illustrated in this report, and actual valve performance. If piping is small in diameter and long in length, then performance may vary from that

illustrated here. Before using the valve in a specific application of importance, upstream and downstream plumbing details for that application should be rigorously defined, and their effect analyzed.

3.3 Valve Performance - The performance of the valve is presented in figures 22 through 27. The performance of the relief mode is illustrated (figures 22 through 25) for suddenly applied, and suddenly removed, flows of 1, 2, 3, and 4 lb/sec of 197° R gaseous fluorine. A propellant tank of constant 10 ft^3 ullage was used as typical of the minimum ullage for a vehicle on which the valve might be used. The performance of the vent mode actuator is shown in figures 26 and 27. Here the valve was assumed to be actuated via a pressure switch controlled solenoid valve, set to operate as a relief valve. It is seen that the vent actuator response was ample for this mode of operation. The method of calculating valve performance has been discussed previously in paragraph 3.2, "Calculation of Valve Response". The design parameters selected for the final valve are presented in Table III. These parameters were strictly adhered to in the detail design of the valve.

3.3.1 In every case, every valve position, flow rate, and pressure was calculated as a function of time. The graphs reproduced were plotted automatically from the digital results, with equipment that was then limited to only one variable vs time. The graphs, therefore, display only tank pressure vs time. This is adequate, since it is the real measure of valve performance. However, for a better engineering understanding of valve performance, the results of the 2 lb/sec calculation, have been plotted by hand, and show all pressures, and both valve positions, as functions of time, on a common graph. This graph is reproduced as figure 28 in paragraph 3.4. The complete set of all calculated variables vs time is too voluminous to reproduce in this report.

TABLE III

SUMMARY OF DESIGN PARAMETERS

The design elements were designed to the following requirements in the final design:

1. AREAS ($in.^2$)

Power bellows effective area =	20.6
Pilot bellows effective area =	1.76
Vent bellows effective area =	4.52
Main valve unbalanced area =	7.07
Pilot valve unbalanced area =	0.110

2. SEAT DIAMETERS (in.)

Main valve seat diameter =	3.00
Pilot valve seat diameter =	0.375

3. PRELOAD FORCES (lb)

Main valve seat preload =	5.0	at zero stroke
Pilot valve preload =	166	at zero stroke

4. SPRING RATES (lb/in.)

Main valve spring rate =	100	(power bellows plus upper & lower flexures)
Pilot valve spring rate =	1246	(pilot bellows plus preload spring)

5. POPPET STROKES (in.)

Main valve stroke =	0.250
Pilot valve stroke =	0.087

6. PRESSURES (psig)

Vent valve:	Operating	500
	Proof	750
	Burst	1250
Relief valve:	Operating	100
	Full Flow	110
	Reseat	95
Main Valve Cavity:	Proof	250
	Burst	375

TABLE III cont'd.

7. FLOW CAPACITY

4.0 lb/sec GF_2 at 197°R at sea level

8. ORIFICES

Total orifice area =	0.0232 in^2
Orifice diameter =	0.122 in.
Number of orifices =	2

9. PACKAGE DIMENSIONS (in.)

Welded type: 7.0 dia x $8\frac{1}{2}$ max width x 10 1/8 height
Bolted type: 6-1/8 dia x 8-1/8 max width x 10-1/8 height

10. PARKER DRAWING NUMBERS

Version	Type	Drawing
Preliminary (welded)	1	5670099
Preliminary (bolted)	2	5670100
Final (welded)	1	5680002
Final (bolted)	2	5680003

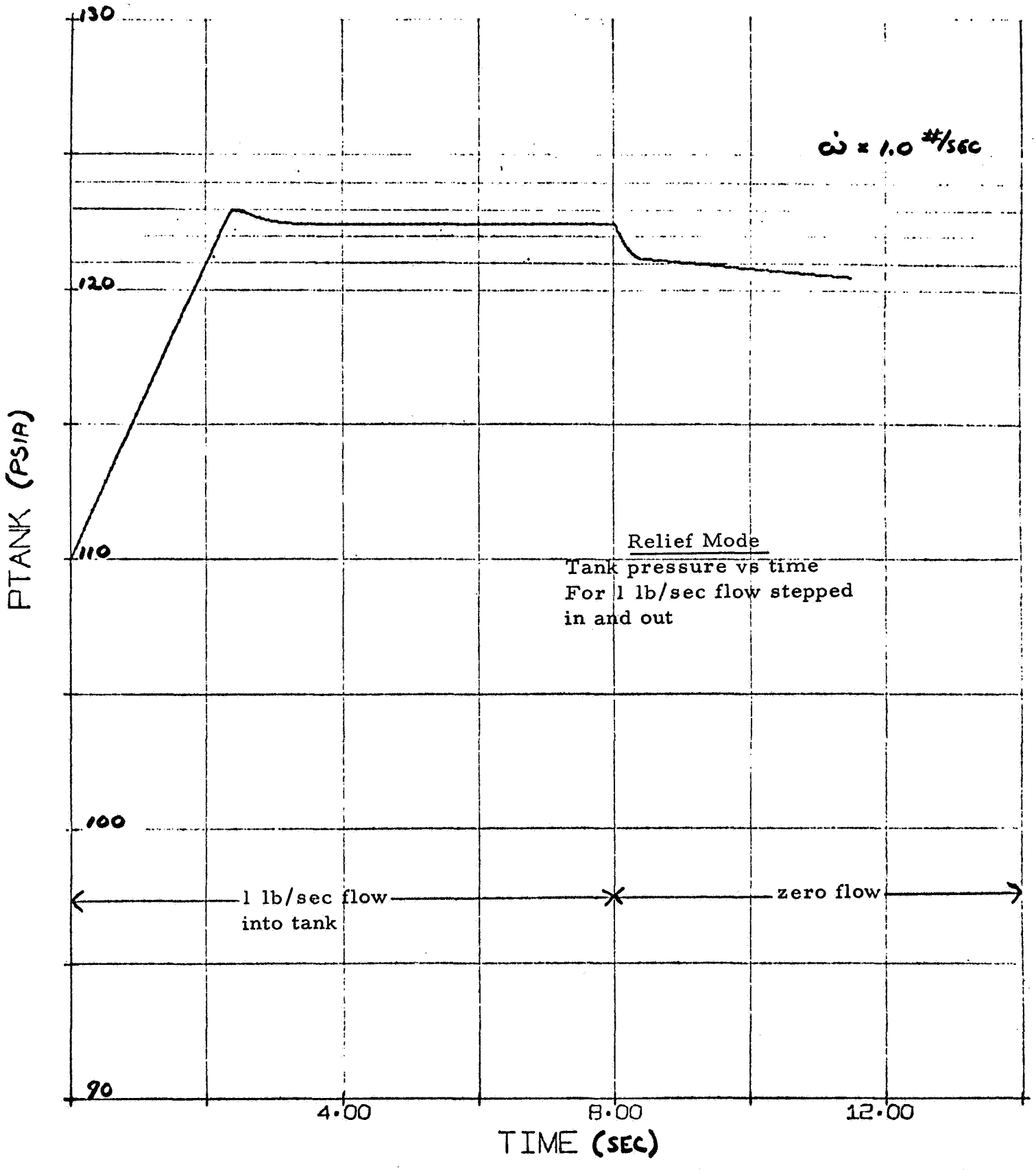

Figure 22 FLUORINE V/R VALVE - RUN 8E -

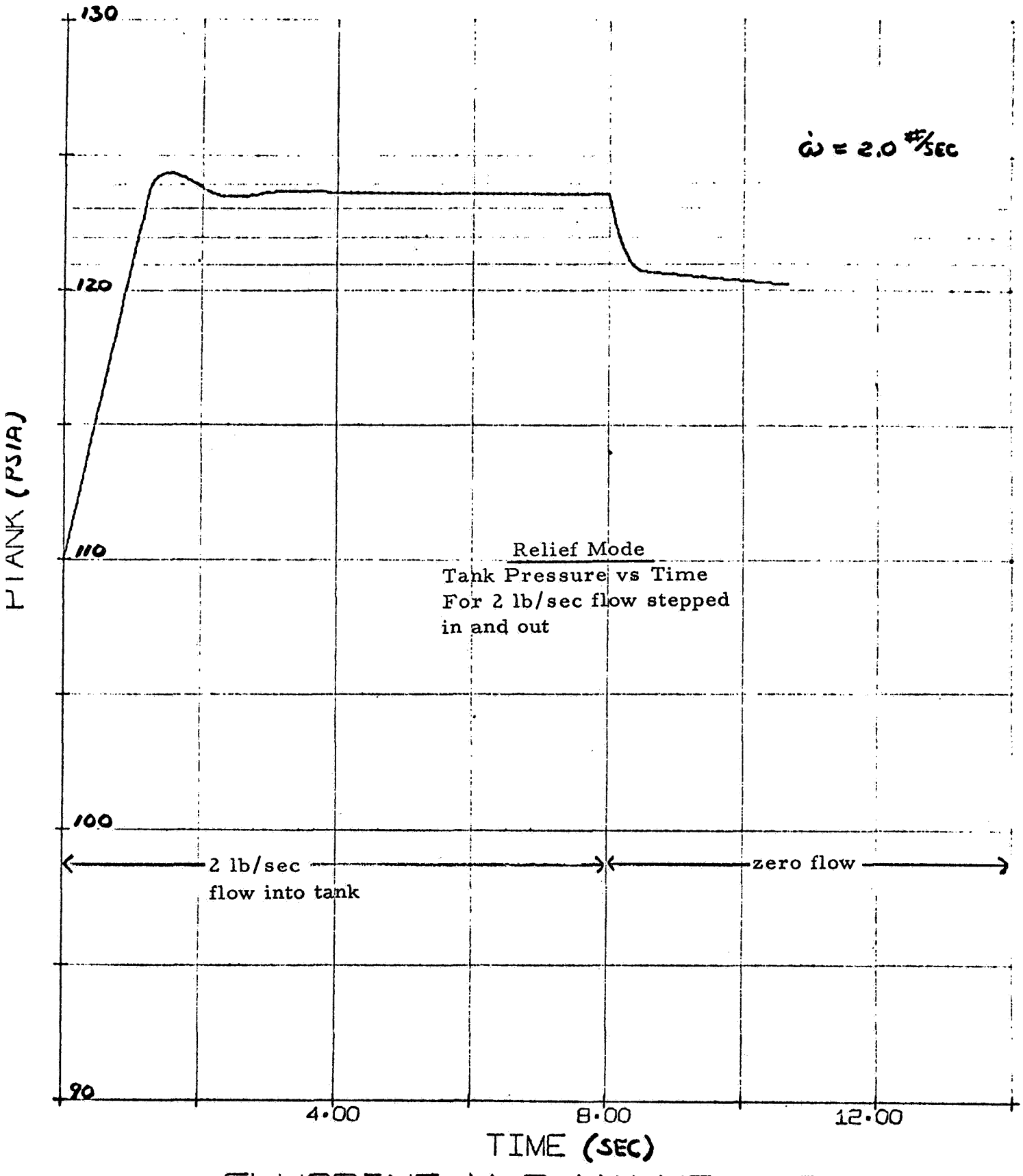

Figure 23 FLUORINE V/R VALVE - RUN 9E -

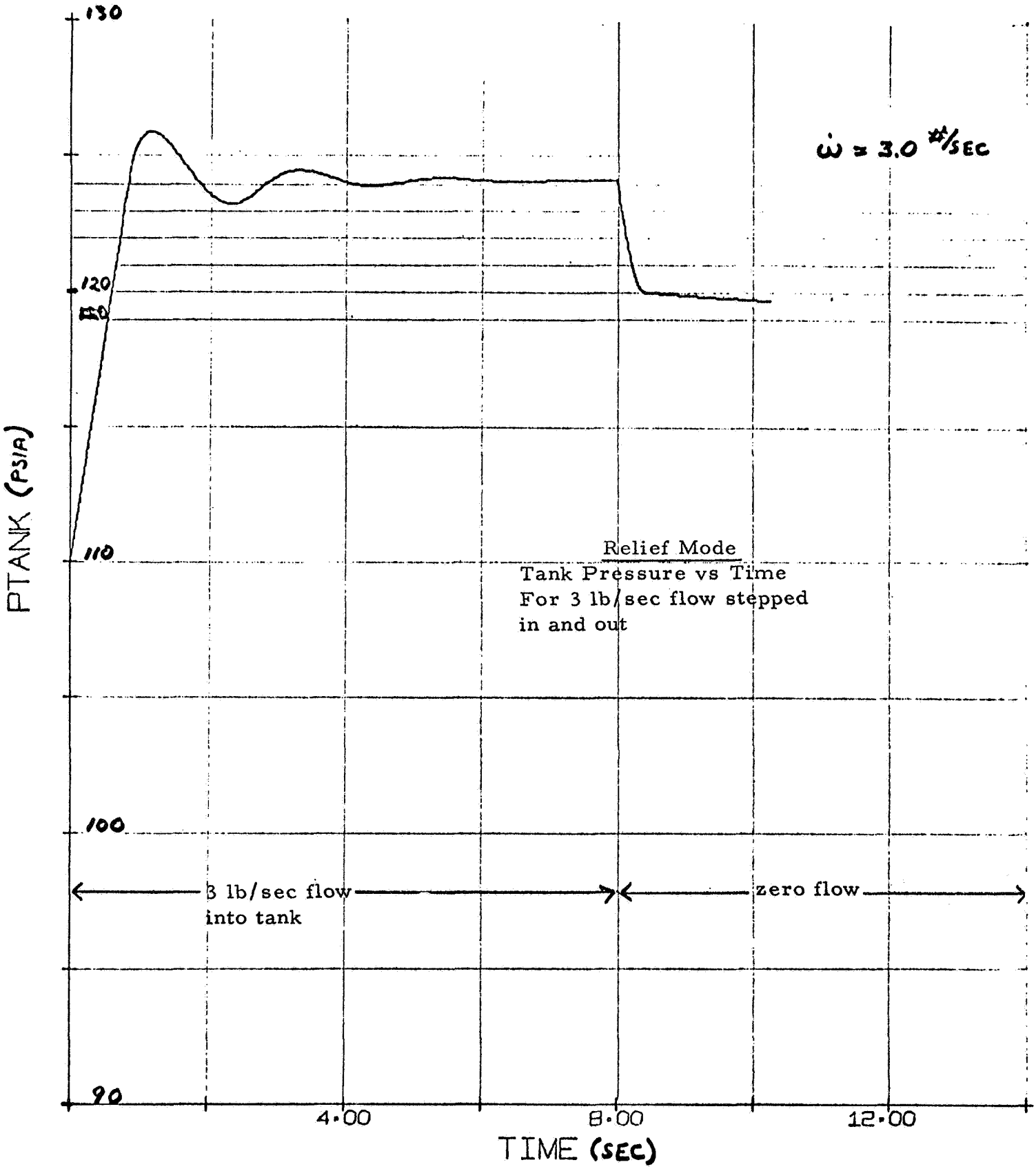

Figure 24 FLUORINE V/R VALVE - RUN 10E -

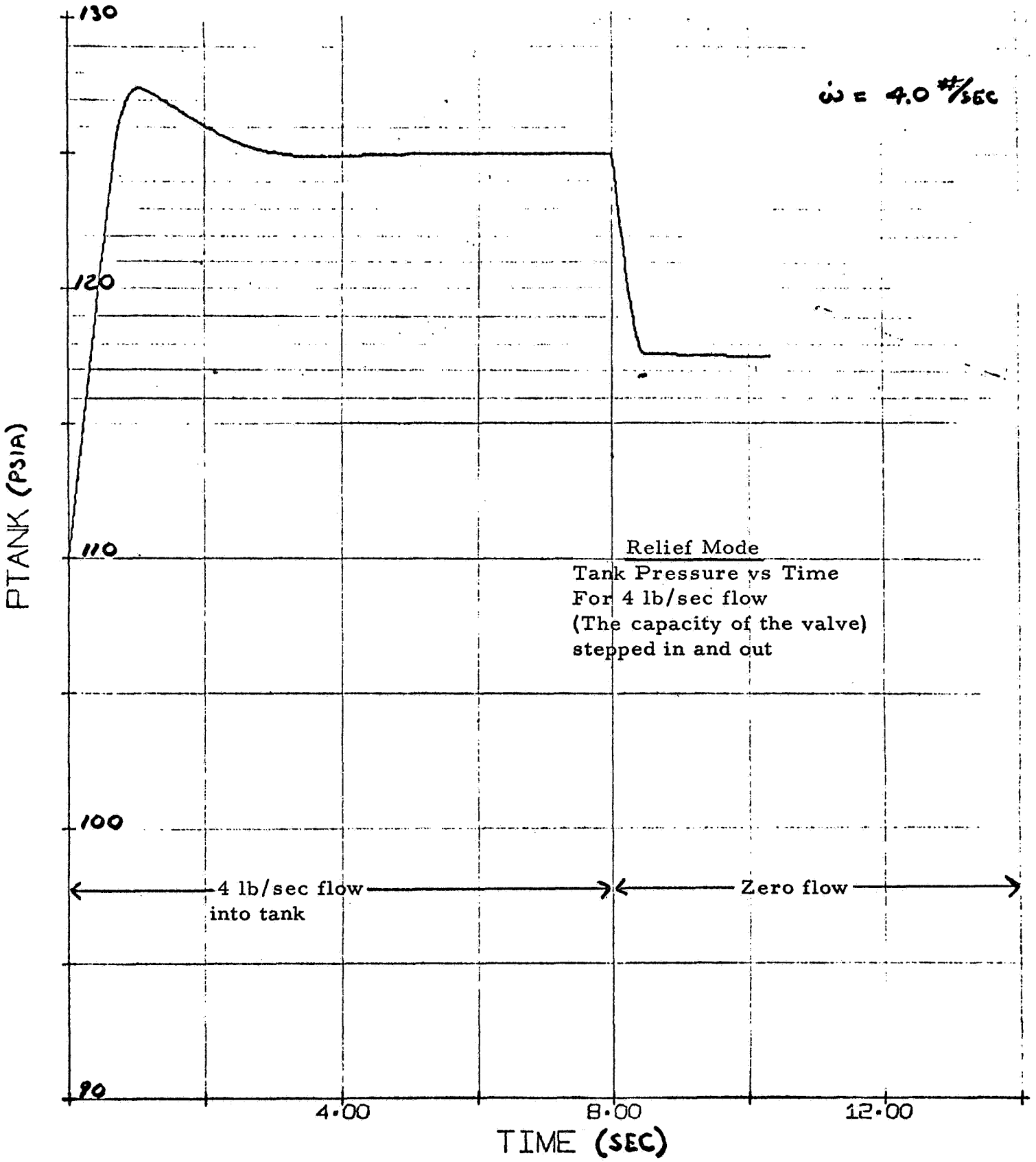

Figure 25 FLUORINE V/R VALVE - RUN 7E -

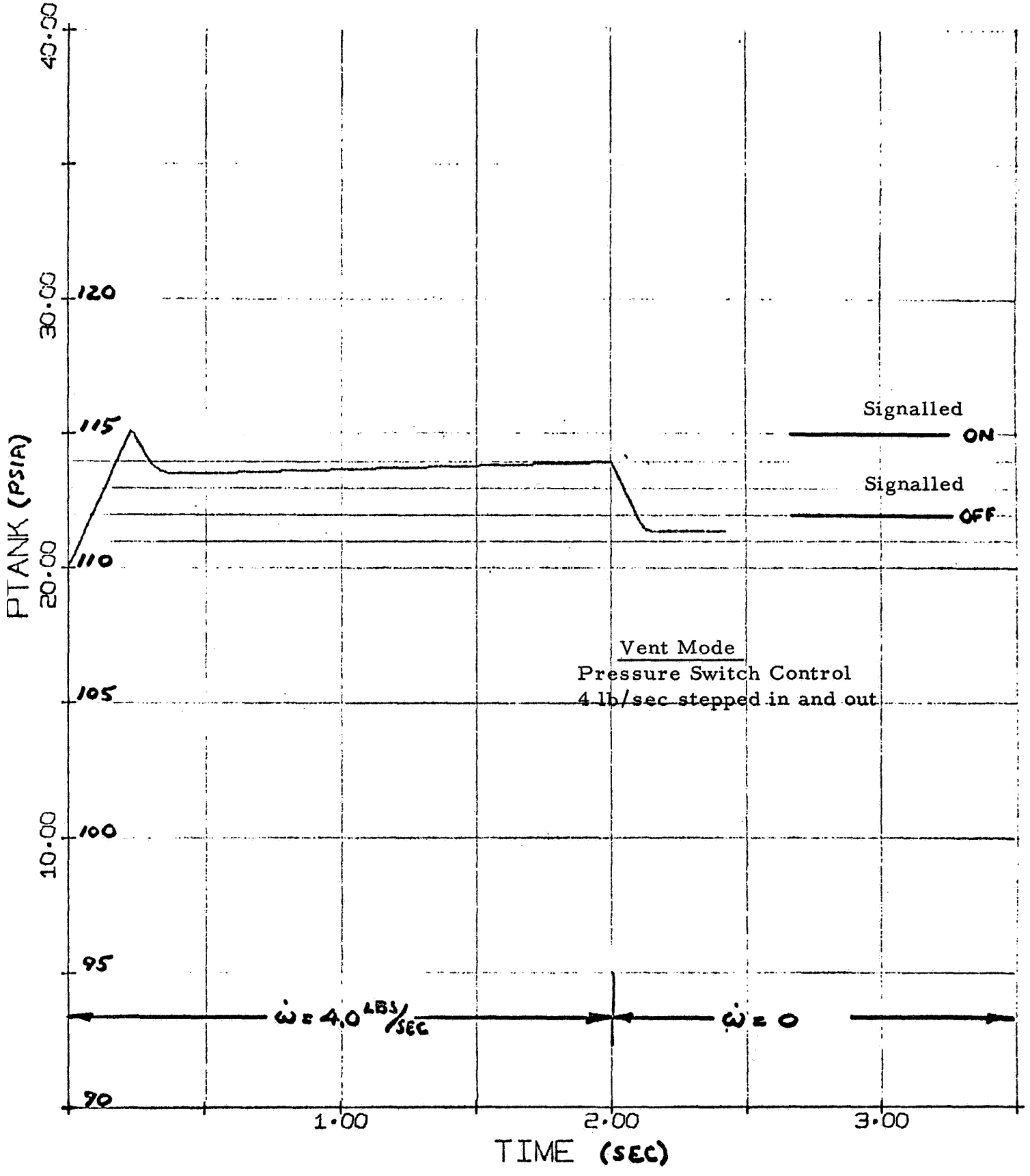

Figure 26 FLUORINE VALVE (P.S.) - RUN 1

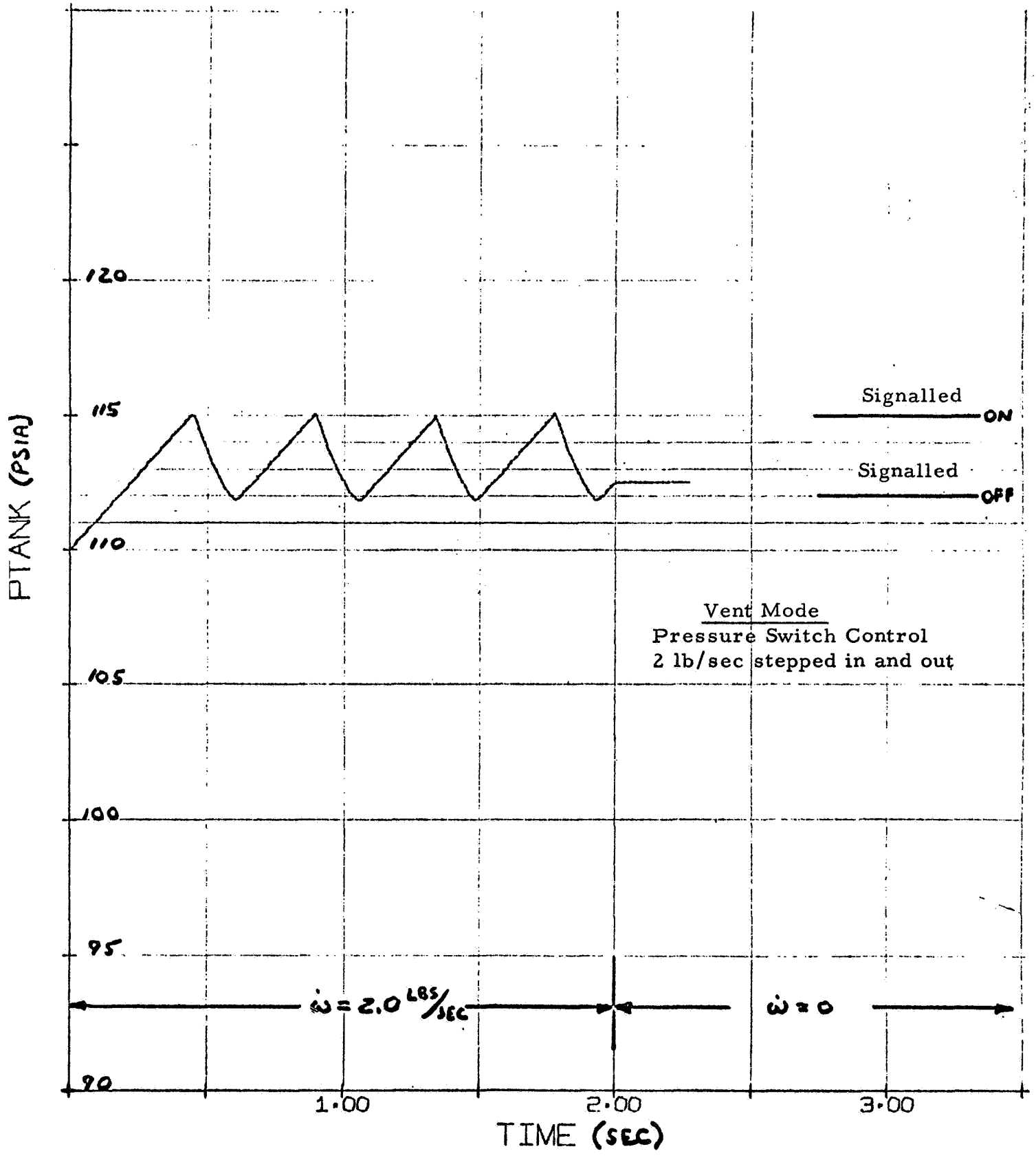

Figure 27 FLUORINE VALVE (P.S.) - RUN 2

TABLE IV

Operating conditions for graphs of figures 22 through 27.

Ambient Pressure	14.7 psi
Cracking Pressure	100 psig (114.7 psia)
Outlet line volume	500 $in.^3$
Outlet line effective flow area	0.872 $in.^2$
Gas constant	488 $in./°R$ (GF_2)
Temperature	197°R
Tank ullage volume	17,280 $in.^3$
Liquid flow from tank	zero
Pressure Switch	
Actuation	115 psia
Deactuation	112 psia
Solenoid Valve Flow Area	
Inlet	0.040 $in.^2$
Exhaust	0.040 $in.^2$
Solenoid Valve Response	Instantaneous

3.4 Design Optimization - Prior to achieving the final design, a number of design changes were made to improve performance. The first response calculations were made using the design parameters from the preliminary design. When it was decided to change from multiple ply to single ply bellows (refer to paragraph 4.2) it became impractical to use bellows strokes as large as originally planned.

3.4.1 It was necessary to increase the valve diameter from its original 2 inches, to the present 3 inches. This permitted a reduced valve stroke while maintaining the same valve flow area. The increased valve diameter dictated an increase in actuator bellows area, in order to still use only 5 of the 10 psi minimum pressure drop to open the valve. With these changes, valve performance was calculated. Results are shown in figures 28 and 29. The performance of this trial configuration was unsatisfactory, since there was an undershoot when flow was stepped out, to below the desired reseat pressure. In addition, there were limit cycle oscillations which occurred at certain flow rates. Study of the calculated results showed that the undershoot was caused by control pressure (which builds up only after the valve has cracked) acting on the downstream side of the pilot valve poppet and exerting a force tending to hold the pilot valve open. This problem could easily be corrected by reducing pilot valve diameter, but too much reduction could cause overshoot when flow was stepped in. The pilot valve diameter was reduced from 0.5 inch to its present value of 0.375 inch. This not only eliminated the excessive undershoot, but also eliminated the limit cycle oscillations. Overshoot remained satisfactory.

3.4.2 The final modification occurred when it was found that spring (20) could not be designed with both the intended spring rate and the intended natural frequency (over 2000 cps). A small increase in spring rate was tried and found to permit a 2000 cps natural frequency, and still retain adequate response. This value of spring rate was selected for the final design.

3.4.3 Performance of the final design, and the selected design parameters are presented in paragraph 3.3.

Relief Mode - Tank Pressure vs Time

2 lb/sec stepped in and out.

(This is not the final design - see text)

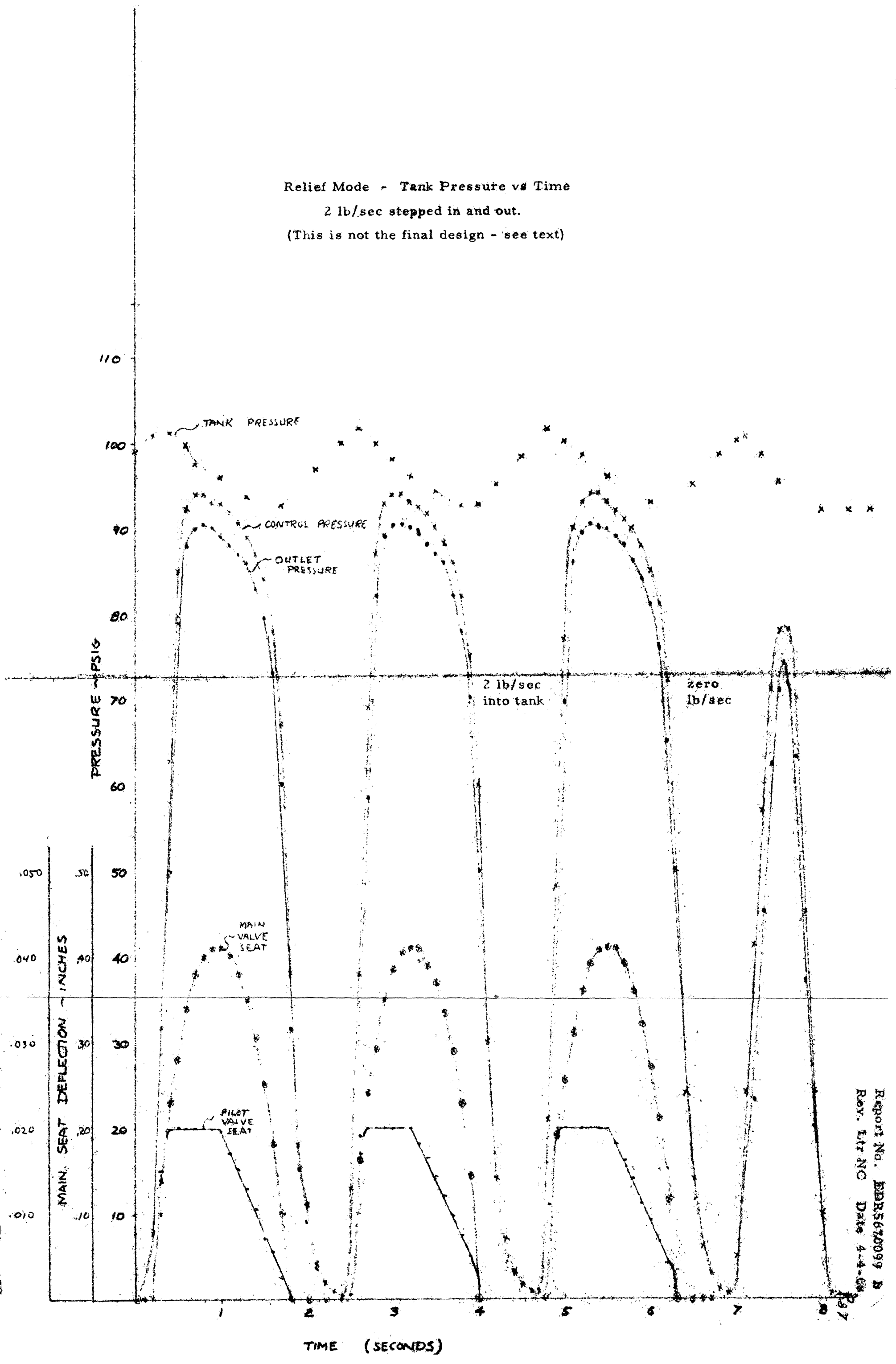

Figure 28 PILOT SEAT DEFLECTION ~ INCHES

Report No. EDR5670099 B
Rev. Ltr NC Date 4-4-68

Relief Mode - Tank Pressure vs Time

4 lb/sec stepped in and out

(This is not the final design - see text)

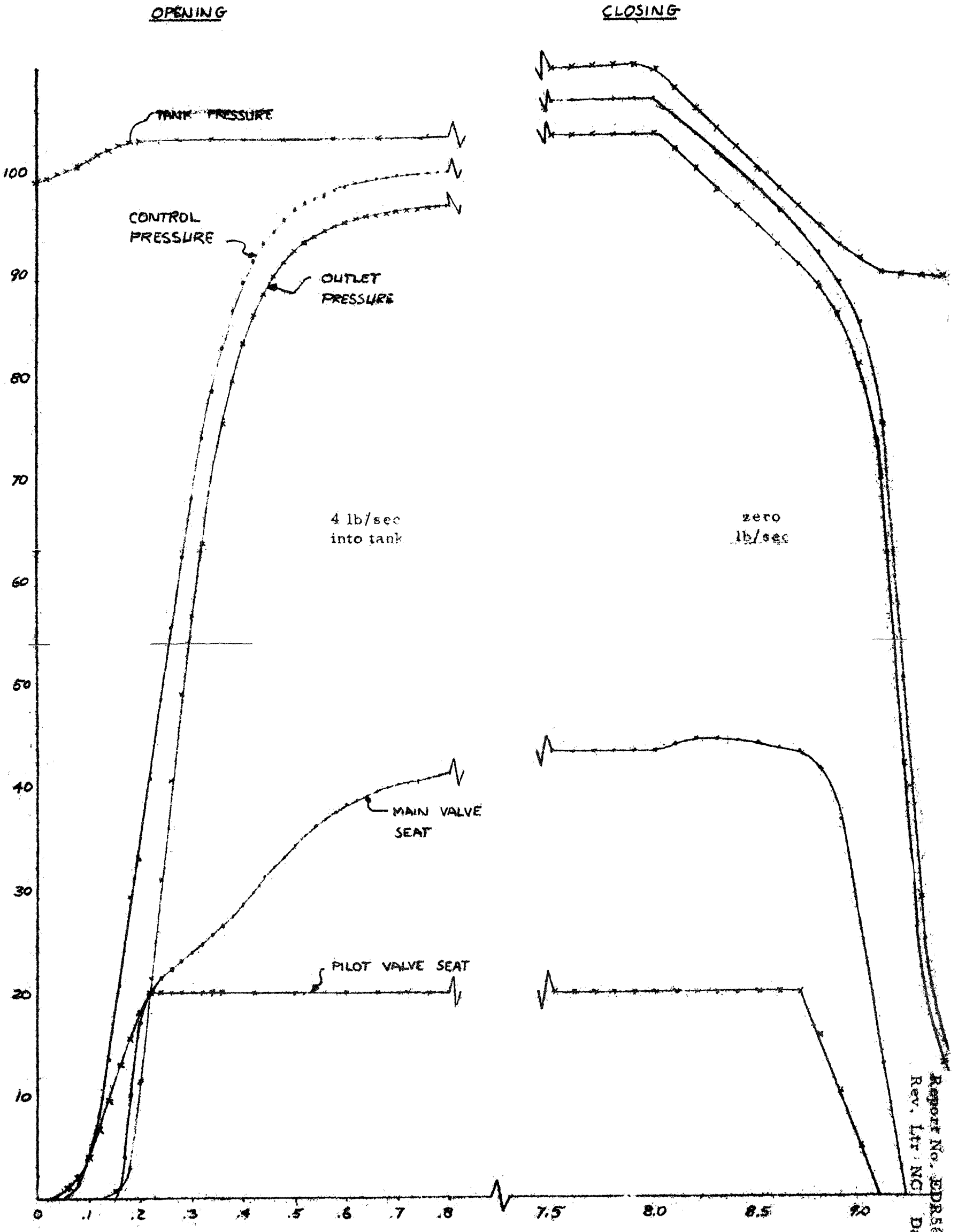

Figure 29

4.0 DESIGN ELEMENT ANALYSES

4.1 Summary - Table V summarizes the design element calculations performed and provides a convenient reference for the dimensions and performance parameters of all parts of the valve. The purpose of the design element analyses was to establish the physical dimensions of the detail parts such that the performance parameters of Table V would be met. As previously explained, the parameters must be held to the values in this table, or the valve assembly will not meet specified performance requirements. The details of the calculations are presented in Appendix B. However, the methods used are discussed in the following paragraphs, along with the reasons for selection of particular design elements.

TABLE V

FLUORINE VENT & RELIEF VALVE
SUMMARY OF CALCULATIONS

1. POWER BELLOWS

Rate =	78 lb/in.
Preload =	5 lb
Effective area =	20.5 in^2
Material =	321, 347
Material thickness =	0.0085 in.
Number convolutions =	12
Stroke =	0.250 in.
Max stress (total) =	42,600 psi (max allowable stress = 190,000 psi for 500 cycle life)

2. VENT BELLOWS

Rate =	1225 lb/in.
Effective area =	4.56 in^2
Material =	321, 347
Material thickness =	0.032 in.
Number convolutions=	14
Stroke =	0.250 in.
Max stress (total) =	155,600 psi (Max allowable stress= 190,00 psi for 500 cycle life)

3. PILOT BELLOWS

Rate =	96 lb/in.
Effective area=	1.76 in^2
Material =	321, 347
Material thickness =	0.0059 in.
Number convolutions =	12
Stroke =	0.087 in.
Max stress (total) =	160,000 psi (Max allowable stress = 190,000 psi for 500 cycle life)

TABLE V cont'd

4. TEMPERATURE COMPENSATOR

Material = Texas Instruments Truflex Alloy Bl
Composition: High expansion side: 22% Ni, 3% Cr, 75% Fe
Low expansion side: Invar (36% Ni, 64% Fe)

5. FLEXURE GUIDES (UPPER AND LOWER)

Rate =	11 lb/in.
Material =	321, 347
Material Thickness =	.0072 in.
Number of convolutions =	2
Max stroke =	0.250 in.
Max stress (motion) =	33, 800 psi

6. PILOT PRELOAD SPRING

Rate =	1140 lb/in.
Material =	Pretempered alloy steel wire
Wire dia =	0.177 in.
No. coils =	1.2
Max stress =	126, 000 psi
Natural frequency =	2030 cps

7. MAIN VALVE SEAT

Seat dia =	3.00 in.
Land width =	0.010 in.
Seat stress at reseat pressure =	7120 psi
Surface finish =	0.5 AA
Material: Seat -	Inconel 718
Poppet -	321 Cres
Calculated leakage =	6.45×10^{-7} lb/sec max

8. PILOT VALVE SEAT

Seat dia =	0.375 in.
Land width =	0.010 in.
Seat stress at reseat pressure =	840 psi
Surface finish =	0.5 AA
Calculated leakage =	3.32×10^{-7} lb/sec max
Material: Seat =	Inconel 718
Poppet =	321 Cres

TABLE V cont'd.

9. STRUCTURAL CALCULATIONS

a) Vent Bellows Housing
Material - Inconel 718
Yield stress = 105,000 psi min
Outer wall: (0.090 in. min)
S= 24,800 psi at 1250 psig burst pressure
Lower plate: (0.140 in. min)
S= 47,350 psi combined pressure stress from burst and bellows spring load.
Upper plate: (0.250 in. min)
S= 59,400 psi at 1250 psig burst pressure

b) Power Bellows Inner Housing
Material - Inconel 718
Yield stress = 105,000 psi min
S= 85,000 psi resulting from forces on stop at vent burst pressure

c) Power Bellows Outer Housing
Material - Inconel 718
Yield stress = 105,000 min
Wall: S= 12,570 psi at burst pressure of 375 psig
End cap: S= 10,000 psi at burst pressure of 375 psig

4.2 Bellows and Spring - The valve requires three "pressure responsive surfaces", a function which can be performed by bellows, diaphragms, or pistons. Each has its advantages and disadvantages. A very strong argument can be made for the use of bellows:

1. They do not leak (very important when fluorine is being handled).

2. They are frictionless, and involve no sliding contact. Thus there is no possibility of sticking, galling, or scraping off fluoride films.

3. They are all metal, and pose no particular material selection problems for fluorine service.

4. They are capable of much larger strokes than metal diaphragms, the only other device possessing all of the above three advantages. The strokes required in the valve are beyond the range of practicality for metal diaphragms (except possibly the pilot valve application).

4.2.1 The use of formed bellows is recommended wherever possible since the greater sophistication of welded bellows increases costs, and provides more opportunity for manufacturing and engineering error. The design and manufacture of bellows are inseparably linked. Bellows performance is very sensitive to small variations in thickness, and convolution shape. Variations which occur due to manufacturing techniques cause significant changes in bellows performance. For example, a 0.010-inch wall thickness bellows does not really have 0.010-inch thick walls. The stretching which occurs during forming of the bellows causes the thickness to vary. Nor is the stress equal to the calculated value because the forming process introduces large residual stresses.

4.2.2 The normal method of "designing" a bellows is to negotiate with potential bellows suppliers, asking them to propose bellows designs which meet specified performance requirements. It was decided not to do this for the fluorine valve since it would have required an unreasonable proposal effort on the part of a vendor.

4.2.3 Parker obtained the use of bellows design equations actually used by a leading bellows manufacturer. The bellows were designed using these equations. The details of the analyses are presented in full in Appendix B. Bellows designed on a commercial business basis are designed using ordinary

stress and deflection equations for flat plates. But the equations are modified empirically to account for the changes in thickness and shape which occur due to the manufacturer's particular forming process. The calculated results should not be used for actual bellows fabrication, because it is unlikely that the forming process will be identical to the one for which the equations were derived. The real meaning of the calculated results is that it is feasible to make a bellows which meets the performance requirements using the forming method of a leading supplier. Other suppliers, therefore, should be able to design the bellows using their own equations, and also meet the performance requirements within essentially the same envelope.

4.2.4 Resonance of bellows due to vibration is a common problem. It is almost impossible to design bellows that will have a resonant frequency greater than 2000 cps, while still meeting other requirements such as effective area, spring rate, and stroke. In fact, the reason vibration testing is seldom carried out above 2000 cps is that almost every part of a vehicle structure has passed through its resonant frequency by then and is attentuating the input movement. The violence of the bellows resonance depends on whether the bellows are single or multiple ply and on the length to diameter ratio of the bellows. As a matter of experience, multiple ply bellows are desirable where vibration is a problem (the friction between plies damps the resonance). However, the Douglas Fluorine Systems Handbook states that multiple ply bellows are not recommended for fluorine service because of the impossibility of being certain that there is no contaminant between the plies.

4.2.5 Parker concedes that present day methods of bellows manufacture may very well make it impossible to use multiple ply bellows that are safe for fluorine service. However, the advantages of multiple ply bellows are so great that serious consideration should be given to special bellows manufacturing facilities where all operations are carried out in modern clean rooms and welding is done by modern techniques which do not produce contamination (such as electron beam welding). This would probably make multiple ply bellows safe for fluorine. But such facilities do not exist today, so the valve has been designed to use single ply bellows. This makes it about 50% larger in diameter than it would have been with multiple ply bellows. It also reduces the amount of vibration which the valve will successfully endure, although it is believed that the specified requirements will be met.

4.2.6 The bellows have deliberately been kept short in length compared to their diameter since this is beneficial in minimizing the effects of resonance. The only really critical resonance problem is in the pilot valve since here resonance could cause shifts in cracking pressure. The pilot valve spring force primarily determines the cracking pressure. Resonance of this

spring must be prevented since it would cause an oscillation in the force determining the cracking pressure, and cause the pilot valve to "chatter", shifting the setting. Therefore the spring is designed with a resonant frequency greater than 2000 cps. The design parameters for the pilot valve were worked out so that this would be possible, while still meeting other performance requirements. The pilot valve bellows does not have a natural frequency greater than 2000 cps, but it is very light compared to the spring, contributes almost no spring force and is a short, squat bellows that does not resonate as violently as longer bellows. Under these circumstances, pilot valve bellows resonance should have little noticable effect.

4.3 Temperature Compensator - All pressure sensing instruments change calibration with temperature. In those instruments using mechanical springs, the change in modulus of elasticity is normally the primary cause. Thermal expansion is usually secondary in effect.

4.3.1 In any relief valve design, it is necessary to either provide temperature compensation or to tolerate a change in setting of roughly 3% per 100°F temperature change. The setting goes up as the temperature goes down.

4.3.2 The simplest type of temperature compensation involves making the spring out of the nickel alloy Ni-Span C, which has a constant modulus of elasticity over a temperature range of roughly -50° to +150°F. Unfortunately, Ni-Span C does not maintain a constant modulus down to cryogenic temperatures. The usual approach to temperature compensation for cryogenic temperatures is to devise a thermal expansion device that will extend the working length of the spring as the temperature decreases. The increased spring rate due to the increased modulus is then cancelled by an increase in the working length of the spring. While such devices are simple, and practical, they tend to be rather bulky. In order to minimize the size of the thermal expansion device, it was decided to use thermostat metal. An order of magnitude more defelection per degree of temperature change can be achieved with this material. Its limitation is that it is difficult to get the compensator rigid enough to bear the loads imposed on it while still maintaining a high deflection per degree. Design changes which make the thermostat metal element more rigid, all reduce the deflection per degree.

4.3.3 The analysis of the temperature compensator is presented in great detail in Appendix B. Several alternate locations were explored, and much trial and error was required before the final design was achieved. The final design meets all objectives.

4.4 Flexure Guide - The flexure guide is novel in design. A larger axial deflection was needed than is practical with conventional flexure guides. The problem was solved by use of very short bellows sections serving as flexure guides. Since the bellows sections are not subjected to any pressure differential, the bellows material can be very thin and a large deflection per convolution may be obtained. A welded style bellows segment was chosen in order to obtain the largest deflection per convolution. . This is important since using too many convolutions would impair the radial stiffness of the flexure guide.

4.4.1 Appendix B presents the details of the flexure guide design. Note that the same methods of analysis are used as for the other bellows, except that there is no pressure stress.

4.5 Structural Considerations - Structural calculations of a routine nature were made to assure the structural integrity of the design. Details are presented in Appendix B.

4.6 Valve Seats - Valve seat leakage was calculated to be sure that the seat stresses and surface qualities selected were consistent with specified maximum leakages. The method used is based on Tellier's comprehensive valve seat leakage studies (Reference 3 of Part I), which is essentially the same as the methods presented in the Fluorine Systems Handbook (Reference 1 of Part I).

5.0 FABRICATION, ASSEMBLY AND INSPECTION

The following outline provides necessary information for fabrication, assembly and inspection of the fluorine vent and relief valve.

5.1 General Requirements -

5.1.1 Documentation and Traceability - Documentation and traceability of raw materials, receiving and inspection of raw materials, manufacturing, and post manufacturing, shall be per paragraph 8.0 Section III of "Fluorine Systems Handbook".

5.1.2 Manufacturing -

5.1.2.1 Cutting and forming coolants shall be as specified in Table III-2.1a of "Fluorine Systems Handbook".

5.1.2.2 Passivation of components shall be as specified in Appendix III-5 of "Fluorine Systems Handbook".

5.1.2.3 Inspection requirements for components shall be as specified in Table III-7.0a of "Fluorine Systems Handbook".

5.1.3 Assembly -

5.1.3.1 All cleaning, inspection, assembly and preservation of cleaned components shall be performed in a clean room meeting the requirements of FED-STD-209, Class 100,000.

5.1.3.2 No dye penetrants shall be used.

5.1.3.3 No lubricants shall be used.

5.1.3.4 Post-weld inspection shall be as specified in Appendix III-4 of "Fluorine Systems Handbook".

5.2 Assembly Procedure - (See drawing 5680002 for Part Identification) Note: Welded version discussed below. Bolted version similar.

5.2.1 Electron beam weld outlet port (28) to main housing (1). Tooling required. Inspection required.

5.2.2 Pressure fit valve seats (2) and (15) into main housing (1) and electron beam weld. Lap valve seats and leak test. Tooling required for welding, lapping and leak testing. Inspection required for weld.

5.2.3 Place lower flexures (14) in main housing (1). Install power bellows housing (10) and bellows (13). Weld (upper and lower joints) bellows (10) to main housing (1) and power bellows housing (10). Tooling required. Inspection required.

5.2.4 Install guide (4) on stem (3) and electron beam weld to main poppet (5). Lap poppet. Tooling required for welding. Inspection required.

5.2.5 Electron beam weld vent bellows (12) to vent cap (11) and lower vent housing (24). Tooling required. Inspection required.

5.2.6 Electron beam weld assembly of (11), (12), and (24) to vent housing (7). Same tooling as paragraph 5.2.5. Inspection required.

5.2.7 Install stem assembly and with nut (27) and tab washer (26). Set preload for main valve seat.

5.2.8 Electron beam weld upper joint of outer housing (8) and vent housing (7). Tooling required. Inspection required.

5.2.9 Functional test of assembly prior to welding to main housing (Pilot valve opening to be used for pressurizing). Upper flexure to installed. Test fixture required.

5.2.10 Electron beam weld outer housing (8) to main housing (1). Tooling required. Inspection required.

5.2.11 Electron beam weld inlet port (6) to main housing (1). No additional tooling required. Inspection required.

5.2.12 Electron beam weld pilot bellows (19) to stop (23) and body flange (29). Tooling required. Inspection required.

5.2.13 Electron beam weld pilot body to pilot bellows assembly. Same tooling as paragraph 5.2.12 required. Inspection required.

5.2.14 Assemble Belleville (21), pilot poppet (16), temperature compensator (22) and electron beam weld to stop plate (30). Same tooling as paragraph 5.2.12 required. Inspection required.

5.2.15 Install spring (20), plug (18),screws (25), shim as required for preload, functional test. Test fixture required.

5.2.16 Electron beam weld pilot valve assembly to main valve assembly. Tooling required. Inspection required.

Appendix E

PRELIMINARY DESIGN OF POPPET SHUTOFF VALVE

E. 1 INTRODUCTION

The preliminary design of the valve shown in Figure 67 was accomplished by McDonnell Douglas under NASA Contract NAS 3-11195. The configuration was evolved during a design study in which several closures including both butterflies and poppets and several mating shapes, such as flat, conical, and spherical, were considered. The valve uses a flat-faced poppet closure and all-metal construction for the subcomponents exposed to fluorine. Welding is used wherever feasible to reduce the number of joints that require sealing. However, for purposes of this design, mechanical joints are retained to permit removal of the poppet and seat for refurbishing. The valve is normally closed and uses both inlet propellant pressure and mechanical springs for closing. Opening the valve requires application of pneumatic pressure to a linear actuator. All the materials used in the valve, the flat-faced sealing concepts (and bumper design), as well as the fabrication, inspection, and cleaning procedures are based on rigid adherence to the tests and design criteria generated by the McDonnell Douglas team under contracts NASw-1351 and Nas 3-11195.

The purchased parts selected for this design are representative of a type of component. Equivalent designs from other vendors would be equally acceptable.

E. 2 VALVE OPERATION

The valve is a normally closed shutoff valve. Two coaxial helical springs in the actuator maintain the valve in the closed position when no external power source is applied. In a normal installation the valve will be oriented in a propellant system so that pressure greater than ambient in the propellant tank will reinforce the valve closing force, increase the valve seat stress, and improve the seal at the valve interface.

The valve is opened by applying pneumatic pressure to the port in the actuator end cap. Use of an orifice in the pressurization line may be desirable to limit the rate of pressure buildup in the actuator and thereby control the valve response time. The valve will translate to the open position when the pressure on the actuator piston becomes sufficiently high to overcome the mechanical spring force, the hydrostatic pressure force on the poppet, and the friction drag forces from the piston seal and the poppet shaft guide bushing.

The cavity on the low-pressure side of the piston must be vented through a low-pressure check valve connected to the port in the side of the actuator housing. The check valve bleeds off any actuator pressurizing gas that leaks by the dynamic piston seal. It must also prevent back flow of any gas from the outside ambient atmosphere which may contain water or other contaminants deleterious to the life and operation of the valve.

Closing of the valve requires bleeding off the pneumatic pressurant in the actuator by means of a suitable control system. When the pressure force on

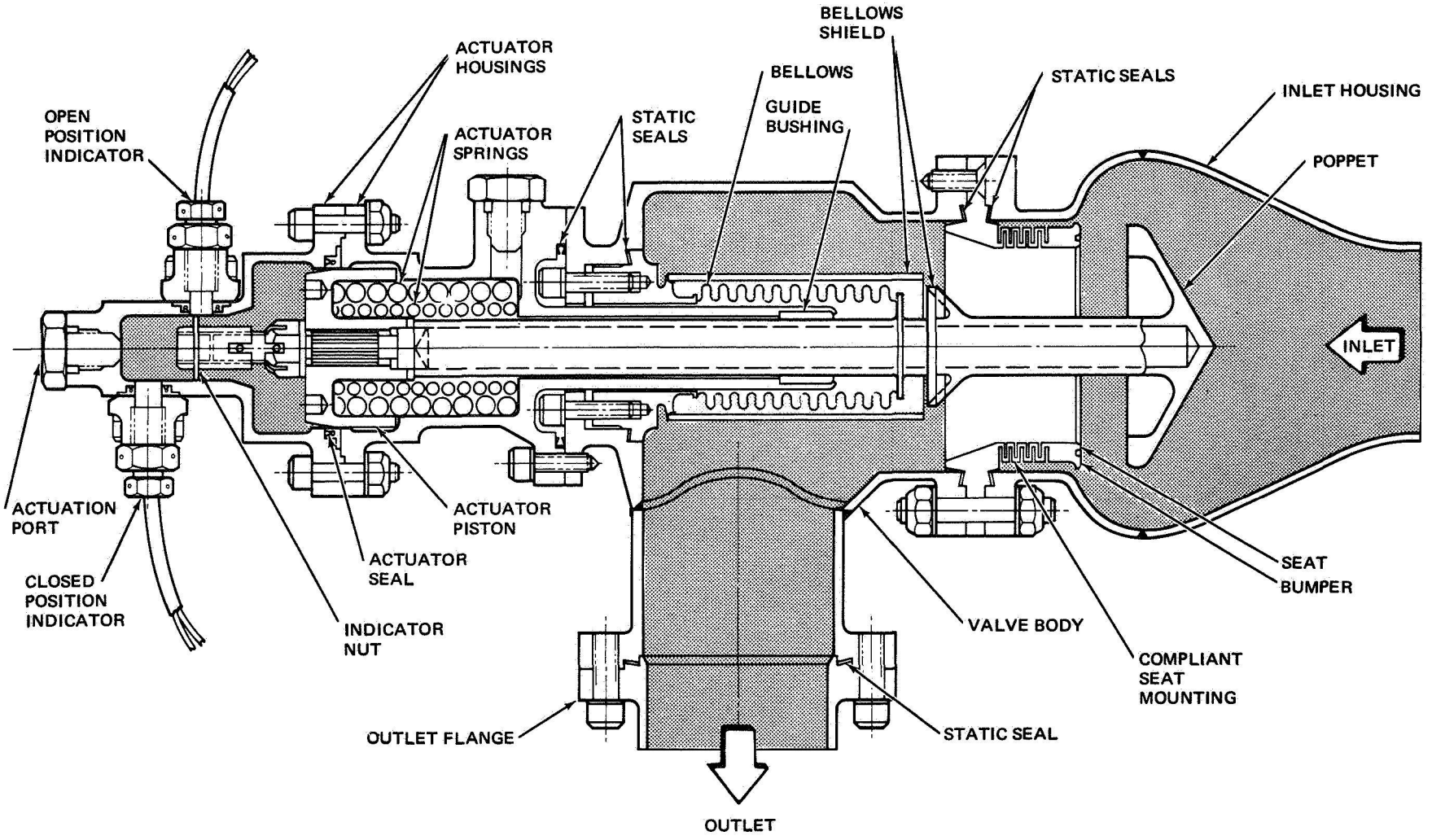

Figure 67. Valve Design

the piston becomes less than the sum of the propellant hydrodynamic force and the spring force on the poppet, the valve will close. As the poppet closes on the seat, the compliance of the seat mounting will deflect to permit completely normal contact between poppet and seat and absorb energy to reduce the impact load between poppet and seat.

E. 3 VALVE SUBCOMPONENTS

E. 3. 1 Poppet

The poppet consists of a rigid conical structure machined integral with a tubular shaft. A relatively wide flat sealing land is machined on the base of the cone. For normal operation, the apex of the conical poppet is pointed upstream into the flow. The poppet shaft is of tubular construction, closed at both ends. This necessitates fabrication of the shaft in two pieces and joining the pieces by butt welding. This construction provides a relatively stiff member without incurring the weight penalty of a solid shaft. The hollow shaft terminates with a cylindrical splined section and an external thread for attachment to the actuator piston. The poppet shaft can be used to hold the poppet while lapping the sealing land to the finish that is required to achieve the desired valve sealing characteristics. The poppet is part of a weld assembly which also includes the shaft seal bellows, the bellows adapter, and the bellows shield.

E. 3. 2 Seat

The valve seat consists of a rigid ring with a flat sealing land machined on the face which mates with the poppet. The opposite side of the ring is integrally attached by a machine-cut, ring-grooved support to a mounting flange which attaches to the valve body with screws. Sealing lands that will mate with the static seals between the valve body and seat flanges and between the valve inlet housing and seat flanges are incorporated on the seat. The ring-grooved mounting provides compliance for poppet-to-seat alignment. The land which seals against the poppet has a 2-μin. AA (5.08×10^{-8} m AA) circular lay surface finish.

E. 3. 3 Bellows

A hydroformed bellows is used for the dynamic seal on the poppet shaft. The bellows isolates the actuator from the fluorine cavity of the valve. Flexing of the bellows permits the valve poppet to move from closed to open without the use of a sliding seal, thereby eliminating a mechanical joint with its potential leakage hazard. One end of the bellows is welded to the poppet shaft and the other end is welded to an adapter that is attached with screws to the valve body.

Welded diaphragm-type bellows are not considered for this application because of problems incurred in reliable, effective cleaning and passivation for LF_2 service.

E. 3. 4 Actuator

The actuator controls the axial position of the poppet and is also used to provide partially the alignment and support for the poppet. The actuator is a simple single-piston design utilizing pneumatic pressure to open the valve and two coaxial helical springs to close the valve and apply the necessary seating loads to maintain minimum leakage at shutoff.

The actuator consists of a piston and a housing mounted externally on the valve. The metal bellows on the poppet shaft provides the dynamic seal between the fluorine cavity in the valve and the actuator.

A static seal is used between the valve body and the actuator housing to permit control of the environment in the cavity between the piston and the shaft bellows. It is necessary to maintain a dry inert atmosphere in this cavity to prevent corrosion and the possible formation of ice when the valve is chilled to cryogenic conditions.

Bearing support and radial alignment for the moving piston and poppet combination are provided by the actuator housing. The piston is guided and supported on the internal bore of the housing and the poppet shaft is supported by a guide bushing in the tip of the housing which extends into the valve body.

The actuator has two position indicators which sense the open and closed positions of the poppet. The indicators work on an inductive-proximity principle and sense the presence of the flange on an aluminum nut attached to the poppet shaft when the conducting flange moves into the sensing range of the detector. The position indicators provide verification of proper valve functioning and also can be used for valve response measurements. These indicators are available from the Bently-Nevada Corporation.

Two mechanical springs apply force on the actuator housing at one end and on the actuator piston at the other. These springs develop a closing force of 285 lb (1.30×10^2 kg) with the valve in the open position and 170 lb (7.73×10^1 kg) with the poppet seated, where a pressure assist of 345 lb (1.57×10^2 kg) results from the differential pressure across the poppet at 100-psig (6.90×10^5 pascals) system pressure.

One sliding dynamic seal is required in the actuator. A commercial seal that has performed well in low-temperature applications was selected for this application. This seal is a combination hat seal and C-section ring with garter spring. Because the basic C-spring has a radial flange outboard of the ring, the actuator piston seal assembly must be attached to the valve housing rather than the piston. With the Omniseal, low-temperature shrinkage enhances the sealing along the piston. Leakage around the outside of the seal is prevented by serrations on the housing which are embedded into the seal flange. The Omniseal is fabricated from Teflon to minimize friction.

E.3.5 Valve Body

The valve body is an Inconel 718 weld assembly made up of two lathe-turned subcomponents. The two ends of the larger subcomponent terminate with bolting flanges, one for mounting the valve seat and the other for mounting the actuator. The smaller subcomponent has a bolting flange on one end which is the valve outlet port. The areas that mate with the static seals are the most critical areas of the valve body. These sealing areas must be free of porosity and pits and have surface finish of 16 μin. AA (4.07×10^{-7} m AA) maximum. Elements of the valve, including poppet, seat, and static seals, must be replaceable; therefore, the sealing lands in the valve body must be considerably harder than the static seal material so that all plastic deformation of material at the sealing interface is confined to the static seals which are expendable when the valve is disassembled.

E.3.6 Static Seals

The static seals used in this valve may be divided into two categories: those which will be directly exposed to fluorine during the normal use of the valve, and those which will be exposed to fluorine only if a failure occurs which permits fluorine leakage into areas not normally exposed. A conical gasket made of annealed type 321 stainless steel has been specified for the static seals which will be exposed directly to the fluorine. The advantage of this seal is that in the installed position the conical gasket is flattened and its inner and outer edges are displaced radially to cause an interference fit with the sealing lands on its mating flanges. The gasket has a lower yield strength than the flanges so that plastic deformation takes place only on the edge of the gasket and not on the flange sealing land. Because of the plastic deformation, a new gasket must be used each time the coupling is separated and reconnected.

A C-section metallic seal made of Inconel X-750 coated with Teflon TFE has been specified for the interface between the valve body and the actuator housing. The primary purpose of this seal is to provide a dry inert environment in the cavity bounded by the poppet shaft bellows seal on one end and the actuator piston on the other. By maintaining a dry inert atmosphere in this cavity, corrosion of the metal components can be eliminated and, of equal importance, water will be excluded thus eliminating any problems from ice formation. Ice on the movable components could cause the valve to become inoperative. Moderate leakage can be tolerated through this valve-to-actuator interface seal. On a normal installation the metal structure of the seal is loaded in the elastic range and the required degree of sealing is achieved by controlling the surface roughness of the sealing interfaces. The Teflon TFE coating has a dual function. It increases the sealing effectiveness because the Teflon is deformed in its plastic range and also it forms a protective barrier between the dissimilar Inconel-X of the seal and the aluminum actuator housing. It is probable that similar seals made by other manufacturers would perform equally well for this application.

Spring-loaded Teflon TFE Omniseals have been specified for the valve position indicator seals. The Teflon jackets of these seals are manufactured in

a C-section and installed so that they are pressure energized by the contained fluid pressure applied to the inner surface of the C-section. Because Teflon has a higher coefficient of expansion than metals, it shrinks at a higher rate than the surrounding metal structure when chilled down from normal ambient to cryogenic temperatures. This greater shrink rate causes a Teflon seal to seal tighter on its inside diameter and separate from the outside sealing surface thus resulting in unacceptable leakage at low temperature. To prevent this leakage around the outside surface the Omniseal is provided with a flange which can be secured to the outside metal structure thus eliminating this leakage path. Spring action is imparted to the Teflon outer jacket by a continuous helical-wound, beryllium-copper spring formed from a flat rectangular cross-section. Springs of 304 CRES, 15-7PH CRES, and 17-7 CRES are also available but the beryllium-copper material is recommended by the vendor for cryogenic applications.

E.4 MATERIALS SELECTION

The materials for the valve components have been selected on the basis of NASA/MDAC experience on materials compatibility with both liquid and gaseous fluorine, as well as adequate physical properties throughout an expected temperature range from -320 to +200°F (77.6 to 366.5°K). The selected materials include Inconel alloys 718 and X-750. Stainless steels which have been used include types A286, 316, 324, and 347. Aluminum alloys A356, 1100, 2024, and 6061 have been selected for the valve actuator components and TFE Teflon seals are used in the actuator. Aluminum bronze coated with Astrocoat-T, a Teflon related polymer, or Teflon TFE has been used for the poppet guide bushing.

E.4.1 Poppet and Seat

Inconel 718 was selected for the poppet and stainless steel A286 was chosen for the seat. In the selection of materials for the poppet and seat sealing interface, a prime requirement as proved in previous NASA/MDAC programs is that the material must be capable of accepting a very smooth finish (2 μin. (5.08×10^{-8} m AA) or less) to provide an acceptable fluid seal. Many other criteria for the selection of materials for the poppet and seat are less clearly definable.

It is generally considered inadvisable to use the same material for two components in direct contact which have motion relative to each other, especially when they must operate under vacuum conditions because of the possibility of cold welding. However, this may not be a problem because fluorine may tend to maintain a fluoride film on the interfacing surfaces preventing the metal-to-metal contact which fosters cold welding. The possible material combination for poppet and seat include a hard metal against a hard metal, and a hard metal against a soft metal, where a hard metal is defined as a metal having a Brinell hardness greater than 250 and a soft metal is defined as one having a Brinell hardness less than 250.

If a hard metal against a hard metal is chosen, the apparent seating stress should be maintained at a level below 80% of the compressive yield strength

of the weaker material, which will eliminate gross plastic deformation of the sealing surfaces. When a soft metal is chosen for one of the closure components, and a hard metal for the other, the apparent seat stress should be greater than the compressive yield stress of the soft material and less than 80% of the compressive yield stress of the hard material. In valves with metal-to-metal sealing closures it is usually necessary to use a narrow sealing land on one of the components to develop a sufficiently high seat stress for good sealing characteristics. The use of different land widths on the two closure elements of a valve introduces a potential danger of damaging the wider land by a cutting action caused by the edge of the narrow land. This could occur if taper exists on the narrow land, or if the mating faces of the two lands are not parallel at the time of their initial contact. Tellier (Reference 3) concluded that this situation could be improved by making the overlapping member at least 20% harder than the narrower land part. A narrow land width on the sealing surface improves the probability of not trapping a solid particle.

In view of the above considerations, it appears that relatively hard materials are the best choice for a flat poppet and seat. For the configuration under consideration, the poppet should be of harder material than the seat. Because of the welded construction which joins the poppet, the shaft seal bellows, and the bellows adapter, it was necessary to select a material which is not only weldable but has good elongation properties and a reasonable fatigue life for the hydroformed bellows. The poppet shaft requires good strength qualities and a resistance to galling at the sliding bearing area and at the threaded end. Inconel 718 was selected as the material which best fulfills all of these requirements. Because of its high nickel and copper content, it is highly resistant to corrosion in fluorine. A hard surface is desired for the reasons discussed above. In the aged condition, Inconel 718 has a Brinnel hardness of approximately 400 which is higher than the attainable hardness for any of the other materials considered suitable for the application. If needed, still higher hardness can be attained by cold working the material.

Inconel 718 has excellent cryogenic properties. Its slow response to precipitation hardening makes it readily weldable (Reference 1). The poppet shaft material should be used in the as-rolled and aged condition providing a minimum tensile strength of 190,000 psi (1.31×10^9 pascals) and a bearing surface in the region on the guide bushing sufficiently hard to resist physical damage such as nicks and scratches which could lead to a valve malfunction due to galling or excessive wear.

The design and fabrication constraints stated in the Fluorine Systems Handbook (Reference 1) were considered for the shaft seal bellows. Establishing a rationale for the fatigue life of the bellows requires some degree of judgment. To provide the required flexibility the bellows wall thickness must be thin [approximately 0.008 in. (2.03×10^{-4} m)]. Because of the thin wall there is little margin of safety to protect against even small discrepancies in the physical properties of the material. Although the service life of the valve may require only a few cycles of operation or even a few hundred cycles, it is not practical to design for a material fatigue life based on a few

cycles of operation. Low cycle fatigue data do not exist for most of the candidate materials for this operation. In view of the above considerations, a fatigue life of 10,000 cycles was selected for the bellows. This value will provide an ample margin of safety over the expected service life for the valve. It is also consistent with criteria being used on a bellows for a 3-in.-diameter (7.6×10^{-2}-m-diameter) LF_2 shutoff valve currently undergoing test evaluation by McDonnell Douglas for AF/RPL.

Inconel 718 is being used by bellows manufacturers to fabricate bellows. Because the material work hardens when it is cold worked, it may be necessary to use two or more stages of forming while annealing the material between stages. Inconel 718 bellows have been subjected to testing in LF_2 on at least two test programs. A machined, convoluted mounting utilized to provide compliance to a butterfly valve seat was tested for NASA to demonstrate criteria for LF_2 feed system components (Reference 2). The mounting was subjected to 200 cycles of opening and closing the butterfly blade while exposed to the LF_2 medium. On a MDAC LF_2 valve test program for AF/RPL, two hydroformed bellows which were designed for a poppet valve shaft seal were submitted to a 10,000 cycle service life test while exposed to LF_2. The excursion of each cycle included the double stroke required for full opening and closing the valve. The bellows was designed for operation only on the compression side of the no-load or free-length position. Both bellows successfully completed the test without evidence of failure. Also, some room temperature fatigue life testing on Inconel 718 bellows was conducted by the Battelle Memorial Institute as part of an R&D program sponsored by the Air Force Rocket Propulsion Laboratory. The final report on this work has not yet been made available, but preliminary information from Battelle indicates that Inconel 718 is a reliable bellows material.

E.4.2 Seat

A-286 stainless steel heat treated to a minimum ultimate tensile strength of 130,000 psi was selected for the valve seat. At this strength level, A-286 stainless steel has a Brinell hardness of approximately 285 which is significantly lower than the Brinell hardness for the poppet. The seat has the narrower land width of the closure interface. Any plastic deformation as a result of impact between poppet and seat will occur on the seat causing an increase in its land width. The harder and wider poppet land will remain flat and free of indentations.

A machined mounting is used to provide compliance for poppet to seat alignment. This mounting is an integral part of the seat. Stainless steel A-286 is a good mounting material which has been successfully tested in LF_2. As part of the original NASA program to develop and demonstrate criteria for LF_2 feed system components (Reference 2), a butterfly valve utilizing a resilient machined bellows seat fabricated from A-286 stainless steel was subjected to 200 opening and closing cycles while exposed to an LF_2 medium.

E. 4. 3 Valve Body

The valve body consists of two lathe-turned components welded together. The areas which mate with the static seals are the most critical areas of the valve. These sealing areas must be free of porosity and pits and have a surface finish of 16 μin. AA (4.07×10^{-7} m AA) maximum. The elements of the valve, including poppet, seat, and static seals, are replaceable; therefore, the sealing lands in the valve body must be considerably harder than the static seal material so that all plastic deformation of material at the sealing interface is confined to the static seals, which are expendable when the valve is disassembled. Inconel 718 was selected for the valve body because it has high physical strength and hardness and has a good weldability rating. Stainless steel (A-286) was considered for this application but was eliminated because of its poorer welding characteristics. An acceptable alternate construction and material for the valve body would be to cast it from S Monel.

E. 4. 4 Actuator Housing

Cast aluminum A356-T6 has been selected for the actuator housing and end cap. A relatively heavy wall thickness for the cylinder is desirable to maintain adequate rigidity. The material stress level is low because the actuation pressure is low. The use of side ports for pressurization line and valve position indicator mounting results in an irregular shape which is ideally suited to casting as a fabrication method. Therefore, aluminum castings are logical choice for these components. Cast aluminum (A356) is also suitable for application of hard anodic surface treatment to the inside surface wall to provide a gall resistant surface at the sliding interface with the piston.

E. 4. 5 Piston

Aluminum 6061-T651 was selected for the piston material. Use of aluminum minimizes the piston weight thus permitting the valve opening and closing response time to be a minimum. Since the piston is directly coupled to the poppet shaft, a minimum weight for this assembly is desirable so that a high acceleration will not cause the poppet to lift from the seat as a result of the g-forces overpowering the valve closing spring. It is desirable to hard anodize the outer cylindrical surface of the piston to provide protection from galling when it slides in the cylinder. This hard-anodized surface must be relatively smooth to reduce friction and also to minimize wear on the Teflon Omniseal. Hard anodizing on aluminum 6061 results in a smoother surface than on other aluminum materials otherwise suitable for this application such as 2014 or 2024 aluminum.

E. 4. 6 Springs

An austenitic stainless steel type 316 spring tempered to a minimum torsional elastic limit of 100, 000 psi (6.90×10^8 pascals) has been selected for the actuator springs. Like most metals, the austenitic stainless steels increase in strength as temperature decreases. However, they retain their

elongation and impact strength properties at much lower temperatures than do most metals. Type 302 stainless steel is an acceptable alternate material but it may be more difficult to obtain with a torsional elastic limit of 100,000 psi (6.90×10^8 pascals). Inconel 718 tempered as noted above is also an acceptable spring material for the application but would be more costly and more difficult to obtain in the required wire sizes.

E.4.7 Inlet and Exit Flanges

Type 347 stainless steel has been specified for the inlet and exit flanges. A prime requirement for these flanges is that they must be suitable for welding to flight weight tubing. The most readily available thin wall stainless steel tubing suitable for welding is type 347. The best weld joint results when the flange and tubing are made from the same alloy. Other stainless steels acceptable for this application are types 304L, 316L, and 321. If the mating tubing is to be one of these alternate materials, then the flanges should be made of the same material.

E.4.8 Poppet Guide Bushing

Aluminum bronze has been selected for the poppet shaft guide bushing material. To provide a minimum coefficient of friction between the bushing and the poppet shaft it has been specified that the inside of the bushing shall be coated with Astrocoat-T which is a Teflon related polymer. A 0.002-in. (5.08×10^{-5} m) thick layer of TFE Teflon suitably bonded to the inside surface of the bushing is an acceptable alternate coating. Aluminum bronze was selected for this component to minimize the possibility of galling between the shaft and bushing if the polymer coating is dissipated. No published data could be found regarding the coefficient of friction between aluminum bronze and Inconel 718; however, brasses and bronzes are used extensively for bushing and bearing applications and have a relatively low friction coefficient when used against steel (Reference 13).

The possibility of making the entire bushing of Teflon was also considered. The Teflon bushing concept was rejected for three reasons. First, it was considered desirable to limit the amount of Teflon near the bellows seal. Because of its thin wall, the bellows is one of the most vulnerable components in the valve. A crack in the bellows would expose the bushing to a highly concentrated fluorine atmosphere and there is a possibility of the Teflon reacting with fluorine. Secondly, the shrinkage of the Teflon bushing during chilldown to the cryogenic temperature would result in an unacceptably large clearance between the bushing and its supporting structure. Third, Teflon cold flows under low-load conditions and the valve sealing could be adversely affected if the radial displacement of the poppet with respect to the seat became excessive.

E.4.9 Position Indicator Nut

Aluminum alloy 2024-T351 was selected for the position indicator nut because of its excellent machinability and weight considerations. The indicator works on inductive-proximity principles and any conducting material could be used for the indicator.

Type A286 stainless steel was chosen for bolts and screws because its physical properties are superior to the properties of the 300 series stainless steels and because of favorable experience at cryogenic temperatures with bolts of this material. The material retains its high ductility and has excellent notch toughness at -320°F (77.6°K).

E.4.10 Threads

It is undesirable to use lubricants on fluorine components because essentially all lubricants are incompatible with fluorine. However, most threaded fasteners will gall if installed clean and dry and torqued to a normal preload. Therefore, the external thread at all locations where galling would result in expensive rework or replacement of a subcomponent will be plated with soft copper. The threads which must be copper plated include the poppet shaft threads and all screws which are installed in tapped holes in the valve body. Copper plating of the screws used with nuts is optional. Although cold welding between the copper plating and the internal thread may occur, the copper has a lower shear strength than the parent metal of the threads; therefore, the fasteners can be removed without destroying the threads.

E.5 VALVE FABRICATION AND ASSEMBLY

The valve has been designed for fabrication by conventional manufacturing methods: casting, metal forming, machining, and welding. Producing the required surface finish on the sealing surfaces of the poppet and seat will be the most stringent requirement for fabrication.

The general requirements specified in Section III of NASA CR-72064 for manufacturing, material processing, and inspection of fluorine system components are applicable. A prime consideration in the manufacture of the valve subcomponents is that a high level of cleanliness is required in the completed component.

E.5.1 Fabrication and Inspection

Conventional tools may be used to fabricate the parts; however, sufficient controls must be applied to ensure a minimum degree of contamination. Petroleum-base coolants or preservatives must not be used during the fabrication of a component. An amine nitrite synthetic coolant which is water soluble is recommended. For operations such as grinding or lapping which make use of abrasive particles, only high-purity abrasives which are compatible with fluorine may be used. When either of these abrasive cutting techniques are used some of the abrasive particles can be expected to become imbedded in the finished surface. Recommended abrasives are diamond and manufactured aluminum oxide.

The valve body is an Inconel 718 weld assembly made up of two lathe-turned components which are welded together. The two ends of the larger component terminate with bolting flanges, one for mounting the valve seat and the other for mounting the actuator. The smaller component has a bolting flange on one end which is a valve outlet port. The welding must be either electron

beam weld or inert gas shielded arc weld. Full penetration of the weld through the joint is required and no cavities or inclusions in the weld are permitted. The weld joint must be given a 100% radiographic inspection.

After welding, the valve body must be stress relieved to minimize potential warpage problems. The final machining of all surfaces which are interfaces with mating components including seals, seat, and actuator must be accomplished after welding and stress relieving. Parallelism between the seat mounting flange and the actuator mounting flange is important to minimize the mismatch tolerances between poppet and seat. These two surfaces must be parallel within 0.01 in. in 10 in. (2.54×10^{-4} m in 2.54×10^{-1} m). The areas on the valve body which require the smoothest surface finish are the sealing lands for the static seals. A surface finish of 16 μin. AA (4.07×10^{-7} m AA) is required on the sealing lands. A surface finish of 125 μin. AA (3.18×10^{-6} m AA) is adequate on the remainder of the valve body.

The A-286 stainless steel material for the valve seat must be heat treated and aged to provide a minimum yield strength of 130,000 psi (8.97×10^{8} pascals). The basic shape may be obtained by turning on a lathe. The required spring rate for the compliant section is 5000 lb/in. (8.75×10^{4} N/m). The exact configuration of the bellows as well as the machining of this section will probably require the services of a vendor who specializes in machined bellows. Producing the required 2 μin. AA (5.08×10^{-8} m AA) surface finish on the seat sealing surface is the most critical of all the manufacturing operations. To obtain the required sealing characteristics, the surface must be lapped with a circular lay to the noted finish. To prevent scratching, the finish must not be inspected with a stylus instrument. It should be inspected optically with an interference microscope to verify that the 2 μin. AA (5.08×10^{-8} m AA) surface finish has been achieved and that the final land width is within the drawing tolerances. If any pits or scratches are found on the sealing surface, they must be evaluated by the cognizant engineer to determine whether their contribution to leakage can be tolerated without exceeding the permissible leak rate of the valve.

The poppet is part of an Inconel 718 weld assembly which also includes the shaft seal bellows, the bellows adapter, and the bellows shield. The Inconel 718 material for the poppet must be solution treated and aged to a minimum tensile strength of 190,000 psi (1.31×10^{9} pascals) before welding. The poppet shaft is a tubular construction closed at both ends. This necessitates fabrication in two pieces and joining the pieces by butt welding. This construction was devised to obtain a relatively stiff member without incurring the weight penalty of a solid shaft. Stress relieving must not be applied after making any of the welds on the poppet assembly because it will reduce the material hardness. It is desirable to maintain a high hardness level on the sealing land of the poppet to prevent surface finish deterioration when the valve is operated. Final machining of the exterior surface details on the shaft and the poppet sealing land must be accomplished after welding the two subcomponents of the poppet shaft together. The poppet sealing land must be lapped with a circular lay to a surface finish of 2 μin. AA (5.08×10^{-8} m AA). The land finish must be inspected optically with an interference microscope. The requirements for inspection of the land are the same as noted above for the seat.

The shaft seal bellows must be fabricated as a single-ply element because of the danger of trapping contamination between plies in multiply construction. Hydroforming of the convolutions is the preferred method of fabricating bellows for fluorine service. Bellows with edge welded convolutions are not considered acceptable because of the possibility of contamination and the difficulty of cleaning the welded areas. It is permissible to make the bellows from sheet stock by rolling the sheet into a tube and butt welding the longitudinal seam. This weld area must be given a 100% radiographic inspection after the convolutions have been formed. The bellows must be stress relieved after forming and prior to welding to the poppet.

The basic shape of the bellows adapter may be turned on a lathe. The Inconel 718 material for the adapter must be solution treated and aged to a minimum tensile strength of 190,000 psi (1.31×10^9 pascals) prior to final machining. All surfaces on the adapter may be finished with a 125 μin. AA (3.18×10^{-6} m AA) surface finish except the sealing land for the static seal which must be finished with a maximum roughness of 16 μin. AA (4.07×10^{-7} m AA).

The bellows shield is also a lathe turned part fabricated from annealed Inconel 718 material A surface finish of 125 μin. AA (3.18×10^{-6} m AA) on the shield is adequate. Four notches 0.13 in. by 0.13 in. (3.3×10^{-2} m by 3.3×10^{-2} m) equally spaced around the circumference of the shield on its weld attachment end are required to provide drainage from the bellows cavity.

A weld jig will be required to hold the subcomponents of the poppet assembly during welding. The orientation of the tapped hole pattern in the bellows adapter must be held in a predetermined position with respect to the serrations on the poppet shaft so that the piston support fixture noted in Subsection E.5.2 can be utilized to assemble the valve. Prior to welding, all subcomponents of the weld assembly must be precleaned in accordance with Subsection E.6. The welding must be either electron beam weld or inert gas shielded arc weld. Full penetration of the weld through the joint is required and no cavities or inclusions in the weld are permitted. All weld joints must be given a 100% radiographic inspection.

The buildup of the weld assembly consists of the following steps:

1. Weld one end of the bellows to the poppet.
2. Inspect the weld radiographically.
3. Slide the bellows shield over the bellows and toward the poppet so that the free end of the bellows is exposed for welding.
4. Place the bellows adapter in the jig and weld the bellows to the adapter.
5. Inspect the weld radiographically.
6. Preclean the assembly per Subsection E.6.
7. Weld the bellows shield to the adapter.

8. Inspect the weld radiographically.

9. Clean and package the assembly for fluorine service per Subsection E. 6.

The piston may be fabricated by turning on a lathe from bar stock. A broaching operation is required to produce the internal serrations which mate with the poppet shaft. The outer cylindrical surface of the piston must be hard anodized with a minimum coating thickness of 0. 002 in. (5. 08 x 10^{-5} m) for abrasion resistance. The coating may be polished if necessary to obtain the required 16 μin. AA (4. 07 x 10^{-7} m AA) surface finish.

The actuator housing and end cap are aluminum sand castings. The end cap requires no special operations other than conventional machining including turning, threading, and milling. The actuator housing however, requires a modification prior to the final machining. The poppet shaft guide bushing is retained by spinning the tip of the housing to a smaller diameter after the bushing is inserted. Cast material does not have sufficient ductility to make this spinning operation feasible. It is therefore necessary to fabricate the final one inch of the housing (that part which contains the bushing) of 6061-T651 aluminum bar and weld it to the cast housing using an inert gas shielded arc weld. After this modification the final machining of the housing can proceed. The housing requires a 0. 002 in. (5. 08 x 10^{-5} m) hard anodic coating for abrasion resistance on the internal surface in contact with the piston. The final operations include installing the poppet guide bushing and spin forming the tip of the housing to retain the bushing.

The poppet guide bushing is a lathe turned element fabricated from aluminum bronze bar. To minimize the friction effects between the poppet shaft and the guide bushing, and also to preclude galling, the bore of the sleeve must be coated with either Astrocoat-T (a Teflon related polymer) or a 0. 002 in. (5. 08 x 10^{-5} m) thick coating of TFE Teflon.

The remaining components include the actuator springs, the piston-to-shaft seal, the position indicator nut, and the position detector seal retainers. All of these items can be fabricated using conventional machine shop techniques.

E. 5. 2 Assembly Instructions

The valve components shall be cleaned and assembled in a clean room. The requirements for the clean room, for cleaning the components and for packaging the assembled valve are presented in Subsection E. 6. The assembly instructions contained in this section identify the specific valve components by item numbers which are identical to the find numbers shown on drawing 1T32095.

Two components, the inlet and outlet flanges (items 7 and 8), are designed for a weld attachment to the vehicle feed system piping. Therefore the attachment of the valve to these components and the installation of the interface seals will be accomplished during the installation of the valve into the vehicle. The valve inlet and outlet ports are to be capped with expendable closures to preclude internal contamination after assembly and prior to installation in the vehicle.

The following special fixtures and tools are required to aid in the assembly of the valve:

1. An assembly support fixture--the fixture would consist of a 1/4 in. (6.35×10^{-3} m) thick aluminum plate with a hole pattern matching the valve outlet port attach flange. The hole pattern must include both the bolt hole pattern and a 2-in. (5.08×10^{-2} m) diameter hole matching the outlet port to provide accessibility to the interior of the valve when it is mounted on the plate. The plate must be of suitable size to provide for gripping in a bench vise when the valve is mounted. The fixture must permit the valve to be oriented with the inlet port in the up direction for installation of the seat and poppet and the actuator end in the up direction for installation of the actuation mechanism.

2. A poppet installation fixture--the fixture would be designed with an outer support structure which would bolt directly to the valve inlet flange. An inner member would be designed to grip the poppet securely by its outer diameter. The interface between the inner and outer components of the fixture would provide the following functions:

   (a) Hold the poppet in axial alignment with the valve body

   (b) Permit rotation of the poppet about its axis for alignment with the valve body

   (c) Provide for holding the poppet in two axial positions, first slightly away from the seat when the poppet shaft seal is being rotationally aligned with its mating bolt pattern in the valve body and secondly firmly in contact with the valve seat when the valve actuation mechanism is being installed.

3. A piston support fixture--The fixture would consist of a 3/4 in. (1.90×10^{-3} m) thick aluminum plate, three inches in diameter with a bolt hole pattern to match the outboard flange of the actuator housing. The plate would have a 13/16-in. (2.06×10^{-2} m) diameter hole through the center to provide socket wrench clearance to install the shaft nut (item 34) and would be counterbored 1.70 (4.32×10^{-2} m) diameter by 7/16 in. (1.1×10^{-3} m) deep to provide piston clearance. Two 3/16-in. (4.77×10^{-3} m) dowel pins would be installed to match the holes in the face of the piston. The primary function of the fixture is to prevent damage to the bellows seal (item 2) due to torsional loading when the shaft nut (item 34) is installed.

4. Poppet and seal installation tongs--Special tongs will be required to reach through the valve outlet port and guide the bellows adapter into position during installation of the poppet and its static seal (item 20).

The following procedure shall be followed to assemble the valve:

1. Mount the assembly support fixture in a bench vise and attach the valve body assembly to the fixture using a minimum of four bolts through the valve outlet flange.

2. Orient the valve with the inlet end up. Prepare for installation of the valve seat (item 6), poppet (item 3) and their static seals by visually inspecting all of the sealing surfaces to ascertain that no damage is evident and no loose particles are present. Place a 59307-27S conoseal gasket (item 20) in the recess at the bottom of the valve body cavity and a 59307-40S Conoseal gasket (item 21) in the recess on the top side of the valve inlet flange. Carefully insert the valve seat through the Conoseal gasket and attach to the valve body with NAS 1189C3P8 screws (item 27). Tighten all screws until the heads just contact the seat, then torque each screw one-half turn in a sequence which will compress the gasket in a uniform manner. Continue this tightening procedure until the seal is compressed and all of the screws have been torqued 20 to 25 lb.-in. (2.32 to 2.88 x 10^{-1} kg-m).

3. Attach the poppet holding fixture to the poppet and carefully insert the poppet shaft through the seat and the Conoseal previously placed at the bottom of the valve cavity using care not to damage any of the sealing surfaces. The poppet must be located in the holding fixture in the position which precludes contact between the sealing surfaces of the poppet and seat so that the poppet can be rotated for alignment of the static seal bolt circle without marring the sealing surfaces. Attach the holding fixture to the valve inlet flange using a minimum of three bolts. Guide the bellows adapter into position by use of the special tongs through the valve outlet port. Align the bolt hole pattern in the bellows adapter (item 4) with the hole pattern in the valve body and install the eight 64566H-3F-20 cap screws and washers (items 39 and 36). Tighten all screws initally finger tight.

4. Invert the valve and holding fixture in the vise to orient the valve inlet down. Torque each of the eight screws installed in the previous step one-half turn in a sequence which will compress the Conoseal gasket in a uniform manner. Continue this tightening procedure until the seal is compressed and all of the screws have been torqued 20 to 25 lb-in. (2.32 to 2.88 x 10^{-1} kg-m).

5. Install the static seal (item 31) and the actuator housing (item 9) using the seven screws and washers (items 39 and 36). Torque screws 20 to 25 lb-in. (2.32 to 2.88 x 10^{-1} kg-m).

6. Adjust the poppet holding fixture until the poppet makes uniform contact with the seat. DO NOT OVERLOAD THE SEAT. The valve seat should not be deflected axially more than 0.040 in. (1.02 x 10^{-3} m) from its no load position.

7. Insert the two actuator springs (items 14 and 14) into the actuator housing and place the aluminum seal washer (item 12) on the shaft. Install the piston (item 11) and the piston support fixture. During this step care must be exercised to engage the serrations between the piston and shaft in an orientation which aligns the bolt hole pattern in the piston support fixture with the hole pattern in the actuator cylinder flange to prevent torsional over-stressing of the bellows seal. Use a minimum of four bolts with long threaded sections to secure the piston support fixture to the actuator housing. Tighten the bolts uniformly one-half turn each in sequence, compressing the actuator springs, until the fixture contacts the actuator housing at each bolt location. Install the shaft washer and nut (items 39 and 34) and torque the nut 40 to 70 lb-in. (4.64 to 8.12 x 10^{-1} kg-m) making certain that the cotter pin hole in the shaft is aligned with a set of slots in the castellated nut. Install the cotter pin (item 35).

8. Remove the piston support fixture, initially unscrewing the attaching bolts uniformly one-half turn each in sequence until all loads in the bolts are removed. Remove the poppet installation fixture. Install the indicator nut (item 13) on the shaft. Initially adjust the nut so that the outboard side of its flange is approximately 1.13 in. (2.87 x 10^{-2} m) from the face of the piston.

9. Make a trial installation of the actuator cap, securing with a minimum of two screws and check the position of the indicator nut flange through the position detector mounting hole nearest to the outboard end of the caop. The outer face of the indicator nut flange should appear in the inboard half of the hole and be within 0.030 in. (7.62 x 10^{-4} m) of the center of the hole.

10. If the indicator nut is not in the required location noted in step 9, remove the actuator cap and readjust the nut. Repeat steps 9 and 10 until the indicator nut is located within the specified tolerance.

11. Remove the actuator cap and secure the indicator nut with a cotter pin.

12. Install the position detectors (item 23) on the actuator cap as a subassembly. First install the jam nuts (item 24) on the detectors, then screw the detectors into the seal retainers (item 16) until the detectors project approximately 0.200 in. (5.08 x 10^{-3} m) through the bases of the retainers. Install the Omniseals (item 40) over the projecting tips then install the detector assemblies on the actuator cap with their mounting screws (item 30). Adjust each detector until its tip is flush with the inner wall of the actuator cap then tighten the jam nuts with 120 to 150 lb-in. (6.96 to 8.70 x 10^{-1} kg-m) torque and lockwire together.

13. Install the Omniseal (item 41) over the piston then install the actuator cap assembly and secure with the eight screws (item 29) and nuts (item 33). Torque the nuts 20 to 25 lb-in. (2.32 to 2.88 x 10^{-1} kg-m).

14. Remove the valve from the assembly support fixture and run an acceptance test on it in accordance with the applicable procedure. The test shall include demonstration of operation and a dry inert gas leak test on all dynamic and static seals to verify compliance with the permissible leakage requirements for the valve.

15. After satisfactory completion of the acceptance test remove the valve from the test stand and cap all ports. Install the two plugs and O-rings (items 25 and 26) in the actuator pressurization ports. Install expendable covers over the valve inlet and exit ports.

16. If the valve is not to be used immediately, package it for storage in accordance with the procedure specified in Section A. 6.

E. 6 CLEANING AND PROCESSING SPECIFICATION FOR PROPOSED LF_2 SHUTOFF VALVE

E. 6. 1 Environmental Requirements

All final cleaning, inspection, assembly, and preservation of cleaned sub-components and assembled components shall be performed within a clean room meeting the requirements of Federal Standard 209a, Class 100, 000.

E. 6. 2 Cleanliness Requirements

Before use, a 500 ml (5.0×10^{-4} m^3) sample of test solvent to verify cleanliness level of components and sub-components shall meet the following:

(a) The nonvolatile residue content shall not exceed 0. 010g. (1.0×10^{-5} kg).

(b) The solvent shall contain no particles over 80 microns (8.0×10^{-5} m) in size.

All significant surfaces of subcomponents and assembled components that are in contact with gaseous or liquid fluorine shall meet the following particle size limitations and nonvolatile-residue content per square foot (9.29×10^{-2} m^2) of area based on 500 ml (5.0×10^{-4} m^3) of solvent sample.

E. 6. 2. 1 Particle Size Limitations

1. No particles greater than 300 microns (3.0×10^{-4} m) in any dimension.

2. Three particles between 121 - 300 microns (1. 21 to 3.0×10^{-4} m).

3. Ten particles between 80 - 120 microns (8.0×10^{-5} to 1.2×10^{-4} m).

E. 6. 2. 2 Nonvolatile Residue Content

The nonvolatile residue content increase shall not be greater than 0. 001g (1.0×10^{-6} kg).

E.6.3 Materials

E.6.3.1 Cleaning Chemicals

Aluminum Cleaner	Kelite Corp. or equivalent
Descaler, RD-16	Carbonic Div., General Dynamics, or equivalent
Hydrofluoric Acid, Technical Grade	0-H-795
Nitric Acid, Technical Grade	0-N-350
Non-Ionic Detergent	MIL-D-16791
Plater's Cleaner	P-C-535a
Scale Conditioner (Permanganate Type)	MIL-D-26549 Amend. 2

E.6.3.2 Cleaning Solvents

Methylene Chloride	MIL-D-6998, Grade A
1, 1, 1, Trichloroethane, stabilized, vapor degreasing grade	MIL-T-81533
Trichlorotrifluoroethane	MSFC-SPEC-237

E.6.3.3 Drying or Preservation Gas

Air

Air used in drying and preservation processes shall be prefiltered to a 100-micron (1.0×10^{-4} m) level (absolute), the hydrocarbon content shall not exceed 0.5 ppm by weight in terms of n-cetane, and the moisture content shall not exceed 26.3 ppm by weight.

Nitrogen

Nitrogen gas used in drying and preservation processes shall be in accordance with MIL-P-27401, type 1, and in addition, shall adhere to the purity requirement listed in paragraph 3.3.1.

E.6.3.4 Packaging Material

Adhesive Tape, cloth back	PPP-T-60, Class 1
Aluminum Foil, Dry Annealed	MIL-F-148, Type 1, Grade B

Fluoro-halocarbon (Aclar or Kel-F) bags	MIL-B-22205A
Fluoro-halocarbon (Aclar or Kel-F) sheet	Richmond Corp. or equivalent

E.6.4 Procedures

The following precleaning procedures shall not be used with assembled components which contain dissimilar metals, Teflon coated subcomponents, or have been certified "fluorine clean" by the supplier. In the event a multi-material component has not been certified "fluorine clean," it shall be completely disassembled and the individual subcomponents pre-cleaned and final cleaned according to the following applicable procedures.

E.6.4.1 Precleaning

Components or subcomponents, except those coated with Teflon, shall be processed outside the clean room for the removal of dirt, grit, shop soil, chips, and other major contaminants by scrubbing with methylene chloride using a bristle brush and purging with compressed air. After removal of major contaminants, the following individual material cleaning procedures shall be used.

NOTE: The use of penetrant type inspection is not permitted on components and subcomponents for fluorine service. All components and subcomponents that show evidence of penetrant inspection shall be rejected from use without any further cleaning and processing.

Aluminum Alloys

Vapor degrease using 1, 1, 1 trichlorethane (or equivalent) until condensation ceases.

Immerse in 5-10% Oakite #61A Alkaline Cleaner (or equivalent) solution for minimum of 10 minutes (600 sec) at 160 ± 10°F (344.3 ± 5.5°K).

Rinse thoroughly with tap water.

Immerse in 15-20% (by volume) nitric acid solution maintained at 110 ± 40°F (316.5 ± 22.2°K) for minimum of 10 minutes.

Rinse thoroughly with tap water.

Oven dry at a maximum temperature of 180°F (355.4°K), or purge dry with filtered air.

Stainless Steel and Nickel Alloys

Vapor degrease using 1, 1, 1 trichlorethane (or equivalent) until condensation ceases.

Immerse in 5-10% Plater's cleaner (or equivalent solution) maintained at 170 ± 10°F (349.8 ± 5.5°K) for minimum of 10 minutes.

Rinse thoroughly with tap water.

Immerse in nitropickle solution (16% nitric acid/1% hydrofluoric acid - by volume), maintain at 140 ± 10°F (333.2 ±5.5°K) for 10 minutes (600 sec) to remove weld scale from components or subcomponents.*

NOTE: Use scale conditioner (or equivalent) followed by an alkaline descaler (or equivalent) both maintained at 190 ± 10°F (360.9 ± 5.5°K) for a minimum of 15 minutes in place of nitropickle to remove weld scale from components and subcomponents that contain critical finished surfaces or openings (polished to 2B or machined to 32 μin. AA (8.13 x 10^{-7} m AA) or finer).

Immerse in 20 - 40% (by volume) nitric acid solution maintained at 110 ± 40°F (316.5 ± 22.2°K) for minimum of 10 minutes.

Rinse thoroughly with tap water.

Oven dry at a maximum temperature of 180°F (355.4°K) or purge dry with filtered air.

E.6.4.2 Final Cleaning

Clean all component/subcomponent surfaces by purging with filtered air or nitrogen prior to transferring to clean room.

Metallic Components and Subcomponents

Use one of the following cleaning methods followed by cleanliness level testing and drying to final clean all significant surfaces that will be exposed to gaseous or liquid fluorine.

Vapor degrease using 1, 1, 1 trichloroethane (or equivalent) until condensation ceases, then flush with clean solvent.

Ultrasonically clean using trichlorotrifluoroethane for 2 to 5 minutes (120 to 300 sec), then flush with clean solvent.

Flush with a solvent listed in Subsection A.6.3.2.

Verify cleanliness level to the requirements of Subsection E.6.2 with test solvent.

Oven dry at a maximum temperature of 180°F (355.4°K) or purge dry with filtered air or nitrogen.

*Omit this step if welded subcomponents do not show evidence of weld scale.

Teflon or Teflon Coated Subcomponents

Wash with 0.1 to 0.5% (by volume) nonionic detergent solution.

Rinse thoroughly with filtered tap water followed by a deionized water rinse.

Oven dry at 240 to 260°F (388.2 to 400.0 °K) for 1 hour.

E.6.4.3 Component Assembly

All final cleaned components and subcomponents significant surfaces must meet the requirements of Subsection E.6.2 prior to assembly.

NOTE: No lubricants shall be used during subcomponent assembly unless specifically called out on the engineering drawing.

If assembly into a component is not forthcoming within a reasonable time, package Subsection E.6.4.4.

Wear nylon protective gloves when handling cleaned components with exposed significant surfaces.

E.6.4.4 Packaging

Wrap all subcomponent and/or component significant surfaces and/or openings with a minimum of two layers of aluminum foil (2 mils (5.08×10^{-5} m) thickness). Secure the foil with tape, completely covering all loose ends, obtaining as tight a seal as possible. Under no conditions shall the tape contact any significant surface.

NOTE: Use fluoro-halocarbon (Aclar or Kel-F) sheet or bags in place of aluminum foil when packaging all critical finished surfaces and openings (polished to 2B or machined to 32 μin. AA (8.13×10^{-7} m AA) or finer).

Place component in an Aclar or Kel-F bag.

Purge the interior of the bag with gas conforming to Subsection A.6.3. Flatten the bag by hand to exhaust excess gas atmosphere.

Heat seal the bag allowing a minimum of 1/2 in. (1.27×10^{-3} m) of material beyond the outer edge of the seal.

Identify per Subsection E.6.4.5.

E.6.4.5 Identification

Firmly affix a tag to the outside of the packaged component above the heat seal without penetrating any portion of the protective bag which forms the

secondary contamination barrier for the component. The tag shall contain the following information:

Part name.

Part number.

Manufacturer's serial number, if applicable.

Cleaned for fluorine service.

Date of cleaning.

Inspection and employee's cleaning stamps.

E.7 POPPET SHUTOFF VALVE ANALYSIS

E.7.1 Valve Sizing

Initial sizing of the valve was based upon the requirements of two-inch (5.08×10^{-2} m) size, 90 gpm (5.68×10^{-3} m^3/sec) flowrate, valve inlet pressure of 100 psia (6.90×10^5 pascals), and pressure loss of 5 psid (3.45×10^4 pascals) maximum. An apparent seat stress of 5,000 to 10,000 psi (3.45 to 6.90×10^7 pascals) was assumed to meet the leakage requirements of Table 27 for the valve closure.

Experience with valve closure tests during contract NASw-1351 and valve leakage analysis conducted as a part of contract NAS 3-11195 indicated a seat width of 0.010 inch (2.54×10^{-4} m) would successfully meet the sealing requirements by providing sufficient seat stress with adequate path length to inhibit leakage. Based on these assumptions, an effective seat and poppet diameter of 2.10 (5.34×10^{-2} m) in. and a poppet stroke of 0.50 in. (1.27×10^{-2} m) were selected.

E.7.2 Flow and Pressure Loss Performance Analysis

Pressure loss requirements for this valve will be met by the proposed design. A good estimate of the losses through the valve are given by Darcy's equation,

$$\Delta P = 1.112 \times 10^{-5} K\rho(Q/A)^2 \qquad \text{(E-1)}$$

where

ΔP = pressure loss, psid (6.90×10^3 pascals)

K = resistance factor

ρ = fluid density, lb/ft^3 (1.60×10 kg/m^3)

Q = flowrate, gpm (6.31×10^{-5} m^3/sec)

A = equivalent flow area, $in.^2$ (6.45×10^{-4} m^2)

Table 27

STATIC FORCE ANALYSIS INPUTS

C_{D_2} = constant for all Q

K_1 = constant for all Q

D_{poppet} = 2.1 in. (5.34×10^{-2} m)

A_{poppet} = 3.45 in.^{2} (2.22×10^{-3} m^2)

Maximum Lift of Poppet = 0.5 in. (1.27×10^{-2} m)

Flow area maximum = 3.14 in.^{2} (2.02×10^{-3} m^2)

at poppet lift = 0.485 in. (1.23×10^{-2} m)

P_1 = 100 psia (6.90×10^5 pascals)

P_2 = 0 psia (valve closed); 94.7 psia (valve fully open)
(0 pascals closed; 6.53×10^5 pascals open)

Shaft Seal Bellows		
Inside diameter, in. (m)	0.90	(2.29×10^{-2})
Outside diameter, in. (m)	1.26	(3.20×10^{-2})
Effective Area, in.^{2} (m^2)	0.92	(5.94×10^{-4})
Spring rate, lb/in. (N/m)	147.0	(2.63×10^3)
Springs		
Preload, lb (N)	170.0	(7.71×10^1)
Spring rate, lb/in. (N/m)	230.0	(4.11×10^3)
Pneumatic operating pressure, psig (pascals)		
Nominal	500	(3.45×10^6)
Minimum	250	(1.73×10^6)

The resistance factor is an empirical coefficient derived from tests of similar valves. This K factor is defined by the relationship:

$$K = fL/D \qquad \text{(E-2)}$$

where

f = Darcy friction factor

L = equivalent length of the flow resistance, inches (2.54×10^{-2} m)

D = equivalent diameter of the flow resistance, inches (2.54×10^{-2} m)

Based upon tests conducted at Calmec Manufacturing Corporation on a vent and relief valve of similar internal configuration to the proposed valve during contract NASw-1351 (Reference 2), together with empirical data given in References 13 and 14, a conservative K factor of six was chosen for the proposed configuration. Based on this value, and assuming that the density of liquid fluorine is 97 lb/ft^3 (1.55×10^3 kg/m^3) at a temperature of -320°F (77.6°K), the pressure loss was calculated as

$$\Delta P = 1.112 \times 10^{-5} \quad (6)(97)\left(\frac{90}{3.14}\right)^2$$

$$\Delta P = 5.3 \text{ psid } (3.7 \times 10^4 \text{ pascals})$$

E.7.3 Static Force Analysis

Figure 68 is a diagram of the valve closure that identifies the significant pressures and areas affecting valve static force analysis. Based upon this diagram a summation of the pressure forces acting on the valve poppet may be written as

$$F_{closing} = P_1A_p - P_2(A_p - A_S) + P_2(A_B - A_S) \qquad \text{(E-3)}$$

which can be reduced to

$$F_{closing} = (P_1 - P_2)A_P + P_2A_B \qquad \text{(E-4)}$$

The pressure behind the valve poppet (P_2) can be seen from Figure 68 to be dependent upon the inlet pressure and the stroke of the valve. To evaluate this pressure, it is first necessary to assume some boundary conditions for valve operation. For example, to maintain a valve inlet pressure of 100 psia (6.90×10^5 pascals) at a flowrate of 90 gpm (5.68×10^{-3} m^3/sec) with the valve fully open, a back pressure of 94.7 psia (6.53×10^5 pascals) must be maintained at the valve outlet. However, the valve leakage requirements are based upon a differential pressure across the valve closure of 100 psid (6.90×10^5 pascals).

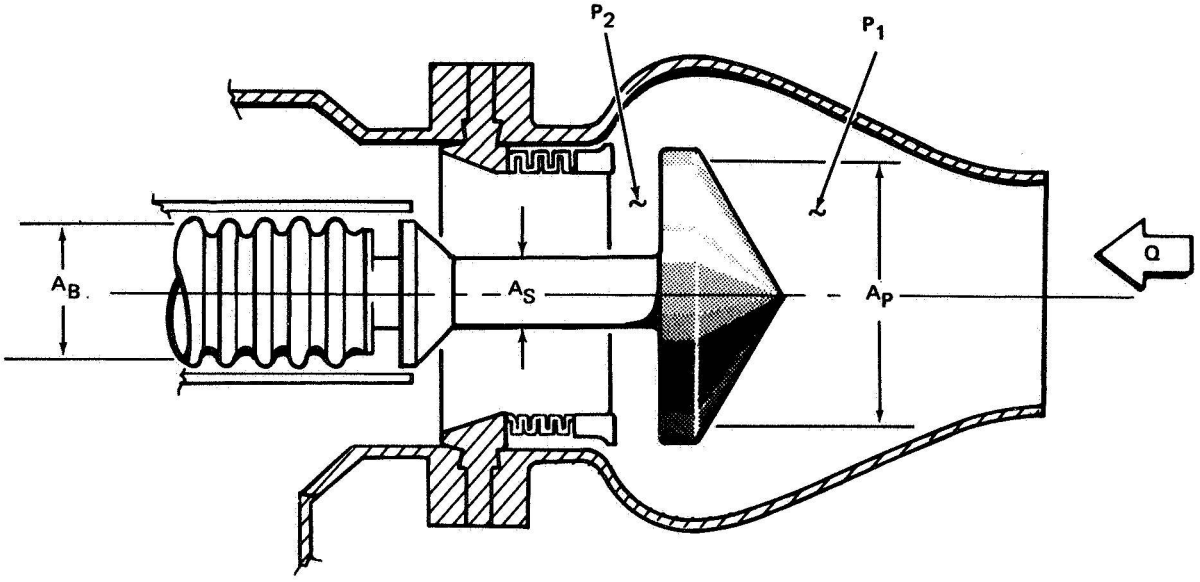

Figure 68. Valve Closure Diagram

These boundary conditions are met by the valve installation shown schematically in Figure 69. This schematic illustrates a flow system with two series flow resistances separating the 100 psia (6.90×10^5 pascals) valve inlet pressure from the ambient vacuum conditions. The valve is the upstream resistance between stations 1 and 2, and is represented in hydraulic symbols as $(K_1^{-1/2} A_1)$. The downstream resistance between stations 2 and 3 is defined only by the assumed boundary conditions, and is symbolized as $(C_{D_2} A_2)$.

Assuming continuity of mass and quasi-steady flow through the system, it is possible to write the expression based upon Bernoulli's equation:

$$Q = 296 K_1^{-\frac{1}{2}} A_1 \sqrt{\frac{(P_1 - P_2)}{\rho}} = 296 C_{D_2} A_2 \sqrt{\frac{(P_2 - P_3)}{\rho}} \qquad \text{(E-5)}$$

or, simplifying

$$K_1^{-\frac{1}{2}} A_1 \sqrt{(P_1 - P_2)} = C_{D_2} A_2 \sqrt{(P_2 - P_3)} \qquad \text{(E-6)}$$

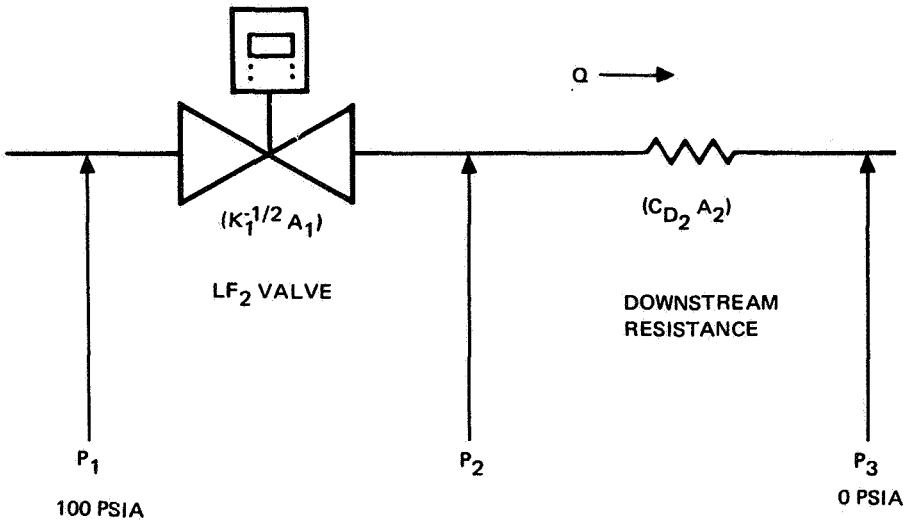

Figure 69. Typical Valve Installation

Taking advantage of the fact that $P_3 = 0$, this equation can be solved for P_2 as

$$P_2 = P_1 \left[\frac{\left(K_1^{-\frac{1}{2}} A_1 \right)^2}{\left(C_{D_2} A_2 \right)^2 + \left(K_1^{-\frac{1}{2}} A_1 \right)^2} \right] \qquad \text{(E-7)}$$

For simplicity, it may be assumed that the resistance coefficients will remain constant with respect to valve stroke. The downstream resistance $(C_{D_2} A_2)$ is evaluated from the first boundary condition as

$$C_{D_2} A_2 = \frac{Q}{296} \sqrt{\frac{\rho}{P_2}} \qquad \text{(E-8)}$$

$$= 0.303$$

The back pressure on the poppet is now given by Equation E-7 as a function of valve flow area. However, for a flat poppet valve, valve flow area is proportional to valve stroke. Therefore, poppet back pressure may conveniently be parameterized as a function of valve stroke. The summation of pressure area forces acting on the poppet may now be computed from Equation E-3.

Table 27 gives a summary of the input variables affecting the valve static forces analysis. From these values, and the preceding analysis, the valve closing forces shown in Figure 70 were calculated. Based upon these data, an actuator or piston pressure area of 2.07 in.^{2} (1.33×10^{-3} m^2) was chosen, providing an actuation safety factor of 2 for the valve.

E.7.4 Main Closure Leakage

Leakage through the main closure of the valve has been calculated by the method derived in Appendix A. As described in that appendix, the theoretical laminar liquid flow is given in pounds per second (4.54×10^{-1} kg/sec) by the equation

$$\dot{w}_{Theo.} = \left(\frac{L}{W}\right) \frac{(hp \times 10^{-6})^3 \ (P_1 - P_2)}{144\mu} \qquad (E-9)$$

Using the values given in Table 28 it was possible to calculate liquid fluorine leakage as a function of surface roughness, Figure 71, and differential pressure, Figure 72.

Table 28

MAIN CLOSURE LEAKAGE ANALYSIS INPUTS

Rated differential pressure, valve closed ($P_1 - P_2$), psid (pascals)	100	(6.90×10^5)
Mean Seat diameter (D), in. (m)	2.10	(5.34×10^{-2})
Seat width (W), in. (m)	0.010	(2.54×10^{-4})
Seal length (L), in. (m)	6.60	(1.68×10^{-1})
Seal area (A), in.^{2} (m^2)	0.066	(4.25×10^{-5})
Apparent seat stress (S), psi (pascals)	8,000	(5.53×10^7)
Surface Roughness, μin. AA (circular lay) (m AA)	2	(5.08×10^{-8})
Equivalent flat plate height (h_p), μin. (m)	6	(1.52×10^{-7})
Fluorine temperature (T), °F (°K)	-320	(77.6)
Fluorine density (ρ), lb/ft^3 (kg/m^3)	97	(1.55×10^3)
Fluorine viscosity (μ), lb-sec/ft^2 (pascal-sec)	6.25×10^{-6}	(2.99×10^{-4})

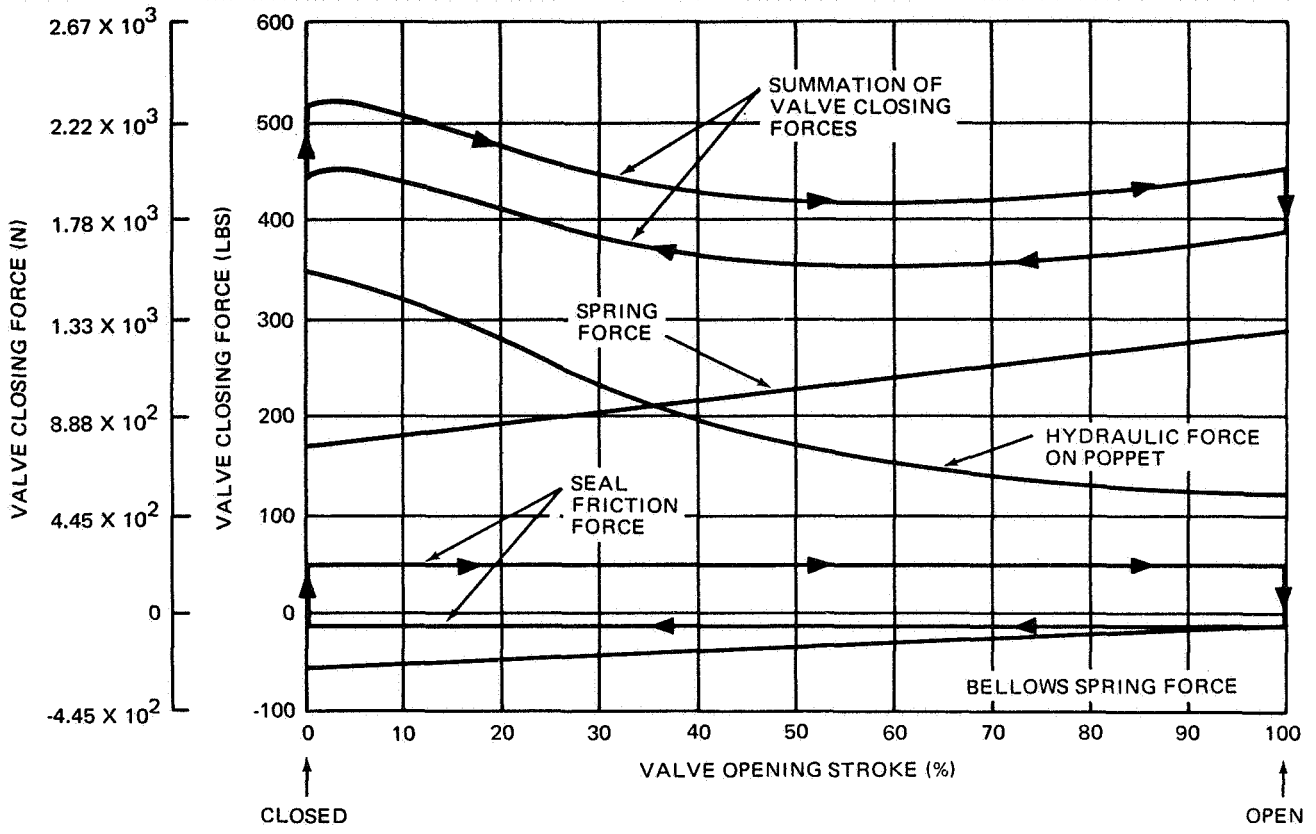

Figure 70. Typical Valve Closing Forces

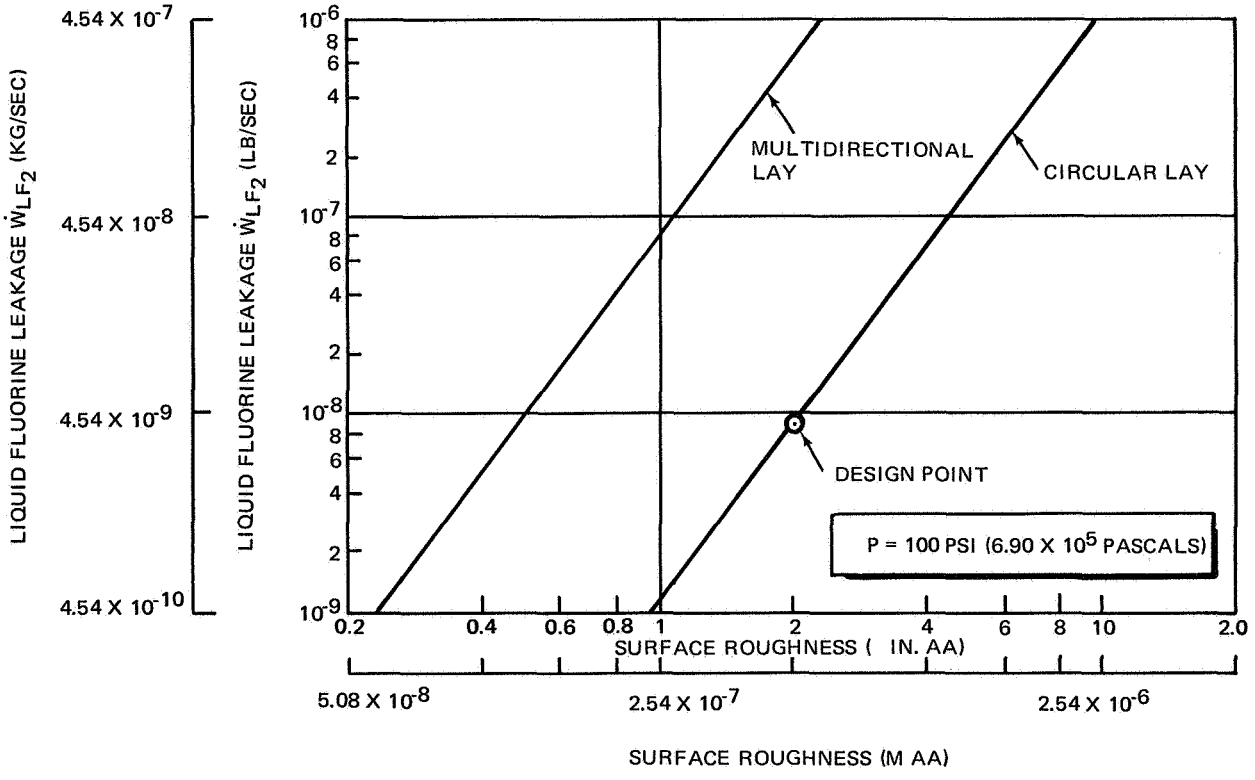

Figure 71. LF_2 Leakage vs Surface Roughness

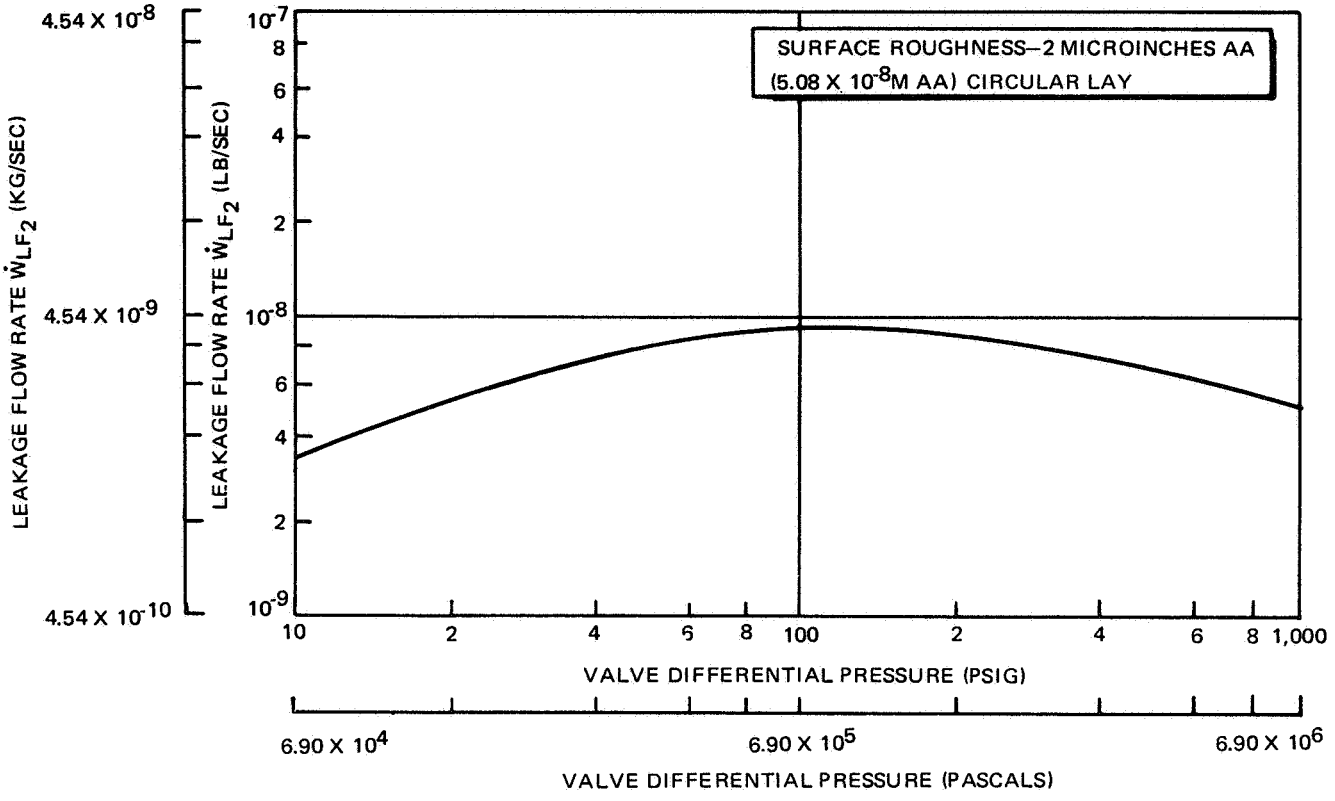

Figure 72. Estimated LF_2 Leakage vs Differential Pressure

Appendix F

ANALYSIS OF MOISTURE IN FLUORINE TANKAGE

If a quantity of liquid fluorine is delivered to the test site and flowed into a new storage tank, and this propellant is later pumped into the tanks of a space vehicle, the LF_2 will have two opportunities to acquire additional water content. Each new tank will contain a certain amount of moisture which will be mixed into the LF_2.

The moisture content of the tanks is generated from two sources. First, there is the water vapor present in the pressurizing gas in the storage tank. Under best conditions, this moisture would all be displaced from the tank with the pressurant with the introduction of the LF_2; however, under worst conditions, it would remain behind to contaminate the LF_2.

A second source of moisture is the thin molecular film of water adhering to the tank walls. It is not likely that this moisture would be displaced from the tank by the entering LF_2. All of this molecular film will probably remain to contaminate the fluorine.

The purpose of this analysis is to evaluate the relative importance of these two sources of moisture, and the resultant effect of the moisture on the LF_2. A typical example will be studied to provide numerical results.

A 50,000-lb (2.27×10^4 kg) load of fluorine at -307°F (85.4°K), has a volume of 532 ft^3 (1.51×10^1 m^3). Assume that this volume of fluorine is transferred into a tank which has been purged continuously with gas until the gas emerging from the tank is found to contain only 200 ppm (by volume) of water vapor. For a storage tank volume of 532 ft^3 (1.51×10^1 m^3), about 6.8×10^{-3} lb (3.09×10^{-3} kg) of water vapor might be expected in the pressurizing gas at room temperature and 1 atmosphere.

To determine the quantity of water adhering to the skin of the storage tank, it is necessary to assume a tank shape. For instance a 532-ft^3 (1.51×10^1 m^3) tank has a surface area of 319 ft^2 (2.96×10^1 m^2) if spherical, and 383 ft^2 (3.56×10^1 m^2) if a 2:1 length-to-diameter cylinder (e.g., a soup can). Assume the latter case to be a worst condition. The weight of water that might be expected to adhere to the skin of a typical aluminum tank having a surface area of 383 ft^2 (3.56×10^1 m^2) is about 2.35×10^{-4} lb (1.07×10^{-4} kg) of water film. The total quantities of water addition to the LF_2 is the sum of 6.8×10^{-3} lb (3.09×10^{-3} kg) due to the gaseous atmosphere in the tank and 2.35×10^{-4} lb (1.07×10^{-4} kg) due to surface film water. The total water addition is, therefore, 7.035×10^{-3} lb (3.19×10^{-3} kg).

The equation for the reaction of the water with LF_2 may be written

$$2H_2O + 2F_2 \rightarrow 4HF + O_2$$

The molecular weight of water is 18, and for hydrogen fluoride, the molecular weight is 20. Therefore, with a complete reaction every 36 lb (1.63×10^1 kg)

of water could yield 80 lb (3.63 X 10^1 kg) of hydrogen fluoride. It follows that the 7.035 X 10^{-3} lb (3.19 X 10^{-3} kg) water could give 1.562 x 10^{-2} lb (7.10 X 10^{-3} kg) increase in hydrogen fluoride. For the 50,000 lb (2.26 X 10^{-4} kg) of LF_2, this is a possible increase of 3.12 x 10^{-5}% by weight in hydrogen fluoride each time the fluorine is detanked to a system that has been open to the atmosphere.

Figure 73 provides a rapid means of estimating the increase in hydrogen fluoride content of LF_2 undergoing a transfer to a new system. The effect of the molecular film of water on the walls has been neglected. The percent increase in hydrogen fluoride is then seen to be independent of container dimensions.

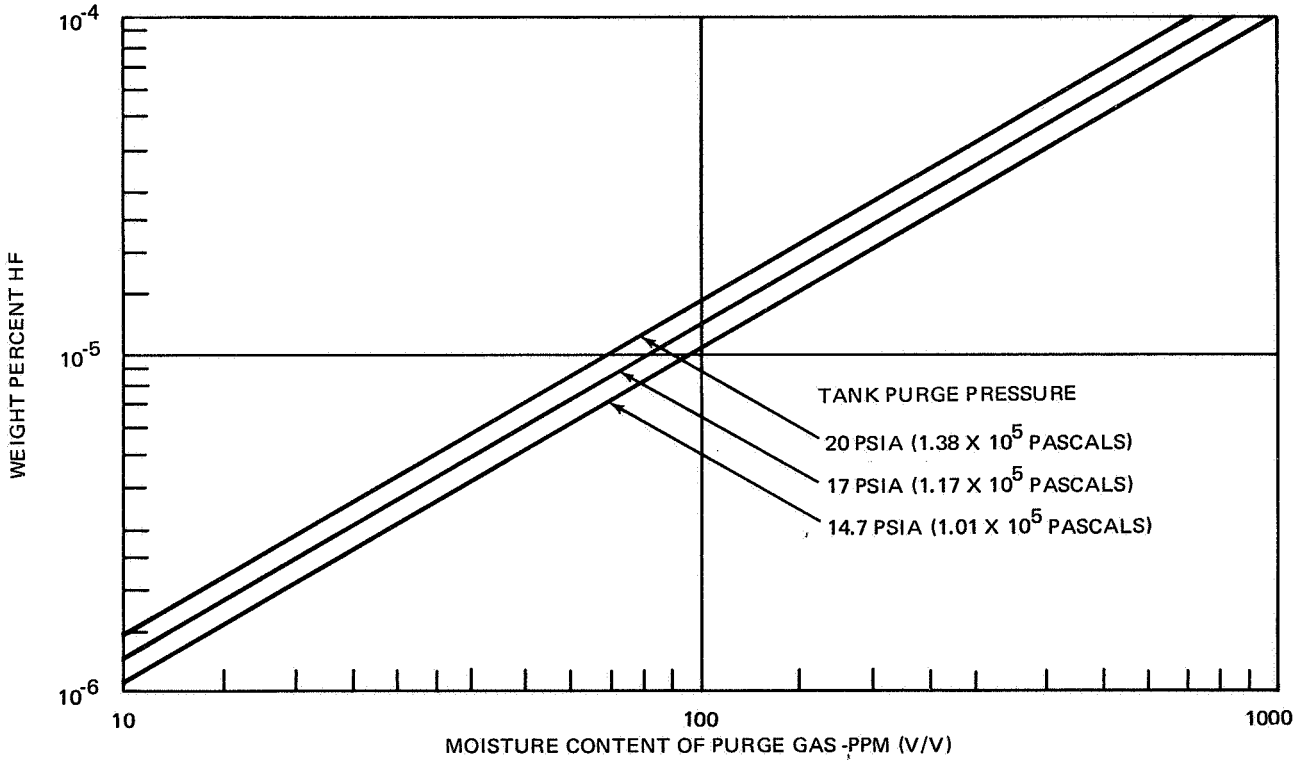

Figure 73. Maximum Hydrogen Fluoride Addition to Tanked Liquid Fluorine

REFERENCES

1. Fluorine Systems Handbook. NASA Report No. CR-72064. McDonnell Douglas Astronautics Company, 1 July 1967.

2. Development and Demonstration of Criteria for Liquid Fluorine Feed System Components. NASA Report No. CR-72063. McDonnell Douglas Astronautics Company, October 1967.

3. G. F. Tellier. Poppet and Seat Design Data for Aerospace Valves. Report No. AFRPL-TR-66-147. Rocketdyne Division of North American Rockwell, July 1966.

4. J. W. Marr. Leakage Testing Handbook. Report No. S-67-1014. General Electric, Schenectady, N. Y., June 1967.

5. R. Kenyon, Fluorine Vent and Relief Valve PN5680002 and PN5680003. Engineering Design Report EDR 5670099. Parker Aircraft Company, 7 May 1968.

6. T. M. Trainer. Development of Analytical Techniques for Bellows and Diaphragm Design, Final Report. Report No. AFRPL-TR-68-22. Battelle Memorial Institute, March 1968.

7. H. W. Schmidt. Handling and Use of Fluorine and Fluorine-Oxygen Mixtures in Rocket Systems. Report No. NASA SP-3037. NASA Lewis Research Center, 1967.

8. W. D. English and D. R. Spicer. Impact Sensitivity in the Fluorine-Ice System. Cryogenic Technology, Vol 1, Sept - Oct 1965.

9. R. M. Spriggs. Expression for Effect of Porosity on Elastic Modulus of Polycrystalline Refractory Materials, Particularly Aluminum Oxide. Journal of American Ceramic Society, December, 1961.

10. S. K. Asunmaa, et al. Halogen Passivation Procedural Guide, Final Technical Report. Report No. AFRPL-TR-67-309. McDonnell Douglas Astronautics Company, December 1967.

11. J. H. Perry. Chemical Engineer's Handbook, Third Edition. McGraw-Hill Book Company, Inc., 1950.

12. R. C. Weast. Handbook of Chemistry and Physics, 46th Edition. The Chemical Rubber Company, 1965.

13. G. W. Howell and T. M. Weathers. Aerospace Fluid Component Designer's Handbook. Report No. RPL-TDR-64-25. TRW, Inc., March 1967.

14. W. G. Kautz. Flow of Fluids Through Valves, Fittings, and Pipe. Technical Paper No. 410, Crane Company, 1965.

Part 1

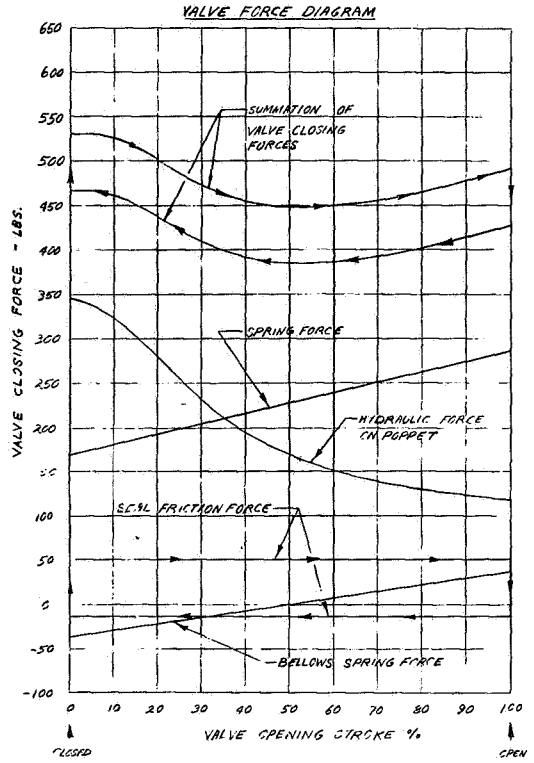

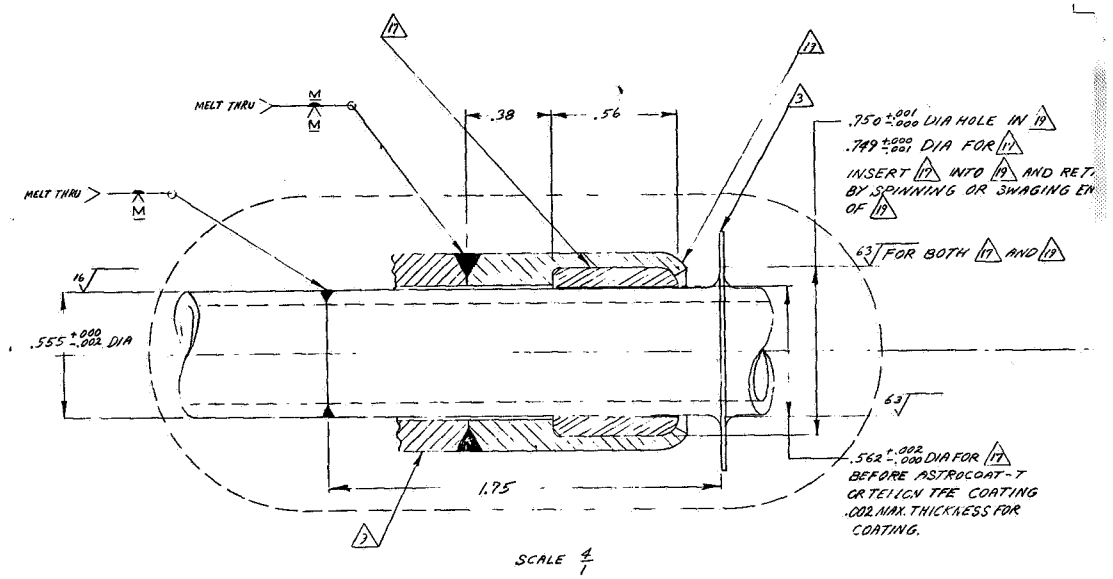

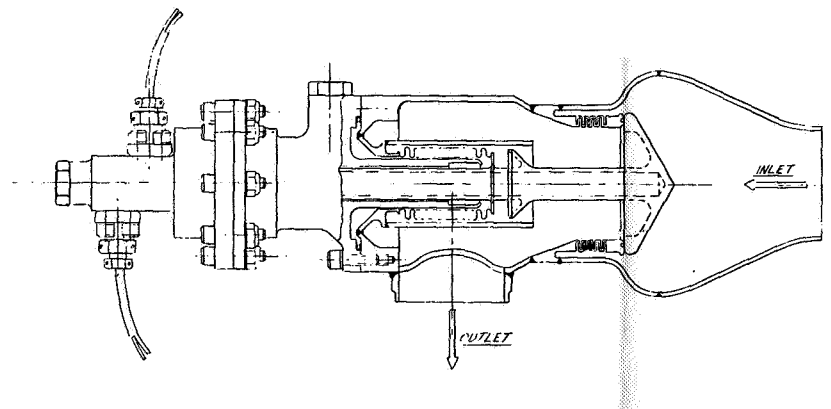

-501 VALVE CONFIGURATION
100% WELDED CONSTRUCTION FOR ALL COMPONENTS EXPOSED TO FLUORINE. ACTUATOR ESSENTIALLY IDENTICAL FOR BOTH -1 & -501 VALVES.
INCONEL 718 MATERIAL FOR ALL FLUORINE EXPOSED COMPONENTS.

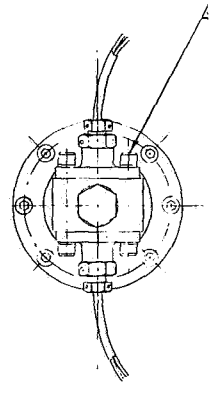

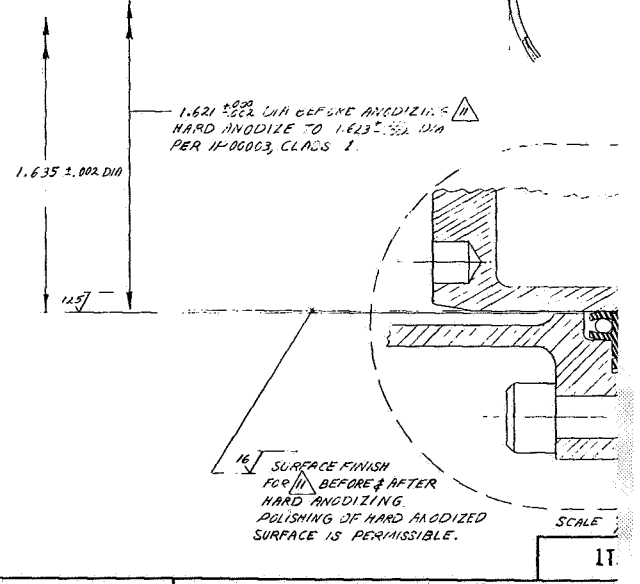

Part 2

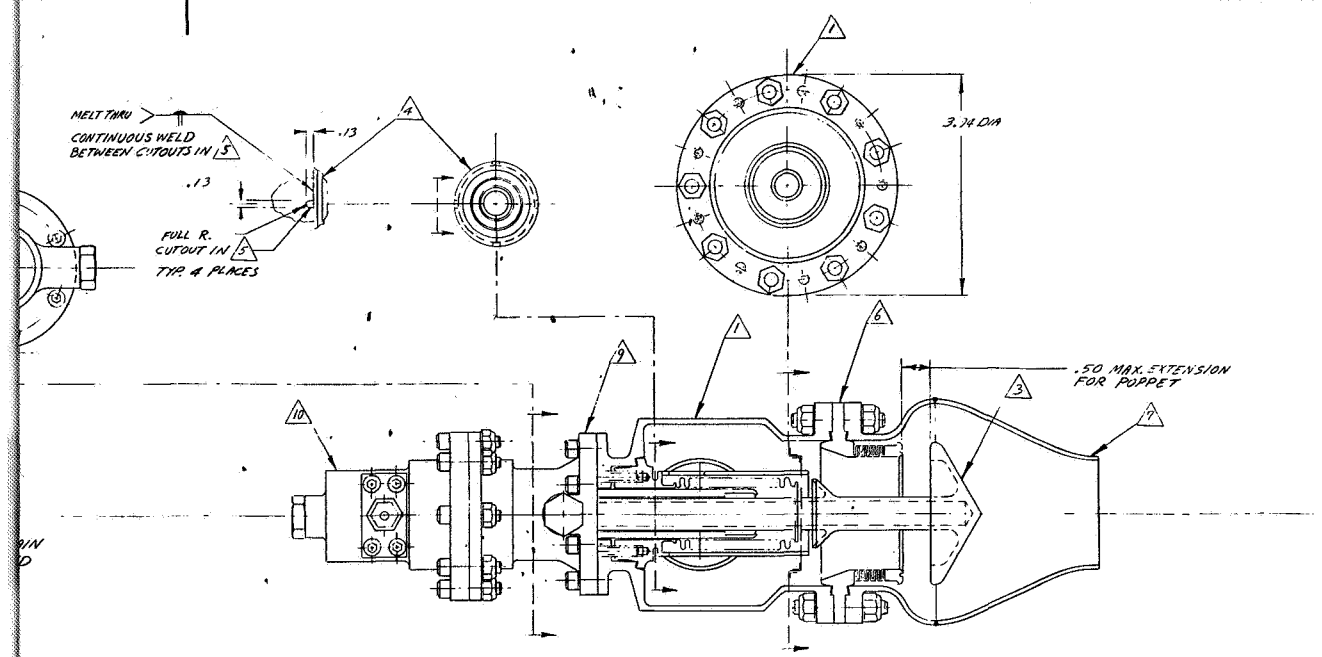

TOP VIEW

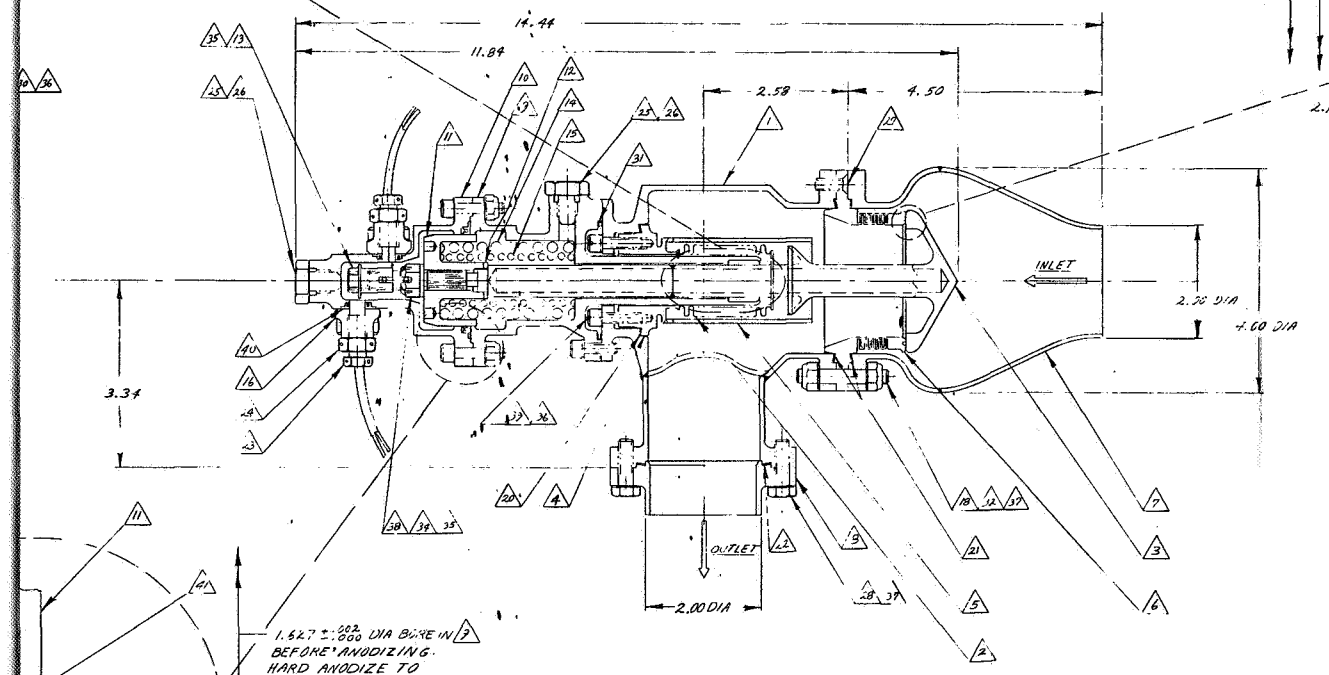

PROFILE VIEW

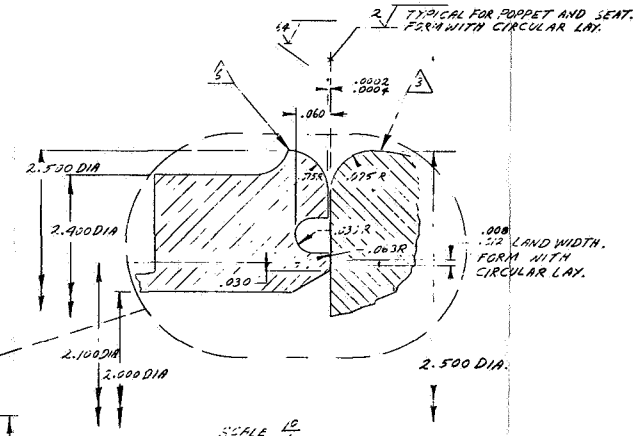

SCALE 10/1

GENERAL NOTES:
UNLESS OTHERWISE SPECIFIED:
1. HIDDEN CAVITIES WHICH CANNOT BE CLEANED ARE NOT PERMITTED IN THE SECTION OF THE VALVE EXPOSED TO FLUORINE
2. BUTT JOINT WELDS ARE PREFERRED. LAP JOINT WELDS ARE PERMISSIBLE ONLY IF BOTH SIDES OF THE JOINT ARE SEALED BY WELDING. FLANGE WELDS MUST BE MELTED THROUGH WITH NO HIDDEN SURFACES REMAINING.
3. WELDING SHALL BE ELECTRON BEAM WELD OR INERT SHIELDED ARC WELD PER MIL-W-8611. FULL PENETRATION OF WELD IS REQUIRED AND NO CAVITIES OR INCLUSIONS ARE PERMITTED. THE APPLICABLE REQUIREMENTS OF NASA CR-72064, APPENDIX III-4 SHALL BE OBSERVED
4. 100% RADIOGRAPHIC INSPECTION OF WELD IS REQUIRED PER RADIOGRAPHIC METHOD MIL STD-453 AND RADIOGRAPHIC INSPECTION SPECIFICATION MIL-R-11468, STD. 1. WRITTEN CERTIFICATION IS REQUIRED.
5. √ INDICATES MACHINED SURFACE ROUGHNESS PER USAS B46.1.
6. ALL MACHINED SURFACE ROUGHNESS 125 PER USAS B46.1 EXCEPT AS NOTED.
7. PROCESS FOR FLUORINE SERVICE PER THE CLEANING PROCEDURE IN NASA CR-72269, APPENDIX III-6.

REVISIONS

SYM	DESCRIPTION	DATE	APPROVED

LIST OF MATERIALS

PART OR IDENTIFYING NO.	NOMENCLATURE OR DESCRIPTION	CODE IDENT NO.	MATERIAL DESCRIPTION	MATERIAL SPECIFICATION	FIND NO.	ZONE
10	SEAL					
9	-37 HOUSING					
	-35 SLEEVING					
8	-33 SEAL RETAINER					
	-31 SPRING					
7	-27 CONE VALVE					
6	-25 VALVE NUT					
5	-23 SEAL					
4	-21 ADAPTER CAP					
3	-19 ADAPTER INLET					
2	-17 INLET FLANGE					
1	-15 INLET HOUSING					
	-13 VALVE SEAT					
1	-11 BELLOWS WELD					
1	-9 BELLOWS ADAPTER					
1	-7 POPPET					
1	-5 BELLOWS					
1	-3 VALVE BODY					

QUANTITY REQUIRED PER NOTED ASSY

DASH NUMBERS OF THIS DRAWING (OD DASH NUMBERS SHOWN / EVEN DASH NUMBERS OPPOSITE)

FINISH

UNLESS OTHERWISE SPECIFIED: DIMENSIONS ARE IN INCHES. TOLERANCES: FRACTIONS ± .03, DECIMALS ± .0 ANGLES ± 1°

MATL | WT CHK | STR CHK | CHECK | PR ENGR | DES ENGR | GR ENGR | PREP BY

DOUGLAS AIRCRAFT COMPANY, INC SANTA MONICA, CALIFORNIA

VALVE, SHUTOFF, POPPET, LIQUID FLUORINE

SEE ENGINEERING RECORDS FOR USAGE DATA

FIRST RELEASE OF PRINTS | ORIGINAL DATE OF DRAWING 13 FEB 68

DESIGN ACTIVITY APPROVAL

CUSTOMER APPROVAL

CODE IDENT NO. 18355 | SIZE J | 1T32095 | SCALE 1/1 | SHEET 1 OF 1

1T32095 | SHEET

DISTRIBUTION LIST

Report Copies R	D	RECIPIENT	DESIGNEE
		National Aeronautics & Space Administration Lewis Research Center 21000 Brookpark Road Cleveland, Ohio 44135	
1		Attn: Contracting Officer, MS 500-313	
5		Liquid Rocket Technology Branch, MS 500-209	
1		Technical Report Control Office, MS 5-5	
1		Technology Utilization Office, MS 3-16	
2		AFSC Liaison Office, MS 4-1	
2		Library	
1		Office of Reliability & Quality Assurance, MS 500-111	
1		D. L. Nored, Chief, LRTB, MS 500-209	
3		L. H. Gordon, Project Manager, MS 500-209	
1		E. W. Conrad, MS 500-204	
2		Chief, Liquid Experimental Engineering, RPX Office of Advanced Research & Technology NASA Headquarters Washington, D. C. 20546	
1		National Aeronautics & Space Administration Goddard Space Flight Center Greenbelt, Maryland 20771 Attn: Library	Merlund L. Moseson, Code 620
1		National Aeronautics & Space Administration John F. Kennedy Space Center Cocoa Beach, Florida 32931 Attn: Library	Dr. Kurt H. Debus
1		National Aeronautics & Space Administration Langley Research Center Langley Station Hampton, Virginia 23365 Attn: Library	Ed Cartwright, Director
1		National Aeronautics & Space Administration Manned Spacecraft Center Houston, Texas 77001 Attn: Library	J. G. Thiobodaux, Jr. Chief, Propulsion & Power Division

1	National Aeronautics & Space Administration George C. Marshall Space Flight Center Huntsville, Alabama 35812 Attn: Library	Keith Chandler, Hans G. Paul, Leon J. Hastings, James Thomas
1	Jet Propulsion Laboratory 4800 Oak Grove Drive Pasadena, California 91103 Attn: Library	Henry Burlage, Jr. Duane Dipprey
1	Defense Documentation Center Cameron Station Building 5 5010 Duke Street Alexandria, Virginia 22314 Attn: TISIA	
1	Office of the Director of Defense Research & Engineering Washington, D. C. 20301 Attn: Office of Asst. Dir. (Chem. Technology)	
1	RTD (RTNP) Bolling Air Force Base Washington, D. C. 20332	
1	Arnold Engineering Development Center Air Force Systems Command Tullahoma, Tennessee 37389 Attn: Library	Dr. H. K. Doetsch
1	Advanced Research Projects Agency Washington, D. C. 20525 Attn: Library	D. E. Mock
1	Aeronautical Systems Division Air Force Systems Command Wright-Patterson Air Force Base, Dayton, Ohio Attn: Library	D. L. Schmidt Code ARSCNC-2
1	Air Force Missile Test Center Patrick Air Force Base, Florida Attn: Library	L. J. Ullian
1	Air Force Systems Command Andrews Air Force Base Washington, D. C. 20332 Attn: Library	Capt. S. W. Bowen SCLT

1	Air Force Rocket Propulsion Laboratory (RPR) Edwards, California 93523 Attn: Library	J. Hartley
1	Air Force Rocket Propulsion Laboratory (RPM) Edwards, California 93523 Attn: Library	
1	Air Force FTC (FTAT-2) Edwards Air Force Base, California 93523 Attn: Library	Donald Ross
1	Air Force Office of Scientific Research Washington, D. C. 20333 Attn: Library	SREP, Dr. J. F. Masi
2	Chief, Liquid Propulsion Technology, RPL Office of Advanced Research & Technology NASA Headquarters Washington, D. C. 20546	
1	Director, Launch Vehicles & Propulsion, SV Office of Space Science & Applications NASA Headquarters Washington, D. C. 20546	
1	Chief, Environmental Factors & Aerodynamics Code RV-1 Office of Advanced Research & Technology NASA Headquarters D Washington, D. C. 20546	
1	Chief, Space Vehicles Structures Office of Advanced Research & Technology NASA Headquarters Washington, D. C. 20546	
1	Director, Advanced Manned Missions, MT Office of Manned Space Flight NASA Headquarters Washington, D. C. 20546	
6	NASA Scientific & Technical Information Facility P. O. Box 33 College Park, Maryland 20740	
1	Director, Technology Utilization Division Office of Technology Utilization NASA Headquarters Washington, D. C. 20546	

1	National Aeronautics & Space Administration Ames Research Center Moffett Field, California 94035 Attn: Library	Hans M. Mark Mission Analysis Division
1	National Aeronautics & Space Administration Flight Research Center P. O. Box 273 Edwards, California 93523 Attn: Library	
1	Space & Missile Systems Organization Air Force Unit Post Office Los Angeles, California 90045 Attn: Technical Data Center	
1	Office of Research Analyses (OAR) Holloman Air Force Base, New Mexico 88330 Attn: Library	Major R. E. Bracken, Code MDGRT
1	U. S. Air Force Washington, D. C. Attn: Library	Col. C. K. Stambaugh, Code AFRST
1	Commanding Officer U. S. Army Research Office (Durham) Box CM, Duke Station Durham, North Carolina 27706 Attn: Library	
1	U. S. Army Missile Command Redstone Scientific Information Center Redstone Arsenal, Alabama 35808 Attn: Document Section	Dr. W. Wharton
1	Bureau of Naval Weapons Department of the Navy Washington, D. C. Attn: Library	J. Kay Code RTMS-41
1	Commander U. S. Naval Missile Center Point Mugu, California 93041 Attn: Technical Library	
1	Commander U. S. Naval Weapons Center China Lake, California 93557 Attn: Library	W. F. Thorm Code 4562

1	Commanding Officer Naval Research Branch Office 1030 E. Green Street Pasadena, California 91101 Attn: Library	
1	Aerospace Corporation 2400 E. El Segundo Blvd. Los Angeles, California 90045 Attn: Library-Documents	J. G. Wilder
1	Arthur D. Little, Inc. 20 Acorn Park Cambridge, Massachusetts 02140 Attn: Library	A. C. Tobey
1	Astropower Laboratory McDonnell-Douglas Aircraft Company 2121 Paularino Newport Beach, California 92163 Attn: Library	Dr. George Moe Director Research
1	Astrosystems, International 1275 Bloomfield Avenue Fairfield, New Jersey 07007 Attn: Library	A. Mendenhall
1	ARO, Incorporated Arnold Engineering Development Center Arnold AF Station, Tennessee 37389 Attn: Library	Dr. B. H. Goethert
1	Susquehanna Corporation Atlantic Research Division Shirley Highway & Edsall Road Alexandria, Virginia 22314 Attn: Library	Dr. Ray Friedman
1	Battelle Memorial Institute 505 King Avenue Columbus, Ohio 43201 Attn: Report Library, Room 6A	
1	Beech Aircraft Corporation Boulder Facility Box 631 Boulder, Colorado Attn: Library	Douglas Pope
1	Bell Aerosystems, Inc. Box 1 Buffalo, New York 14205 Attn: Library	T. Reinhardt W. M. Smith

1	Director (Code 6180) U. S. Naval Research Laboratory Washington, D. C. 20390 Attn: Library	H. W. Carhart J. M. Krafft
1	Picatinny Arsenal Dover, New Jersey 07801 Attn: Library	I. Forsten
1	Air Force Aero Propulsion Laboratory Research & Technology Division Air Force Systems Command United States Air Force Wright-Patterson AFB, Ohio 45433 Attn: APRP (Library)	R. Quigley C. M. Donaldson
1	Electronics Division Aerojet-General Corporation P. O. Box 296 Azusa, California 91703 Attn: Library	W. L. Rogers
1	Space Division Aerojet-General Corporation 9200 East Flair Drive El Monte, California 91734 Attn: Library	S. Machlawski
1	Ordnance Division Aerojet-General Corporation 11711 South Woodruff Avenue Downey, California 90241 Attn: Library	
1	Propulsion Division Aerojet-General Corporation P. O. Box 15847 Sacramento, California 95803 Attn: Technical Library 2484-2015A	R. Stiff
1	Aeronutronic Division of Philco Ford Corp. Ford Road Newport Beach, California 92663 Attn: Technical Information Department	D. A. Carrison Dr. L. H. Linder
1	Bendix Systems Division Bendix Corporation 3300 Plymouth Street Ann Arbor, Michigan Attn: Library	John M. Brueger

1	Bellcomm 955 L'Eufant Plaza, S. W. Washington, D. C. Attn: Library	H. S. London
1	Boeing Company Space Division P. O. Box 868 Seattle, Washington 98124 Attn: Library	J. D. Alexander C. F. Tiffany
1	Boeing Company 1625 K Street, N. W. Washington, D. C. 20006	
1	Boeing Company P. O. Box 1680 Huntsville, Alabama 35801	Ted Snow
1	Chemical Propulsion Information Agency Applied Physics Laboratory 8621 Georgia Avenue Silver Spring, Maryland 20910	Tom Reedy
1	Chrysler Corporation Missile Division P. O. Box 2628 Detroit, Michigan Attn: Library	John Gates
1	Chrysler Corporation Space Division New Orleans, Louisiana Attn: Librarian	
1	Curtiss-Wright Corporation Wright Aeronautical Division Woodridge, New Jersey Attn: Library	G. Kelley
1	University of Denver Denver Research Institute P. O. Box 10127 Denver, Colorado 80210 Attn: Security Office	
1	Fairchild Stratus Corporation Aircraft Missiles Division Hagerstown, Maryland Attn: Library	J. S. Kerr

1	General Dynamics/Convair P. O. Box 1128 San Diego, California 92112 Attn: Library	Frank Dore R. Roberts
1	Missiles and Space Systems Center General Electric Company Valley Forge Space Technology Center P. O. Box 855 Philadelphia, Pa. 19010 Attn: Library	F. E. Schultz F. Menger
1	General Electric Company Flight Propulsion Lab. Department Cincinnati 15, Ohio Attn: Library	D. Suichu
1	Grumman Aircraft Engineering Corporation Bethpage, Long Island, New York Attn: Library	Joseph Gavin
1	Hercules Powder Company Allegheny Ballistics Laboratory P. O. Box 210 Cumberland, Maryland 21501 Attn: Library	
1	Honeywell Inc. Aerospace Division 2600 Ridgeway Road Minneapolis, Minn. Attn: Library	Gordon Harris
1	ITT Research Institute Technology Center Chicago, Illinois 60616 Attn: Library	C. K. Hersh
1	Kidde Aer-Space Division Walter Kidde & Company, Inc. 567 Main Street Belleville 9, New Jersey Attn: Library	R. J. Hanville
1	Ling-Temco-Vought Corp. P. O. Box 5907 Dallas, Texas 75222 Attn: Library	Warren G. Trent
1	Lockheed Missiles & Space Company P. O. Box 504 Sunnyvale, California 94087 Attn: Library	V. C. Lee J. Guill

1	Lockheed-California Company 10445 Glen Oaks Blvd., Pacoima, California Attn: Library	G. D. Brewer
1	Lockheed Propulsion Company P. O. Box 111 Redlands, California 92374 Attn: Library, Thackwell	H. L. Thackwell
1	Marquardt Corporation 16555 Saticoy Street Box 2013--South Annex Van Nuys, California 91409	W. D. Boardman, Jr. Howard McFarland
1	Martin-Marietta Corporation Baltimore Division Baltimore, Maryland 21203 Attn: Library	John Calathes C. E. Thomas
1	Denver Division Martin-Marietta Corp. P. O. Box 179 Denver, Colorado 80201 Attn: Library	Dr. Morganthaler F. R. Schwartzberg I. W. Murphy
1	Stanford Research Institute 333 Ravenswood Avenue Menlo Park, California 94025 Attn: Library	Thor Smith Dr. Gerald Marksman P. R. Gillette
1	Thiokol Chemical Corporation Reaction Motors Division Denville, New Jersey 07834 Attn: Librarian	A. Sherman Dwight S. Smith
1	Thiokol Chemical Corporation Redstone Division Huntsville, Alabama Attn: Library	John Goodloe
1	TRW System Group 1 Space Park Redondo Beach, California 90278 Attn: STL Tech. Lib. Doc. Acquisitions	G. W. Elurum
1	TRW Incorporation TAPCO Division 23555 Euclid Avenue Cleveland, Ohio 44117	P. T. Angell E. A. Steigerwald

1	United Aircraft Corporation Corporation Library 400 Main Street East Hartford, Connecticut 06108 Attn: Library	Dr. David Rix Erle Martin
1	United Aircraft Corporation Pratt & Whitney Division Florida Research & Development Center P. O. Box 2691 West Palm Beach, Florida 33402 Attn: Library	R. J. Coar Erle Martin R. A. Schmidtke
1	Orlando Division Martin-Marietta Corp. Box 5837 Orlando, Florida Attn: Library	J. Fern
1	Western Division McDonnell Douglas Aircraft Company, Inc. 3000 Ocean Park Blvd. Santa Monica, California 90406 Attn: Library	R. W. Hallet G. W. Burge Paul Klevatt
1	McDonnell Douglas Aircraft Corporation P. O. Box 516 Lambert Field, Missouri 63166 Attn: Library	R. A. Herzmark
1	Northrop Space Laboratories 3401 West Broadway Hawthorne, California Attn: Library	Dr. William Howard
1	Purdue University Lafayette, Indiana 47907 Attn: Technical Librarian	S. Fairweather
1	Radio Corporation of America Astro-Electronics Division Defense Electronic Products Princeton, New Jersey Attn: Library	S. Fairweather
1	Rocket Research Corporation Willow Road at 116th St. Redmond, Washington 98052 Attn: Library	Fy McCullough, Jr.

1	Rocketdyne Division of Rockwell North American Rockwell, Inc. 6633 Canoga Avenue Canoga Park, California 9134 Attn: Library, Department 596-306	Dr. R. J. Thompson S. F. Iacobellis
1	Rohm and Haas Company Redstone Arsenal Research Division Huntsville, Alabama 35808 Attn: Librarian	
1	United Aircraft Corporation United Technology Center P. O. Box 358 Sunnyvale, California 94088 Attn: Librarian	Dr. David Altman
1	North American Rockwell, Inc. Space & Information Systems Division 12214 Lakewood Boulevard Downey, California 90241 Attn: Technical Librarian	H. Storms
1	Pyronetics Inc. Santa Fe Springs, Calif. Attn: Library	
1	Conax Corporation 2300 Walden Ave. Buffalo, New York 14225 Attn: Library	
1	Pelmec, Division of Quantic Industries, Inc. 1011 Commercial St. San Carlos, California 94070 Attn: Library	
1	Pyrodyne, Div. of William Wald Corp. Santa Monica, California Attn: Library	
1	Holex Corp. Hollister, Calif. Attn: Library	